

University of Warwick institutional repository: <http://go.warwick.ac.uk/wrap>

A Thesis Submitted for the Degree of PhD at the University of Warwick

<http://go.warwick.ac.uk/wrap/4235>

This thesis is made available online and is protected by original copyright.

Please scroll down to view the document itself.

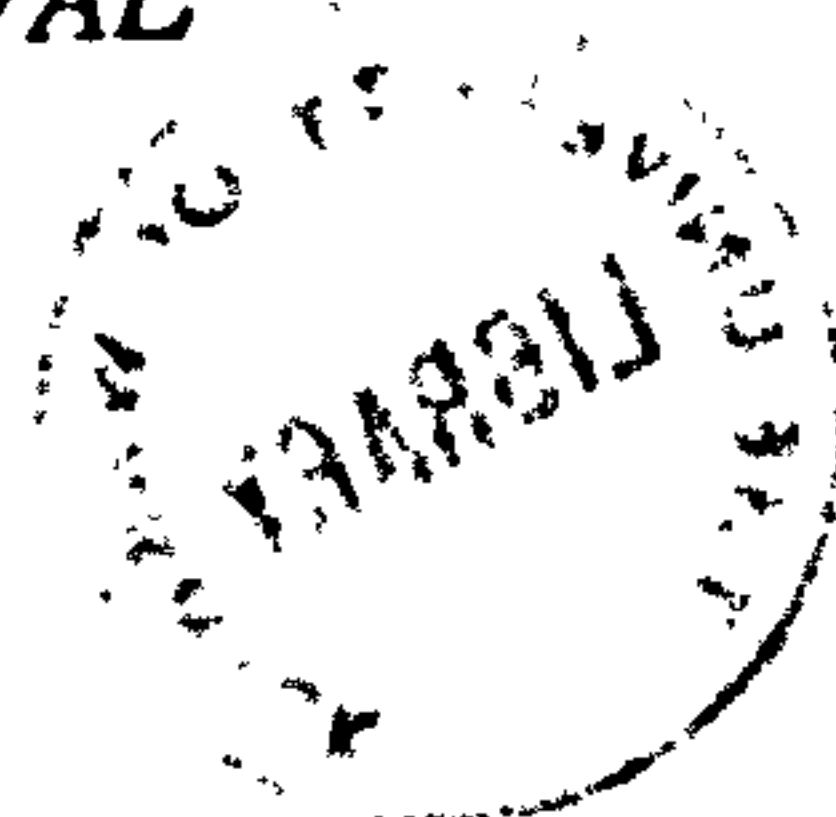
Please refer to the repository record for this item for information to help you to cite it. Our policy information is available from the repository home page.

THE ELECTROCHEMISTRY OF REDOX ENZYMES

RICHARD GEORGE WHITAKER, BSc.

A thesis submitted for the degree of Doctor of Philosophy
of the University of Warwick

Department of Chemistry
University of Warwick
Coventry CV4 7AL
England



May 1989

To Steph

Science

SCIENCE! to you.

*I have long bid a last and a careless adieu:
Still flying from nature to study her laws,
And dulling delight by exploring its cause,
You forget how superior, for mortals below,
Is the fiction they dream to the truth that they know.
Oh! who, that has ever had a rapture complete,
Would ask how we feel it, or why it is sweet;
How rays are confused, or how particles fly,
Through the medium refined of a glance or a sigh!
Is there one who but once would not rather have known it,
Than written, with Harvey, whole volumes upon it?*

Thomas Moore

TABLE OF CONTENTS

	<i>Page</i>
Contents	i
List of Figures	v
List of Tables	xi
Acknowledgements	xiii
Summary	xv
 Chapter 1 Introduction	 1
1.1 Electron Transfer in Biological Systems	2
1.2 The Effect of Distance on Electron Transfer Rates	5
1.3 The Characteristics of Redox Enzymes	6
1.4 The Electrochemistry of Flavoenzymes	12
1.4.1 Unmediated Electrochemistry	13
1.4.2 Mediated Electrochemistry	15
1.5 The Electrodeposition of Organic Polymers	26
1.6 The Electrochemical Immobilisation of Flavoenzymes	27
1.7 Summary of Work Presented in this Thesis	28
 Chapter 2 Apparatus and Experimental Techniques	 30
2.1 Controlling Electronics	30
2.1.1 Modular Instrumentation	30
2.1.2 Ring-Disc Circuit	31
2.2 Commercial Instrumentation	31
2.3 Electrodes	35
2.4 Rotation Apparatus	38
2.5 Electrochemical Cells	38
2.6 Temperature Control and Deoxygenation of Solutions	40
2.7 Solutions and Chemicals	41
2.8 Enzyme Assays	42
2.8.1 The Oxygen Electrode Assay	43
2.8.2 Spectrophotometric Determination of Glucose Oxidase Activity	46
2.8.3 Spectrophotometric Determination of Active GOD Concentration	48
2.9 The Covalent Modification of Glucose Oxidase with Electron Relays	50
2.9.1 Preparation	50
2.9.2 Gel Filtration	52
2.10 Ellipsometry	53
2.10.1 Preparation of Gold Substrates	55
2.10.2 Ellipsometry and Film Growth	56

Chapter 3 Theory	58
3.1 Oxygen Mediation to an Immobilised Enzyme	59
3.1.1 The Kinetic Scheme	59
3.1.2 Case A: $(k_{cat} + ka)s > K_M ka$	62
3.1.3 Case B: $(k_{cat} + ka)s < K_M ka$	64
3.1.4 Non-linear Dependence of Current on Substrate Concentration	71
3.2 Reaction of the Mediator on the Conducting Polymer Immobilisation Matrix	82
3.2.1 The Kinetic Scheme	83
3.3 Comparison to Previous Theoretical Models	91
 Chapter 4 The Immobilisation of Glucose Oxidase in Organic Polymer Films; Electrochemical Detection of Hydrogen Peroxide	 93
4.1 Electrodeposition of Polypyrroles from Aqueous Solutions	94
4.2 The Development of a Polymerisation System Compatible with Enzyme Immobilisation	97
4.3 Ellipsometric Measurement of Film Thickness	99
4.3.1 Determination of the Charge-Thickness Relationship	101
4.4 Electrochemical Immobilisation of Glucose Oxidase in Polypyrrole	104
4.5 Electrochemical Immobilisation of Glucose Oxidase in Poly- <i>N</i> - methylpyrrole	108
4.5.1 The Detection of Hydrogen Peroxide	108
4.5.2 Enzyme Immobilisation	119
4.5.3 Response to Glucose	125
4.6 Comparison of the Results to Theory	127
4.6.1 The Effect of Film Thickness	127
4.6.2 Variation of the Enzyme Loading	131
4.6.3 Discussion	139
4.7 The Stability of the Glucose Electrode	142
4.8 Determination of the pH Optimum of the Immobilised Enzyme	145
4.9 The Electrochemical Immobilisation of GOD in other Organic Polymers	149
4.9.1 Polyaniline	149
4.9.2 Analysis of pAn-GOD Electrode Responses	152
4.9.3 Polyphenol	157
4.9.4 Analysis of the pPh-GOD Data	160
4.9.5 Comparison of Response Characteristics	163
4.10 Conclusions	167
4.11 Electrochemical Immobilisation of Two-enzyme Systems	168
4.11.1 A Coupled β -fructosidase-GOD System	168
4.11.2 Coimmobilisation	169
4.11.3 Production of a Bilayer Two-Enzyme System	171

Chapter 5 The Immobilisation of Glucose Oxidase in Conducting Poly- N-methylpyrrole films; Mediation by a Ferrocene Derivative	174
5.1 A Gas Tight Electrochemical Cell.....	175
5.1.1 Levich Currents.....	176
5.1.2 Alberly-Hitchman Determination of Diffusion Coefficients.....	178
5.1.3 Coulometric Titration in the Gas Tight Cell.....	181
5.2 The Reaction of FMA at Clean and Poly-N-methylpyrrole Coated Platinum Electrodes	184
5.2.1 Oxidation of FMA at a Platinum Electrode.....	184
5.2.2 Reaction of FMA at Poly-N-methylpyrrole Coated Electrodes.....	186
5.3 Responses to Glucose	189
5.3.1 The Cyclic Voltammetry of the FMA Mediated GOD-pNMP System....	194
5.4 Analysis of the Glucose Responses	196
5.4.1 Film Thickness (l)	197
5.4.2 Substrate Concentration (s_g)	200
5.4.3 Mediator Concentration (a_g)	205
5.4.4 Enzyme Loading (e_g)	208
5.5 Comparison and Discussion of the Experimentally Determined Parameters...	209
5.6 The Site of FMA Oxidation.....	211
5.7 Conclusions.....	212
 Chapter 6 The Covalent Modification of Redox Enzymes	213
6.1 Introduction.....	213
6.1.1 The Effect of Distance on Electron Transfer Rates.....	214
6.1.2 Electron Transfer between Modified Redox Enzymes and Simple Metallic Electrodes	216
6.1.3 Techniques for the Production of Modified Flavoenzymes.....	218
6.2 Types of Modified Redox Enzyme Produced.....	225
6.2.1 Ferrocene Modified Flavoenzymes.....	225
6.2.2 Ruthenium Pentaamine Modified Flavoenzymes	229
6.3 A Series of Ferrocene Carboxylic Acid Modified Enzymes	235
6.3.1 Preparation and Determination of Iron Content	235
6.3.2 Electrochemistry.....	236
6.4 Responses to Glucose	237
6.4.1 Stationary Electrode Studies.....	237
6.4.2 Analyses of the Glucose Responses.....	241
6.4.3 Estimation of the Redox Potentials of the Modified Enzymes.....	244
6.5 Stability Studies.....	247
6.5.1 Stability on Storage.....	247
6.5.2 Operational Stability.....	251
6.5.3 Loss of Electrochemical Response	254

6.6 Reagentless Membrane Electrodes	257
6.6.1 Electrode Construction	257
6.6.2 Response to Glucose.....	257
6.6.3 Analysis of the Glucose Response.....	258
6.8 Conclusions.....	263
 Chapter 7 Concluding Remarks	265
7.1 Overall Conclusions.....	265
7.2 Future Work.....	265
 References.....	267
 Appendix I : Previous Publications	282

LIST OF FIGURES

	<i>Page</i>
1.1 Schematic representation of the transmembrane arrangement of respiratory carriers and dehydrogenase enzymes in the mitochondrion	3
1.2 The structure and redox reactions of the flavins	8
1.3 Scheme for the classification of flavoenzymes	9
1.4 The homogeneous mediation of flavoenzyme electrochemistry.....	16
Plate 2.1	31
2.1 The potentiostat configuration.....	33
2.2 The Sallen and Key filter.....	34
2.3 The calomel reference electrode (twice actual size)	37
2.4 Schematic representation of a water jacketed two compartment electrochemical cell.....	39
2.5 Relationship of GOD activity to rate of oxygen depletion in the oxygen electrode assay.....	44
2.6 Absorption spectra for free and enzyme bound FAD.....	49
2.7 The relationship between GOD concentration and solution absorbance at 450nm.....	51
2.8 Column elution profile for the G-25 sepadex separation of modified enzyme from low molecular weight components.....	54
3.1 General kinetic scheme for the immobilised enzyme reaction	61
3.2 A plot of the dimensionless flux, ψ , as a function of the normalised film thickness, l/X_K	67
3.3 Plots of the normalised concentration profiles for S (a) and B (b) in the film as a function of x/l . The values of l/X_K are shown for each curve. ($\phi_S = s/K_{s_2}$, $\phi_B = b D_B / D_S K_{s_2}$).	69
3.4 Case diagram for the system showing three cases and approximate expressions for j_S and j_B in each case. The bold lines show the case boundaries.....	70
3.5 Case diagram showing the relationship between the different j_S expressions when an approximation is used to describe a saturation type current response (section 3.1.4).	76
3.6 Case diagram showing the relationship between the different j_B expressions when an approximation is used to describe a saturation type current response (section 3.1.4).	81

3.7	Kinetic scheme for the reaction of the reduced mediator at the electrode or polymer surface.	84
3.8	Case diagram showing the relationship between the different j_s expressions for the situation described in section 3.2.	90
4.1	Current transients for the potentiostatically controlled polymerisation of <i>N</i> -methylpyrrole at a series of potentials.....	100
4.2	Poly- <i>N</i> -methylpyrrole film thickness as a function of time (each sample is 20ms) and applied potential (50 mmol dm ⁻³ <i>N</i> -methylpyrrole, 0.1 mol dm ⁻³ sodium phosphate, 0.15 mol dm ⁻³ TEA TFB pH 7.0, 20°C).....	102
4.3	Film thickness as a function of charge density during film growth (taken from the data presented in figure 4.2).	103
4.4	Polarogram for the oxidation of hydrogen peroxide (5×10 ⁻⁵ mol cm ⁻³) in buffered electrolyte (0.1 mol dm ⁻³ sodium phosphate, 0.15 mol dm ⁻³ TEA TFB, pH 7.0, 25°C in the absence of molecular oxygen) at a poly- <i>N</i> -methylpyrrole coated platinum electrode ($A=0.385\text{cm}^2$, $W=4\text{ Hz}$).....	110
4.5a	Koutecky-Levich plots for the oxidation of hydrogen peroxide at a poly- <i>N</i> -methylpyrrole coated platinum rotating disc electrode ($A=0.385\text{ cm}^{-3}$, $l=4.18\pm0.11\times10^{-5}\text{ cm}$) at concentrations between 1×10^{-7} and $1\times10^{-6}\text{mol cm}^{-3}$ hydrogen peroxide (pH 7.0, 25°C).	113
4.5b	Plot of the Koutecky-Levich (K-L) intercept as a function of reciprocal hydrogen peroxide concentration.	113
4.5c	Plot of the K-L slope as a function of reciprocal hydrogen peroxide concentration.	114
4.6	Plot of the K-L intercept as a function of film thickness for hydrogen peroxide oxidation at poly- <i>N</i> -methylpyrrole coated electrodes.	116
4.7	Dependence of the limiting current on the bulk hydrogen peroxide concentration ($l=3.1\times10^{-5}\text{ cm}$, $W=9\text{ Hz}$).....	118
4.8	Short-time current transients for the initial phase of polymer growth from a solution containing <i>N</i> -methylpyrrole (50 mmol dm ⁻³) and glucose oxidase (5 mg cm ⁻³) at a variety of applied potentials.....	122
4.9	Plot of the logarithm of the slopes of the i vs t^2 plots as a function of potential applied for polymerisation.	124
4.10	The response of the glucose oxidase electrode to additions of glucose. Each arrow represents an increase in glucose concentration of 6.6 mmol dm ⁻³ . The electrode was rotated at 9 Hz ($E=0.95\text{V vs SCE}$). The inset shows a typical plot of current as a function of bulk glucose solution.....	126
4.11	Plot of the gradient of the glucose calibration plot as a function of charge passed to grow the glucose oxidase / poly- <i>N</i> -methylpyrrole films ($A=0.385\text{ cm}^2$, $W=9\text{ Hz}$).....	128

- 4.12 Comparison of the experimental variation of the electrode response to glucose as a function of l with the theoretical expression. The points represent the experimental data and the solid line is drawn according to equation (4.6)... 130
- 4.13 The variation of the electrode response with the rotation speed for thin films ($l \ll X_K$) with high enzyme loadings ($e_\Sigma = 2.08 \text{ mg cm}^{-3}$, $Q = 25 \text{ mC}$, $A = 0.385 \text{ cm}^2$). The glucose concentration was 6.3 mmol dm^{-3} (pH 7.0, 25°C). 133
- 4.14 Plot of j_{obs} as a function of $W^{-1/2}$. The intercept of this plot gives an estimate of j_B (data from figure 4.13). 135
- 4.15 Comparison of the experimental variation of the electrode response to added glucose as a function of e_Σ with the theoretical expression. The points represent the experimental data and the solid line is calculated from equation 4.6. The inset shows the fit of experiment to theory ($l = 40 \text{ mC}$, $A = 0.385 \text{ cm}^2$, $W = 9 \text{ Hz}$, pH 7.0, 25°C). 136
- 4.16 Effect of glucose oxidase concentration on the response of the resulting electrode. A plot of response as a function of the time spent in the polymerisation solution at 0 volts is shown. 137
- 4.17 The response of the glucose electrodes as a function of time stored at 25°C (pH 7.0 phosphate) after preparation. ($l = 3 \times 10^{-5} \text{ cm}$, $e_\Sigma = 5 \text{ mg cm}^{-3}$). 143
- 4.18 pH profiles for free (O) and electrochemically immobilised (■) glucose oxidase. Reaction rates (0.1 mol dm^{-3} glucose) determined at 0.95 V vs SCE, 9 Hz for the immobilised enzyme. 146
- 4.19 Potentiostatic current time transients for the polymerisation of aniline at a platinum electrode surface ($A = 0.385 \text{ cm}^2$) at a number of applied potentials. 151
- 4.20 Response curves for the glucose oxidase - polyaniline electrodes at three different thicknesses (circles $Q = 8 \text{ mC}$, squares $Q = 24 \text{ mC}$, diamonds $Q = 18 \text{ mC}$). The inset shows a typical experimental $i-t$ trace with each arrow representing a 6 mmol dm^{-3} increase in the bulk glucose concentration. 153
- 4.21a Electrode response, at low glucose concentration (6.6 mmol dm^{-3}) as a function of charge density for film growth..... 155
- 4.21b Electrode response, at saturating glucose concentration (65 mmol dm^{-3}) as a function of charge density for film growth..... 155
- 4.22 Polarogram for polyphenol coated and clean platinum electrodes in ferricyanide solution (potassium ferricyanide, 5 mmol dm^{-3} , TEA TFB 0.15 mol dm^{-3} , phosphate 0.1 mol dm^{-3} , pH 7.2, 25°C) at $W = 9 \text{ Hz}$ 159
- 4.23 Response curves for the glucose oxidase - polyphenol electrode to glucose. The plot shows the calibration curve obtained for additions of glucose. The inset shows the $i-t$ trace for additions of glucose. The arrows represent stepwise increases in the bulk glucose concentration of 5 mmol dm^{-3} 161

4.24	Plot showing the electrode response as a function of rotation speed (0.1 mol dm^{-3} glucose).....	164
4.25	Plot of response as a function of $W^{-1/2}$ (data taken from figure 4.24).	165
4.26a	Oxygen electrode trace for the addition of sucrose to the coupled enzyme system in solution.....	170
4.26b	The pH profile for this coupled enzyme system.....	170
4.27	Responses of the coimmobilised bienzyme system. Each arrow represents a stepwise increase in the substrate concentration of 6.6 mmol dm^{-3}	172
4.28	Response for the two layer bienzyme system on the addition of sucrose.....	172
5.1	Drawing of the perspex gas tight electrochemical cell and electrodes (to scale 1:1).....	177
5.2	Albery-Hitchman plot for oxidation of ferrocyanide ion at a rotating electrode (0.5V vs Ag/AgCl).	180
5.3	Nernst plot for the progressive oxidation of ferrocene acetic acid.	183
5.4	Polarogram for the oxidation / reduction of ferrocene monocarboxylic acid at a rotating disc electrode (9 Hz).	185
5.5	Corrected Tafel plot for the oxidation / reduction of ferrocene monocarboxylic acid (data from figure 5.4).....	187
5.6	Levich plots for the oxidation of ferrocene monocarboxylic acid. Solid points for data at a pNMP-GOD coated platinum RDE, open points for data at a clean platinum RDE.....	188
5.7	Plot of the Levich slope as a function of bulk mediator concentration. Open points for data at a pNMP-GOD coated platinum RDE, solid points for data at a clean platinum RDE.	190
5.8	Schematic representation of recycling of the mediator in the enzyme containing conducting polymer film.	192
5.9	Plot of electrode response ($i_{total} - i_{Levich}$) as a function of bulk glucose concentration. The lower inset shows the experimental trace of current as a function of time. The arrows indicate the points at which glucose was injected and the numbers signify the final concentration of glucose after each addition to the bulk solution.....	193
5.10	Cyclic voltammetric response for a pNMP-GOD film in the presence of FMA ($5.5 \times 10^{-4} \text{ mol dm}^{-3}$) for different concentrations of glucose.	195
5.11	Plot to show electrode response as a function of film thickness. Solid squares represent data for low glucose concentration ($1.25 \times 10^{-6} \text{ mol cm}^{-1}$) and solid circles represent data for saturating glucose ($1 \times 10^{-4} \text{ mol cm}^{-1}$).....	199
5.12	Case diagram for situations when $k_M e_{\Sigma} < k'$ and $k_M e_{\Sigma} > k'$	202

5.13	Current response as a function of substrate concentration for a “thin” film situation ($l = 9.1 \times 10^{-6}$ cm).	203
5.14	Current response as a function of substrate concentration for a “thick” film situation ($l = 3.2 \times 10^{-5}$ cm).	206
5.15	Current response as a function of mediator concentration ($s_{\infty} = 1 \times 10^{-4}$ mol cm ⁻³ , $l = 3.2 \times 10^{-5}$ cm, $[enz] = 5$ mg cm ⁻³).	207
6.1	Schematic representation of the electron transfer distances involved in a) the native enzyme, and b) the redox modified enzyme.....	217
6.2	Reaction sequence for coupling of electron relays to a redox enzyme via amide bonds.....	226
6.3	Ruthenium pentaamine isonicotinamide modified glucose oxidase coupling site.	231
6.4	Ruthenium pentaamine azo coupling site.	231
6.5	Ruthenium pentaamine relays coordinated to available imidazole rings of glucose oxidase.....	233
6.6	D.c. cyclic voltammograms for: a) the unmodified GOD enzyme in buffered electrolyte (0.085 mol dm ⁻³ phosphate pH 7.0) at zero glucose (platinum or glassy carbon electrode, 5 mV s ⁻¹); b) the ferrocene carboxylic acid modified GOD (4.6 mg cm ⁻³); c) the ferrocene acetic acid modified GOD (2.0 mg cm ⁻³); d) the ferrocene butanoic acid modified GOD (0.65 mg cm ⁻³).....	238
6.7	D.c. voltammogram for: (a) ferrocene acetic acid, (b) ferrocene butanoic acid, and (c) ferrocene carboxylic acid modified glucose oxidase at a glassy carbon electrode (3mm diameter), sweep rate 5 mV s ⁻¹ . In all cases the glucose concentration is 100 mmol dm ⁻³ and the enzyme concentration is 1 mg cm ⁻³ . All at pH 7.0, 25°C.....	239
6.8	Glucose response curve for the ferrocene acetic acid modified GOD (4.5 mg cm ⁻³) at a glassy carbon electrode (3mm diameter) at pH 7.0, 25°C in the absence of atmospheric oxygen.....	240
6.9	Plot of equation 6.4 for ferrocene acetic acid modified GOD using data for three different enzyme concentrations (0.45, 1.13 and 4.5 mg cm ⁻³).....	242
6.10	Corrected Tafel plots for the modified enzymes: A) ferrocene butanoic acid modified, B) ferrocene acetic acid modified, and C) ferrocene carboxylic acid modified. All for saturating glucose concentration (0.1 mol dm ⁻³ , pH 7.0).	245
6.11	The effect of different storage conditions on the activity of the ferrocene carboxylic acid modified GOD to glucose.	249
6.12	Comparison of the storage stability of: a) ferrocene acetic acid modified GOD to b) ferrocene carboxylic acid modified GOD, at 4°C, pH 7.0, in the absence of atmospheric oxygen.	250

- 6.13 The stability of A) ferrocene acetic acid modified and B) ferrocene carboxylic acid modified GOD to continuous potential cycling (5 mV s^{-1} , 20°C). 253
- 6.14 Membrane electrode responses to a) zero glucose, b) $2.4 \times 10^{-3} \text{ mol dm}^{-3}$, and c) $6.54 \times 10^{-3} \text{ mol dm}^{-3}$ glucose, with inset calibration curve showing plateau current as a function of bulk glucose concentration (20°C , pH 7.0)..... 259
- 6.15 Analysis of the modified enzyme membrane electrode response. a) Plot of s_∞/i against s_∞ , giving an estimate of k_{ME}' . b) Plot of Y against ρ , giving an estimate of K_{ME} and k_s'/k_{ME}' 261

LIST OF TABLES

	<i>Page</i>
1.1 Sequential redox reactions in the electron transfer chain of the mitochondrion	4
1.2 Classification of flavin-containing redox enzymes	11
1.3 Homogeneous mediation of flavoenzyme electrochemistry.....	18-20
2.1 Working electrodes.....	35
3.1 Expressions for the concentration and fluxes of S and B in the different limiting cases.....	66
3.2 Expressions for j_s and the rate dependencies for each case.....	75
3.3 Expressions for j_B and the dependencies in each case	82
3.4 The different j_s expressions for each case	91
4.1 Glucose oxidase immobilised in polypyrrole.....	106
4.2 Diffusional parameters for oxidation of hydrogen peroxide.....	117
4.3 Optimum conditions for growth of polymer films containing glucose oxidase.....	119
4.4 Kinetics and mass transport parameters obtained for the detection of hydrogen peroxide produced by GOD immobilised in films of poly- <i>N</i> -methylpyrrole.	140
4.5 Comparison of the response characteristics of the immobilised glucose oxidase systems	166
5.1 Diffusion coefficients determined by the Albery-Hitchman method.....	179
5.2 The dependence of the flux j_s on the experimental variables	197
5.3 Ferrocene monocarboxylic acid mediation – best fit data	210
6.1 Possible coupling sites and coupling methods.....	221-2
6.2 The amino acid composition of two flavoenzymes.....	223
6.3 Comparison of no. of relays incorporated to no. of possible coupling sites in GOD	234
6.4 The iron content of the various modified enzymes	236
6.5 Kinetic constants determined for the modified GOD-glucose reactions.....	241
6.6 Redox potentials for the modified enzymes	246
6.7 Stability data for the ferrocene modified glucose oxidases.....	251

6.8 Stability data for the ferrocene acetic acid modified glucose oxidase 256

6.9 The kinetic parameters obtained for the modified GOD-membrane electrode 262

ACKNOWLEDGEMENTS

I would like to thank Dr P.N. Bartlett for his helpful and patient supervision of this work and also for his many excellent suggestions during its course.

Financial support by Genetics International (now MediSense) is gratefully acknowledged.

I would also like to thank Dr A. Hamnett of the I.C.L., Oxford University, for his generosity both with his time and the use of his equipment.

Finally, I would like to express my gratitude to the other members of the research group for their useful comments and suggestions during the course of this work.

DECLARATION

The work presented in this thesis was conducted solely by the author. Where previously published material has been included the appropriate publication is bound into the thesis as an appendix. Where the work of other authors has been discussed this is clearly indicated.

This work was conducted in the Department of Chemistry, University of Warwick, between January 1986 and October 1988, under the supervision of Dr P.N.Bartlett.

Signed Richard G. W. Walker

SUMMARY

The work presented in this thesis is of two types. Firstly methods for the electrochemical immobilisation of redox enzymes in organic polymers are described. The electrochemical monitoring of the immobilised enzyme reaction by detection of one of the enzyme's products is discussed, and the results obtained for such a system under a variety of experimental conditions are presented.

A good understanding of the way in which such a system operates was obtained by using a specially developed kinetic model. This model is explained fully in the theory chapter of this thesis.

A variety of organic polymers were used in the electrochemical immobilisation process, with varying degrees of success. The flexibility of this approach is demonstrated by the use of a variety of immobilisation matrices and also by the development of bienzyme and bilayer devices.

The final experimental chapter presents work on the covalent modification of redox enzymes with a variety of redox centres based on ferrocene. Although attempts to electrochemically immobilise a modified enzyme were not successful, some interesting information about the kinetic behaviour and stability of a series of modified enzymes was obtained.

An indication of possible work forming an extension to this thesis is given in the final part of this thesis. The electrochemical immobilisation techniques and the procedure for covalently modifying enzymes using electroactive groups are relatively recent ideas. Much work remains to be done before a better understanding of these systems is gained.

CHAPTER ONE

INTRODUCTION

The work presented in this thesis is concerned with electrochemical methods for the immobilisation and study of redox enzymes⁽¹⁻⁵⁾. In immobilised enzyme systems the enzyme, a highly specific biological catalyst⁽⁶⁾, is immobilised in a support matrix. When the enzyme is entrapped at an electrode surface it is possible, in many cases, to monitor the enzyme reaction electrochemically.

A novel electrochemical enzyme immobilisation technique is described. This enables a redox enzyme to be entrapped at an electrode surface using a single step procedure. The resulting immobilised enzyme retains activity towards its substrate. The results presented for such an electrochemically immobilised enzyme system are analysed in terms of a new theoretical model describing the kinetic and transport processes occurring within the enzyme containing film at an electrode surface.

In the final part of this thesis the development and electrochemical behaviour of a specially modified redox enzyme is described. Results demonstrating the direct oxidation of such modified enzymes at a simple metallic electrode are presented and analysed by the use of an appropriate kinetic model.

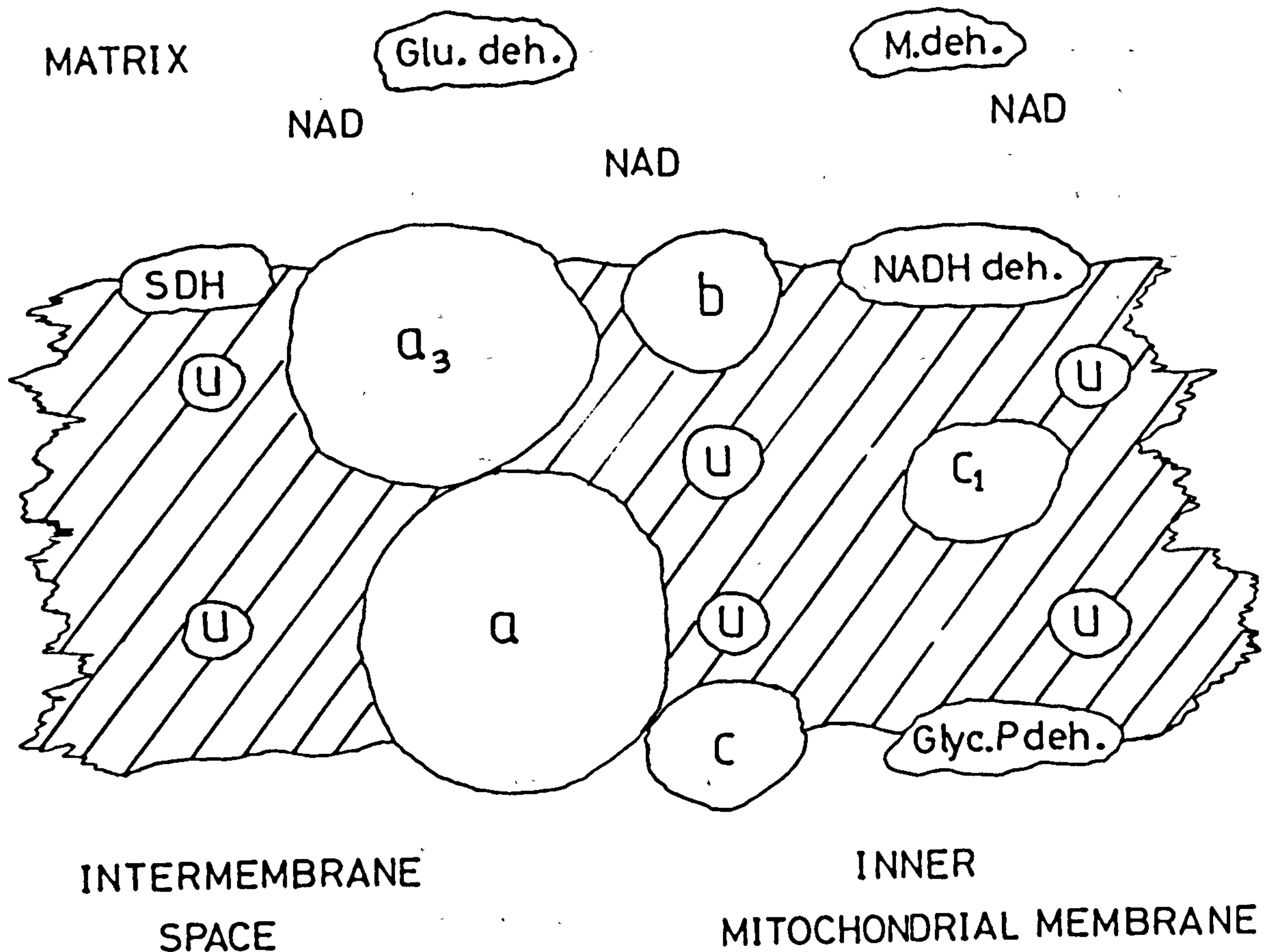
In this introduction we begin by briefly describing the role of electron transfer in biological systems and the characteristics of redox enzymes. We then describe the methods used to immobilise redox enzymes, at electrode surfaces and electrochemical procedures for monitoring the activity of immobilised enzymes. Finally the electrochemistry of redox modified enzymes is reviewed. Since no attempt was made to produce a viable analyte sensing device the applications of immobilised enzyme systems will not be discussed. The work presented concentrates on the development of a theoretical model system to explain the results in terms of the processes occurring in different types of immobilised enzyme film.

1.1 ELECTRON TRANSFER IN BIOLOGICAL SYSTEMS

In all living systems the sequential and specific transfer of electrons is of vital importance in maintaining pH and ionic gradients, fueling biosynthetic reactions and in a variety of other highly specific energy requiring processes within the cell. Energy derived from oxidisable substrates and light are fed into electron transport or electron transfer chains^(1,7,8). These chains are a complex series of redox centres, many of which are membrane bound. The asymmetric transfer of electrons through a specific series of redox centres is linked to the production of high energy phosphorylated molecules in the cell^(9,10). Examples of this type of electron transport chain are the respiratory chain, the photosynthetic pathway, nitrogen fixation and the Cytochrome P-450 system⁽⁵⁾. Figure 1.1 shows the mitochondrial electron transport chain. The specific spatial and sequential arrangement of the electron carriers is shown schematically in this figure. Hydrogen atoms derived from the catabolism of carbohydrates are incorporated into nicotinamide adenine dinucleotide (NADH) and flavoproteins. The NADH produced donates two electrons and one proton to the dehydrogenase enzymes on the mitochondrial membrane surface. The electrons are transferred through a series of electron transfer proteins and soluble mediators to molecular oxygen (Table 1.1).

At this stage of the introduction it is important to distinguish between the electron transfer, or redox proteins and redox enzymes. The redox proteins are relatively low molecular weight proteins containing a redox centre at the periphery of the protein. The protein associated with the redox centre serves only to ensure that the redox protein undergoes electron transfer with its specific partners alone. Failure to do this would result in the random transfer of electrons and the death of the cell.

Figure 1.1 Schematic representation of the transmembrane arrangement of respiratory carriers and dehydrogenase enzymes in the mitochondrion



a, a₃, b, c, c₁ are cytochromes

SDH = succinate dehydrogenase (a flavoenzyme)

Glu.deh. = glutamate dehydrogenase

NADH.deh. = NADH dehydrogenase

GlyP.deh. = glycerophosphate dehydrogenase (a flavoenzyme)

M.deh. = malate dehydrogenase

U = ubiquinone

Table 1:1

Sequential Redox Reactions in the Electron Transfer Chain of the Mitochondrion

Redox reaction	Redox potentials of components / mV vs SHE	E° (pH 7.0) / mV vs SHE
$\text{NADH} + \text{H}^+ + \text{FAD}^{\text{a)}} \rightarrow \text{NAD}^+ + \text{FADH}_2$	NADH/FADH ₂ -320 -50	+270
$\text{FADH}_2 + \text{UQ}_{\text{ox}} \rightarrow \text{FAD} + \text{UQ}_{\text{red}}$	UQ _{red} +100	+150
$\text{UQ}_{\text{red}} + 2\text{Cytb}_{\text{ox}} \rightarrow$ $\text{UQ}_{\text{ox}} + 2\text{Cytb}_{\text{red}} + 2\text{H}^+$	Cytb _{red} +40	-60
$2\text{Cytb}_{\text{red}} + 2\text{Cytc}_{1\text{ox}} \rightarrow$ $2\text{Cytb}_{\text{ox}} + 2\text{Cytc}_{1\text{red}}$	Cytc _{1red} +220	+180
$2\text{Cytc}_{1\text{red}} + 2\text{Cyta}_{\text{ox}} \rightarrow$ $2\text{Cytc}_{1\text{ox}} + 2\text{Cyta}_{\text{red}}$	Cyta _{red} +290	+70
$2\text{Cyta}_{\text{red}} + \frac{1}{2}\text{O}_2 + \text{H}^+ \rightarrow$ $2\text{Cyta}_{\text{ox}} + \text{H}_2\text{O}$	H ₂ O +820	+530

a) represents flavin centres in flavoenzymes

UQ is ubiquinone

cyt. represents a cytochrome

The redox enzymes are a larger, more complex series of proteins, which catalyse the specific oxidation or reduction of a substrate, or group of substrates, within the cell. These enzymes have redox centres buried in the protein away from the periphery. Here the substrate must diffuse into the enzyme interior to the active site before any redox process can occur. The characteristics of redox enzymes will be discussed in section 1.3.

In order to study the oxidation and reduction of these biological macromolecules at electrode surfaces it is important to understand the effect of inter-redox centre distance on the rate of electron transfer. In the next section we

consider the large distances over which protein-electrode electron transfer must occur.

1.2 THE EFFECT OF DISTANCE ON ELECTRON TRANSFER RATES

The aim of this work is to investigate electron transfer between redox enzymes and electrodes. The large size of many redox proteins makes distance a controlling factor in the rate of electron transfer.

The effect of distance on electron transfer in redox proteins and biological systems remains the subject of much research. The topic has been reviewed by several authors⁽¹¹⁻¹⁴⁾. In order to quantify this distance effect we must relate the electrochemical rate constant k' to the distance over which the electron transfer must occur. The general expression for the electrochemical rate constant is: ⁽¹⁵⁻¹⁷⁾

$$k' = k_E' \nu k_{el}(r) e^{-G^*/RT} \quad (1.1)$$

where k' is the heterogeneous electrochemical rate constant,

k_E' describes the diffusion pre-equilibrium,

ν is the effective frequency of motion along the reaction coordinate,

k_{el} is the electronic transmission coefficient, which depends upon r , the distance over which the electron transfer occurs, and

G^* is the activation energy.

For the electrode reaction of small molecules k_{el} is taken to be close to 1 when the electrons can transfer adiabatically, and less than 1 in other cases. For the electron transfer reaction of large biological molecules at macroscopic electrodes, electron transfer must occur over large distances. Under such conditions we must account for this distance dependence.

$$\nu k_{el} = \nu_0 e^{-\beta(r-r_0)} \quad (1.2)$$

where r_0 is the distance at which νk_{el} equals some preassigned value, ν_0 . If we take

ν_0 equal to a typical vibrational frequency, 10^{13} s^{-1} , we assume that the electron transfer is adiabatic when $r = r_0$.

The value of β in equation 1.2 can be estimated from the results of studies of the electron transfer kinetics for a number of systems where the electron transfer distance has been systematically varied. Such experiments give a value of β of around 12 nm^{-1} for non-biological systems. This value appears to be consistent with studies on electron transfer proteins⁽¹³⁾. The β value will depend on the nature of the medium through which electron transfer must occur. If we interpret β simply in terms of tunneling through a square potential barrier, and use the standard quantum mechanical tunneling formula

$$\beta = (4\pi/h) (2mV_0)^{1/2} \quad (1.3)$$

to estimate the barrier height, for values of β between 11 and 15 nm^{-1} we find barrier heights of between 1.1 and 2.1 eV respectively.

We must consider additional factors when dealing with macromolecular biological redox couples. Firstly the protein molecules are not spherically symmetric so that the $(r-r_0)$ in equation 1.2 must be replaced by the actual separation. Secondly the protein around the redox site is inhomogeneous, so that certain paths for electron transfer may be energetically favoured.

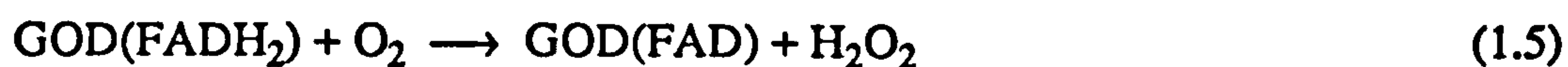
Even though these complicating factors exist, it is apparent that as the electron transfer distance increases the probability of electron transfer decreases. This observation has profound effects on the electrochemical study of any large biological redox species.

1.3 THE CHARACTERISTICS OF REDOX ENZYMES

The redox enzymes contain a number of types of redox active group. The two largest groups of redox enzymes are the nicotinamide coenzyme dependent dehydrogenases, which are not included in this work, and the flavin containing

oxidoreductases. The latter group comprises over 80 enzymes containing either FAD (flavin adenine dinucleotide) or FMN (flavin mononucleotide) at the active centre or centres⁽¹⁸⁾. Of these the majority are FAD containing flavoenzymes. The flavin group is strongly associated with the protein structure⁽¹⁹⁾ with dissociation constants in the range 10^{-8} to 10^{-11} mol dm⁻³. In certain cases, such as that of succinate dehydrogenase (E.C. 1.3.99.1), the isoalloxazine ring of FAD is covalently linked to an amino acid residue in the protein structure⁽²⁰⁾. During the catalytic redox cycle of flavoenzymes, the flavin centres remain firmly associated with the enzyme protein.

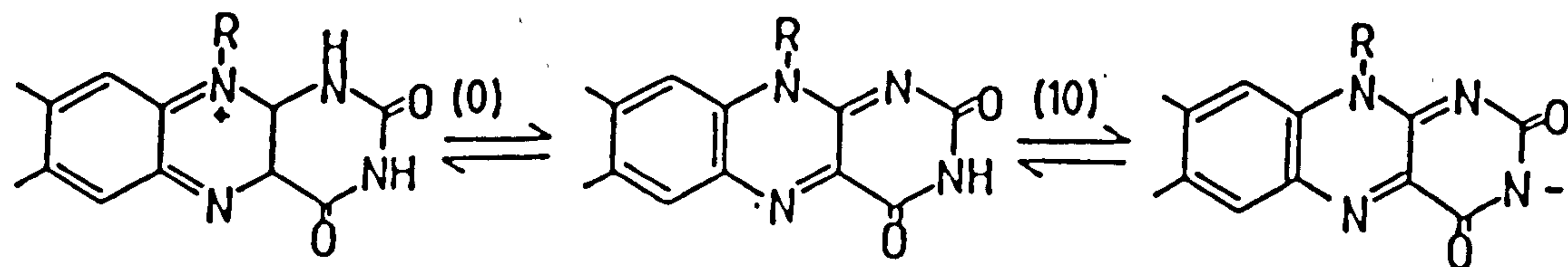
The structure of the flavins along with their redox reactions are shown in figure 1.2. The structure and redox reactions of the flavin isoalloxazine ring systems is described in detail by Hemmerich *et al* and Janik and Elving^(21,22). The classification of the flavoenzymes, with respect to their metal requirements, if any, and their redox properties will be described below. The classification scheme, showing the way in which glucose oxidase (E.C. 1.1.3.4), the main enzyme of interest in this work, fits into the flavoenzyme group, is shown in figure 1.3. The flavoenzymes are classified as either oxidases or dehydrogenases. The distinction is made on the basis of their reactivity towards molecular oxygen when the flavin redox centres of the enzyme are in a reduced state. Flavo-oxidases are readily reoxidised by molecular oxygen, which accepts two protons and two electrons from the reduced flavin centre to produce hydrogen peroxide as the reaction byproduct⁽²³⁾. This type of reaction is illustrated by the action of glucose oxidase (GOD) on its substrate β -D-glucose in the presence of molecular oxygen.



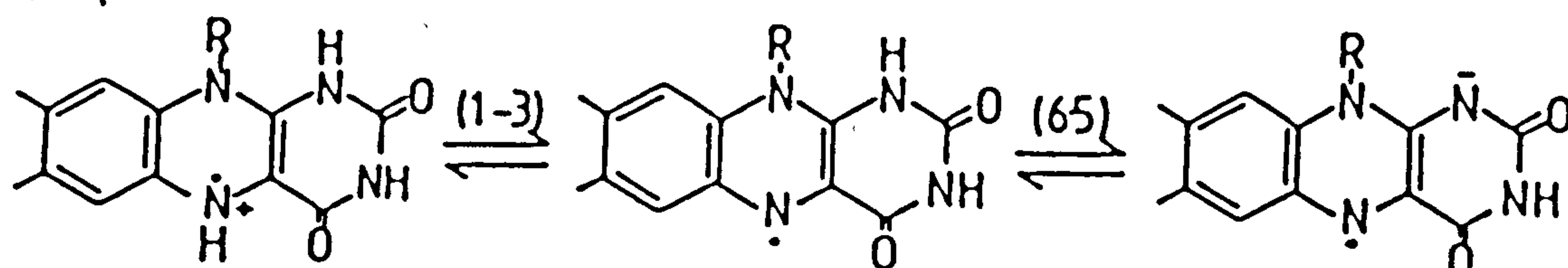
Reactions (1.4) and (1.5) are of a type catalysed by flavo-oxidases in general. The

Figure 1.2 The structure and redox reactions of the flavins

Quinone state (FAD or FMN)



Semiquinone state



Hydroquinone state (FADH₂ or FMNH₂)

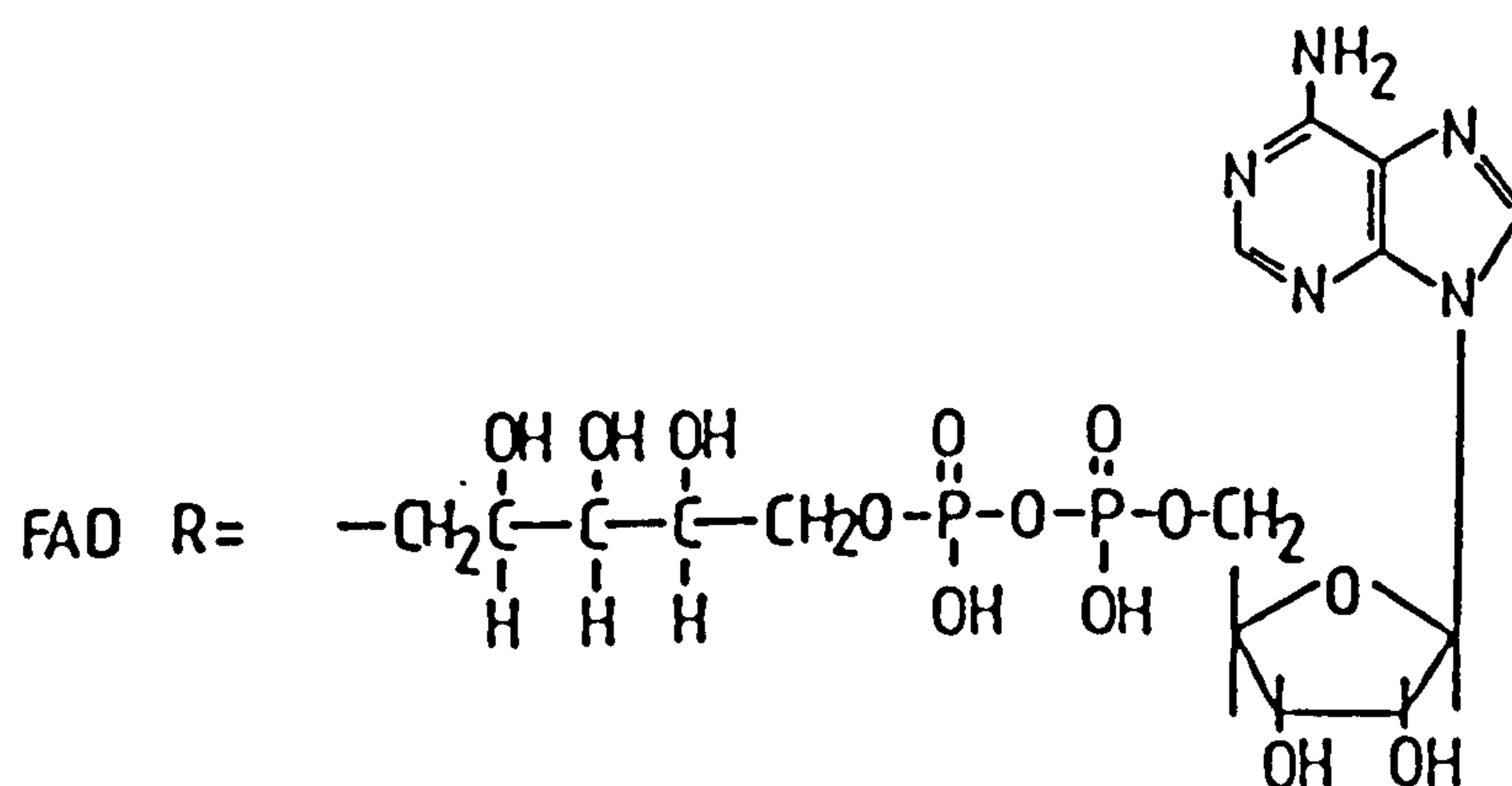
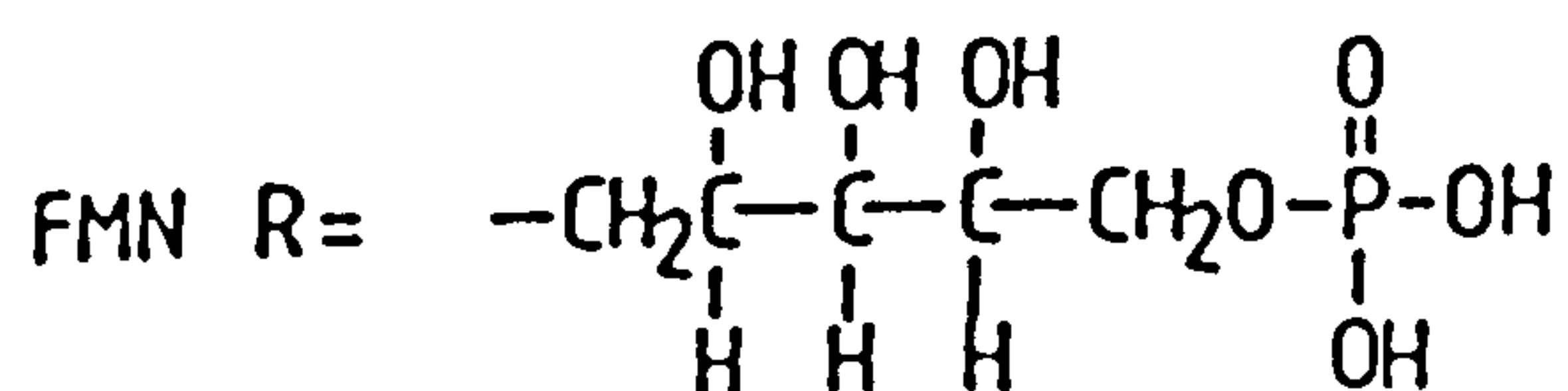
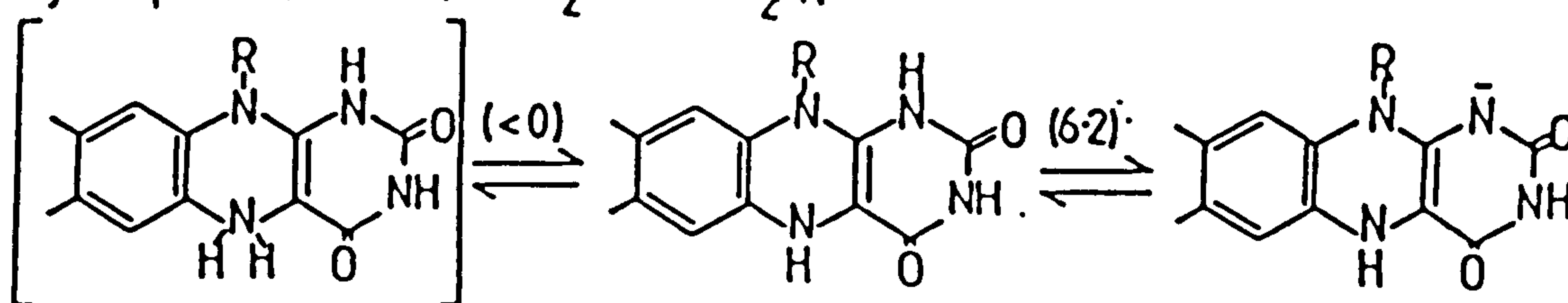
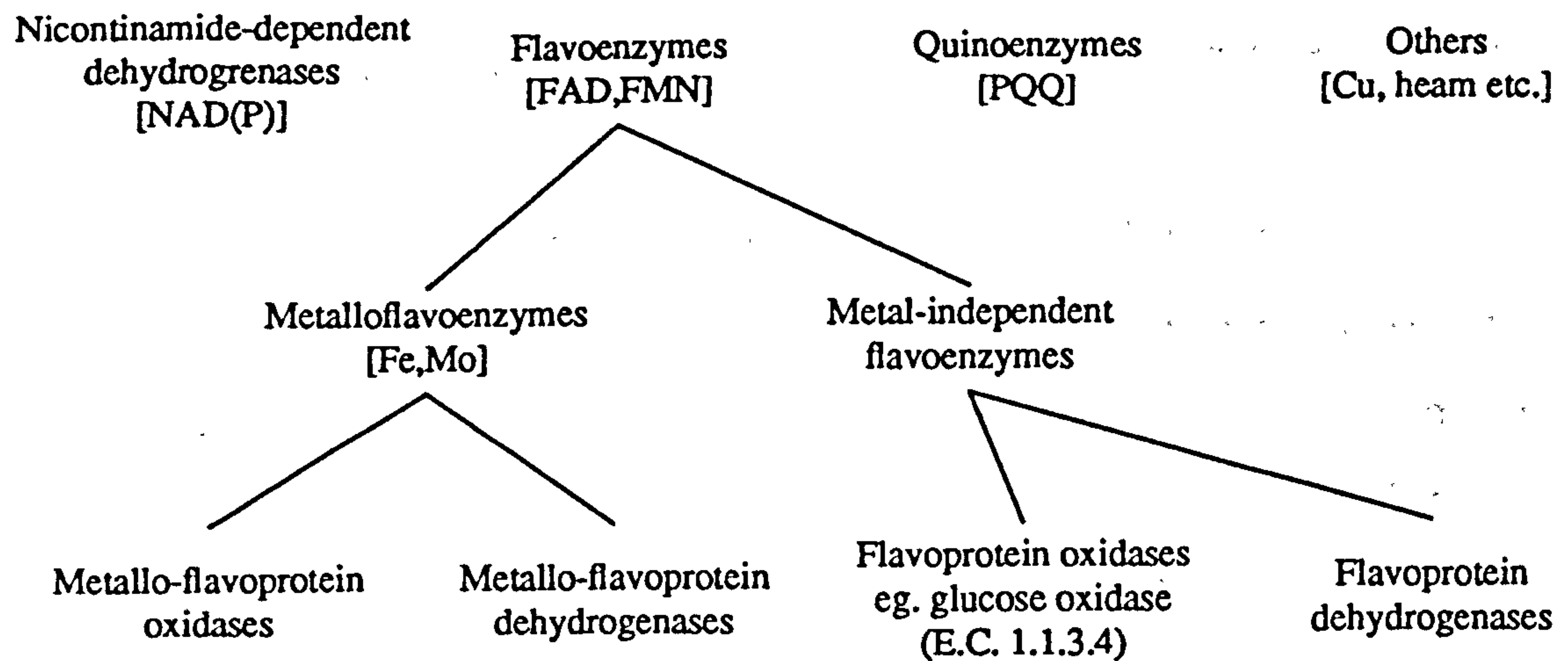


Figure 1.3 Scheme for the Classification of Flavoenzymes



PQQ is pyrrolo-quinoline quinone

[2,7,9-tricarboxy-1H-pyrrolo- (2,3-f-quinoline-4,5-dione)]

production of hydrogen peroxide in this way has implications for the electrochemical monitoring of flavo-oxidase activity. These will be discussed in detail in section 1.4.

The flavo-dehydrogenases, on the other hand, show little tendency to become reoxidised by molecular oxygen⁽²⁴⁾ and utilise alternative organic electron acceptors. These enzymes do not produce hydrogen peroxide.

A further classification is made on the basis of whether the flavoenzyme in question requires the presence of metal ions within the enzyme protein to exert redox activity. Flavoenzymes which have a specific metal requirement (commonly for molybdenum or iron) are defined as metalloflavoenzymes. It is known that xanthine oxidase⁽²⁶⁾ (E.C. 1.2.3.2) is an example of a metalloflavoenzyme, although the exact role of the metal is still unclear⁽²⁷⁾. A further group of flavoenzymes, such as D-aminoacid oxidase (E.C. 1.4.3.3) appear to have no metal cofactor requirement⁽²⁸⁾. Examples of a number of flavoenzymes and their classification are shown in Table 1.2. It is apparent that these enzymes have high molecular weights, typically greater than 1×10^5 D. The position of the redox active flavin prosthetic groups within these enzymes is largely ill defined.

The location of the flavin prosthetic groups within the enzyme protein has profound effects on any attempt to study the direct electrochemistry of flavoenzymes at simple metal electrodes. In the following section the apparently direct electron transfer observed by a number of authors when studying adsorbed or covalently immobilised flavoenzymes will be discussed. Following this a number of methods used to study the indirect, or mediated, electron transfer from flavoenzymes are described, and the advantages of using these indirect methods are outlined.

Table 1.2
Classification of Flavin-Containing Redox Enzymes

Enzyme	Molecular wt (Daltons)	Prosthetic Group		
		Flavin	Metal	Other
Flavoprotein oxidases				
Glycolate oxidase (plants) E.C. 1.2.3.5	100 000	FMN	—	—
Glucose oxidase (molds) E.C. 1.1.3.4	160 000	2 FAD	2 Fe	?
D-aminoacid oxidase (kidney) E.C. 1.4.3.3	138 000	2 FMN	—	—
L-aminoacid oxidase (liver) E.C. 1.4.3.2	100 000	2? FAD	—	—
Flavoprotein dehydrogenases				
NADPH-cytochrome c reductase (yeast) E.C. 1.6.2.4	78 000	FMN	—	—
Lipoyl dehydrogenase (respiratory particles)	100 000	2 FAD	—	-S-S-
Metalloflavoprotein oxidases				
Xanthine oxidase (milk) E.C. 1.2.3.2	300 000	2 FAD	8 Fe, 2 Mo	(a)
Metalloflavoprotein dehydrogenases				
L-lactate dehydrogenase (yeast) E.C. 1.1.2.3	200 000	2 FMN	heme Fe	—
Succinate dehydrogenase (beef heart) E.C. 1.3.99.1	300 000	FAD (b)	8 Fe	(a)
Choline dehydrogenase (liver) E.C. 1.1.99.1	800 000	FAD	4 Fe	(a)

(a) protein contains acid labile sulphur

(b) FAD is bound covalently to the protein

1.4 THE ELECTROCHEMISTRY OF FLAVOENZYMES

In order to successfully study the electron transfer reaction occurring between the prosthetic groups of flavoenzymes and simple metallic electrodes, it is important to once more consider the effect of distance on the rate of electron transfer (section 1.2). Assuming that the electron transfer in question is thermodynamically favourable, it is likely that the major obstacle for the transfer is the relatively large size of the protein coat surrounding the redox centre of interest at the enzyme's active centre. The presence of this outer protein sphere, although vital for the biological role of an enzyme, represents a shortcoming in any attempt to observe direct electron transfer. Even when the enzyme is adsorbed onto or is directly adjacent to the electrode, the enzyme protein ensures that the redox active centre is spatially distant from the electrode material.

To illustrate this effect it is informative to consider an example. Glucose oxidase (E.C. 1.1.3.4) from *A.niger*⁽²⁵⁾ has received considerable attention from electrochemists. This enzyme has a molecular weight in the region of 160 000 Daltons⁽²⁹⁾. It consists of two identical subunits, each containing one FAD centre, and has a hydrodynamic radius of 4.3 nm⁽²⁹⁾. The exact structure of this enzyme is not, at present, known, as X-ray crystallographers have yet to solve the crystal structure of this very large molecule. This lack of knowledge means that it is not possible to know the exact position of the FAD centres within the molecule. Consequently it is difficult to estimate the electron transfer distances that would be involved if direct electron transfer was to occur. Certain evidence is, however, available concerning the the location of the active centres in this and other flavoenzymes. In glucose oxidase the FAD centres are located at an undefined distance beneath the glycoprotein coat of the enzyme and are known to be partly inaccessible to solvent⁽³⁰⁾. This indicates that the flavin centres are not simply exposed at the enzyme's periphery.

It is interesting to consider a further example of a less commonly studied flavoenzyme for which the structure has been solved by X-ray crystallography. Glutathione reductase (E.C. 1.6.4.2) has a flavin bound in an extended conformation with the adenine group at the enzyme surface and the flavin buried in the protein's centre⁽³¹⁾. Consequently this enzyme shows no observable direct electrochemistry at a pyrolytic graphite electrode⁽³²⁾.

A number of authors have described the apparent direct electrochemistry of flavoenzymes at a number of electrode materials. Examples from the literature are discussed in the next section and conclusions are drawn about the viability of studying this type of direct electrochemistry.

1.4.1 Unmediated Electrochemistry

Much of the earlier work in this area made use of mercury electrodes. This is a material which is now thought to be largely incompatible with biological proteins.

It is known that a number of proteins become irreversibly adsorbed onto mercury surfaces⁽³³⁻³⁶⁾. This phenomenon is known to occur during studies of flavoenzymes at mercury electrodes^(37,38). This means that any direct electron transfer observed is due to the presence of an enzyme which is intimately associated with the mercury electrode surface and is not simply a heterogeneous solution process. When a flavoenzyme becomes adsorbed onto mercury it becomes 'flattened' due to the formation of Hg-disulphide bonds⁽³⁹⁾.

A distortion in the protein structure results, which may cause loss of enzyme-bound FAD. It is likely that it is the presence of these small amounts of soluble flavin which gives rise to the apparent direct response. It is therefore disadvantageous to use mercury electrodes in conjunction with flavoenzymes. Furthermore, a number of authors have concluded that direct electron transfer in this type of system is not possible^(40,41).

In a study of the 'direct' electrochemistry of glucose oxidase at platinum

electrodes the authors conclude that it is not possible to distinguish between electron transfer from free FAD and that from enzyme bound FAD⁽⁴²⁾. They hypothesize that the apparent direct electron transfer is due to traces of free flavin able to diffuse within the solution.

In an attempt to alleviate problems associated with the denaturation of flavoenzymes at simple metal electrodes a number of authors have immobilised flavoenzymes onto carbon electrodes using covalent coupling and crosslinking techniques. The idea here is to secure the enzyme in a rigid conformation and thus prevent protein flattening. The results from such experiments appear to be unpredictable and, as might be expected, are sensitive to the immobilisation technique employed.

When L-amino-acid oxidase⁽⁴³⁾, xanthine oxidase⁽⁴³⁾ or glucose oxidase⁽⁴⁴⁾ were immobilised onto cyanuric chloride modified graphite electrodes, an apparent direct electron transfer was observed. However, when glucose oxidase was chemically grafted onto glassy carbon electrodes using carbodiimide coupling no direct response was seen and the authors demonstrated enzyme activity by detecting hydrogen peroxide in the presence of glucose⁽⁴⁵⁾. Furthermore, when glucose oxidase was immobilised onto a carbon paste electrode using glutaraldehyde-albumin crosslinking no direct response was reported⁽⁴⁶⁾.

It is apparent that the occurrence of direct electron transfer is intimately dependent on the nature of the covalent immobilisation procedure. Also it is likely that, as in the case of adsorbed flavoenzymes, the response is due to the release of small amounts of free flavin during or after the coupling procedure. It is difficult to differentiate with any certainty between an electrochemical response due to electron transfer from enzyme bound flavin and that from free flavin.

In conclusion it can be seen that a more widely applicable and better understood method of effecting electron transfer between the flavin centres of redox enzymes and metallic electrodes is desirable. A number of indirect techniques have

been developed towards this goal. The use of a wide range of low molecular weight redox couples to 'mediate' electron transfer has resulted in considerable success in studying the widespread and persistent electrochemistry of flavoenzymes. These indirect techniques are discussed in the following section.

1.4.2 Mediated Electrochemistry

In the living cell the reduced flavin groups of the flavoenzymes become reoxidised by low molecular weight electron acceptors. In the case of the flavo-oxidases the electron acceptor is usually molecular oxygen⁽²³⁾. The small oxygen molecules are able to diffuse into the interior of the molecule and accept electrons from the FADH₂ centres. The hydrogen peroxide produced, equation (1.5), is able to diffuse back into the bulk solution to be removed by other enzyme systems.

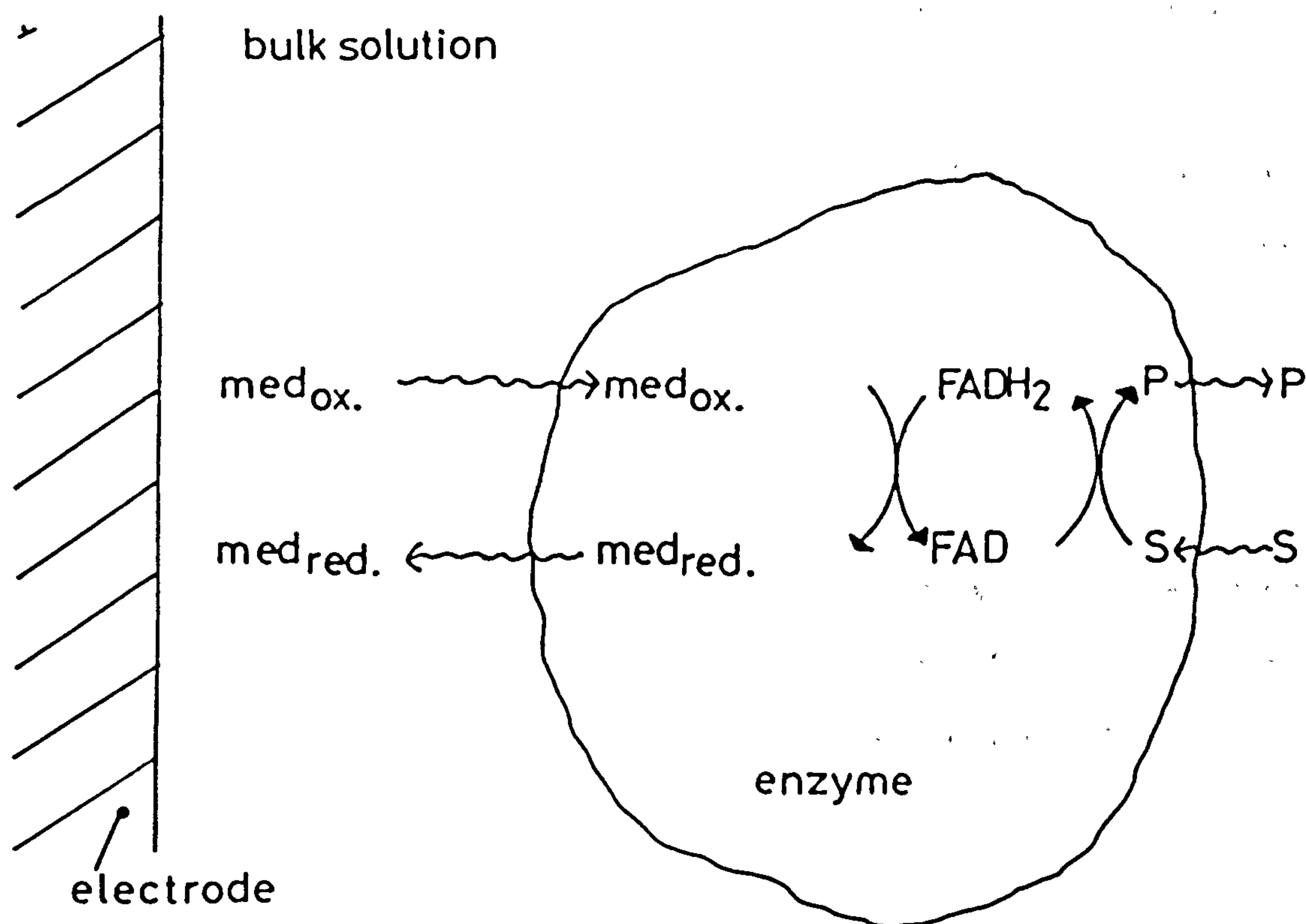
Many flavo-oxidase enzymes are able to utilise artificial electron acceptors, usually called mediators⁽²⁴⁾. It is possible to use mediators to shuttle charge between the flavin centres of an enzyme and an electrode. This mediated, or indirect electrochemistry has formed the basis of a great deal of recent research work in this area of electrochemistry. The mediator is regenerated at the electrode resulting in a cyclic process, figure 1.4.

To be effective, a mediator must compete with the enzymes natural substrate, often molecular oxygen. Many potential mediators do not fulfill this requirement and are of little use except in deoxygenated solution.

The criteria for an ideal redox mediator have been described by several authors^(47,48). Traditionally organic dyes, such as phenazine methosulphate, and methylene blue, and inorganic ions such as ferricyanide have been used. These do not, however, satisfy many of the requirements for an ideal redox mediator. A major problem is that these organic dyes and inorganic redox ions are not readily amenable to chemical substitution to tailor their individual redox potentials.

The majority of recent work has utilised ferrocene derivatives as redox

Figure 1.4 The homogeneous mediation of flavoenzyme electrochemistry



S is the substrate, P is the product (produced by oxidation of S) and $\text{med}_{\text{ox.}} / \text{med}_{\text{red.}}$

are the oxidised and reduced form of the soluble redox mediator. FAD/FADH_2

represents the oxidised and reduced forms of the flavin at the enzyme's active site.

mediators. These compounds exhibit reversible electrochemistry and fast enzyme kinetics with a number of flavoenzymes⁽³²⁾. They are also amenable to chemical substitution so that their redox potential can be tuned to match the required enzyme reaction. Also their net charge can be easily altered by chemical derivitisation. The charge on the mediator molecule appears to influence the rate of the enzyme reaction in certain cases⁽⁴⁹⁾. Ferrocene derivatives appear to be the mediators of choice for the indirect study of enzyme electrochemistry.

The enzyme/mediator reaction can occur in several ways with both of the species free in solution, or one or both of the species immobilised at an electrode surface. The simplest situation, in which both species are free in solution, will be described first.

1.4.2.1 Homogeneous Mediation

With both species free in solution the mediator shuttles electrons between the electrochemically inactive enzyme and the electrode (figure 1.4). The redox reaction of the flavin prosthetic group, FAD, is a two electron process. It is apparent, therefore, that when using a one-electron redox couple, such as ferrocenes, two molecules are required for each cycle.

The effectiveness of a particular mediator/enzyme combination has commonly been assessed by use of simple d.c. cyclic voltametry^(50,51), or amperometry⁽⁷⁹⁾. The results obtained are analysed using the theory developed for the EC' (catalytic) case. This enables the second order rate constant for the enzyme/mediator molecule reaction to be estimated⁽⁵²⁾. A number of flavoenzyme/mediator combinations have been studied in this way. Table 1.3 collects together results from the literature for this type of homogeneous mediation. It is apparent that a range of mediators including inorganic ions, quinones and ferrocenes have been employed to accept electrons from reduced flavoenzymes in solution.

It would be greatly advantageous if a mediator could be chosen for a particular

Table 1.3

Homogeneous Mediation of Flavoenzyme Electrochemistry

Enzyme	Mediator	Mediator redox potential / mV vs SCE, pH 7.0	$k_s \times 10^{-3} / \text{dm}^3 \text{mol}$	Comments	Refs.
Glucose oxidase (<i>A. Niger</i>) E.C.1.1.3.4	1,1'-dimethyl ferrocene	100	44	Rate constants measured by cyclic voltammetry at a graphite electrode. Effect of pH, temperature and oxygen investigated.	32,53-57
	ferrocene	165	15		
	vinyl ferrocene	250	18		
	ferrocene-COOH	275	110		
	1,1'-ferrocene di-COOH	395	15		
	(dimethylamino)-methyl ferrocene	400	525		
	trimethylamino-ferrocene	400	300	25°C, pH 7.0	54
	ferrocene-lidocaine conjugate	300		Use in immunoassays.	56,58
	[Ru(CN) ₆] ⁴⁻ [Ru(NH ₃) ₅ py] ²⁺	685 50	10 100	Comparison of Ru complexes to mediators such as ferrocenes and ferricyanide.	59
	[Fe(CN) ₆] ³⁻	180			66,67
Glucose oxidase (<i>P. Vitale</i>)	DCPIP	0		pH 6, fuel cell	68
	Fe(CN) ₆ ³⁻	119	0.32 28	25°C, pH 7.0 25°C, pH 4.0	85
	Co(phen) ₃ ³⁺	180	1.60 3.64	25°C, pH 7.0 25°C, pH 4.0	85
	Co(dipy) ₃ ³⁺	130	0.09 0.13	25°C, pH 7.0 25°C, pH 4.0	85
	TCNQ	120	1500	25°C, pH 7.0	85
	2 bromo-1,4-benzoquinone	70	590	25°C, pH 7.0	85
	tetrabromo-1,4-benzoquinone	50	263	25°C, pH 7.0	85
	1,4-benzoquinone	30	197	25°C, pH 7.0	85
	2-methyl-1,4-benzoquinone	-30	53	25°C, pH 7.0	85
	1,2-napthoquinone	-100	110	25°C, pH 7.0	85
	TCNQ (Li salt)	-130	34	25°C, pH 7.0	85
	PMS	-121	18	30°C, pH 7.0	85

Enzyme	Mediator	Mediator redox potential / mV vs SCE, pH 7.0	$k_s \times 10^{-3} / \text{dm}^3 \text{mol}$	Comments	Refs.
	2,3-dichloro-1,4-naphthoquinone	-161	4.9	25°C, pH 7.0	85
	2-methyl-5-methoxy-1,4-benzoquinone	-161	3.5	25°C, pH 7.0	85
	1,4-naphthoquinone	-197	3.5	25°C, pH 7.0	85
	9,10-phenanthrene-quinone	-220	3.9	25°C, pH 7.0	85
	pyocyanin	-280	7.6	30°C, pH 7.0	85
	1,2-naphthoquinone-4-sulphonate	-30	0.86	25°C, pH 7.0	85
CO-acceptor-oxido-reductase (<i>P.Thermocarboxydovorous C2</i>)	ferrocene-COOH 1,1'-dimethylferrocene methylene blue PES TMPD [Fe(CN) ₆] ³⁻ thionine	275 100 -230 -170 -10 180 -181	40	Mediators used in a variety of fuel cell and enzyme electrode configurations	60,61
Cholesterol oxidase (<i>S.Commune</i>) E.C.1.1.3.6	hydroxymethyl-ferrocene	190	6	The only cholesterol oxidase which has been shown to use ferricinium ion as electron acceptor.	63
Sacrosine oxidase (<i>Arthrobacter</i>) E.C.1.5.3.1	ferrocene-COOH [Fe(CN) ₆] ⁴⁻ [W(CN) ₈] ⁴⁻ Ni(II)cyclam [Mo(CN) ₈] ⁴⁻ DCPIP hydroquinone	280 180 280 440 540 0 60	1 2.5 12 1.9 15 1.9 6.8	20-25°C, pH 7.0, edge plane pyrolytic graphite electrode.	32,65
Lactate oxidase (<i>Pedioccus</i>)	[Fe(CN) ₆] ⁴⁻ [W(CN) ₈] ⁴⁻ ferrocene-COOH Ni(II)cyclam [Mo(CN) ₈] ⁴⁻ DCPIP hydroquinone	180 280 280 440 540 0 60	3.8 63 19 2 38 12 55	20-25°C, pH 7.0, edge plane pyrolytic graphite electrode.	65
Glycolate oxidase (<i>S.Oleracea</i>) E.C.1.1.3.1	ferrocene-COOH 1,1'-dimethylferrocene	275 100	115	25°C, pH 8.3	64
L-amino acid oxidase (<i>C.adamenteus</i>)	ferrocene-COOH 1,1'-dimethylferrocene	275 100	40	37°C, pH 7.8	64

Enzyme	Mediator	Mediator redox potential / mV vs SCE, pH 7.0	$k_s \times 10^{-3} / \text{dm}^3 \text{mol}$	Comments	Refs.
E.C.1.4.3.2 Pyruvate oxidase E.C.1.2.2.3	ferrocene-COOH	275	20	20°C, pH 7.0	32
Xanthine oxidase (bovine) E.C.1.2.3.2	ferrocene-COOH	275	400	20°C, pH 7.0	32
Liopamide dehydrogenase E.C.1.6.4.3	ferrocene-COOH	275	20	20°C, pH 7.0	32
Glutathione reductase E.C.1.2.2.3	ferrocene-COOH	275	200	20°C, pH 7.0	32
Lactate dehydrogenase (cyt.b ₂) (yeast) E.C.1.1.2.3	ferrocene-COOH	275	6700	20°C, pH 7.0	32,62
	[Fe(CN) ₆] ³⁻	180		Membrane electrode 25°C, pH 7.0	69
Diaphorase (<i>C.Kluyeri</i>) E.C.1.6.99.2	hydroxymethyl ferrocene	190	880	Use in an NAD ⁺ independent cholesterol assay system.	63
	2(amino ethyl)- ferrocene HCl	160	650		
	ferroceneboronic acid	210	250		

DCPIP is 2,6-dichlorophenolindophenol

phen is 1,10-phenanthroline

dipy is 2,2'-bipyridine

TCNQ is tetracyano-p-quinodimethane

PMS is phenazine methosulphate

PES is phenazine ethosulphate

TMPD is 1,1,1',1'-tetramethylphenylenediamine

enzyme system with a knowledge of redox potentials and enzyme/mediator overall charges. It is therefore informative to consider a well studied example and to see if any apparent trends occur. Glucose oxidase is known to utilise a number of artificial electron acceptors. These include organic dyes such as phenazine methosulphate (PMS), 2,6-dichlorophenolindophenol (DCPIP) and N,N,N',N'-tetramethyl-4-phenylenediamine^(68,70). Also inorganic species, such as hexacyanoferrate^(66,67,85), hexacyanoruthenate⁽⁵⁹⁾ and pentaamine pyridine ruthenium⁽⁵⁹⁾ act as electron acceptor for soluble GOD. However, due to the instability and pH sensitivity of the organic dyes and quinones and the fact that chemical modification of the simple inorganic ions is not feasible the effectiveness of a large range of ferrocene derivatives as mediators for GOD was investigated⁽⁵³⁻⁵⁸⁾.

The derivatives investigated have varying charge and water solubility and redox potentials ranging from 100 to 400 mV (vs SCE)⁽⁵³⁾. There does not appear, however, to be any direct correlation between the redox potential of the ferrocene mediator and the second order rate constant for the enzyme/mediator reaction. This implies that it is not the electron transfer which is rate limiting in this system. Another possibility is that there is a significant shift in the redox potential of the mediator when in the interior of the enzyme. The exact mechanism of enzyme/mediator interaction must remain the topic of some speculation.

Certain valid assumptions about the enzyme bound FAD/mediator electron transfer can be made. It is known that the FAD centres of GOD cycle between the fully reduced (FADH_2) and fully oxidised (FAD) states with no semiquinone (FADH^\bullet) intermediate occurring when molecular oxygen is the electron acceptor⁽⁷¹⁾. When the ferricinium ion acts as electron acceptor only single electron transfer is possible due to the ferrocene molecule being a one electron (zero proton) acceptor. This must imply that the semiquinone form of FAD is involved since a simultaneous electron transfer involving enzyme bound FADH_2 and two ferricinium ions is highly unfavourable. It seems likely, therefore, that the use of this type of artificial electron

acceptor results in a mechanism different from that observed with the natural acceptor, oxygen.

Until a better understanding of the mechanism of enzyme/mediator electron transfer is obtained, the choice of suitable mediators for a particular enzyme will remain largely arbitrary.

In the next section systems in which one of the components, flavoenzyme or mediator, is immobilised at the electrode surface will be described. This type of system has a direct relationship to certain aspects of the work presented in the experimental chapters of this thesis.

1.4.2.2 Heterogeneous mediation

A large number of systems have been described in which a flavoenzyme or its mediator is immobilised at an electrode surface. The majority of this work focuses on the use of an immobilised flavoenzyme/soluble (or localised) mediator combination. This type of system will be discussed first.

An early report⁽⁷²⁾ describes the heterogeneous electron transfer between glucose oxidase (GOD) and the hydroquinone/benzoquinone couple. Here the enzyme is entrapped in a gelled layer using a simple procedure. In systems of this type the mediator is free to shuttle electrons between the active centre of the immobilised enzyme and the electrode surface. This removes the prohibitive effects of distance and electrode fouling due to protein denaturation encountered during attempts to demonstrate unmediated electron transfer from immobilised flavoenzymes^(40,41).

Further examples of such heterogeneous systems have used GOD in conjunction with ferrocene⁽⁷³⁾, phenazine methosulphate⁽⁷⁴⁾ and benzoquinone and xanthine oxidase in conjunction with ferricyanide⁽⁷⁵⁾.

A more recent development involves the use of covalently immobilised glucose oxidase (GOD)⁽⁴⁵⁾ in conjunction with a mediator localised within the

immobilisation matrix. In this system the mediator, 1,1'-dimethylferrocene or tetrathiofulvalene⁽⁴⁸⁾, is applied to the immobilised enzyme matrix in an organic solvent. The solvent is allowed to evaporate leaving the water insoluble mediator confined to the electrode surface. The oxidised form of the mediator is, however, water soluble to some degree and free to shuttle charge. Hence the mediator is not strictly immobilised, and can be lost from the modified electrode surface.

An extension of this work has been described by Iwakura *et al*⁽⁷⁹⁾. The authors use an electrochemical deposition method (section 1.6) to immobilise both GOD and a ferrocene monocarboxylic acid mediator in a conducting polymer film. The mediator becomes localised within the organic enzyme immobilisation matrix and is able to carry charge between the immobilised enzyme and the electrode surface.

It is apparent that a variety of electrode configurations are possible in which the enzyme is immobilised, either covalently or by physical entrapment, at an electrode surface and the mediator is free to diffuse. There are far fewer reports, however, of successful systems in which the mediating species alone is immobilised at the electrode surface and the flavoenzyme is free in solution. This is not surprising given the nature of such systems. The mediating species, whilst immobilised at the electrode surface, must still be able to access the enzyme's active site.

Three approaches to this problem will be discussed briefly in this section. One postulated approach is to covalently link the flavin group to an electrode surface via an electron conducting support⁽⁸⁰⁾, and to then add the apo-enzyme in the hope that it can somehow recombine with the immobilised flavin prosthetic group. This approach comes some way between an immobilised enzyme, and an immobilised mediator. Predictably, no evidence to support the viability of this approach has been reported. Presumably the immobilised flavin cannot gain access to the active site of the apo-enzymes, such as GOD.

A second approach is to modify the electrode with a polymeric species having mediatory groups as pendant arms, in the hope that they can in some way gain access to the flavin prosthetic group of a flavoenzyme in solution. Cenas *et al* have studied this approach⁽⁸¹⁾ using p-quinone polymers deposited onto glassy carbon electrodes and soluble GOD. The authors conclude that the small currents observed are due to electron transfer through the polymer matrix being rate limiting and not the electron transfer between GOD and the p-quinone groups. This is surprising considering the large size of the enzyme and inaccessibility of the active sites. The authors further conclude that if soluble xanthine oxidase is used then the enzyme-mediator reaction becomes rate limiting.

The small catalytic currents observed at a potential close to the E^0 of the mediating group could in theory be due to the presence of a low concentration of a quinone redox couple in solution. This may be difficult to avoid during the preparation of this type of modified electrode. A further effect mentioned by the authors is that due to 'hard mediator fixation' onto the modifying polymer it is unlikely that the quinone centres can penetrate deep into the large globular enzymes employed. This would again account for the small current increases observed in the presence of substrate.

The final approach to be discussed here is one in which a low molecular weight mediator, such as tetracyano-quinodimethane (TCNQ) is applied to an electrode⁽⁸²⁾. In the presence of soluble GOD and its substrate a mediated response is noted. It seems likely that in this case the mediator is free to leave the electrode and diffuse between the enzyme's active sites and the electrode material.

Considering these three approaches it is apparent that there is little real evidence to suggest that a strictly immobilised mediator is able to gain access to the prosthetic groups of redox enzymes such as GOD. This type of behaviour is predicted from an understanding of the effect of inter-centre distances on the rate of electron transfer.

In the final part of this section literature describing systems in which both flavoenzyme and mediator are immobilised at an electrode surface is discussed. Few reports of this type exist.

1.4.2.3 Systems with both flavoenzyme and mediator immobilised

In systems where both reactants are immobilised it is difficult to understand how rapid electron transfer between the redox centres can occur. However electron transfer between covalently immobilised GOD and strongly adsorbed N-methylphenazinium ion or polyvinylferrocenes⁽⁸⁴⁾ has been reported. In the former case it is likely that a small amount of the mediator is lost from the electrode to diffuse between the GOD and the electrode material. In the case of polyvinylferrocenes, however, it is far more difficult to understand how this type of immobilised high molecular weight mediator can accept electrons from immobilised GOD. Indeed, it has been reported that polyvinylferrocene does not act as a mediator for soluble GOD⁽⁷³⁾. It seems likely that the mediated responses reported by Turner *et al*⁽⁸⁴⁾ are due to the presence of a small quantity of diffusible ferrocene derivatives, or possibly the presence of some free flavin species.

In this section the use of soluble electron acceptors/donors to mediate the electron transfer between the inaccessible active site of high molecular weight flavoenzymes and electrode surfaces has been described. This technique overcomes the many problems encountered in studies of the direct electrochemistry of flavoenzymes. Configurations where the enzyme is immobilised and the mediator is free to diffuse are also successful but immobilisation of both reactants results in a large distance being present between the redox centres and a less successful approach.

In the following sections the immobilisation technique used in the work presented in this thesis is discussed. A detailed review of previous work on the use of an electrodeposition technique to immobilise flavoenzymes is given in chapter 4.

1.5 THE ELECTRODEPOSITION OF ORGANIC POLYMERS

The aim of this section is to describe the type of organic polymers which have been produced by electrochemical methods. A comprehensive survey of the extensive literature devoted to conducting polymers is not included here as this topic has been reviewed by several authors⁽⁸⁶⁻⁸⁹⁾.

A wide range of organic polymers, both conducting and insulating, can be electrochemically deposited onto electrode surfaces. Many of these are potential candidates for the electrochemical immobilisation of redox enzymes described in the next section.

The electrodeposition of polypyrroles^(87,90-95), polythiophenes⁽⁹⁶⁻¹⁰²⁾, polyfurans⁽¹⁰³⁾, polyindoles^(103,104), polyanilines⁽¹⁰⁵⁻¹⁰⁷⁾, polyfluorenes⁽¹⁰⁸⁾, polypyridines⁽¹⁰⁹⁾, polyphenylenes^(110,111) and polyphenols^(112,113) has been reported. These polymers are produced by the electro-oxidation of the appropriate monomer in an electrolyte solution, with the notable exception of polypyridines which are deposited cathodically.

Apart from this wide range of parent polymers there has been much recent interest in the production of organic polymers which are modified with a variety of electroactive and catalytic groups (chapter 4). Furthermore a number of copolymers have been produced by electrodeposition from monomer mixtures. This brief discussion demonstrates the large number of polymers which can be produced electrochemically. This provides a wide choice of possibilities for any electrochemical enzyme immobilisation scheme.

The electrochemical immobilisation of redox enzymes in organic polymers provides a number of advantages over previous immobilisation techniques⁽¹⁶⁸⁾. Firstly, the growth of organic polymers can be performed quickly and reproducibly enabling a single step immobilisation procedure to be used. A further important advantage is that the electrodeposition of polymers can be controlled accurately

allowing the spatial distribution, thickness and porosity of the immobilisation matrix to be varied. Finally, due to the wide range of candidates available it is possible to choose a polymer with the required redox and stability properties when attempting to produce an immobilised enzyme device.

The work presented in this thesis is concerned with the development of successful enzyme immobilisation technology using both conducting and insulating organic polymers. No effort was exerted to determine the mechanism of the electrodeposition process. Much time was devoted instead to understanding the operation of model immobilised enzyme systems.

At the onset of this work there were few reports of successful strategies for electrochemical immobilisation of redox enzymes. However during the course of the experiments described in this thesis a number of reports concerning the electrochemical immobilisation of the enzyme glucose oxidase in a variety of organic polymers have appeared. The literature dealing with this novel immobilisation method will be fully reviewed in chapter 4 of this thesis.

1.6 THE ELECTROCHEMICAL IMMOBILISATION OF FLAVOENZYMES

There are few reports of the electrochemical immobilisation of redox enzymes in organic polymers^(74,114-118). The work reported invariably uses glucose oxidase (GOD) and the authors concentrate on the detection of hydrogen peroxide or oxygen, the enzyme's natural electron acceptor, to monitor the enzyme reaction. Alternatively, artificial mediators are used to accept electrons from the immobilised GOD⁽⁷⁴⁾.

It would be advantageous if a self contained system could be developed in which a mediator is included in the organic polymer film and is unable to diffuse into the surrounding bulk solution. This is necessary since there is no evidence to suggest that GOD can transfer electrons directly to the surrounding polymer.

The covalent immobilisation of the mediating species is not a widely successful strategy (section 1.4.2.2) as this approach results in the redox centres of the enzyme and mediator being spatially distant. A more realistic approach is to localise the mediating species within the enzyme containing polymer. Here the mediator is free to carry electrons from the enzyme but not to diffuse into the bulk solution. The design of this type of system might make use of a negatively charged mediator and a positively charged conducting polymer resulting in the electrostatic localisation of mediator within the film. A recent report⁽⁷⁹⁾ demonstrates that co-immobilisation of GOD and a mediator within a polypyrrole film results in a viable device. However due to the charge on the ferrocene derivative used being 0/+1 it is difficult to see how the mediator is retained within an oxidised polypyrrole film of positive charge for extended periods of time. The authors do not comment on the stability of this system.

A second promising approach to this problem is to covalently attach the electron transferring groups throughout the enzyme molecule. It should then be possible to electrochemically immobilise the redox modified enzyme within an organic polymer. It should be noted that this approach will only work if the redox centres are relatively close, within the protein, and the modified enzyme can transfer electrons rapidly to the surrounding polymer matrix.

Chapter 6 of this thesis describes work on the production of this type of redox modified enzyme. Although a successful electrochemical immobilisation strategy for this type of enzyme has not yet been developed the production of a working device seems possible given the correct choice of organic polymer matrix.

1.7 SUMMARY OF WORK PRESENTED IN THIS THESIS

In the following chapter of this thesis all experimental techniques used during the course of the work are described. This includes all electrochemical and

biochemical instrumentation and methods.

In chapter 3 a working theory is presented which is used in chapter 4 to explain the operation of immobilised glucose oxidase systems using oxygen as an electron acceptor. Results are presented in terms of the kinetic and transport parameters determined for this system using the theoretical treatment.

In chapter 5 an artificial mediator is employed to transfer electrons between the immobilised glucose oxidase and the conducting immobilised matrix. Again the response of this device is rationalised in terms of a specially developed kinetic model. A good understanding of the operation of such a system is gained.

In the final experimental chapter methods for the covalent modification of glucose oxidase with ferrocene derivatives is presented. Although a successful electrochemical immobilisation strategy has not yet been devised, evidence to suggest that this type of modified enzyme is able to exchange electrons directly with clean metal and polymer coated electrodes is described. This electron transfer is rapid and does not appear to be accompanied by electrode fouling or significant enzyme denaturation.

Finally in chapter 7 the implications of this work are discussed in terms of gaining a fuller understanding of the kinetics of the electrochemically immobilised enzyme reaction. The wide variety of work which could be undertaken as an extension to this thesis is outlined in the last part of chapter 7.

CHAPTER TWO

APPARATUS AND EXPERIMENTAL TECHNIQUES

All experimental techniques and apparatus used in this thesis are described below. This includes all aspects of the instrumentation and methods used for electrochemistry. Also, methods used to assay enzyme activity and to modify redox enzymes are detailed. In the final section of this chapter the technique of ellipsometry is included and the use of this method to measure the thickness of polymer films is described.

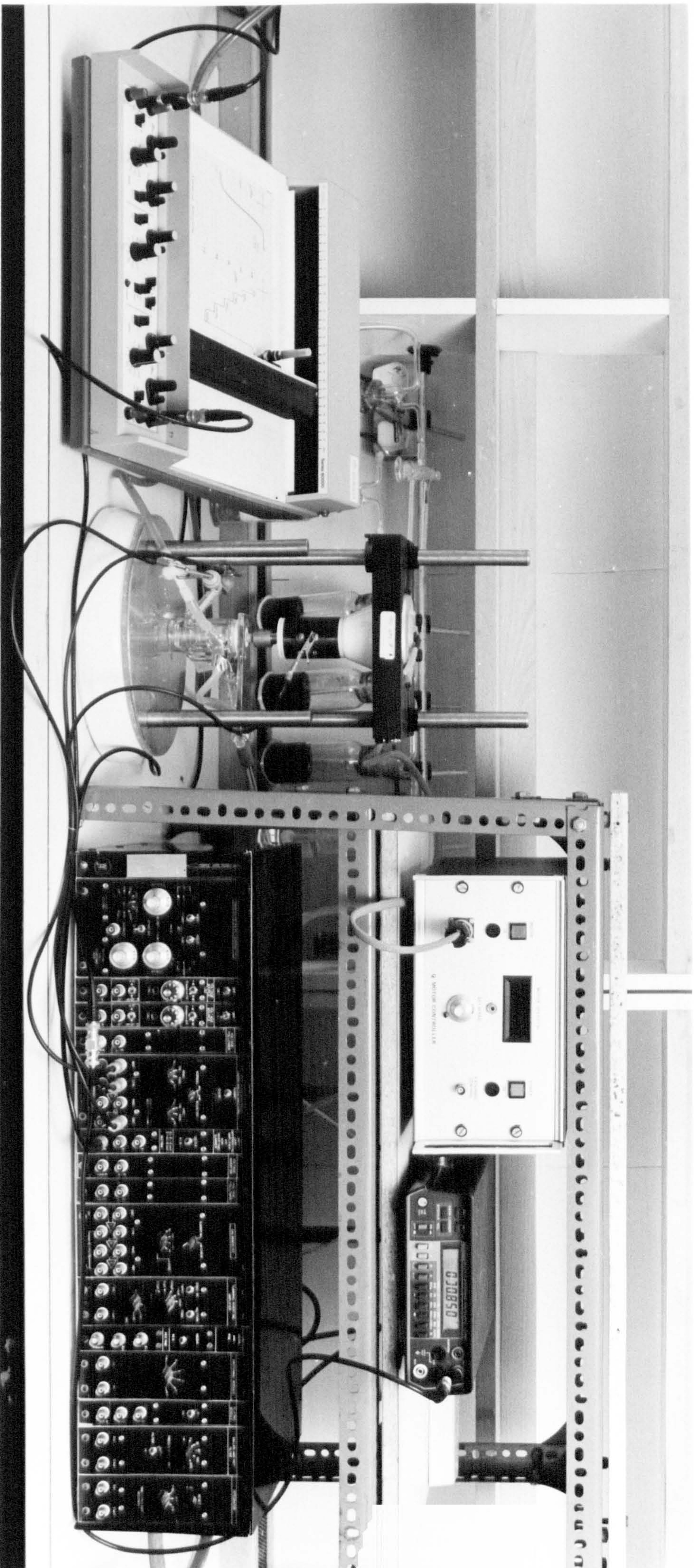
2.1 CONTROLLING ELECTRONICS

The controlling electronics used in the majority of the electrochemical work were of a home-made modular design. These non-commercial modules are described in this section. The use of such modular components enables the construction of a number of types of control circuits for use in the different types of electrochemical experiments.

2.1.1 Modular Instrumentation

The individual modular components are housed in a rack-type system, allowing their interconnection in any required configuration. Power is supplied to these modules via an independent d.c. source of ± 9 Volts. The rack system is housed in a home-made aluminium box in order to reduce the pickup of electrical noise. This rack system, in conjunction with the other components of the control and recording systems, is shown in plate 2.1. The following types of individual modules were used:

Plate 2.1



- Potentiostat
- Galvanostat
- Voltage sources (0 to 1 volt, and 0 to 5 volt)
- Voltage followers
- Triangular wave generator
- Unity gain differential amplifiers

The potentiostat used was of a four electrode type, allowing simultaneous control of ring and disc electrodes. The configuration of this potentiostat, in which the reference electrode is held at earth, is shown in figure 2.1.

When measuring nanoamp currents at a conventional macro-electrode (area greater than 0.10 cm^2) it is often necessary to employ a low pass Sallen and Key filter to smooth the signal. The circuit diagram for this type of filter is shown in figure 2.2.

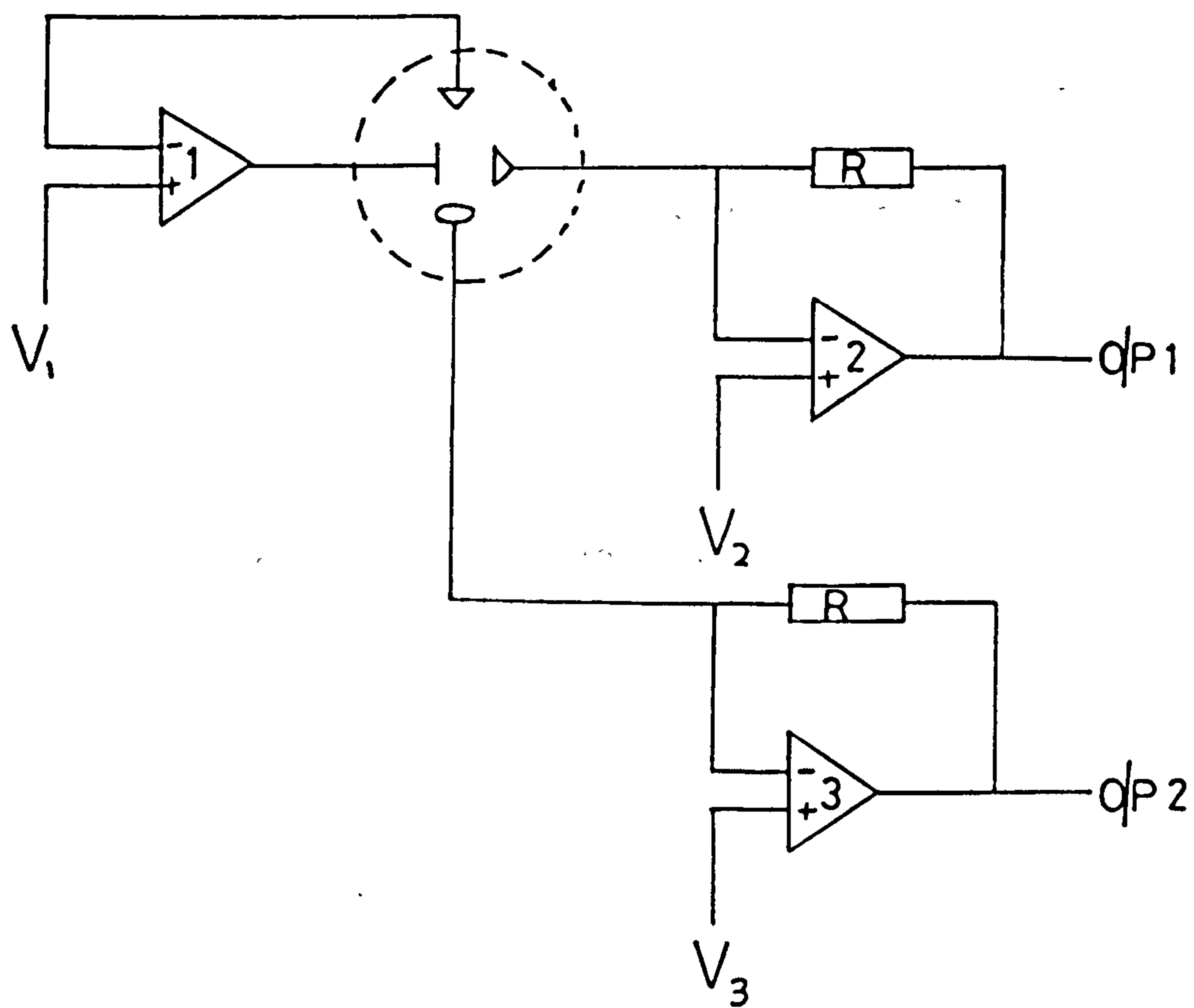
2.1.2 Ring-Disc Circuit

The use of modular electronics allows the construction of circuits to provide potentiostatic or galvanostatic control of the ring and disc electrodes. In most cases simple potential control of the disc electrode alone was required. In certain cases, however, the need to provide independent control of the ring and disc potentials was present. Using the four electrode potentiostat described above, the voltage of one electrode can be ramped whilst the other electrode is maintained at a constant potential. The output from the two electrodes was measured by employing independent differential amplifiers and chart recorders.

2.2 COMMERCIAL INSTRUMENTATION

Modular instrumentation was either home-made (section 2.1) or consisted of a rack system containing a potentiostat, triangular wave generator, and differential amplifier, supplied by Oxford Electrodes. Voltage outputs were recorded on an XY-t

Figure 2.1 The potentiostat configuration

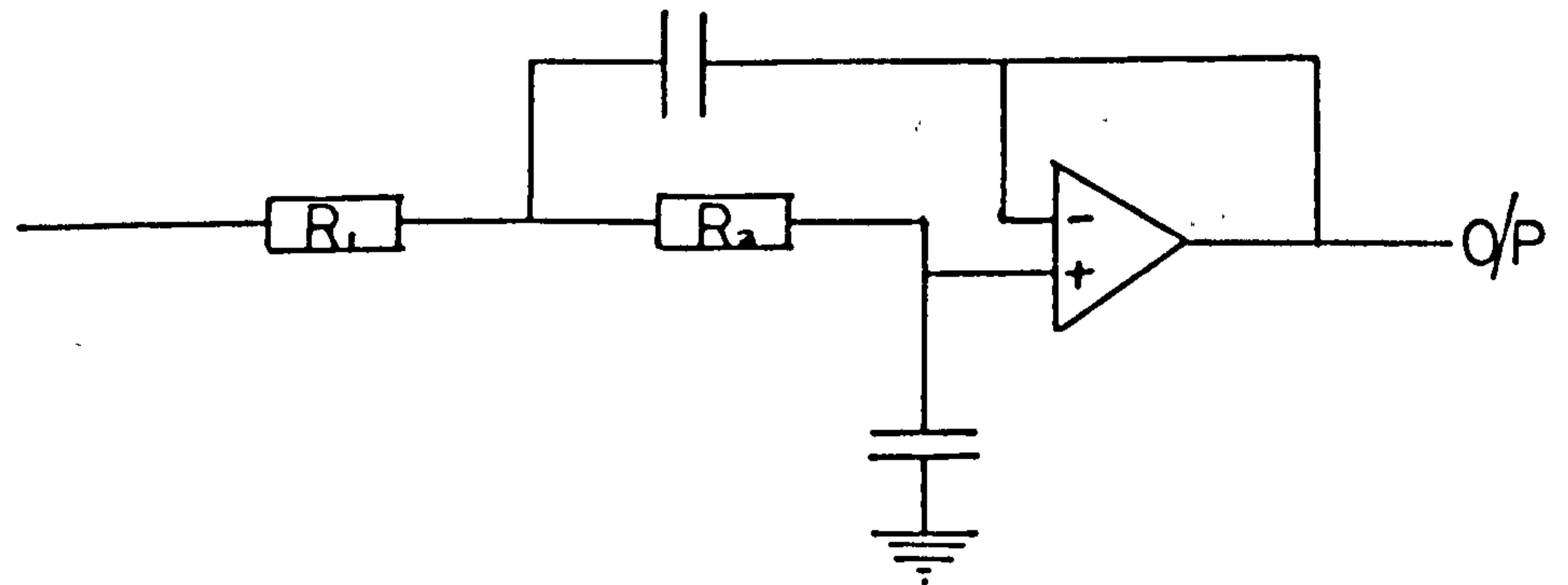


R = variable measuring resistors ($R = 1, 10, 100, \text{ or } 1000 \text{ k}\Omega$)

1,2,3 are LM11 operational amplifiers

V_1, V_2, V_3 are voltage inputs (V_1 is at earth)

Figure 2.2 The Sallen and Key filter



R_1 and R_2 are variable resistors (1, 10, 100, 1000 ohms)

$$f_0 = \frac{1}{2\pi\sqrt{C_1 C_2 R_1 R_2}}$$

where C_1 and C_2 are the circuit capacitors, $C_1 = 1\mu\text{F}$ and $C_2 = 0.5\mu\text{F}$.

recorder, either model PL3 (J.J. Instruments) or a series 60000 (Gould). Alternatively measurements were made using a digital multimeter (Keithley model 175 or 197).

Short time current transients were captured on a digital storage oscilloscope (Gould model OS4020) equipped with roll out facility. Once stored the transient data was down loaded to an XY-t recorder.

2.3 ELECTRODES

Platinum disc and ring-disc electrodes were supplied by Oxford Electrodes. Stationary platinum and glassy carbon disc electrodes were specially designed for use with small volume cells, and were produced to order by Oxford Electrodes. The specification of all working electrodes used in this work are given in table 2.1.

Table 2.1
Working electrodes

Marking	Type	Disc area (cm ²)	Encasing material
Pt/Pt/A	RRDE	0.390	Araldite
Pt/T	RDE	0.393	KEL-F
Pt/E	RDE	0.385	Araldite
Pt small	stationary disc	0.127	Teflon
GC small	stationary disc	0.126	Araldite

All electrodes were polished in the following manner on receipt from Oxford Electrodes. Initially electrodes were polished with 25 micron aluminium oxide powder (Buehler) in glycerol on a mechanical purpose-built polishing device. In the second stage of the polishing procedure the electrodes were washed thoroughly with distilled water, to prevent carry-over of particles of abrasive, and polished with 6 and then 3 micron diamond lapping spray (Engis). These sprays were applied to the lapping cloth along with Hyprez lubricating fluid (Engis). Final polishing was done by hand with a slurry of 1.0 and then 0.3 micron alumina (Banner Scientific) in

distilled water. This was applied to the electrodes using cotton wool. It is important that all polishing materials are kept dust free during polishing and storage to prevent contamination by unwanted particles of abrasive. Final polishing to 0.3 microns produces a mirror finish and was repeated prior to each experiment. In certain cases where the electrode became contaminated with particularly adherent polymeric materials it was necessary to revert to a 6 micron polish and again work down to 0.3 micron polish to ensure that the electrode was free from contamination.

The geometrical dimensions of all working electrode surfaces were measured by use of a travelling microscope. Ten random measurements of each electrode diameter were taken and the mean used to calculate the geometrical electrode area in each case.

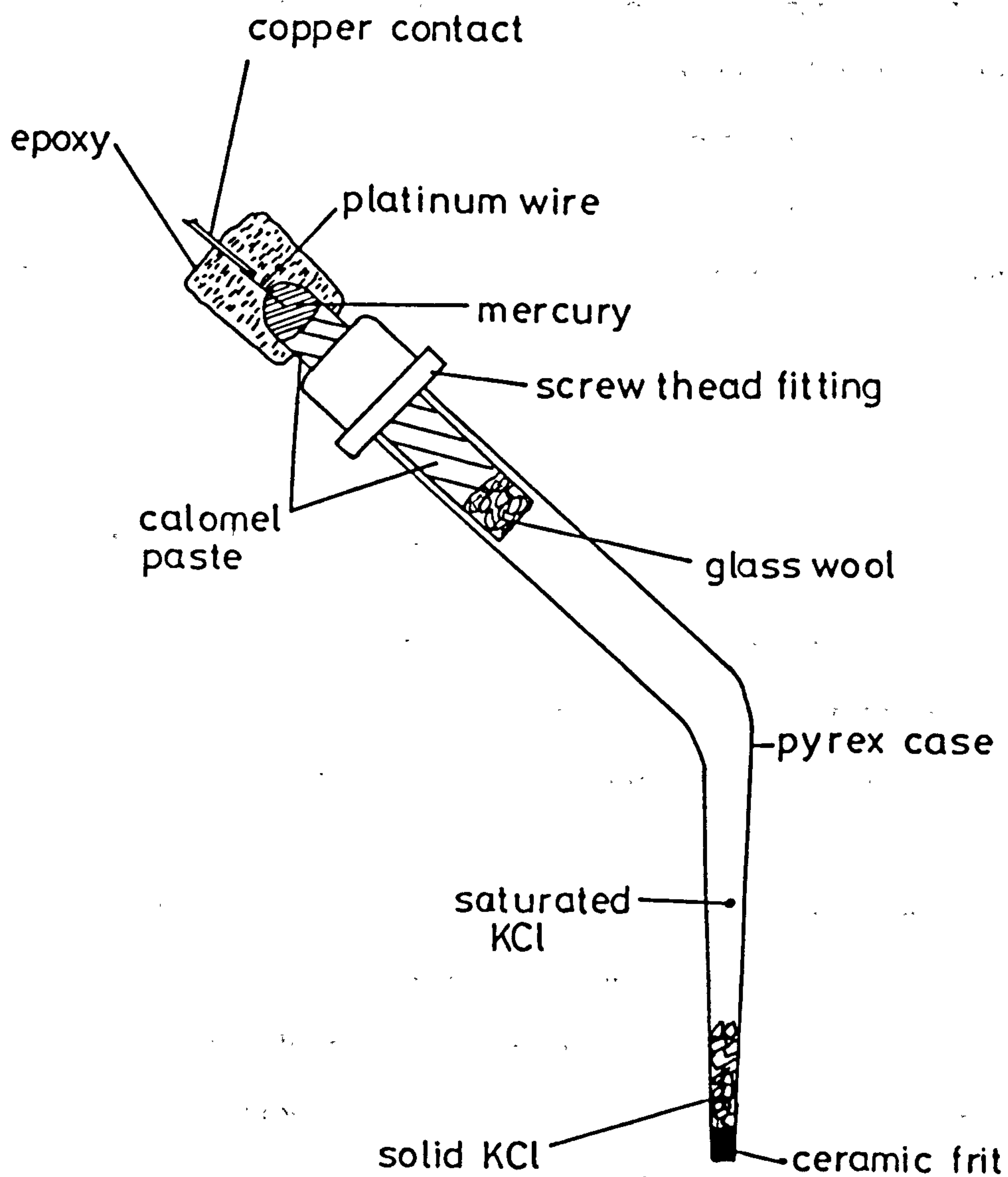
Counter electrodes were constructed of platinum gauze (approximately 2 cm²) which was spot welded onto a length of platinum wire to allow external connection.

Alternatively, a coiled length of platinum wire (external diameter 0.5 mm) was used in conjunction with the small volume cells, or the air-tight perspex cell. The design of these cells is detailed in section 2.5 below.

Potentials were measured with respect to a saturated calomel electrode (SCE) except where the air-tight perspex cell was employed, in which case a silver/silver chloride (Ag/AgCl) reference electrode was used. The calomel electrodes were either a commercially available type (Radiometer) or were of a specially designed home-made type. These purpose built reference electrodes incorporate a screw-thread fitting to prevent leakage of the internal filling solution and resultant failure of the electrode due to dissolution of the external solder contact. The thread fitting is sealed to the inner glass section by means of a gas-tight teflon ring. The design of this type of electrode is shown in figure 2.3. Contact to the external solution is made via a low porosity ceramic frit (a gift from Kent Industrial Measurements Ltd).

The potential of the home-made calomel electrodes was regularly checked against that of a commercial calomel electrode and was found to be within $\pm 2\text{mV}$.

Figure 2.3 The calomel reference electrode (twice actual size)



Any electrode found to deviate from this potential range was repacked with calomel and retested before further use.

2.4 ROTATION APPARATUS

Rotating disc and ring-disc electrodes were mounted on a bearing block (Oxford Electrodes) by means of an internal brass screw-thread contact. Rotation is achieved by direct drive from a printed armature d.c. motor and motor controller (Oxford Electrodes). The electrode rotation speed is continuously monitored by means of a slotted opto-switch connected to the motor drive shaft and displayed in a digital form. This control system allows the accurate determination of electrode rotation speed, giving speeds of between 1 and 50 Hz (± 0.01 Hz). The electrode rotator block and motor controller are illustrated in plate 2.1.

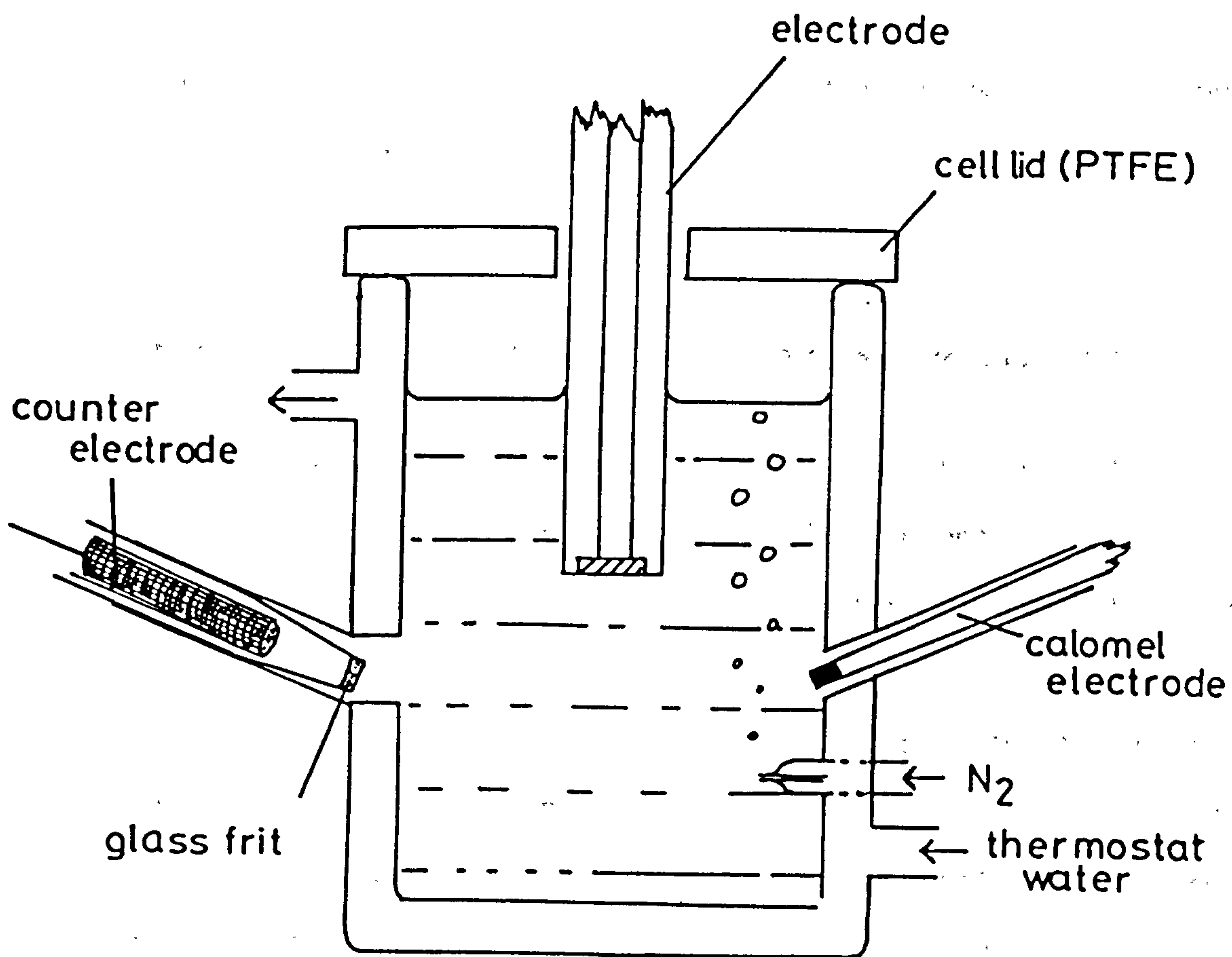
2.5 ELECTROCHEMICAL CELLS

Three types of specially designed electrochemical cell were used in the course of this work. The use of different types of cell enabled the use of a range of sample volumes, temperature control and the rigorous exclusion of oxygen from the sample solutions when required.

The majority of work utilized two compartment water jacketed pyrex cells of volume 15 or 150 cm³ in conjunction with rotating disc and ring-disc electrodes respectively. The design of this type of cell, figure 2.4, enables a stream of oxygen free nitrogen to be passed through the solution in the inner cell compartment prior to the start of an experiment. Oxygen is then prevented from diffusing back into the solution, during the course of the experiment, by maintaining a positive pressure of nitrogen in the cell.

The counter electrode is placed in a second compartment behind a high porosity glass frit. This prevents contamination of the bulk solution by products of

Figure 2.4 Schematic representation of a water jacketed two compartment electrochemical cell.



the counter electrode reaction. The cells are covered with a close fitting teflon lid which has holes for sample injection if required.

The use of a 2 cm³ sample volume was allowed by the development of small pyrex cells and purpose made electrodes. These cells are of a simple two compartment design in which the reference electrode is contacted to the bulk solution by means of a capillary.

The design and use of a purpose built gas-tight cell is described in chapter 5. This type of cell allows the complete exclusion of oxygen from sample solutions where required.

2.6 TEMPERATURE CONTROL AND DEOXYGENATION OF SOLUTIONS

Solutions were thermostatted at 25°C ($\pm 0.2^\circ\text{C}$) by use of a water bath and circulator (Grant Instruments model SE15), unless otherwise specified.

Deoxygenation of solutions used for electrochemistry was achieved by purging with nitrogen which had previously had traces of oxygen removed by passage through a train of dreschel bottles containing a caustic solution of anthraquinone-2-sulphonate in contact with zinc amalgam. This pretreatment was found to provide adequate solution deoxygenation and the use of the anthraquinone reagent is convenient since it is self indicating, turning from deep red to straw yellow when exhausted.

Alternatively, oxygen-free nitrogen (Air Products) was used. Nitrogen was presaturated by passage through the solution in use before entering the cell. Deoxygenation was continued for at least 20 minutes prior to the start of an experiment. All solutions used for electrochemistry were treated in this way unless otherwise specified.

2.7 SOLUTIONS AND CHEMICALS

All solutions were freshly prepared using water from a MilliQ water purification system (Millipore). The system contains two nuclear grade ion exchange and two organic scavenging cartridges. After purification the water passes through a 0.2 micron filter to remove any fine particulate matter. The resulting water has a resistance of greater than 15 megohms.

All glassware was cleaned by immersion in Decon 90 overnight, followed by a thorough rinsing in purified water. Glassware which was not completely cleaned by this procedure was immersed in hydrochloric acid solution (5 mol dm^{-3}) and, if need be, sonicated prior to reimmersion in Decon 90 overnight.

All simple inorganic chemicals were of analytical reagent grade and were used without further purification unless otherwise specified. All buffer reagents were supplied by Fisons or BDH and were of analytical reagent grade.

Ferrocene monocarboxylic acid (Aldrich Chemicals) was purified by recrystallisation from toluene⁽¹¹⁹⁾ before use. Ferrocene ethanoic acid and ferrocene butanoic acids were a gift from MediSense (UK) Inc. These acids were obtained in a pure form.

Pyrrole and N-methylpyrrole (Aldrich Chemicals) were distilled under reduced pressure before use and stored under nitrogen at -20°C for periods of less than a week. Aniline (Fisons) was distilled under reduced pressure and stored at 4°C until required.

Glucose oxidase (EC 1.1.3.4) from *A.niger* was a gift from MediSense (UK) Inc. and was obtained as a concentrated solution (240 to 277 mg cm^{-3}) with an activity of between 36800 and 48400 U cm^{-3} . The units specified are described in full in section 2.8. The glucose oxidase concentrate is stable for extended periods if stored in air tight vials at 4°C .

β -fructosidase (EC 3.2.1.26) from yeast was purchased from Boehringer

Mannheim in a lyophilised form and was stored dessicated at 4°C. This preparation has an activity of 300 U mg⁻¹.

Peroxidase (EC 1.11.1.7) from Horseradish was purchased from Sigma (type II) in a lyophilised form with an activity of 150 U mg⁻¹. This preparation was stored dessicated at -20°C.

Catalase (EC 1.11.1.6) from beef liver was purchased from Boehringer Mannheim as a solution in glycerol (30% v/v) and ethanol (10% v/v). This preparation has an activity of 260000 U cm⁻³. Before use this enzyme preparation was dialysed against phosphate buffer (3×250 cm³ of sodium phosphate, 0.085 mol dm⁻³, pH 7.0 at 4°C). This ensured the complete removal of all unwanted low molecular species. The dialysed concentrate was stored in sealed vials at 4°C until required.

2.8 ENZYME ASSAYS

This section describes all procedures employed to determine the activity and protein concentration of all glucose oxidase (GOD) solutions used. The activity of the GOD concentrates was determined regularly to ensure that these solutions were stable to storage. Activity assays consisted either of an oxygen electrode based assay or a dye-linked spectrophotometric procedure.

The unit of enzyme activity used in all cases is defined as follows. One unit of GOD is that amount of enzyme required to convert 1 μmole of glucose to product per minute at pH 7.0 and 30°C. Alternatively 1 unit of enzyme is that amount which consumes 1 μmole of molecular oxygen per minute (equivalent to 22.4 μl of molecular oxygen per minute) under identical conditions.

The stock glucose solution (1.000 mol dm⁻³) used in these assays was allowed to equilibrate for 24 hours at room temperature before use. The assay procedures are described below.

2.8.1 The Oxygen Electrode Assay

A conventional oxygen electrode (Rank Bros.) was used to monitor the uptake of oxygen by GOD in the presence of β -D-glucose⁽¹²⁰⁾. Output from the oxygen electrode was recorded on a Gould Series 60000 XY-t recorder. The sample chamber of the oxygen electrode and all assay solutions were thermostatted at 25°C ($\pm 0.2^\circ\text{C}$). A polarising voltage of 0.60 volts was used for oxygen detection. A constant stir rate was used throughout to produce controlled mass transport of oxygen to the membrane surface. Each GOD activity assay contained the following components:

- glucose (0.10 mol dm^{-3})
- GOD ($2 \text{ to } 40 \mu\text{g cm}^{-3}$)
- buffer of required pH to a final volume of 2 cm^3 .

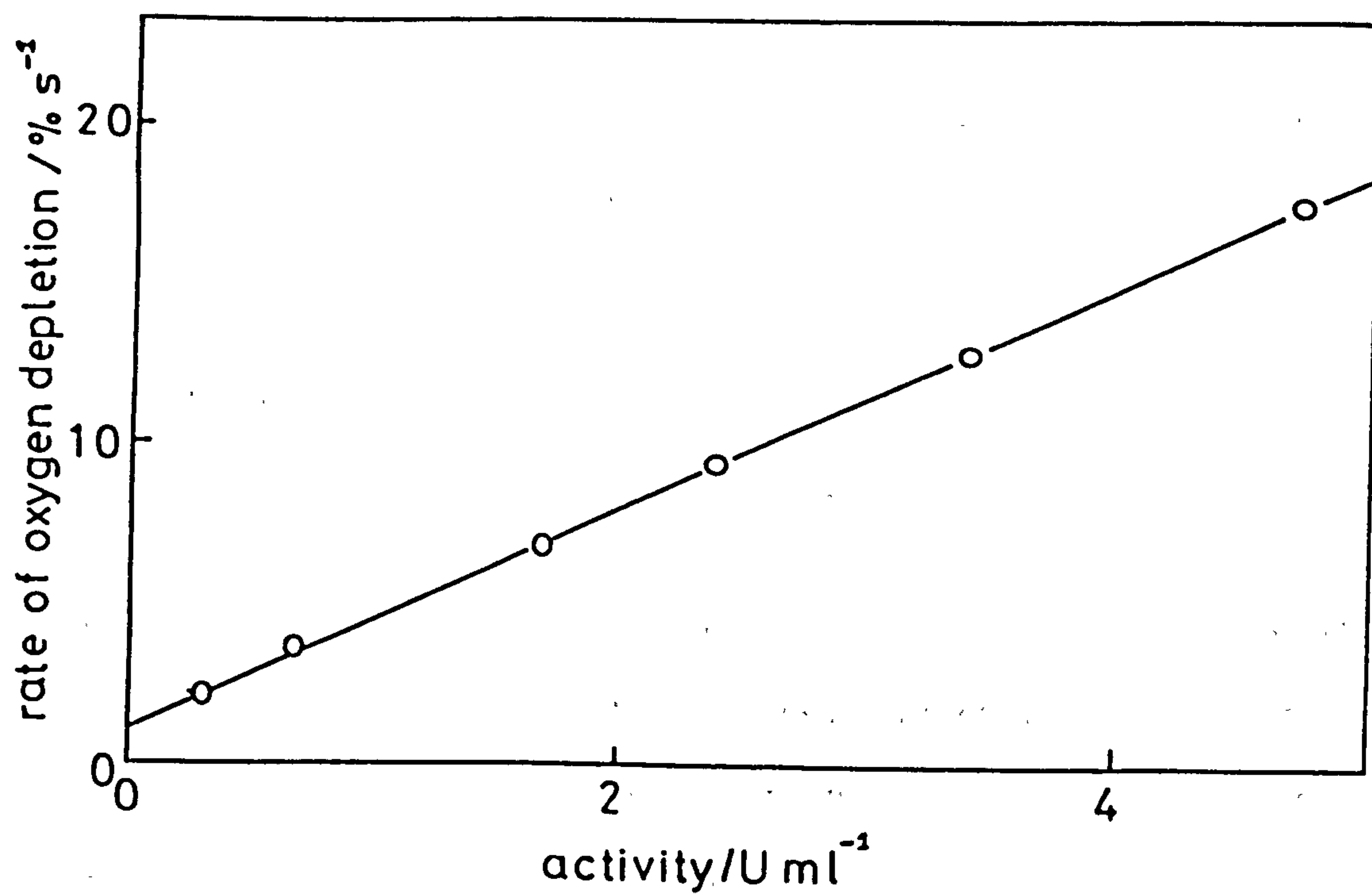
Buffer and enzyme were introduced into the sample chamber and the lid fitted so as to exclude atmospheric oxygen. Once a constant oxygen tension was reached glucose was injected into the sample chamber using a microsyringe and the initial rate of oxygen depletion was measured.

By varying the concentration of freshly obtained GOD in the assay a calibration curve was constructed which relates the rate of oxygen depletion ($\% \text{ sec}^{-1}$) to the enzyme activity (U cm^{-3}). Such a plot is shown in figure 2.5. The activity of the stock GOD solutions could thus be measured at suitable time intervals by measuring the initial rate of oxygen depletion at a known GOD concentration.

Assays were normally carried out at pH 7.0. A series of assays were, however, carried out at a range of pH values in order to determine the pH profile of the enzyme. Buffer solutions used were of three types. For pH 1 to 4 a glycine-HCl buffer was used, and for pH 5 to 7 and 8 to 11 phosphate-citrate and glycine-NaOH buffers respectively were used.

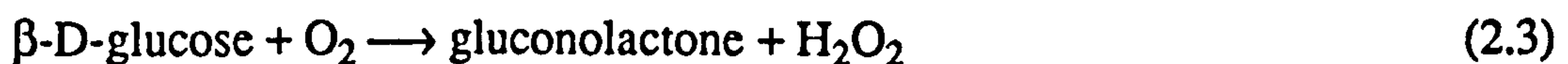
It was important to check that these buffer systems did not exert any unwanted inhibitory or destabilising effects on the enzyme. By comparing the pH profile

Figure 2.5 Relationship of GOD activity to rate of oxygen depletion in the oxygen electrode assay.



obtained with those present in the literature this effect was determined. The pH profile obtained was directly comparable to those previously determined for this enzyme⁽¹²¹⁻¹²³⁾. This indicates that the buffer systems used are suitable for use in the development and determination of pH optimum of GOD linked bi-enzyme assays.

A further oxygen electrode based assay was developed to determine the pH optimum of a coupled GOD- β -fructosidase system. The consumption of sucrose by β -fructosidase was coupled to the oxidation of glucose by GOD⁽¹²⁴⁾. This coupled system is described by the following reactions.



Reaction (2.2), the mutarotation of α -D-glucose, was found to proceed at a sufficient rate for the requirement of a second coupling enzyme mutarotase (Aldase-1-epimerase EC 5.1.3.3) to be eliminated⁽¹²⁵⁾. The oxygen electrode assay developed contained the following components.

- Sucrose (0.10 mol dm^{-3})
- GOD (50 U cm^{-3})
- β -fructosidase (220 U cm^{-3})
- buffer, of required pH, to a final volume of 2 cm^3 .

An excess of the coupling enzyme was included in order to minimise any lag period produced by the coupling of the two systems.

The sucrose and buffer solutions were equilibrated at 25°C . Buffer and both enzymes were then introduced into the sample chamber and the lid fitted. Again a constant stirrer speed was used throughout. Once a stable oxygen tension had been reached the sucrose was injected into the sample chamber and the rate of oxygen

consumption was measured. Initial seconds after sucrose addition were discounted from the initial rate measurement due to the existence of a short lag period.

Using the range of buffers described above, the pH optimum for the coupled enzyme system was determined.

2.8.2 Spectrophotometric Determination of Glucose Oxidase Activity

A second glucose oxidase (GOD) activity assay was also used which involved a colourimetric reaction. This was found to give directly comparable results to the simple oxygen based assay described above.

The spectrophotometric assay utilises the peroxidase enzyme in conjunction with a chromogenic electron acceptor⁽¹²⁶⁾ and is based on the following system:



The procedure used was a modification of that described by Trinder^(127,128). The chromogen 4-aminoantipyrine (AAP) undergoes a colour reaction with 3,5-dichloro-2-hydroxybenzene sulphonic acid (DHSA) in the presence of peroxidase and hydrogen peroxide⁽¹²⁹⁾. By measuring the rate of production of the oxidised electron acceptor, reaction (2.5) in the presence of saturating glucose the rate of glucose consumption by GOD can be determined. The coloured product has an adsorption maximum at 520nm. The initial rate of increase in absorption at 520nm ($\Delta A_{520} \text{ min}^{-1}$) therefore gives a measure of the GOD activity. The assay contained the following components.

- glucose (0.10 mol dm^{-3})
- DHSA ($1.95 \times 10^{-3} \text{ mol dm}^{-3}$)
- peroxidase (0.003% w/v)
- 4-AAP ($2.0 \times 10^{-4} \text{ mol dm}^{-3}$)
- buffer ($0.133 \text{ mol dm}^{-3}$ sodium phosphate containing $1 \times 10^{-3} \text{ mol dm}^{-3}$ EDTA) to a final volume of 2 cm^3).

The assay components were equilibrated at 30°C and then thoroughly mixed. The reaction was initiated by addition of $50 \mu\text{l}$ of GOD sample and the A_{520} monitored. The absorbance was found to have a linear time dependence over the first 60 seconds of reaction. Samples of GOD giving $\Delta A_{520} \text{ min}^{-1}$ of greater than unity were diluted as required. The GOD activity was calculated using the following relationship.

$$\text{Activity} = \frac{\Delta A_{520} \cdot x \cdot M}{c \cdot y} \text{ Units mg}^{-1} \quad (2.6)$$

where ΔA_{520} is the absorbance change per minute at 520 nm , x is the conversion factor to give ΔA_{520} for a 1 cm^3 addition of GOD sample (for a $50 \mu\text{l}$ sample $x = 20$), M is the molecular weight of GOD (160000), c is the concentration of GOD in mg cm^{-3} , and y is a unit conversion factor for ΔA_{520} produced in the presence of $1 \times 10^{-6} \text{ mol dm}^{-3}$ hydrogen peroxide by peroxidase. The factor y has a value of 12 for this assay system.

In conjunction with the protein concentration assay described below this activity measurement was used to assay all GOD samples. The enzyme unit described is defined as follows. One unit of GOD is that amount of enzyme required to catalyse the oxidation of 1×10^{-6} moles of β -D-glucose per minute at pH 7.0 and 30°C , as previously specified.

In the following section a method for the determination of the concentration of active, flavin adenine dinucleotide (FAD) containing, GOD is described.

2.8.3 Spectrophotometric Determination of Active GOD Concentration

It is essential that the concentration of glucose oxidase (GOD) in all stock and assay solutions can be accurately determined to enable a good estimate of activity to be obtained.

The enzymatically active form of GOD is known to contain two FAD centres per enzyme molecule^(121,130-132). In the presence of the atmosphere, and the absence of the substrate, these FAD centres are in the oxidised form due to reaction with molecular oxygen. The absorbance spectra of free and GOD bound FAD are shown in figure 2.6. It is apparent that both free FAD⁽¹³³⁾ and GOD bound FAD⁽¹³⁴⁾ show pronounced absorption peaks at around 450nm in the oxidised state.

By measuring the absorbance at 450nm (A_{450}) of a GOD solution and with a knowledge of the molar absorption coefficient of enzyme bound FAD the concentration of active GOD, containing two FAD centres per molecule of enzyme, can be determined using the Beer Lamber law⁽¹³⁵⁾.

$$A = \epsilon c_M l \quad (2.7)$$

where A is the absorbance, ϵ is the molar extinction coefficient ($\text{dm}^3\text{mol}^{-1}\text{cm}^{-1}$), c_M is the molar concentration, and l is the pathlength (cm). The molar concentration of GOD is therefore given by

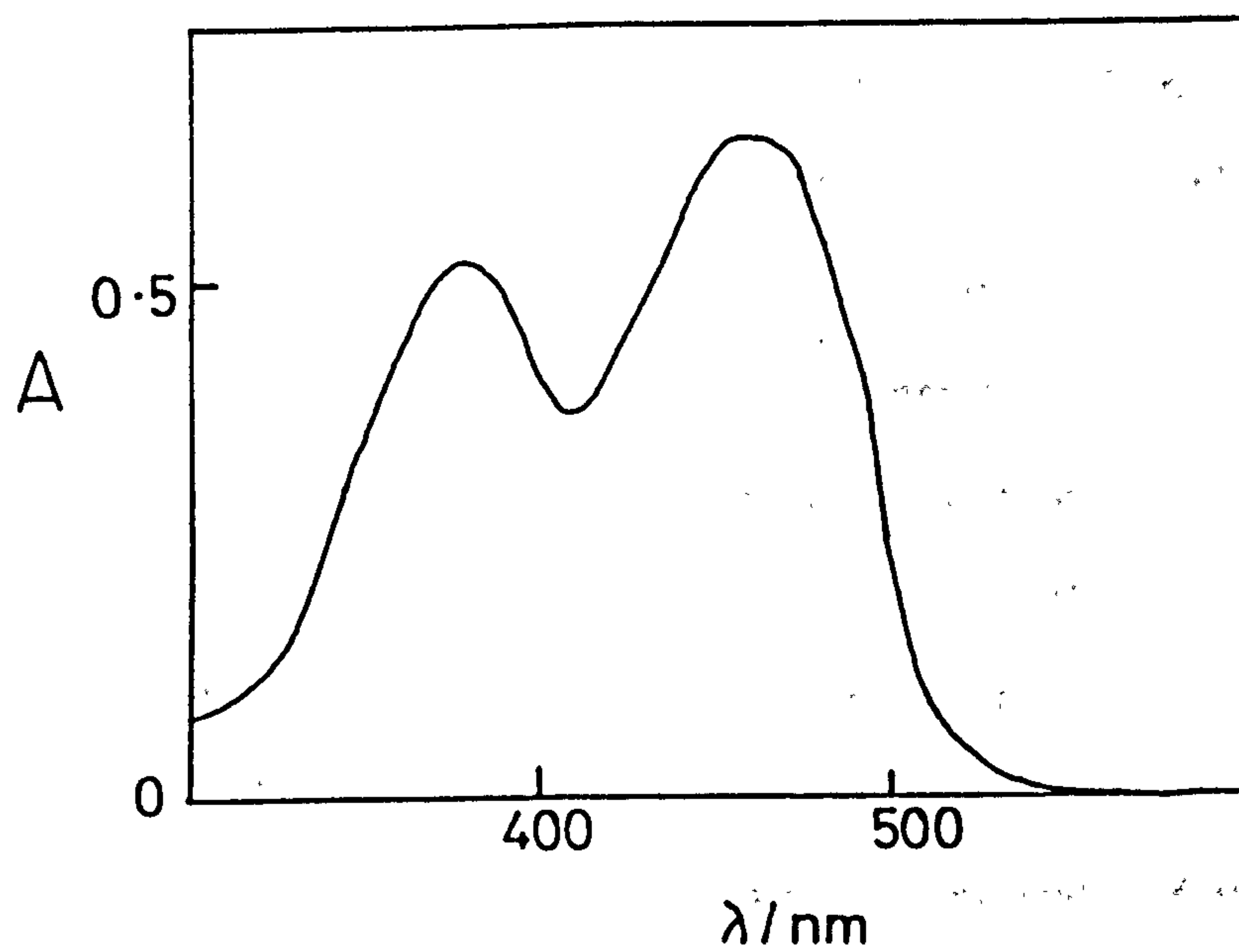
$$c_M = A_{450} / \epsilon l \quad (2.8)$$

It is usual, however, to express protein concentrations in units of mg cm^{-3} . Using a cell pathlength of 1cm and allowing for the fact that there are two FAD centres per GOD molecule, it can be seen that

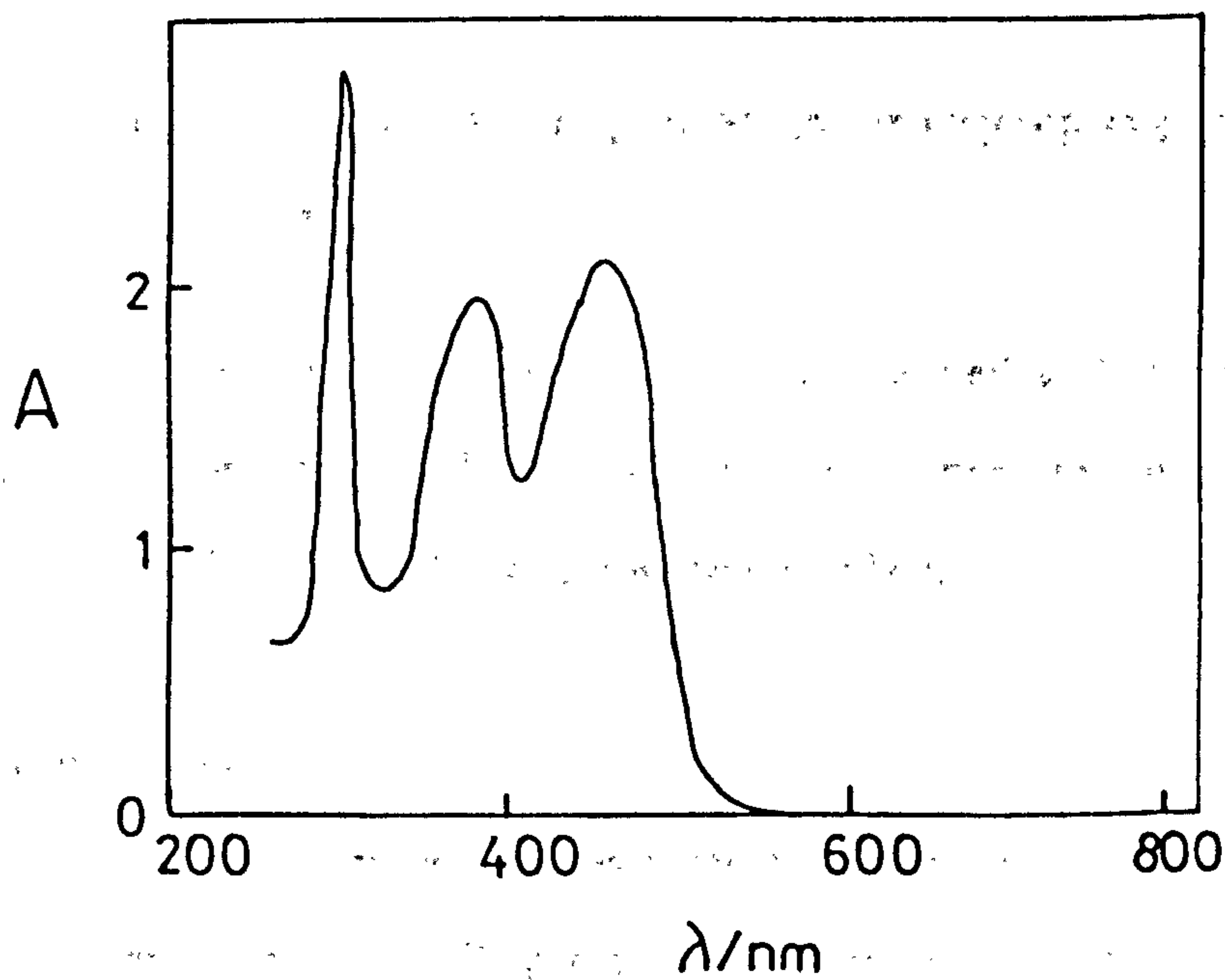
$$c = \frac{A_{450} \cdot M}{\epsilon \cdot 2} \quad (2.9)$$

where c is the concentration of GOD (mgcm^{-3}) and M is its molecular weight. A value of ϵ for GOD has been previously determined as $1.41 \times 10^4 \text{ dm}^3 \text{ mol}^{-1} \text{ cm}^{-1}$ ⁽¹³¹⁾.

Figure 2.6 Absorption spectra for free and enzyme bound FAD.



a) Free FAD ($1.0 \times 10^{-2} \text{ mol dm}^{-3}$, pH 7.0, phosphate buffer)



b) GOD bound FAD ($7.5 \times 10^{-6} \text{ mol dm}^{-3}$, pH 7.0, phosphate buffer)

This fixed wavelength concentration assay was used to determine GOD concentrations in all aspects of this thesis. A calibration plot relating A_{450} to GOD concentration was produced by measuring the absorbance of a range of GOD solutions (figure 2.7). The slope of this plot is $0.175 \text{ mg}^{-1} \text{ cm}^3$. The GOD concentrations of all sample solutions was calculated by multiplying the A_{450} value by the reciprocal of the calibration slope, providing a simple and accurate concentration assay. Samples giving A_{450} readings outside the calibration range (0 to 2) were diluted as required. This assay was found to give an accurate measure of GOD concentrations greater than 0.05 mg cm^{-3} (or $3.1 \times 10^{-7} \text{ mol dm}^{-3}$).

The GOD concentration of all stock solutions was found to lie in the range 240 to 277 mg cm^{-3} . The activity of these solutions was calculated as 36800 to 48400 Unit cm^{-3} . Stock solutions were stable for periods exceeding 6 months when stored at 4°C in sealed vials.

In the following section the procedures employed in the covalent modification of GOD with ferrocene carboxylic acid derivatives is described.

2.9 THE COVALENT MODIFICATION OF GLUCOSE OXIDASE WITH ELECTRON RELAYS

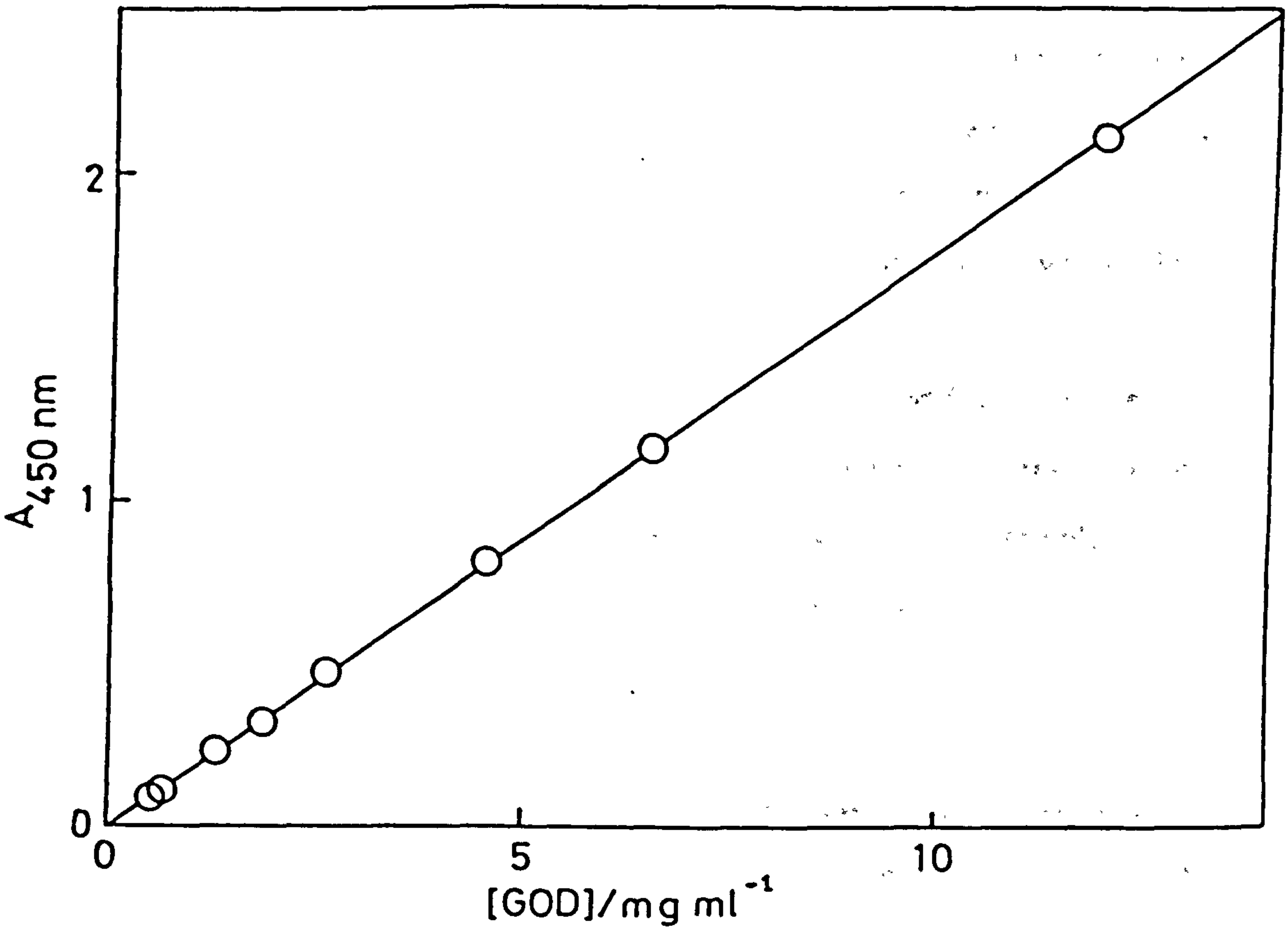
Glucose oxidase (GOD) was chemically modified with a series of ferrocene carboxylic acid derivatives. Techniques used in the preparation and purification of these modified GOD molecules will now be described.

2.9.1 Preparation

The modification procedure described by Degani and Heller^(136,137) was used to produce three modified GOD species in which three different ferrocene carboxylic acid derivatives were used as the modifying electron relays.

In this procedure a water soluble carbodiimide coupling reagent

Figure 2.7 The relationship between GOD concentration and solution absorbance at 450nm.



(1-(3-dimethylaminopropyl)-3-ethylcarbodiimide, DEC) was used to produce amide bonds between the amine groups of lysine residues present in the GOD protein and carboxylate groups of ferrocene carboxylic acid derivatives. The experimental pH and temperature values were those previously described by Degani and Heller. Other experimental procedures were also those previously described by these authors except that once combination of all reagents was complete the mixture was removed from the ice bath, sealed and maintained at 2°C for 14 to 16 hours. After this period the reaction mixture was allowed to warm to room temperature, shaken to resuspend any solid matter, and centrifuged. The supernatant fluid was then centrifuged again and the modified GOD was separated from unwanted low molecular weight molecules by gel filtration.

Control preparations were run in each case. Here the modification procedure was identical except that DEC was excluded from the reaction mixtures. Control samples were then purified in an identical manner to modified GOD samples. The use of gel filtration to purify the modified enzyme is described below.

2.9.2 Gel Filtration

This technique is particularly well suited to the separation of proteins of different molecular size⁽¹³⁸⁾. In the case of the separation of modified GOD (molecular weight > 160000) from starting materials and reaction biproducts (molecular weight <1000) this technique provides a particularly fast and effective separation. This is of great importance because it is essential that the modified enzyme obtained is free from any non-covalently bound, diffusible ferrocene species.

Gel filtration was performed on Sephadex G-15 or G-25 (medium, Pharmacia) in a 1.6×40 cm glass column (Pharmacia). The gel was preswollen at room temperature in the sodium phosphate running buffer (0.085 mol dm⁻³, pH 7.0) for 4 hours prior to column packing.

After decanting fine particles from the surface of the gel suspension and washing the gel with fresh running buffer the column was packed by continuous pouring under gravity. Buffer was then run through the column for 2 hours to ensure complete settling and swelling of the gel. At this point the column was checked for cracks or air pockets with a 100W electric lamp.

The sample was then applied to the top of the gel and the column run. Elution was achieved either by use of a peristaltic pump (Pharmacia P-3) at a rate of $18.6\text{ cm}^3\text{ h}^{-1}$ or under gravity giving a flow rate of $20\text{ cm}^3\text{ h}^{-1}$. Collection of eluted fractions was either automatic or manual with fraction volumes of 2 or 4 cm^3 . Each fraction was assayed for enzyme activity and concentration and ferrocene derivative concentration before being placed in the fridge in air tight vials or used for electrochemical experiments.

The concentration of low molecular weight ferrocene species in the eluant was monitored by measuring the peak height in cyclic voltammetry or by measuring the absorbance at 330nm. Although this wavelength is close to an absorption maxima exhibited by the enzyme (at 450nm and 370nm) there was no significant interference by FAD on the spectrophotometric determination of free ferrocene species. Any doubts about the validity of such measurements were allayed by electrochemical monitoring.

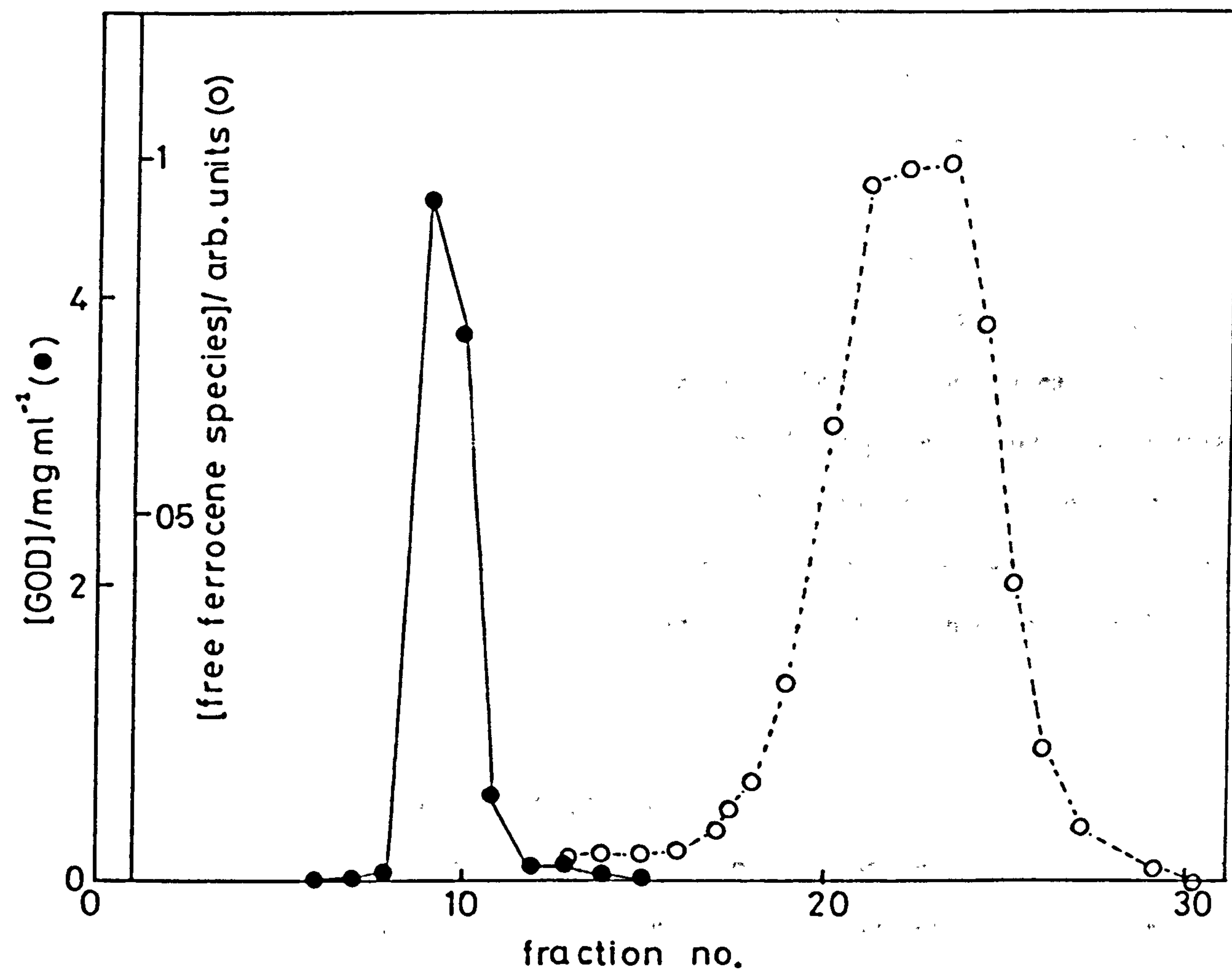
A plot showing the concentration of modified GOD and free ferrocene derivatives as a function of fraction number is shown in figure 2.8. This shows that the separation was complete.

2.10 ELLIPSOMETRY

In this section the use of ellipsometry^(139,140) to determine the thickness and certain other characteristics of a growing poly-*N*-methylpyrrole film is described.

The technique of ellipsometry is an accurate method for measuring optical

Figure 2.8 Column elution profile for the G-25 sepadex separation of modified enzyme from low molecular weight components.



Flow rate = 18.6 cm³ hr⁻¹

Each fraction = 4 cm³

Initial sample volume = 4.0 cm³ (containing 60mg of GOD)

constants of reflecting surfaces, and also for the determination of the thickness of thin films deposited onto such surfaces. This technique is based on the measurement of changes in the state of polarisation of light reflected from the surface under investigation. From the point of view of the electrochemist, ellipsometry is useful since light with wavelengths in the visible region can be used permitting the *in situ* study of an electrode surface in an aqueous electrolyte medium.

The three parameter ellipsometer employed measures α (azimuth), ϵ (ellipticity) and I (intensity) very accurately.

The following sections describe the preparation of gold substrates for ellipsometry and the ellipsometric equipment used to make measurements on a growing conducting polymer film. The aim of the ellipsometric measurements is to provide an accurate relationship between the charge passed during polymer growth and the thickness of the growing polymer film. This thickness parameter becomes important when the response of glucose oxidase containing poly-*N*-methylpyrrole films is interpreted in terms of a theoretical model which contains the film thickness (1).

2.10.1 Preparation of Gold Substrates

Substrates for ellipsometry were prepared by sputtering gold (99.99%) onto glass microscope slides (Chance Propper Ltd., Smethwick). The glass slides were washed in acetone and soaked in Decon 90 for 24 hours prior to use. After rinsing with distilled water and drying in an oven the slides were placed into the vacuum chamber of a sputter coater (Emscope Model SC500). The vacuum chamber was evacuated and purged with the ionising gas, argon. Gold was then sputtered onto the upper surface of the slide using a solid gold sputtering target and a fixed potential of 1kV. A current of between 10 and 15mA was passed during gold deposition. The rate of metal deposition and the film thickness were monitored using a film thickness monitor (Edwards model FTM4). A rate of deposition of around $1 \times 10^{-6} \text{ cm min}^{-1}$

was used to give a final film thickness in the region of 1×10^{-5} cm.

The slides made in this way gave uniform cyclic voltammograms in background electrolyte and were found to be suitable for polymer electrodeposition.

2.10.2 Ellipsometry and Film Growth

Polymer films were deposited from solutions of *N*-methylpyrrole (50 mol dm^{-3}) in a buffered electrolyte ($0.015 \text{ mol dm}^{-3}$ sodium phosphate, 0.10 mol dm^{-3} tetraethylammonium tetrafluoroborate). In all cases film growth was potentiostatic and used a fresh home-made gold substrate.

The ellipsometer used was a Rudolph Research rotating analyser automatic ellipsometer (model RR2000). The optical components are mounted on an optical bench. The light leaving the light source, a 633nm helium neon laser (5mW, Hughes) enters a polariser before being incident on the sample. An angle of incidence of 61.46° was used in all cases. The reflected light then enters a rotating analyser and a 633nm filter before entering a photomultiplier tube. The rotating analyser consists of a quartz prism which is rotated at 50Hz by means of an electric motor. The use of interference filters positioned before the photomultiplier tube allow single wavelengths across the visible spectrum to be selected.

Values of α , ϵ and I can be recorded for each analyser rotation (every 0.02 seconds) allowing a rapidly changing electrode process such as the electrodeposition of an organic polymer to be followed. For longer duration experiments, several minutes, the ellipsometer can be employed to average every 10 or 100 readings taken.

A Matmos PC was used to control the potentiostat via a 12-bit digital-to-analogue converter and also to record the optical measurements made by the ellipsometer. This Matmos PC is interfaced to the ellipsometer electronics unit via a parallel input/output (PIO) board. Use of appropriate software⁽¹⁴¹⁾ allows a variety of potential/time profiles to be employed and the readings of α , ϵ and I as well as

potential and sample number to be collected and stored on disk.

In order to obtain the required values of film thickness the values of α and ϵ , the experimental parameters, were converted to values of Δ and Ψ as the theoretical models are expressed in terms of these latter parameters, where

$$\cos 2\Psi = -\cos 2\epsilon \cos 2\alpha \quad (2.10)$$

$$\tan \Delta = \tan 2\epsilon / \sin 2\alpha \quad (2.11)$$

Values for the changes in Δ , Ψ and I , corresponding to film growth, are entered into the appropriate analysis and fitting program⁽¹⁴¹⁾ along with initial guesses for the refractive indices (n and k). The fitting routine then iterates parameters until a best fit is found.

The relationship between charge passed and film thickness produced in the case of poly-*N*-methylpyrrole was investigated in this way.

Further simple experiments to follow the proposed adsorption of the enzyme glucose oxidase onto a clean platinum surface were undertaken. In this case the slide was equilibrated in the buffer prior to injection of enzyme solution to give a final concentration of 1 mg cm^{-3} . Data was collected and analysed to reveal the extent of enzyme adsorption. Initial seconds after the injection of enzyme were discounted as this period was used to mix the solution thoroughly. The result of this type of adsorption experiment, although qualitative in nature, has profound consequences on the enzyme immobilisation experiments presented in chapters 4 and 5 of this thesis.

CHAPTER THREE

THEORY

In this section of the thesis a theoretical treatment of the different types of immobilised enzyme systems studied is presented. The theory below describes a situation where the enzyme is fixed in space within a polymer film on an electrode surface and is not free to diffuse within this film. The mediator described is either the natural electron acceptor for flavo-oxidases, molecular oxygen, or an artificial one electron acceptor ferrocene monocarboxylic acid. Surprising differences are seen in the way in which the two systems operate when using the same enzyme/polymer combination. An examination of the theoretical treatments for the two systems reveals that this difference arises not from the enzyme/mediator reaction, although the mechanism of this reaction is probably different from one system to the other, but from the site of reoxidation of the reduced mediator.

The polymer used in this comparative work was conducting poly-*N*-methylpyrrole. However, insulating films of polyaniline and polyphenol were also used to immobilise glucose oxidase (GOD). The theory describing the saturation kinetics observed in such cases is also described.

It is interesting to note that the saturation responses observed are not due to Michaelis-Menten type kinetic turnover, at least in the case of the GOD-polyaniline system, but rather to a different rate limiting reaction. Such systems are described in detail in the latter part of this chapter.

Whenever possible kinetic and diffusional parameters were extracted from the fit between experimental data and the appropriate theoretical model. These parameters are presented in chapters 4 and 5 and results from the different systems are compared.

Finally, in this chapter, the theoretical results for limiting cases in the oxygen mediated GOD reaction are compared to the theoretical results obtained by other

authors for digital simulation of a similar system. This comparison is presented in section 3.3.

We begin by describing the theoretical model the operation of GOD immobilised in conducting poly-*N*-methylpyrrole when oxygen is the mediator. Conclusions about the reaction site of the hydrogen peroxide produced and the kinetic processes occurring are drawn in the following chapter where the fit of experiment to this theory is detailed.

3.1 OXYGEN MEDIATION TO AN IMMOBILISED ENZYME

The theoretical expressions developed to describe the operation of immobilised enzyme/diffusible mediator systems contain different expressions for the flux as a function of film thickness, enzyme loading, mediator concentration and substrate concentration in the bulk solution. The appropriate expression for the observed flux in each case depends on which reaction in the enzyme containing film is rate limiting under the experimental conditions used. In this section theoretical results for the limiting cases are presented. Initially the kinetic scheme of reactions occurring within the polymer film is described.

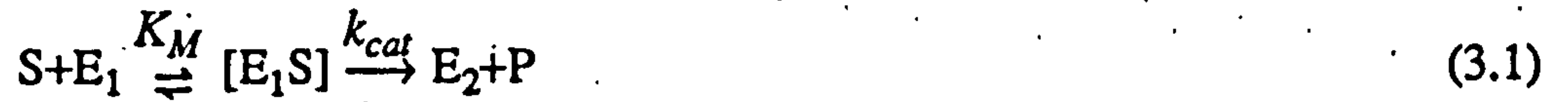
3.1.1 The Kinetic Scheme

In the model presented we assume that oxygen, the mediator, is available in the bulk solution and is not significantly depleted by enzymic removal. A second more important assumption is that there is no significant concentration polarisation of the substrate, glucose, in the external bulk solution.

The substrate, *S*, has a bulk concentration of s_{∞} , a partition coefficient *K*, for entry into the polymer film, and a diffusion coefficient D_s in the film. Thus the surface concentration of *S* in the film is given by Ks_{∞} .

In all sections of this chapter a convention of using lower case letters to denote

concentrations of the various species is adopted. The kinetic scheme is shown in figure 3.1. The kinetic processes occurring are represented as follows:



Here E_1 and E_2 are the oxidised and reduced forms of the enzyme respectively. The reaction of E_1 with the substrate, S , occurs throughout the film to form E_2 and the product P . This reaction is described by normal Michaelis-Menten kinetics where K_M and k_{cat} have their usual meanings^(142,143). The E_1 form of the enzyme is regenerated by reaction with the oxidant, A , to form E_2 and the reduced oxidant, B . B has a diffusion coefficient D_B and is reoxidised to form A either on the electrode surface or on the conducting polymer⁽¹⁴⁴⁾.

We can start by constructing equations describing the concentrations of the three species of interest in the film.

$$\frac{de_2}{dt} = \frac{k_{cat}s(e_\Sigma - e_2)}{K_M + s} - kae_2 \quad (3.4)$$

$$\frac{ds}{dt} = D_S \frac{d^2s}{dx^2} - \frac{k_{cat}s(e_\Sigma - e_2)}{K_M + s} = 0 \quad (3.5)$$

$$\frac{db}{dt} = D_B \frac{d^2b}{dx^2} + kae_2 = D_A \frac{d^2a}{dx^2} - kae_2 = 0 \quad (3.6)$$

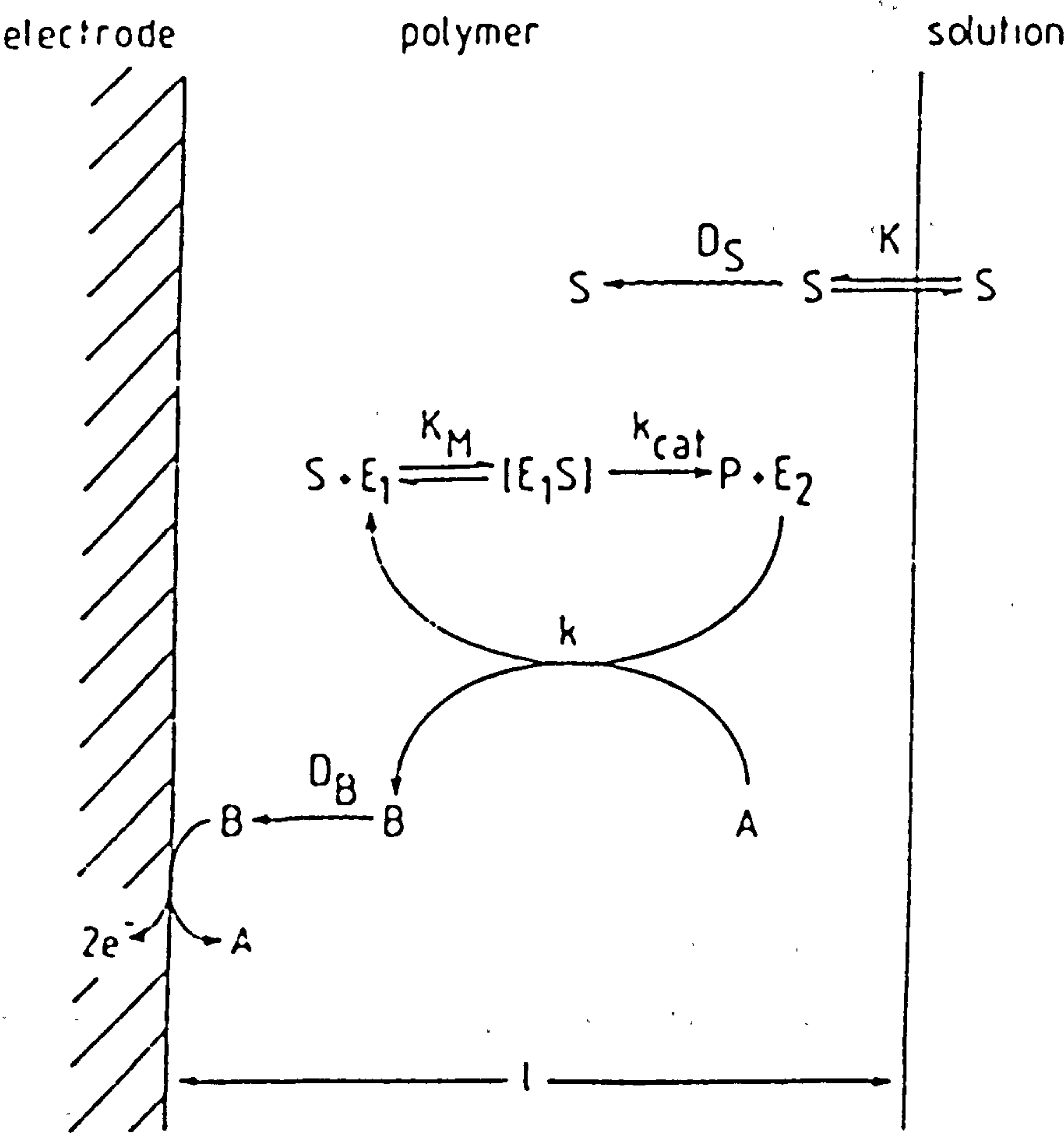
where x is the distance from the electrode surface and e_Σ is the total concentration of immobilised enzyme given by the enzyme conservation equation

$$e_\Sigma = e_1 + e_2 \quad (3.7)$$

Applying a steady state approximation to equation (3.4) gives

$$\frac{k_{cat}s(e_\Sigma - e_2)}{K_M + s} = kae_2 \quad (3.8)$$

Figure 3.1 General kinetic scheme for the immobilised enzyme reaction



Substituting into equations (3.5) and (3.6) and rearranging gives

$$D_S \frac{d^2 s}{dx^2} - \frac{k_{cat} kase_{\Sigma}}{k_{cat}s + K_M ka + kas} = 0 \quad (3.9)$$

$$D_B \frac{d^2 b}{dx^2} + \frac{k_{cat} kase_{\Sigma}}{k_{cat}s + K_M ka + kas} = 0 \quad (3.10)$$

Two possible situations exist in this case; the reduced mediator, B, can become reoxidised either on the conducting polymer or on the underlying metal electrode surface:

To obtain an expression for the flux if B reacts rapidly on the conducting polymer, we must solve equation (3.9) with the boundary conditions

$$\text{at } x = 0 \quad \frac{ds}{dx} = 0 \quad (3.11a)$$

$$\text{at } x = l \quad s = K_{s_-} \quad (3.11b)$$

Alternatively, if B reacts at the electrode surface alone we must solve equation (3.9) for s , substitute into equation (3.10) and solve with the boundary conditions

$$\text{at } x = 0 \quad b = 0 \quad (3.12a)$$

$$\text{at } x = l \quad b = 0 \quad (3.12b)$$

In this case it is instructive to consider a number of approximate solutions obtained when the different reactions involved are assumed to be rate limiting. In section 3.3 these approximate solutions are compared to the results obtained by digital simulation of such a system by Mel and Maloy⁽¹⁴⁵⁾.

3.1.2 Case A: $(k_{cat} + ka)s > K_M ka$

The rate limiting step in this case is either the breakdown of the enzyme-substrate complex, described by k_{cat} , or regeneration of E_1 , described by ka . Under these conditions equation (3.9) becomes

$$D_S \frac{d^2 s}{dx^2} - \frac{k_{cat} kae_{\Sigma}}{k_{cat} + ka} = 0 \quad (3.13)$$

and equation (3.10) becomes

$$D_B \frac{d^2 b}{dx^2} + \frac{k_{cat} kae_{\Sigma}}{k_{cat} + ka} = 0 \quad (3.14)$$

Equations (3.13) and (3.14) must now be solved for S and B respectively.

Integrating equation (3.13) twice shows that the solution is of the form

$$s = \frac{k_{cat} kae_{\Sigma} x^2}{2D_S(k_{cat} + ka)} + A_1 x + B_1 \quad (3.15)$$

Similarly the solution to equation (3.14) is of the form

$$b = \frac{-k_{cat} kae_{\Sigma} x^2}{2D_B(k_{cat} + ka)} + A_2 x + B_2 \quad (3.16)$$

Substitution of boundary conditions (3.11a) and (3.11b) to find A_1 and A_2 , and rearrangement gives the following expression for s

$$s = \frac{k_{cat} kae_{\Sigma}}{2D_S(k_{cat} + ka)} (x^2 - l^2) + K s_{\infty} \quad (3.17)$$

The expression for the flux of s, j_s , is given by the following

$$j_s = D_S \left[\frac{ds}{dx} \right]_{x=l} = \frac{k_{cat} kae_{\Sigma} l}{k_{cat} + ka} \quad (3.18)$$

Equation (3.18) shows that in this case the flux of substrate consumed by the film is simply the product of the film thickness with the slower of the two steps, k_{cat} or ka . It is interesting to note that in either of these cases the rate limiting step is independent of s . Equation (3.18) is appropriate if B reacts on the conducting polymer. If B reacts only at the electrode surface we must obtain an expression for b .

Substitution of boundary conditions (3.12a) and (3.12b) into equation (3.16)

gives the following expression

$$b = \frac{k_{cat} k a e_{\Sigma}}{2D_B(k_{cat} + ka)}(lx - x^2) \quad (3.19)$$

The flux of B reacting at the electrode surface, j_B , is given by

$$j_B = D_B \left[\frac{db}{dx} \right]_{x=0} = \frac{k_{cat} k a e_{\Sigma} l}{2(k_{cat} + ka)} \quad (3.20)$$

This expression is appropriate if B reacts only on the electrode surface. It can be seen that $j_B = j_s/2$. This arises because in this case B is being generated at a uniform rate throughout the film and is equally likely to be lost to the bulk solution as to react at the electrode.

3.1.3 Case B: $(k_{cat} + ka)s < K_M ka$

In this case the rate limiting step is the enzyme, E_1 , substrate reaction. The rate now becomes dependent on the concentration of substrate. Under these conditions equation (3.9) becomes

$$D_s \frac{d^2 s}{dx^2} - \frac{k_{cat} s e_{\Sigma}}{K_M} = 0 \quad (3.21)$$

and equation (3.10) becomes

$$D_B \frac{d^2 b}{dx^2} + \frac{k_{cat} s e_{\Sigma}}{K_M} = 0 \quad (3.22)$$

The solution for s is then of the form

$$s = A_3 \exp\left(\frac{x}{X_K}\right) + B_3 \exp\left(\frac{-x}{X_K}\right) \quad (3.23)$$

where

$$X_K = (D_s K_M / k_{cat} e_{\Sigma})^{1/2}$$

Substitution of the boundary conditions (3.11a) and (3.11b) and rearrangement gives

the required expression for s

$$s = K_{s_{\infty}} \cosh(x/X_K) / \cosh(l/X_K) \quad (3.24)$$

The flux of s , j_s , is then given by

$$j_s = D_s K_{s_{\infty}} \tanh(l/X_K) / X_K \quad (3.25)$$

Once again j_s is only appropriate if B reacts on the polymer. If B reacts on the electrode alone then we must obtain the appropriate expression for the flux of B, j_B .

Substitution of equation (3.24) into equation (3.22) and integration gives

$$b = \frac{-K_M \cosh(x/X_K)}{\cosh(l/X_K)} + A_4 x + B_4 \quad (3.26)$$

Determination of A_4 and B_4 by substitution of boundary conditions (3.12a) and (3.12b) gives

$$b = [D_s K_{s_{\infty}} / D_B \cosh(l/X_K)] [\{\cosh(l/X_K) - 1\}x/l + 1 - \cosh(x/X_K)] \quad (3.27)$$

The flux of B to the electrode surface, j_B , is obtained by differentiation of equation (3.27) and substitution into (3.28)

$$j_B = D_B \left[\frac{db}{dx} \right]_{x=0} \quad (3.28)$$

to give the following

$$j_B = D_s K_{s_{\infty}} [1 - \operatorname{sech}(l/X_K)] / l \quad (3.29)$$

The expressions for s , b , j_s and j_B in each case are summarised in table 3.1.

Table 3.1

Expressions for the concentration and fluxes of S and B in the different limiting cases.

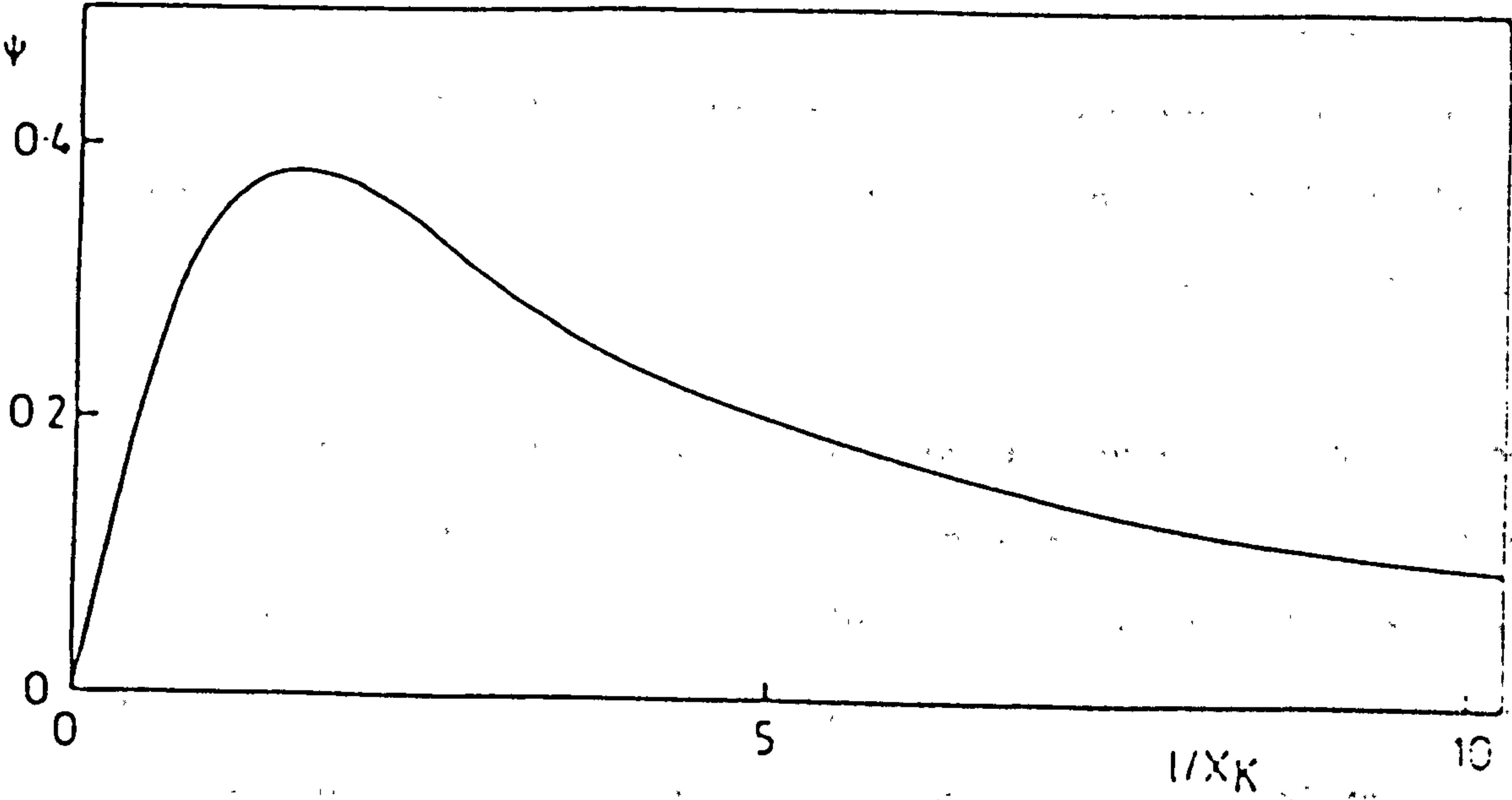
Parameter	Expression	Eqn.no.
Case A: $(k_{cat}+ka)s > K_M ka$		
s	$[k_{cat}kae_{\Sigma}/2D_S(k_{cat}+ka)](x^2-l^2)+K_{S_{\infty}}$	3.17
b	$[k_{cat}kae_{\Sigma}/2D_B(k_{cat}+ka)](lx-x^2)$	3.19
j_s	$k_{cat}kae_{\Sigma}l/(k_{cat}+ka)$	3.18
j_B	$k_{cat}kae_{\Sigma}l/2(k_{cat}+ka)$	3.20
Case B: $(k_{cat}+ka)s < K_M ka$		
s	$K_{S_{\infty}}\cosh(x/X_K)/\cosh(l/X_K)$	3.24
b	$[D_S K_{S_{\infty}}/D_B \cosh(l/X_K)] [\{\cosh(l/X_K)-1\}x/l+1-\cosh(x/X_K)]$	3.27
j_s	$D_S K_{S_{\infty}} \tanh(l/X_K)/X_K$	3.25
j_B	$D_S K_{S_{\infty}} [1-\text{sech}(l/X_K)]/l$	3.29

Equation (3.29) predicts a maximum in j_B as a function of l . A plot of the dimensionless flux, given by $j_B X_K / (D_S K_{S_{\infty}})$ as a function of the normalised film thickness, l/X_K , is shown in figure 3.2. Equation (3.29) shows that when the film thickness is much less than the kinetic length ($l \ll X_K$) then

$$j_B \approx K_{S_{\infty}} e_{\Sigma} l / 2 K_M \quad (3.30)$$

In this “thin” film situation increasing l or e_{Σ} increases the current because S is being consumed uniformly across the film. However when the film is significantly thicker than the kinetic length ($l \gg X_K$) then equation (3.29) becomes

Figure 3.2 A plot of the dimensionless flux, ψ , as a function of the normalised film thickness, l/X_K .



$$j_B \approx D_s K_s / l \quad (3.31)$$

In this situation all of the substrate is consumed by reaction in the film. Corresponding concentration profiles for this “thick” film situation are shown in figure 3.3. Here increasing the film thickness decreases the response. Furthermore changing the enzyme loading does not affect the current response. As the reaction is occurring mainly near to the polymer-solution interface then increasing the film thickness means that B produced must simply diffuse further to reach the electrode. This explains the theoretical decrease in response with increasing film thickness described by equation (3.31). The different cases are collected together on the case diagram in figure 3.4.

In this theoretical treatment we have not used an approximation to describe Michaelis-Menten kinetics since the observed electrode responses are linear to very high substrate concentrations. This linearity is indicative of a low partition coefficient for substrate into the polymer film in the case of poly-*N*-methylpyrrole. However the current responses observed when other polymers are used are seen to saturate. This reflects a change in partition coefficient between different polymers and the adjacent aqueous phase.

In cases where a saturation response to substrate is observed we must use an approximation for the Michaelis-Menten kinetics in the development of a useful theoretical treatment. By comparing experimental results to the appropriate theoretical model it is possible to determine whether the saturation response, seen at high substrate concentrations is due to a Michaelis-Menten type kinetic turnover. However if this is not the case the reaction limiting the response at high substrate concentration can be identified.

A further advantage in the use of the approximation is that it allows fitting of all the experimental data in cases where non-linear response curves are obtained. In the case of poly-*N*-methylpyrrole systems, in which oxygen is the mediator, this type

Figure 3.3 Plots of the normalised concentration profiles for S (a) and B (b) in the film as a function of x/l . The values of l/X_K are shown for each curve. ($\phi_S = s/K_{s\infty}$, $\phi_B = b D_B/D_S K_{s\infty}$).

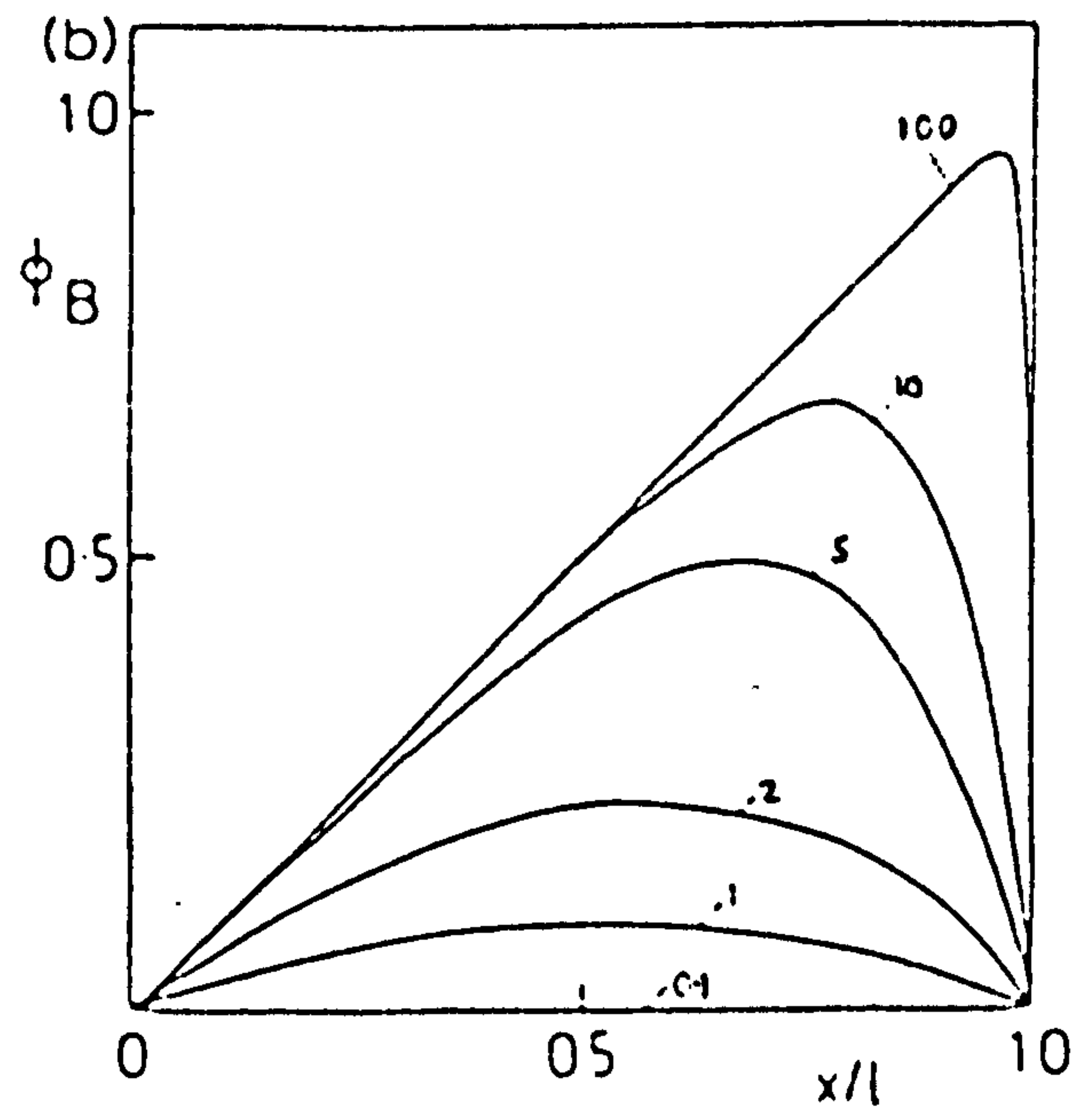
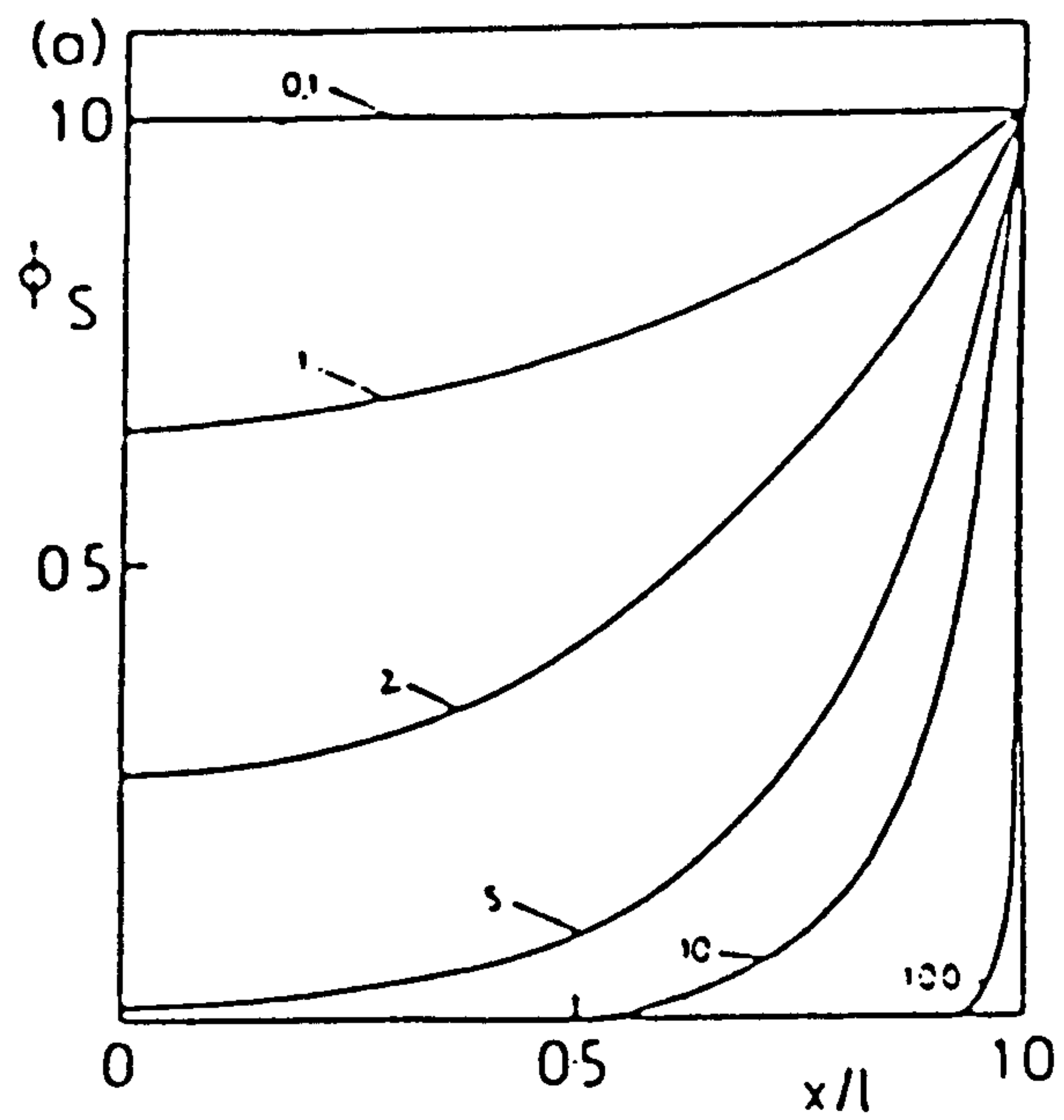
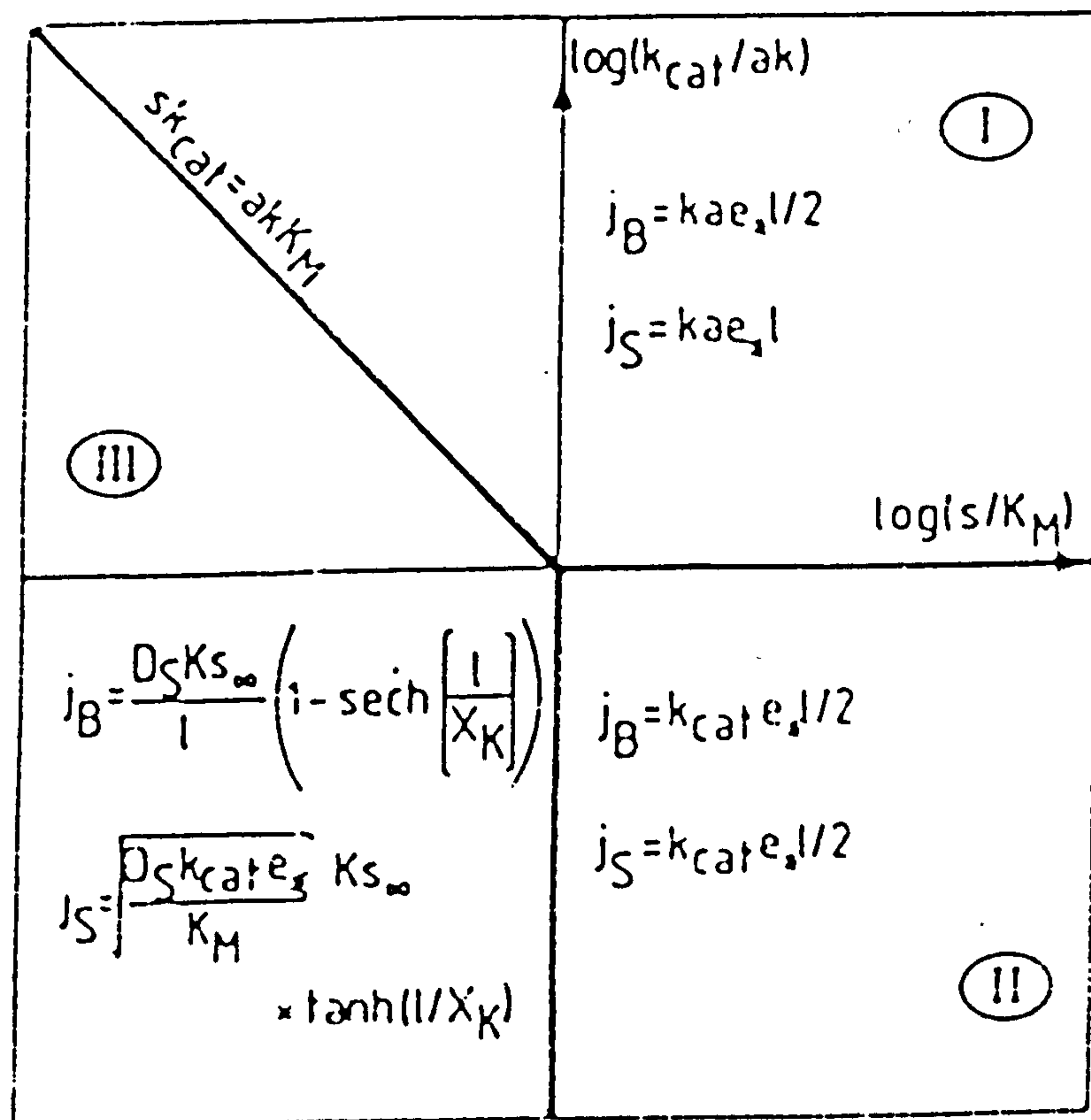


Figure 3.4 Case diagram for the system showing three cases and approximate expressions for j_S and j_B in each case. The bold lines show the case boundaries.



of theoretical model is not advantageous since linear current responses were observed in all cases.

In the following sections a theory for the response of an immobilised enzyme system in which a non-linear substrate response is seen will be described. Polymers found to give this type of response, with oxygen as mediator, were of a non-conducting type. This means that detection of the reduced oxidant, B, can now only occur at the electrode surface.

3.1.4 Non-linear Dependence of Current on Substrate Concentration

In this section an extension of the previous theory is presented. This enables us to fit all data from experiments using polymer/enzyme combinations which do not give linear substrate response curves. Use of the previous theory would only allow fitting of the data for limiting conditions; for example very high and very low substrate concentrations.

This improved theoretical treatment of an immobilised enzyme system uses an approximation to deal with saturation kinetics and makes similar assumptions to those made initially in section 3.1.1. We assume, once again, that a is a constant. This means that there is no concentration polarisation of the mediator oxygen.

From the previous theoretical treatment, equation (3.9)

$$D_s \frac{d^2 s}{dx^2} - \frac{k_{cat} k_a e_\Sigma}{k_{cat} s + K_M k_a + k a s} = 0$$

We can define a number of parameters in order to simplify the derivation of the theory.

$$v = s/s_\infty$$

and as was shown previously, in section 3.1.3

$$X_K = (D_s K_M / k_{cat} e_\Sigma)^{1/2}$$

Using the ratio v then

$$\frac{d^2v}{d\chi^2} - \frac{K_M kav}{K_M ka + (k_{cat} s_{\infty} + ka s_{\infty})v} = 0 \quad (3.32)$$

where χ is the dimensionless distance given by x/X_K . In order to simplify this expression further we can define the following ratio parameters

$$\beta = k_{cat}/ka \quad \text{and} \quad \gamma = s_{\infty}/K_M.$$

Substitution of these parameters into (3.32) gives

$$\frac{d^2v}{d\chi^2} - \frac{v}{1 + \gamma(1 + \beta)v} = 0 \quad (3.33)$$

We now use the approximation

$$\frac{u}{1 + Au} \approx \frac{A + u}{(1 + A)^2}, \quad 0 \ll u \ll 1 \quad (3.34)$$

where u is the normalised substrate concentration given by v and A is equal to $\gamma(1 + \beta)$. Now

$$\frac{d^2v}{d\chi^2} - \frac{\gamma(1 + \beta) + v}{\{1 + \gamma(1 + \beta)\}^2} = 0 \quad (3.35)$$

The solution to this expression is then of the form

$$\gamma(1 + \beta) + v = B_1 \exp\left(\frac{\chi}{1 + \gamma(1 + \beta)}\right) + B_2 \exp\left(\frac{-\chi}{1 + \gamma(1 + \beta)}\right) \quad (3.36)$$

and

$$\frac{dv}{d\chi} = \frac{B_1}{1 + \gamma(1 + \beta)} \exp\left(\frac{\chi}{1 + \gamma(1 + \beta)}\right) - \frac{B_2}{1 + \gamma(1 + \beta)} \exp\left(\frac{-\chi}{1 + \gamma(1 + \beta)}\right) \quad (3.37)$$

Solution of equation (3.37) with the boundary conditions

$$\begin{aligned} \text{at } x = 0 \quad ds/dx &= 0 \\ \text{at } x = l \quad s &= s_{\infty} \end{aligned}$$

shows that

$$B_1 = B_2 = 1 + \gamma(1 + \beta) / 2 \cosh[l / X_K \{1 + \gamma(1 + \beta)\}]$$

Substitution of the integration constants B_1 and B_2 into equation (3.37) gives

$$v = 1 + \gamma(1 + \beta) \frac{\cosh\left(\frac{\chi}{1 + \gamma(1 + \beta)}\right)}{\cosh\left(\frac{l}{X_K \{1 + \gamma(1 + \beta)\}}\right)} - \gamma(1 + \beta) \quad (3.38)$$

If b reacts on the polymer we must obtain an expression for j_s , the flux of S .

$$\left. \frac{dv}{d\chi} \right|_{\chi=l/X_K} = \left[\frac{l}{X_K \{1 + \gamma(1 + \beta)\}} \right]$$

and

$$j_s = \frac{D_s s_\infty}{X_K} \left. \frac{dv}{d\chi} \right|_{\chi=l/X_K}$$

so that

$$j_s = \frac{D_s s_\infty}{X_K} \tanh\left(\frac{l}{X_K \{1 + \gamma(1 + \beta)\}}\right) \quad (3.39)$$

We can obtain j_s expressions for each possible case by making assumptions about the rate limiting reaction.

i) $k_{cat}/ka \gg 1$

In this case it is the reaction between E_2 and the mediator A which is rate limiting, so that

$$j_s = \frac{D_s s_\infty}{X_K} \tanh\left(\frac{l}{X_K (1 + \gamma\beta)}\right) \quad (3.40)$$

If we assume that $\gamma\beta \gg 1$ then

$$j_s = \frac{D_s s_\infty}{X_K} \tanh\left(\frac{l}{\gamma\beta X_K}\right) \quad (3.40a)$$

and when

$$\begin{aligned}
l/\gamma\beta X_K &\ll 1, \quad j_s = k_a e_\Sigma l && \text{Case I} \\
l/\gamma\beta X_K &\gg 1, \quad j_s = s_\infty (D_s k_{cat} e_\Sigma / K_M)^{1/2} && \text{Case IIIa}
\end{aligned}$$

Alternatively, when $\gamma\beta \ll 1$ then

$$j_s = \frac{D_s s_\infty}{X_K} \tanh\left(\frac{l}{X_K}\right) \quad (3.40b)$$

and when

$$\begin{aligned}
l/X_K &\gg 1, \quad j_s = s_\infty (D_s k_{cat} e_\Sigma / K_M)^{1/2} && \text{Case IIIa} \\
l/X_K &\ll 1, \quad j_s = s_\infty k_{cat} e_\Sigma l / K_M && \text{Case IIIb}
\end{aligned}$$

ii) $k_{cat}/k_a \ll 1$

In this case the reaction described by k_{cat} becomes rate limiting so that

$$j_s = \frac{D_s s_\infty}{X_K} \tanh\left(\frac{l}{X_K(1+\gamma)}\right) \quad (3.41)$$

If we assume that $\gamma > 1$ then

$$j_s = \frac{D_s s_\infty}{X_K} \tanh\left(\frac{l}{\gamma X_K}\right) \quad (3.41a)$$

and when

$$\begin{aligned}
l/\gamma X_K &< 1, \quad j_s = k_{cat} e_\Sigma l && \text{Case II} \\
l/\gamma X_K &> 1, \quad j_s = s_\infty (D_s k_{cat} e_\Sigma / K_M)^{1/2} && \text{Case IIIa}
\end{aligned}$$

Alternatively, when $\gamma < 1$ then

$$j_s = \frac{D_s s_\infty}{X_K} \tanh\left(\frac{l}{X_K}\right) \quad (3.41b)$$

and when

$$\begin{aligned}
l/X_K &> 1, \quad j_s = s_\infty (D_s k_{cat} e_\Sigma / K_M)^{1/2} && \text{Case IIIa} \\
l/X_K &< 1, \quad j_s = s_\infty k_{cat} e_\Sigma l / K_M && \text{Case IIIb}
\end{aligned}$$

The expressions for j_s together with the dependence on each of the reactants are

given in table 3.2. It is apparent that a unique pattern of reaction orders is found for each theoretical case.

Table 3.2
Expressions for j_s and the rate dependencies for each case

Case	j_s expression	Reaction order			
		e_Σ	l	a_∞	s_∞
I	$kae_\Sigma l$	1	1	1	0
II	$k_{cat} e_\Sigma l$	1	1	0	0
IIIa	$s_\infty (Dk_{cat} e_\Sigma / K_M)^{1/2}$	1/2	0	0	1
IIIb	$s_\infty k_{cat} e_\Sigma l / K_M$	1	1	0	1

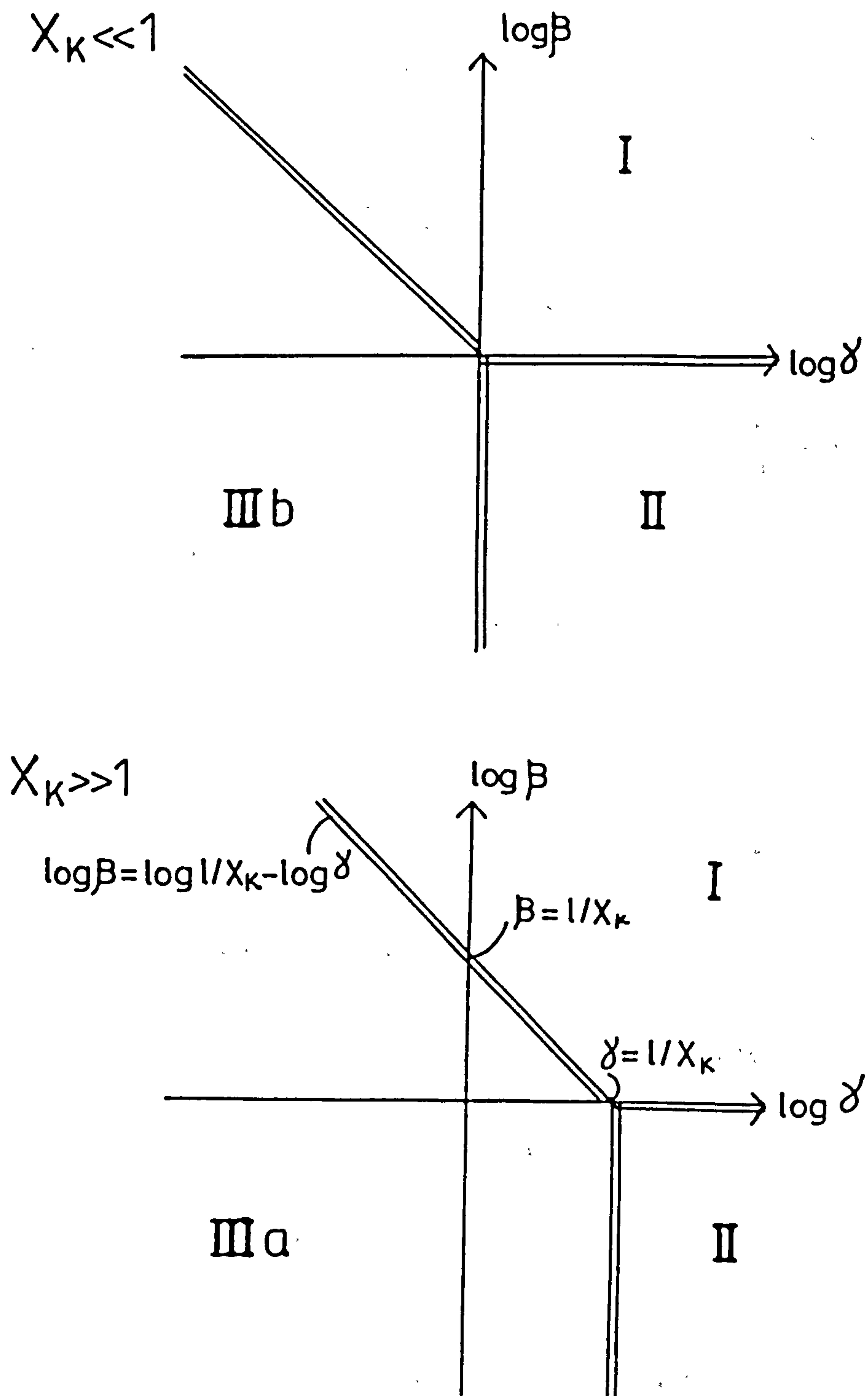
The case diagrams demonstrating the relationship of these cases to each other is shown in figure 3.5. This is essentially similar to the case diagram in figure 3.4. However we now have expressions describing crossover of the case boundaries so that data in all regions of the case diagram can be fitted to the appropriate theoretical expression.

These expressions for j_s are appropriate only if B reacts on the conducting polymer. However, data obtained for this type of situation was from experiments using insulating polymers. In such cases B must diffuse to the electrode surface to react and, once again, we are interested in expressions for j_B , the flux of B to the electrode surface.

To find j_B we must substitute equation (3.38) into the expression for b , equation (3.10).

$$D_B \frac{d^2 b}{dx^2} + \frac{k_{cat} k_a s e_\Sigma}{k_{cat} s + K_M k_a + k a s}$$

Figure 3.5 Case diagram showing the relationship between the different j_s expressions when an approximation is used to describe a saturation type current response (section 3.1.4).



Making $u = b/a_\infty$ then

$$\frac{d^2u}{d\chi^2} + \frac{D_s s_\infty v}{D_B a_\infty [1+\gamma(1+\beta)v]} = 0 \quad (3.42)$$

Integration of equation (3.42) with the following boundary conditions gives the required expression for j_B

$$\text{at } x=0 \quad b=0$$

$$\text{at } x=l \quad b=0$$

Taking equation (3.42) we once again use approximation (3.34) so that

$$\frac{d^2u}{d\chi^2} + \frac{D_s s_\infty}{D_B a_\infty} \left\{ \frac{\gamma(1+\beta)+v}{[1+\gamma(1+\beta)]^2} \right\} = 0 \quad (3.43)$$

Substitution of v from equation (3.38) gives

$$\frac{d^2u}{d\chi^2} + \frac{D_s s_\infty}{D_B a_\infty \{1+\gamma(1+\beta)\}} \frac{\cosh[\chi/\{1+\gamma(1+\beta)\}]}{\cosh[l/X_K \{1+\gamma(1+\beta)\}]} = 0 \quad (3.44)$$

Integration of this expression gives

$$\frac{du}{d\chi} + \frac{D_s s_\infty}{D_B a_\infty} \frac{\sinh[\chi/\{1+\gamma(1+\beta)\}]}{\cosh[l/X_K \{1+\gamma(1+\beta)\}]} + B_3 = 0 \quad (3.45)$$

Integration again gives

$$u + \frac{D_s s_\infty}{D_B a_\infty \{1+\gamma(1+\beta)\}} \frac{\cosh[\chi/\{1+\gamma(1+\beta)\}]}{\cosh[l/X_K \{1+\gamma(1+\beta)\}]} + B_3 \chi + B_4 = 0 \quad (3.46)$$

Substitution of the boundary conditions shows that

$$u = \frac{D_s s_\infty}{D_B a_\infty} \frac{\{1+\gamma(1+\beta)\}}{\cosh[l/X_K \{1+\gamma(1+\beta)\}]} \left\{ \frac{X_K}{l} [\cosh[l/X_K \{1+\gamma(1+\beta)\}] - 1] \chi + 1 - \cosh[\chi/\{1+\gamma(1+\beta)\}] \right\} \quad (3.47)$$

Now we require an expression for j_B where

$$j_B = D_B \left. \frac{db}{dx} \right|_{x=0} = D_B \frac{a_\infty}{X_K} \left. \frac{du}{d\chi} \right|_{\chi=0} \quad (3.48)$$

and

$$\frac{du}{d\chi} = \frac{D_s s_\infty \{1+\gamma(1+\beta)\}}{D_B a_\infty \cosh[l/X_K \{1+\gamma(1+\beta)\}]} \left\{ \frac{X_K}{l} \left[\cosh[l/X_K \{1+\gamma(1+\beta)\}] - 1 \right] - \frac{\sinh[\chi l \{1+\gamma(1+\beta)\}]}{\{1+\gamma(1+\beta)\}} \right\} \quad (3.49)$$

Substituting in for $\chi = 0$ gives

$$\left. \frac{du}{d\chi} \right|_{\chi=0} = \frac{D_s s_\infty \{1+\gamma(1+\beta)\}}{D_B a_\infty \cosh[l/X_K \{1+\gamma(1+\beta)\}]} \frac{X_K}{l} \left\{ \cosh[l/X_K \{1+\gamma(1+\beta)\}] - 1 \right\} \quad (3.50)$$

and for $\chi = l/X_K$

$$\left. \frac{du}{d\chi} \right|_{\chi=l/X_K} = \frac{D_s s_\infty \{1+\gamma(1+\beta)\}}{D_B a_\infty \cosh[l/X_K \{1+\gamma(1+\beta)\}]} \left\{ \frac{X_K}{l} \left[\cosh[l/X_K \{1+\gamma(1+\beta)\}] - 1 \right] - \frac{\sinh[l/X_K \{1+\gamma(1+\beta)\}]}{\{1+\gamma(1+\beta)\}} \right\} \quad (3.51)$$

It is apparent that

$$\begin{aligned} \left. \frac{du}{d\chi} \right|_{\chi=0} - \left. \frac{du}{d\chi} \right|_{\chi=l/X_K} &= \frac{D_s s_\infty \{1+\gamma(1+\beta)\}}{D_B a_\infty \cosh[l/X_K \{1+\gamma(1+\beta)\}]} \left\{ \frac{\sinh[l/X_K \{1+\gamma(1+\beta)\}]}{\{1+\gamma(1+\beta)\}} \right\} \\ &= \frac{D_s s_\infty}{D_B a_\infty} \tanh[l/X_K \{1+\gamma(1+\beta)\}] \end{aligned} \quad (3.52)$$

The fluxes of S and B are seen to balance as expected in this system

$$j_{B(\chi=0)} - j_{B(\chi=l/X_K)} = j_{S(\chi=l/X_K)}$$

As the expression for j_B is given by

$$j_B = D_B \frac{a_\infty}{X_K} \left. \frac{du}{d\chi} \right|_{\chi=0}$$

then the required expression is given by

$$j_B = \frac{D_s s_\infty 1+\gamma(1+\beta)}{X_K \cosh[l/X_K \{1+\gamma(1+\beta)\}]} \frac{X_K}{l} \left\{ \cosh[l/X_K \{1+\gamma(1+\beta)\}] - 1 \right\} \quad (3.53)$$

so that

$$j_B = \frac{D_s s_\infty (1+\gamma(1+\beta))}{l} \left\{ 1 - \text{sech}[l/X_K \{1+\gamma(1+\beta)\}] \right\} \quad (3.54)$$

We can obtain j_B expressions for each possible case by making assumptions about the rate limiting reaction.

iii) $k_{cat}/ka \gg 1$

In this case we are again assuming that it is the reaction between E_2 and the mediator which is limiting.

$$j_B = D_s s_\infty (1+\gamma\beta)/l \{1 - \text{sech}[l/X_K \{1+\gamma(1+\beta)\}]\} \quad (3.55)$$

If we now assume that $\gamma\beta \gg 1$ then

$$j_B = D_s s_\infty \gamma\beta/l \{1 - \text{sech}[l/X_K \gamma\beta]\} \quad (3.55a)$$

and when

$$\begin{aligned} l/X_K \gamma\beta \ll 1, \quad j_B &= k a_\infty e_\Sigma l/2 & \text{Case I} \\ l/X_K \gamma\beta \gg 1, \quad j_B &= D_s s_\infty^2 k_{cat}/l K_M k a_\infty & \text{Case IV} \end{aligned}$$

Alternatively when $\gamma\beta \ll 1$ then

$$j_B = D_s s_\infty/l \{1 - \text{sech}[l/X_K]\} \quad (3.55b)$$

and when

$$\begin{aligned} l/X_K \gg 1, \quad j_B &= D_s s_\infty/l & \text{Case IIIa} \\ l/X_K \ll 1, \quad j_B &= k_{cat} e_\Sigma s_\infty l/2 K_M & \text{Case IIIb} \end{aligned}$$

iv) $k_{cat}/ka \ll 1$

In this case it is the reaction described by k_{cat} that is assumed to be rate limiting so that

$$j_B = D_s s_\infty (1+\gamma)/l \{1 - \text{sech}[l/X_K (1+\gamma)]\} \quad (3.56)$$

If we assume that $\gamma > 1$ then

$$j_B = D_s s_\infty \gamma / l \{ 1 - \text{sech}[l / \gamma X_K] \} \quad (3.56a)$$

and when

$$l / \gamma X_K < 1, \quad j_B = k_{cat} e_\Sigma l / 2 \quad \text{Case II}$$

$$l / \gamma X_K > 1, \quad j_B = D_s s_\infty^2 / l K_M \quad \text{Case V}$$

Alternatively when $\gamma < 1$ then

$$j_B = D_s s_\infty / l \{ 1 - \text{sech}[l / X_K] \} \quad (3.56b)$$

and when

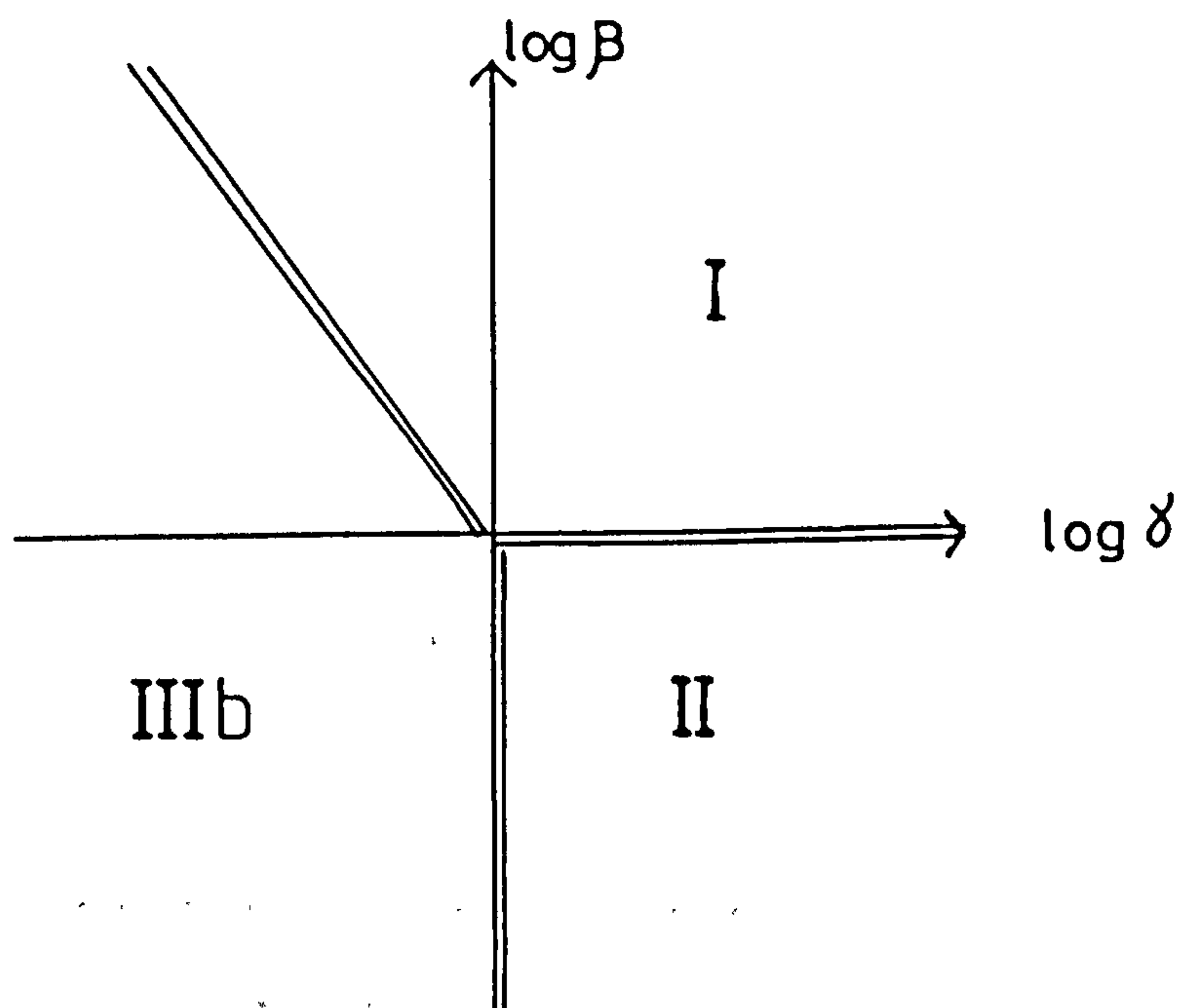
$$l / X_K > 1, \quad j_B = D_s s_\infty / l \quad \text{Case IIIa}$$

$$l / X_K < 1, \quad j_B = s_\infty k_{cat} e_\Sigma s_\infty l / 2 K_M \quad \text{Case IIIb}$$

The expressions for the flux of B to the electrode surface, j_B , and the reaction orders with respect to each of the reactants are summarised in Table 3.3. Once again it is apparent that there is a unique pattern of reaction order dependencies in each case. This should allow the data from each experiment to be placed on the case diagram and the boundary crossing concerned to be identified. The case diagram showing the relationships of the 6 cases is shown in figure 3.6. In chapter 4 data obtained for polyaniline / glucose oxidase and polyphenol / glucose oxidase system are fitted to this theory and the resulting kinetic parameters presented.

Figure 3.6 Case diagram showing the relationship between the different j_B expressions when an approximation is used to describe a saturation type current response (section 3.1.4).

$l/X_K \ll 1$



$l/X_K \gg 1$

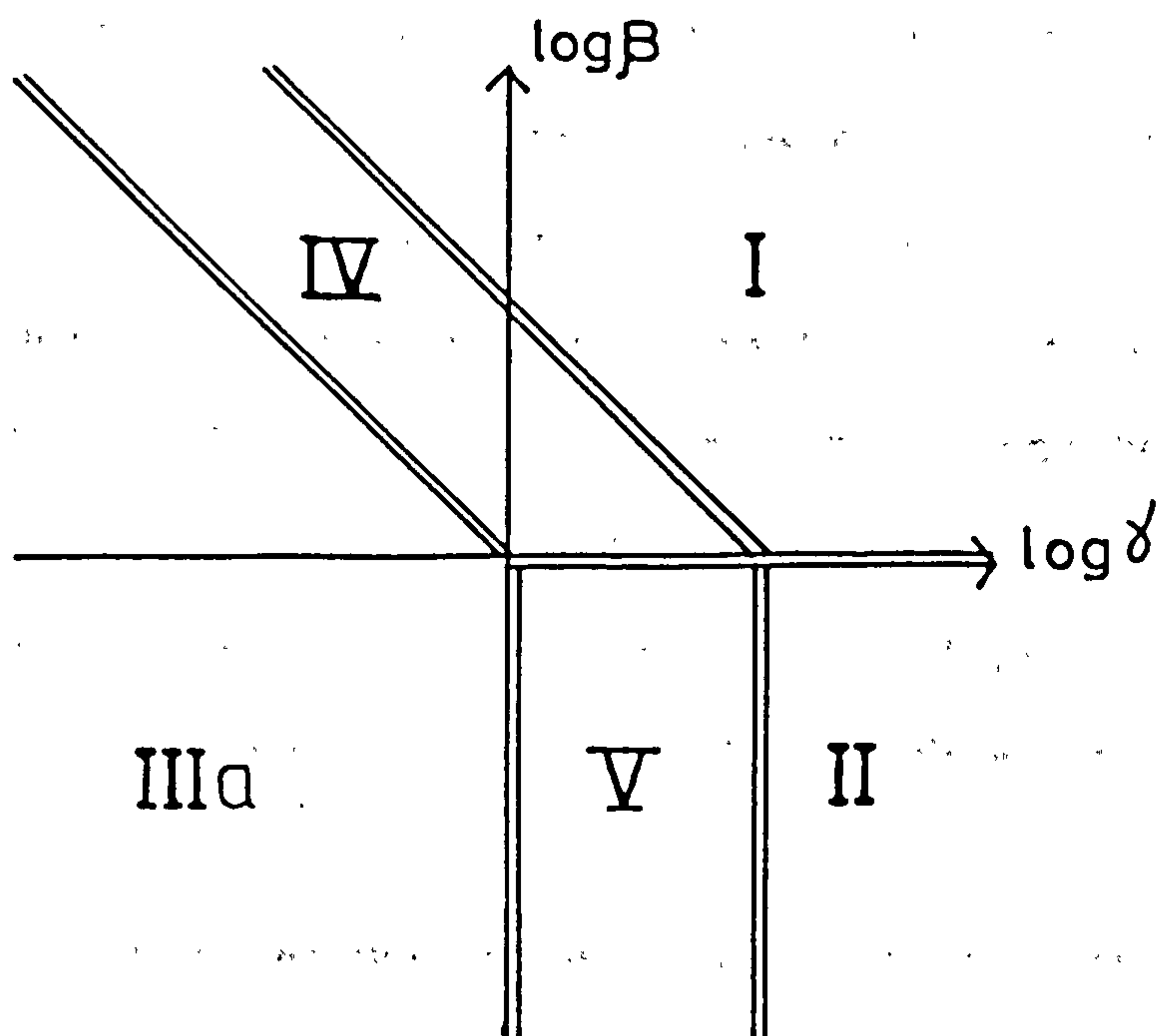


Table 3.3

Expressions for j_B and the dependencies in each case

Case	j_B expression	Reaction order			
		e_Σ	l	a_∞	s_∞
I	$ka_\infty e_\Sigma l/2$	1	1	1	0
II	$k_{cat} e_\Sigma l/2$	1	1	0	0
IIIa	$D_s s_\infty/l$	0	-1	0	1
IIIb	$k_{cat} e_\Sigma s_\infty l/2K_M$	1	1	0	1
IV	$D_s s_\infty^2 k_{cat} l/K_M k a_\infty$	0	-1	-1	2
V	$D_s s_\infty^2/lK_M$	0	-1	0	2

3.2 REACTION OF THE MEDIATOR ON THE CONDUCTING POLYMER IMMOBILISATION MATRIX

In the theoretical model presented in section 3.1 expressions for j_s and j_B were derived for each possible kinetic case. This theory relates to a situation in which the enzymically active, oxidised, form of the mediator, A, is present in the bulk solution. Furthermore there is no provision in this theory for concentration polarisation of A. Chapter 4 shows that all data from experiments involving the detection of hydrogen peroxide fits well to this theory when the j_B expressions are used to describe reaction of B at the electrode surface. In such cases there is no available evidence to suggest that reaction of B occurs on the polymer itself or that A is concentration polarised.

When the artificial mediator ferrocene monocarboxylic acid is used to accept electrons from the reduced form of the immobilised enzyme a different situation

arises. Now the reduced form of the mediator is added to the bulk solution. This is oxidised within the polymer to produce the enzymically active form of this mediator.

The theory developed below describes a situation in which the mediator, A, is produced electrochemically within the polymer film, or on the electrode surface and the enzymically produced reduced form of the mediator, B, is detected either on the polymer film or on the electrode surface. A study of the experimental data obtained from such a system allows the reaction site of the mediator to be determined. Such an analysis is presented in chapter 5 of this thesis.

We will begin by describing the kinetic scheme for such a system.

3.2.1 The Kinetic Scheme

In this system the reduced mediator is oxidised with a rate constant k' . The oxidised form of the enzyme then reoxidises the substrate reduced enzyme with a rate constant k_m . The kinetic scheme is shown in figure 3.7.

We begin by constructing equations for the concentrations of A and S, the species which react directly with the enzyme.

$$D_A \frac{d^2 a}{dx^2} + k'(a_\infty - a) - \frac{k_M k_E s e_\Sigma a}{k_M a + k_E s} = 0 \quad (3.57)$$

and

$$D_s \frac{d^2 s}{dx^2} - \frac{k_M k_E s e_\Sigma a}{k_M a + k_E s} = 0 \quad (3.58)$$

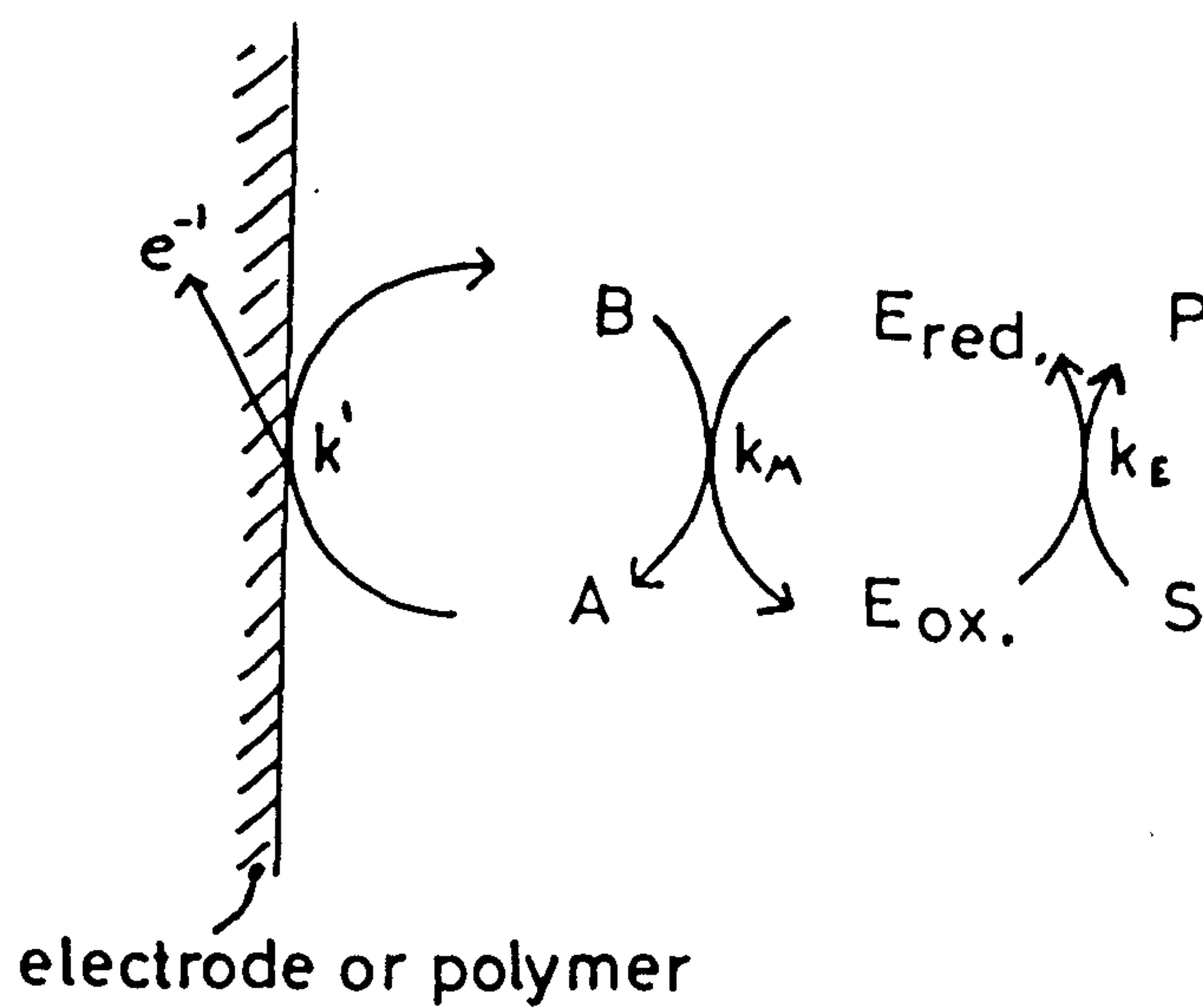
We also define a number of ratios at this stage. This will allow the derivation of the theory to be simplified. These dimensionless variables are as follows

$$u = a/a_\infty$$

$$v = s/s_\infty$$

$$X_K = (D/k')^{1/2}$$

Figure 3.7 Kinetic scheme for the reaction of the reduced mediator at the electrode or polymer surface.



The notation used is described fully in section 3.2.

$$\phi = a_{\infty}/s_{\infty}$$

$$\gamma = k_M a_{\infty}/k_E s_{\infty}$$

$$\beta = k_M e_{\Sigma}/k'$$

Use of these dimensionless variables allows equation (3.57) to be written in the form

$$\frac{d^2 u}{d\chi^2} + (1-u) = \frac{\beta uv}{\gamma u+v} = 0 \quad (3.57a)$$

and equation (3.58) to be written as

$$\frac{d^2 v}{d\chi^2} + \frac{\beta uv \phi}{\gamma u+v} = 0 \quad (3.58a)$$

Looking at the kinetic scheme, figure 3.7, it can be seen that

$$\gamma \gg 1, k_M a_{\infty} \gg k_E s_{\infty} \text{ all enzyme in } E_1 \text{ form.}$$

$$\gamma \ll 1, k_M a_{\infty} \ll k_E s_{\infty} \text{ all enzyme in } E_2 \text{ form.}$$

$$\beta \gg 1, k_M e_{\Sigma} \gg k' \text{ all mediator in B form.}$$

$$\beta \ll 1, k_M e_{\Sigma} \ll k' \text{ all mediator in A form.}$$

$$\phi \gg 1, a_{\infty} \gg s_{\infty}$$

$$\phi \ll 1, s_{\infty} \gg a_{\infty}$$

We start by considering the situation when $\gamma \ll 1$.

i) $k_M a_{\infty} \ll k_E s_{\infty}$

In this situation equations (3.57a) and (3.58a) become

$$\frac{d^2 u}{d\chi^2} + (1-u) - \beta u = 0 \quad (3.59)$$

and

$$\frac{d^2 v}{d\chi^2} + \beta u \phi = 0 \quad (3.60)$$

Rearranging equation (3.59) gives

$$\frac{d^2u}{d\chi^2} - (1+\beta)u + 1 = 0 \quad (3.61)$$

The solution to this expression is of the form

$$(1+\beta)u - 1 = B_5 \exp\left[\chi(1+\beta)^{1/2}\right] + B_6 \exp\left[-\chi(1+\beta)^{1/2}\right] \quad (3.62)$$

Using the boundary conditions

$$\begin{aligned} \chi = 0 \quad u &= 1 \\ \chi = l/X_K \quad u &= 1 \end{aligned}$$

and substituting into (3.62) gives expressions for the two integration constants.

$$B_5 = \frac{\beta[1 - \exp(-l(1+\beta)^{1/2}/X_K)]}{2\sinh(l(1+\beta)^{1/2}/X_K)}$$

and

$$B_6 = \frac{\beta[\exp(l(1+\beta)^{1/2}/X_K) - 1]}{2\sinh(l(1+\beta)^{1/2}/X_K)}$$

Substitution back into equation (3.62) gives the required expression for u as

$$u = \frac{1}{1+\beta} \left[1 + \beta \left[\frac{\sinh\{\chi(1+\beta)^{1/2}/X_K\} + \sinh\{(l-\chi)(1+\beta)^{1/2}/X_K\}}{\sinh\{l(1+\beta)^{1/2}/X_K\}} \right] \right] \quad (3.63)$$

so

$$\frac{d^2v}{d\chi^2} + \frac{\beta\phi(1+\beta)}{1+\beta} \left[\frac{\sinh\{\chi(1+\beta)^{1/2}/X_K\} + \sinh\{(l-\chi)(1+\beta)^{1/2}/X_K\}}{\sinh\{l(1+\beta)^{1/2}/X_K\}} \right] = 0 \quad (3.64)$$

Integration of equation 3.64 gives

$$\frac{dv}{d\chi} + \frac{\beta\phi\beta}{1+\beta} \left[\frac{\cosh\{\chi(1+\beta)^{1/2}/X_K\} - \cosh\{(l-\chi)(1+\beta)^{1/2}/X_K\}}{(1+\beta)^{1/2}\sinh\{l(1+\beta)^{1/2}/X_K\}} \right] + B_7 = 0 \quad (3.65)$$

In order to obtain an expression for j_s

$$\chi = 0 \quad dv/d\chi = 0$$

so that

$$\frac{\beta\phi}{1+\beta} \left[\frac{\beta[1 - \cosh\{l(1+\beta)^{1/2}/X_K\}]}{(1+\beta)^{1/2} \sinh\{l(1+\beta)^{1/2}/X_K\}} \right] = B_7$$

Substitution for B_7 into equation (3.65) gives

$$\begin{aligned} \frac{dv}{d\chi} + \frac{-\beta\phi}{1+\beta} \left[\chi + \frac{\beta}{(1+\beta)^{1/2} \sinh\{l(1+\beta)^{1/2}/X_K\}} [\cosh\chi(1+\beta)^{1/2} \right. \\ \left. - \cosh\{l(1+\beta)^{1/2}/X_K - \chi(1+\beta)^{1/2}\} - 1 + \cosh\{l(1+\beta)^{1/2}/X_K\}] \right] \end{aligned} \quad (3.66)$$

The expression for j_s is given by

$$j_s = D_s \left. \frac{ds}{dx} \right|_{x=l} = \frac{D_s s_\infty}{X_K} \left. \frac{dv}{d\chi} \right|_{\chi=l/X_K}$$

Therefore the required expression for j_s is given by

$$\begin{aligned} j_s = \frac{-D_s s_\infty}{X_K} \frac{\beta\phi}{1+\beta} \left[\frac{l}{X_K} + \frac{2\beta}{(1+\beta)^{1/2}} \left\{ \frac{1}{\tanh\{l(1+\beta)^{1/2}/X_K\}} \right. \right. \\ \left. \left. - \frac{1}{\sinh\{l(1+\beta)^{1/2}/X_K\}} \right\} \right] \end{aligned} \quad (3.67)$$

Different limiting cases can be obtained from this expression. If we assume that $l(1+\beta)^{1/2}/X_K \ll 1$ then

$$j_s + \frac{-D_s s_\infty \beta \phi l}{X_K^2 (1+\beta)} \quad (3.68)$$

and when

$$\begin{aligned} \beta \gg 1, \quad j_s &= -D_s s_\infty \phi l / X_K^2 = k' a_\infty l & \text{Case I} \\ \beta \ll 1, \quad j_s &= -D_s s_\infty \phi \beta l / X_K^2 = k_M e_\Sigma a_\infty l & \text{Case II} \end{aligned}$$

Further limiting cases are obtained when we assume that $l/X_K \ll 2\beta(1+\beta)^{1/2}$. In this

case

$$j_s = \frac{-2D_s s_\infty \beta^2 \phi}{X_K (1+\beta)^{3/2}} \quad (3.69)$$

and when

$$\begin{aligned} \beta \gg 1, j_s &= -2D_s s_\infty \phi \beta^{1/2} / X_K^2 = 2a_\infty (D_s k_M e_\Sigma)^{1/2} & \text{Case III} \\ \beta \ll 1, j_s &= -2D_s s_\infty \phi \beta^2 / X_K \end{aligned}$$

The situation when $\beta \ll 1$ is not a possible solution since we have assumed that $l(1+\beta)^{1/2}/X_K \gg 1$.

Solution for j_s when $k_M a_\infty \ll k_E s_\infty$ gives 3 clearly different cases depending on the rate limiting reaction. Now we will alter the limiting conditions for the j_s expression to $\gamma \gg 1$.

ii) $k_M a_\infty \gg k_E s_\infty$

In this case we are assuming that the reaction of E_2 with A is fast with respect to the E_1/S reaction. This means that all the enzyme is present in E_1 form.

Here equations (3.57a) and (3.58a) become

$$\frac{d^2 u}{d\chi^2} + (1+u) = \frac{\beta v}{\gamma} = 0 \quad (3.70)$$

and

$$\frac{d^2 v}{d\chi^2} + \frac{\beta v \phi}{\gamma} = 0 \quad (3.71)$$

In this case we must solve for v . The solution is of the form

$$v = B_8 \exp(\chi(\beta\phi/\gamma)^{1/2}) + B_9 \exp(-\chi(\beta\phi/\gamma)^{1/2})$$

Differentiation of this expression gives

$$\frac{dv}{d\chi} + (\beta\phi/\gamma)^{1/2} B_8 \exp(\chi(\beta\phi/\gamma)^{1/2}) - (\beta\phi/\gamma)^{1/2} B_9 \exp(-\chi(\beta\phi/\gamma)^{1/2}) \quad (3.72)$$

Substitution of the appropriate boundary conditions

$$\text{at } \chi = l/X_K \quad v = 1$$

$$\text{at } \chi = 0 \quad dv/d\chi = 0$$

and evaluation of the constants of integration gives

$$B_8 = B_9 = 1/2 \cosh\{l(\beta\phi/\gamma)^{1/2}/X_K\}$$

and substitution of B_8 and B_9 into equation (3.72) gives

$$\frac{dv}{d\chi} = (\beta\phi/\gamma)^{1/2} \frac{\sinh\{\chi(\beta\phi/\gamma)^{1/2}\}}{\cosh\{l(\beta\phi/\gamma)^{1/2}/X_K\}} \quad (3.73)$$

Using the expression for j_s

$$j_s = D_s \left. \frac{ds}{dx} \right|_{x=l} = \frac{D_s s_\infty}{X_K} \left. \frac{dv}{d\chi} \right|_{\chi=l/X_K}$$

the required expression for j_s , for the case $\gamma \gg 1$ is

$$j_s = \frac{-D_s s_\infty}{X_K} (\beta\phi/\gamma)^{1/2} \tanh\{l(\beta\phi/\gamma)^{1/2}/X_K\} \quad (3.74)$$

Again we can obtain the limiting cases for the above expression of j_s .

$$(l/X_K)(\beta\phi/\gamma)^{1/2} \gg 1, \quad j_s = (D_s s_\infty/X_K)(\beta\phi/\gamma)^{1/2}$$

$$j_s = s_\infty (D_s k_E e_\Sigma)^{1/2}$$

Case IV

$$(l/X_K)(\beta\phi/\gamma)^{1/2} \ll 1, \quad j_s = D_s s_\infty \beta\phi/X_K^2 \gamma$$

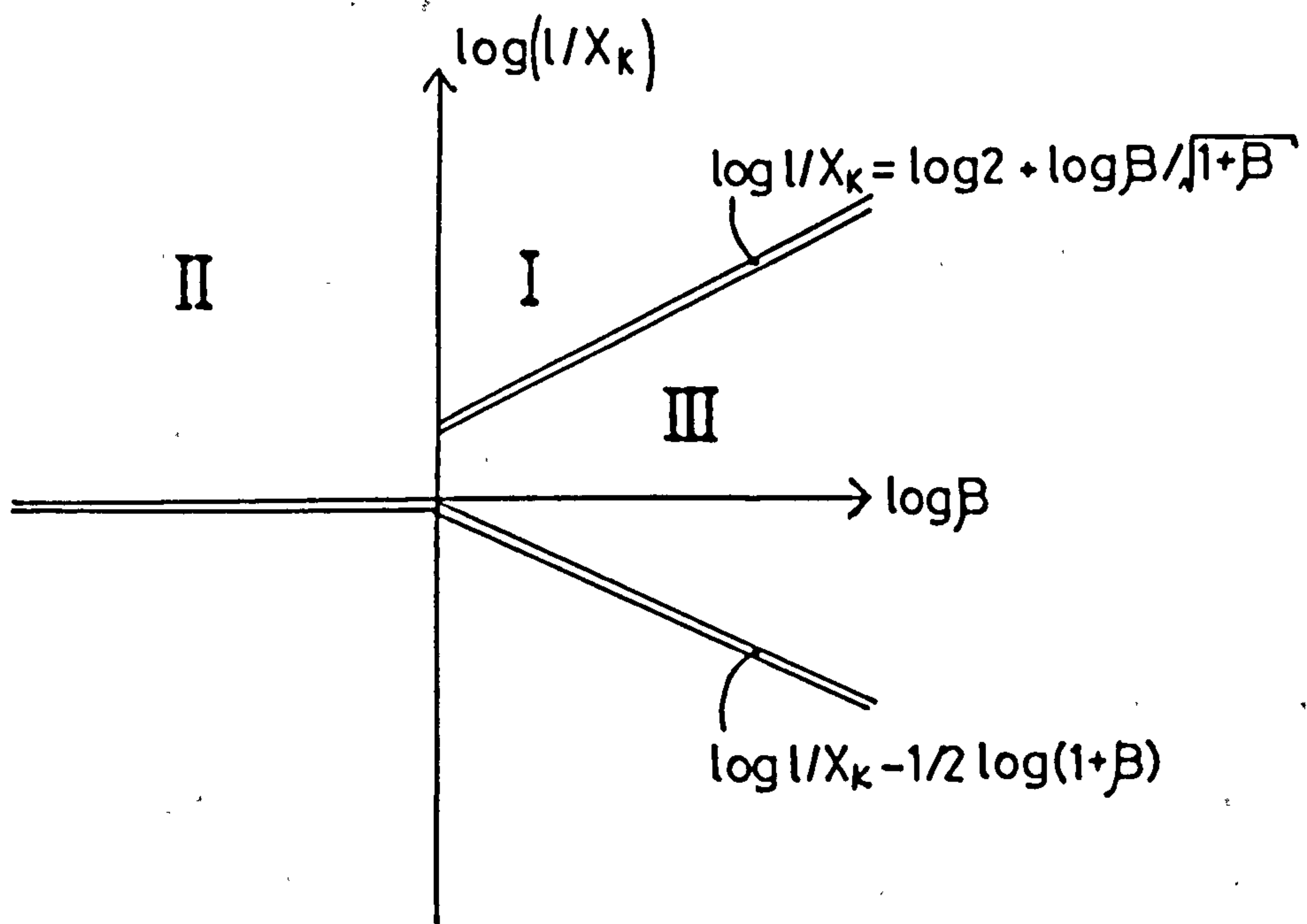
$$j_s = s_\infty l k_E e_\Sigma$$

Case V

It is apparent that there are 5 different cases arising from this analysis. These are summarised in table 3.4. This form of the model is the most general form presented and as such is applicable to a number of enzyme / mediator systems. Again a unique combination of reaction order dependencies are obtained for each of the 5 cases. The relationship between these cases is demonstrated on the case diagrams of figure 3.8.

Figure 3.8 Case diagram showing the relationship between the different j_s expressions for the situation described in section 3.2.

$\delta \ll 1$



$\delta \gg 1$

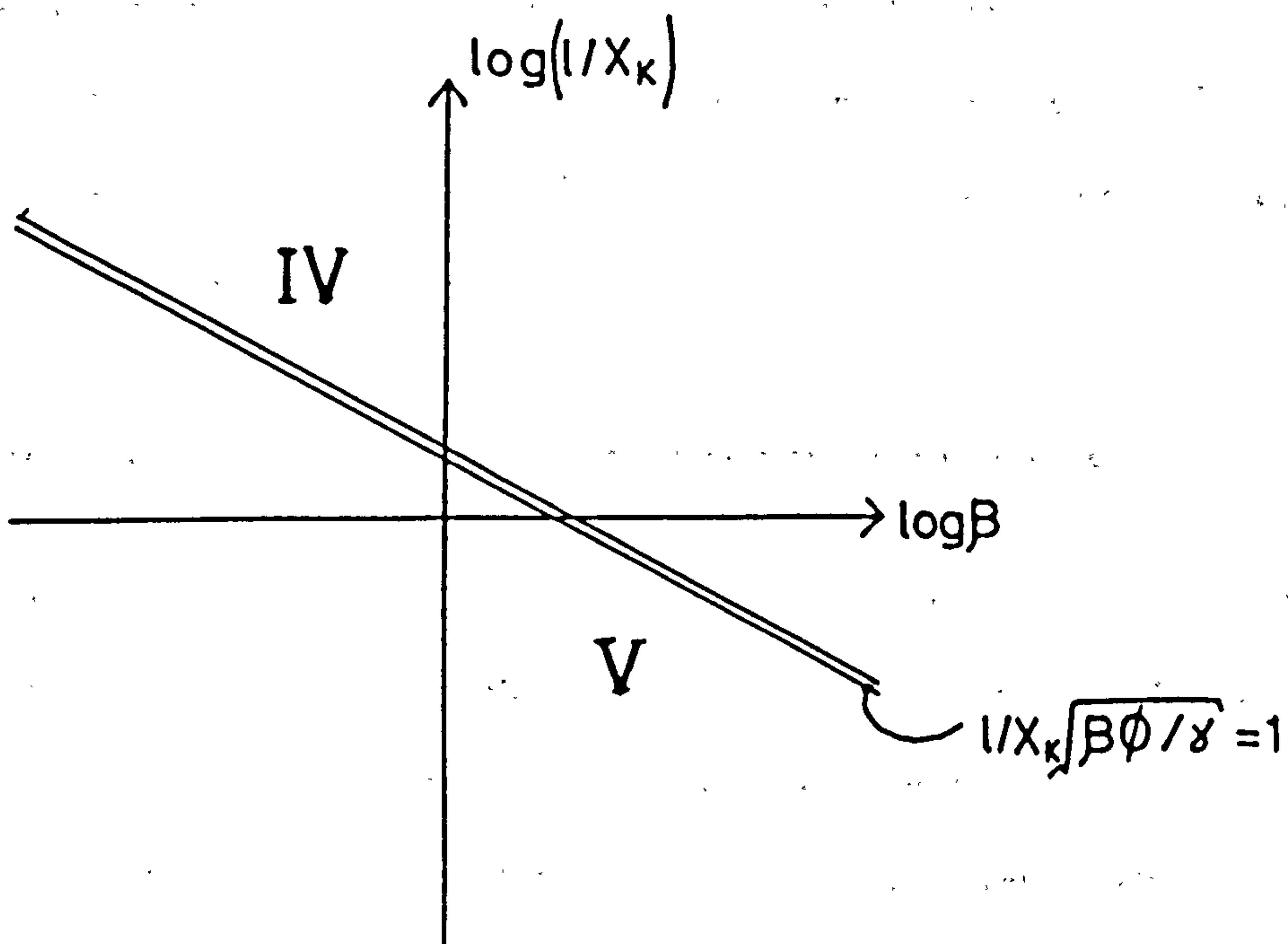


Table 3.4
The different j_s expressions for each case

Case	j_s expression	Reaction order			
		a_{∞}	s_{∞}	l	e_{Σ}
I	$k'a_{\infty}l$	1	0	1	0
II	$k_M e_{\Sigma} a_{\infty} l$	1	0	1	1
III	$2a_{\infty}(D_s k_M e_{\Sigma})^{1/2}$	1	0	0	$1/2$
IV	$s_{\infty}(D_s k_E e_{\Sigma})^{1/2}$	0	1	0	$1/2$
V	$k_E s_{\infty} e_{\Sigma} l$	0	1	1	1

A systematic variation of a_{∞} , s_{∞} , l and e_{Σ} in a conducting polymer / immobilised enzyme with ferrocene monocarboxylic acid as mediator in solution is presented in chapter 5. The data obtained is fitted to the above theory and kinetic parameters describing the processes occurring over a wide range of experimental conditions are presented. Some interesting differences between the use of oxygen and the ferrocene derivative as a mediator are apparent. The way in which the two systems operate is also discussed in chapter 5 following presentation and interpretation of all the relevant experimental data.

3.3 COMPARISON TO PREVIOUS THEORETICAL MODELS

The theoretical work of Mell and Maloy⁽¹⁴⁵⁾ is directly comparable to the theoretical treatment presented in the first section of this chapter. In this short section good agreement between the two theoretical approaches is demonstrated. Whereas this chapter describes a number of approximate solutions, corresponding to the limiting cases, the work of Mell and Maloy involves digital simulation of an

enzyme/mediator reaction.

In their work, these authors assumed that the regeneration of the reduced enzyme by reaction with oxygen was rapid. This corresponds to the case where $ka \gg k_{cat}$ in our notation. The digital simulation results will now be compared to those described in the initial section of this chapter. Equation (18) of reference 145 can be written in our notation. Rearrangement of this expression gives

$$j_B^{-1} = \frac{mk_{cat}e_{\Sigma}l^2}{D_s s_{\infty} K} + \frac{2}{lk_{cat}e_{\Sigma}} \quad (3.75)$$

where m is a function of l^2/X_K^2 . It can be seen from equation (3.75) that the first term corresponds to equation (3.29) and that the function m introduced in reference 145 is

$$m = [1 - \text{sech}(l/X_K)]^{-1} \quad (3.76)$$

The second term in equation (3.75) corresponds to equation (3.20) when we put $ka \gg k_{cat}$. It is apparent, therefore, that there is good agreement between the two approaches to this problem.

In the next two chapters experimental results for a number of immobilised enzyme systems are presented. The data obtained are interpreted by use of the appropriate theoretical model.

CHAPTER FOUR

THE IMMOBILISATION OF GLUCOSE OXIDASE IN ORGANIC POLYMER FILMS; ELECTROCHEMICAL DETECTION OF HYDROGEN PEROXIDE

This chapter describes the electrochemical immobilisation of glucose oxidase (GOD) in organic films produced by the electropolymerisation of simple organic monomers. The technique of electropolymerisation may result in conducting polymers, in the case of polypyrroles^(88,91,146) and polyanilines^(105,107,147), or in polymers that are usually insulators in the case of polyphenols^(113,148,149).

Conducting polymer films have been used to immobilise a number of electroactive and catalytic groups at electrode surfaces. In many cases this has been achieved by covalent binding of the functional centre of interest to the pyrrole monomer prior to electropolymerisation. Examples of functionalised conducting polymers are numerous and include pyrroles modified with viologens (N,N'-dialkyl 4,4'-bipyridium salts)⁽¹⁵⁰⁾, ferrocenes⁽¹⁵¹⁻¹⁵³⁾, 2,2'-bipyridine complexes of ruthenium⁽¹⁵⁴⁻¹⁵⁶⁾ or copper⁽¹⁵⁷⁾, quinones⁽¹⁵⁸⁾, nickel (II) cyclam⁽¹⁵⁹⁾ and porphyrins⁽¹⁶⁰⁻¹⁶²⁾.

A more straightforward method of immobilising a charged species in a conducting polymer is to use the species of interest as a dopant, or counter ion, for the polymer. This approach is effective since polypyrroles have an overall cationic charge in their oxidised, conducting state. Anions which have been used as dopants for conducting polypyrrole include simple species such as ferricyanide^(163,164) and cobalt(II)acetate⁽¹⁶⁵⁾, porphyrins⁽¹⁶⁶⁾, phthalocyanines⁽¹⁶⁷⁾ and more recently the large redox enzyme glucose oxidase^(74,114,115).

In this chapter the electrochemical immobilisation of glucose oxidase (GOD) in organic polymer films is described. The response of the entrapped enzyme to the substrate glucose (equation 1.4) is determined electrochemically by monitoring one of the products of the enzyme reaction, hydrogen peroxide. An amperometric mode

of hydrogen peroxide detection is described⁽¹⁶⁸⁾. The responses of the immobilised GOD systems are interpreted fully in terms of the specially formulated kinetic models presented in the previous chapter of this thesis.

Initially the GOD/poly-*N*-methylpyrrole system is discussed and results for such systems interpreted. This system was the subject of much investigation and is well understood. Following this data for GOD electrochemically immobilised in polyaniline and finally polyphenol are presented and interpreted.

In the last section of this chapter the flexibility of this type of electrochemical immobilisation technique is illustrated in terms of a bienzyme system involving either coimmobilisation of two enzymes or the electrodeposition of one enzyme containing layer on top of another⁽¹⁶⁸⁾.

A widely applicable immobilisation technique of this type must involve the electrodeposition of enzyme containing polymers from aqueous solution. It is preferable that these growth solutions contain a relatively high buffer capacity since the electropolymerisation process liberates protons which could have a detrimental effect on the enzyme. The production of conducting polymers from buffered aqueous solutions will now be discussed.

4.1 ELECTRODEPOSITION OF POLYPYRROLES FROM AQUEOUS SOLUTIONS

There have been many reports, over the past decade, concerning the electrodeposition of conducting polypyrroles on electrode surfaces^(87,88,91,169-172). The vast majority of this work has used an organic solvent, commonly acetonitrile, as the polymerisation medium. Although redox enzymes, such as alcohol dehydrogenase, have been used as catalysts in organic solvents^(173,174), a number of problems have been highlighted when attempting to use an enzyme/organic solvent mixture.

The solubility of many redox enzymes in organic solvents, such as acetonitrile and ethyl acetate⁽¹⁷⁴⁾, is limited and problems associated with enzyme instability persist.

A recent report⁽¹¹⁶⁾ describes the electrodeposition of glucose oxidase containing polyindole from an acetonitrile/electrolyte medium. However, the use of an organic electrodeposition medium, such as acetonitrile, does not represent a widely applicable immobilisation strategy. Many of the redox enzymes which will be of interest in the development and characterisation of this type of enzyme system are not as robust as glucose oxidase. For this reason any immobilisation procedure which is designed to be applicable to a range of enzymes must make use of a buffered, aqueous electrodeposition medium.

There are relatively few reports of the polymerisation and characterisation of polypyrroles in aqueous media. It has been known for some time that the pyrrole can be chemically oxidised in aqueous solutions to form a polymeric species⁽¹⁷⁵⁾. In a recent example the ferric ion is used to chemically oxidise pyrrole in acidic solution⁽¹⁷⁶⁾. In the context of enzyme immobilisation this work serves only to illustrate that the polymerisation of pyrroles in aqueous solutions is feasible. The use of electro-oxidation to produce conducting polypyrrole films on electrodes from a variety of aqueous solutions has been reported^(93,94,177-179). These reports have excluded the use of buffers to control the solution pH during the electrodeposition procedure. Genies and Syed have studied films of polypyrrole and poly-*N*-methylpyrrole, deposited from acetonitrile, in aqueous solutions of different pH⁽¹⁸⁰⁾. They found that the stability to potential cycling and the apparent redox potential of these polymers depends strongly on the pH of the bulk solution. This clearly demonstrates the importance of controlling the solution pH during any investigation of the electrochemical properties of polypyrrole.

A further important consideration is the pH of aqueous solutions used for the electrodeposition of polypyrroles. A detailed account of the effect of pH on the

electrodeposition of polypyrrole⁽¹⁸¹⁾ and poly-*N*-methypyrrole⁽¹⁸²⁾ has been given by Pletcher and co-workers. They found that the potential, pH and choice of electrolyte were all important factors in determining the electrochemical and physical properties of the resulting polymer films. Good quality films of both polypyrrole and poly-*N*-methypyrrole were produced from neutral solutions containing potassium nitrate as electrolyte.

A surprising difference between the mechanism of electrodeposition of the two polymers was observed. Although the initial stage of growth proceeds by instantaneous nucleation and three-dimensional growth in both cases it was found that in the case of poly-*N*-methypyrrole the growth became diffusion controlled after the point at which a peak in the $I-t$ transients occurred. In contrast it was observed that the electropolymerisation of pyrrole in neutral solutions was never diffusion controlled. Correspondingly it was found that the falling portions of the $I-t$ transients for polypyrrole growth were potential dependent whereas those for poly-*N*-methypyrrole were not. Analysis of the rising portion of the $I-t$ transients gave linear plots of I vs t^2 over the potential ranges studied. This is consistent with a growth mechanism involving instantaneous nucleation with three-dimensional growth for both these polymers.

Accurate control of the growth potential was found to be essential. The use of high potentials, greater than 800 mV (SCE) and 900 mV in the case of pyrrole and *N*-methypyrrole respectively, lead to a decrease in the charge under the resulting $I-t$ transients. This is explained by these authors in terms of overoxidation of the polymers at such high potentials resulting in loss of conjugation of the polymer chain and the production of polymer films of poor quality and low conductivity. The use of high potentials is obviously disadvantageous in the production of polypyrroles.

A study of the cyclic voltammetry of the two monomers at a clean metal electrode revealed two anodic peaks, in each case, on the first potential sweep. The first peak was found to correspond to the oxidation of the monomer and the second

peak to the destructive over-oxidation process already described. In the case of poly-*N*-methylpyrrole these peaks are well separated (by around 250 mV) so that undesirable polymer characteristics, seen when the potential is taken to a value higher than the first peak, can be avoided. In the case of pyrrole, however, the two peaks are almost indistinguishable, making it very difficult to prevent polymer overoxidation.

For this reason it is advantageous to use poly-*N*-methylpyrrole and not the parent polymer as an electrode material. This allows overoxidation of the polymer chains to be avoided and a reproducible, stable electrode material to be produced.

A more recent report demonstrates that good quality film of polypyrroles can be produced from neutral aqueous solutions by potential cycling, potentiostatic or galvanostatic techniques⁽¹⁸³⁾. Also the choice of anion, but not cation, was seen to have a profound affect on the electrochemical characteristics of the resultant polymer.

It is apparent, therefore, that a variety of techniques can be used to electropolymerise pyrroles from aqueous solutions of defined pH. A polymerisation system was needed in which the reproducible growth of stable and adherent polymer films from buffered, and ultimately enzyme containing, growth solutions could be achieved. The development of such a system is described below.

4.2 THE DEVELOPMENT OF A POLYMERISATION SYSTEM COMPATIBLE WITH ENZYME IMMOBILISATION

The electrodeposition of polypyrrole and poly-*N*-methylpyrrole from a range of aqueous electrolyte solutions was investigated with a view to developing a system compatible with enzyme immobilisation.

In initial investigations polypyrrole films were produced from aqueous solutions of pyrrole (0.01 to 0.10 mol dm⁻³) in sodium chloride electrolyte (0.10 to

0.25 mol dm⁻³). This resulted in good quality polymer films when a potential step from zero to between 700 and 900 mV (vs SCE) was applied. The resulting polypyrrole films were even, adherent and stable to potential cycling over several hours. The addition of buffer (0.15 mol dm⁻³ sodium phosphate, pH 7.2) to the solutions resulted in a shift in the potential range producing adherent polymers (800 to 1000 mV vs SCE) and a decrease in the electrochemical stability of the films was noticed. The electroactivity of these films was quickly destroyed by potential cycling in buffered background electrolyte.

The effect of buffering the solutions is to maintain neutral pH at the electrode surface. This is not the case in unbuffered solutions since the electropolymerisation of pyrrole is known to liberate protons⁽¹⁸⁴⁾. In this unbuffered case a pH gradient develops during the electropolymerisation procedure. The reason why polymerisation of pyrrole in the presence of phosphate buffer produces unstable films is unclear. Due to the unsuitability of pyrrole, as previously described, the monomer was changed to *N*-methylpyrrole. This monomer has already been shown to have advantages over the parent polymer when used for electropolymerisation^(180,182).

Once again films were grown potentiostatically from solutions of monomer (0.01 to 0.10 mol dm⁻³) in the presence of sodium phosphate (0.15 mol dm⁻³, pH 7.2) and electrolyte (0.10 to 0.25 mol dm⁻³). Poly-*N*-methylpyrrole films produced in this way were found to be of greater stability to potential cycling than corresponding polypyrrole films. The most stable films were produced using monomer (0.05 mol dm⁻³), sodium phosphate (0.15 mol dm⁻³, pH 7.2) and tetraethylammonium tetrafluoroborate (TEA TFB, 0.1 mol dm⁻³). Potential steps from 0 volts to between 750 and 900 mV (vs SCE) were found to give even, adherent and electrochemically stable poly-*N*-methylpyrrole films. These films gave a stable and reproducible background current when potentiostated at 850 to 950 mV (vs SCE) in background buffered electrolyte once the polymer charging current was

allowed to decay. Current-time ($I-t$) transients for this potentiostatic film growth are shown in figure 4.1. The growth procedure employed resulted in good reproducibility of the growth transients and therefore in films of reproducible thickness and properties. Careful potential control (± 2 mV) of the working electrode is essential in order to achieve a high degree of reproducibility.

A detailed analysis of the $I-t$ transients in the absence and presence of enzyme is given later in this chapter. Conclusions are also drawn about the mechanism of film growth, with and without enzyme, later in this section.

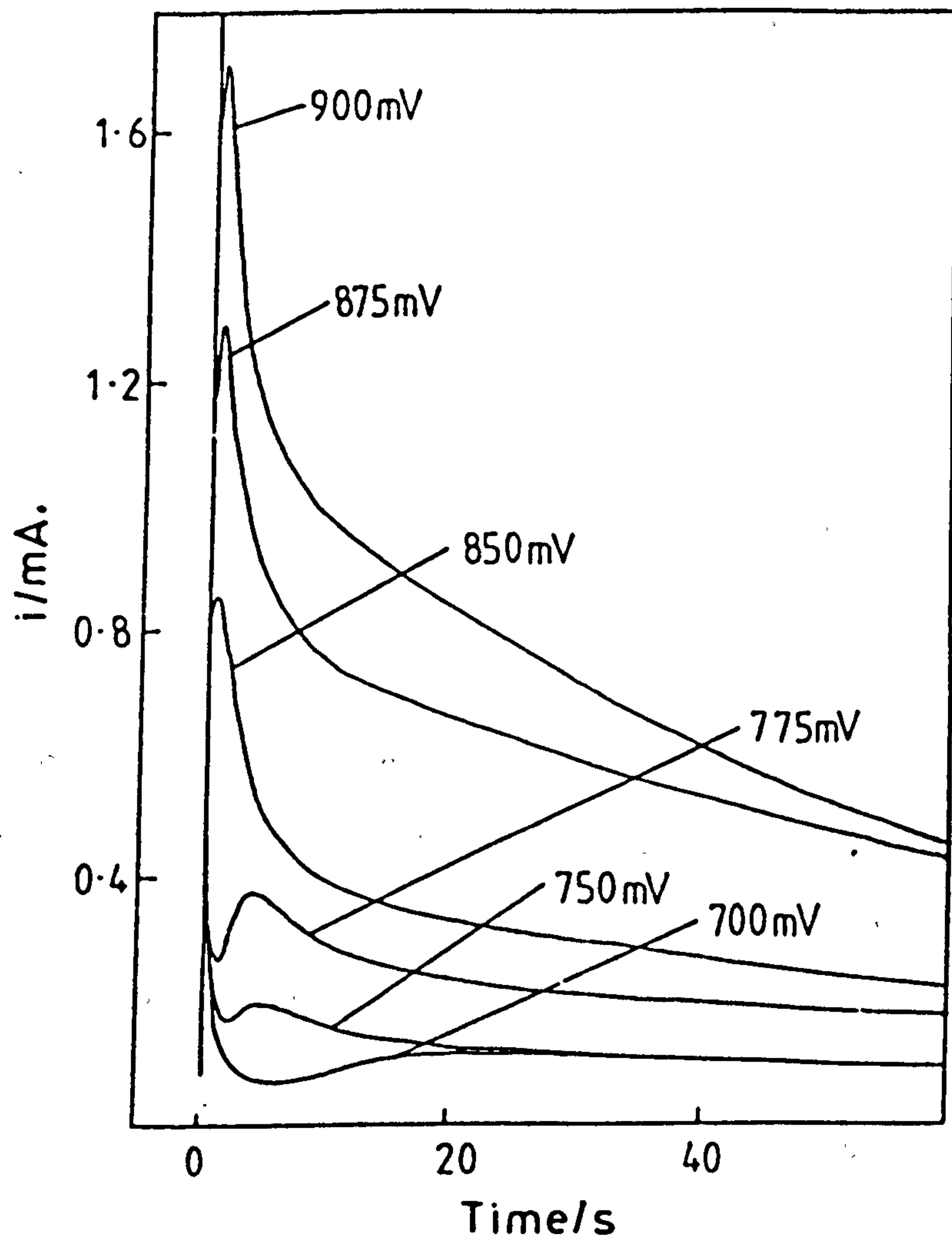
Once this reproducible method of poly-*N*-methylpyrrole film growth had been developed an attempt was made to accurately determine the relationship between charge passed during polymer growth and film thickness for this system. The use of ellipsometry^(139,140) to determine the thickness of poly-*N*-methylpyrrole films *in situ* is described in the following section.

4.3 ELLIPSOMETRIC MEASUREMENT OF FILM THICKNESS

An accurate measure of film thickness as a function of charge passed during film growth was required. Several attempts have been reported in the literature to measure the thickness of similar types of film. Methods of film thickness measurement which involve removal of solvent from a polymer are of little use in estimating the thickness of a solvated film realistically. Therefore an *in situ* technique is required which can give estimates of the solvated film thickness at short time intervals during film growth, without the need to dry or in any way alter the morphology of the film under examination.

Multiple beam interferometry has been used to estimate the thickness of a cobalt doped polypyrrole film⁽¹⁶⁵⁾. This technique gave a value of approximately 100 Å for a charge of 12 mC cm⁻² passed during film growth. Also ellipsometry⁽¹³⁹⁾ has been employed to determine the thickness of polypyrrole-tetra-fluoroborate⁽¹⁸⁵⁾.

Figure 4.1 Current transients for the potentiostatically controlled polymerisation of *N*-methylpyrrole at a series of potentials.



A linear correlation between film thickness and charge passed was found over the range studied (40 to 75 mC cm⁻²). This gave a value of around 16 Å mC⁻¹cm² which is in reasonable agreement to that determined by multiple beam interferometry⁽¹⁶⁵⁾. However, a large discrepancy exists between this data and the previously established estimate of 0.1 µm when passing 24 mC⁻¹cm². Assuming a linear charge-thickness relationship this is equivalent to 42 Å mC cm⁻² (186).

Apart from this conflicting data there does not appear to be a good estimate of film thickness of polypyrrole films. Furthermore there is no information available relating to the thickness of poly-*N*-methylpyrrole films deposited from buffered aqueous solutions. Using ellipsometry a reliable estimate of film thickness as a function of charge was obtained. This is needed since the theory used to interpret the data obtained from enzyme containing poly-*N*-methylpyrrole films later in this chapter contains a parameter describing film thickness.

In the following section data will be presented for ellipsometric measurement of film thickness measure *in situ*.

4.3.1 Determination of the Charge-Thickness Relationship

In order to measure the film thickness as a function of charge passed films were grown potentiostatically and a current-time transient was measured at the same time as the ellipsometric parameters I , α and ϵ (see section 2.10.2). Thicknesses were calculated and plotted against the appropriate value of charge obtained by integrating the area under the current-time transient. A plot of potential and thickness against time is shown in figure 4.2. This shows a linear increase of thickness with time on stepping from zero volts to a polymer growth potential. A plot of charge passed against film thickness is shown in figure 4.3. This shows that the film growth is linear as a function of charge passed over the range studied. The graph has a slope of 2.2 nm mC⁻¹cm² (22 Å mC⁻¹cm²). This value will be used in

Figure 4.2 Poly-*N*-methylpyrrole film thickness as a function of time (each sample is 20ms) and applied potential (50 mmol dm⁻³ *N*-methylpyrrole, 0.1 mol dm⁻³ sodium phosphate, 0.15 mol dm⁻³ TEA TFB pH 7.0, 20°C).

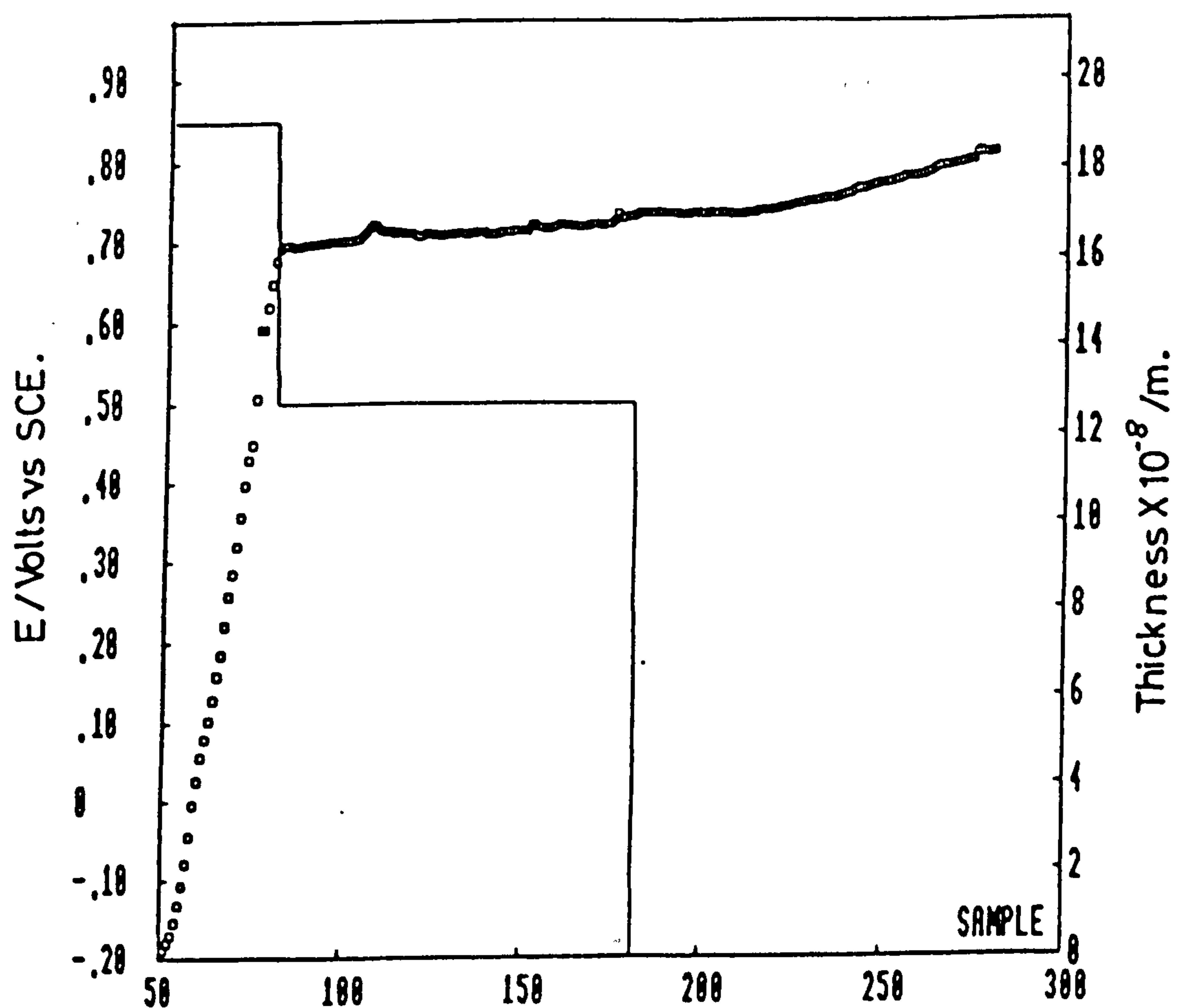
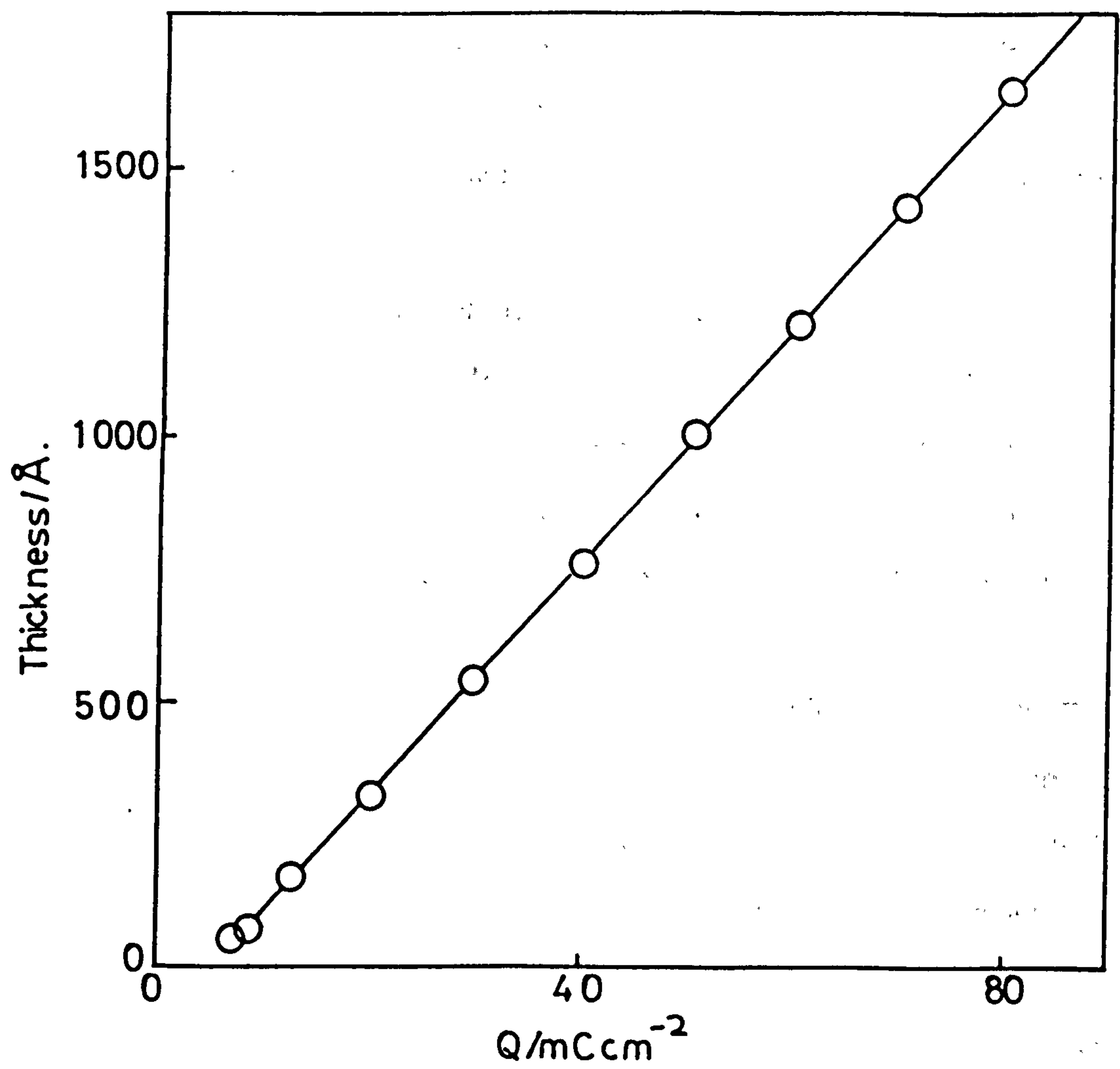


Figure 4.3 Film thickness as a function of charge density during film growth
(taken from the data presented in figure 4.2).



the determination of kinetic and mass transport parameters later in this chapter and compares to one of $16 \text{ Å mC}^{-1}\text{cm}^2$ for polypyrrole⁽¹³⁹⁾. It is likely that the higher value obtained for the *N*-methyl substituted polymer is at least partly due to the steric bulk of the methyl groups in this film.

4.4 ELECTROCHEMICAL IMMOBILISATION OF GLUCOSE OXIDASE IN POLYPYRROLE

This section will review work on the use of conducting polypyrrole as an immobilisation matrix for redox enzymes. Workers in this field have invariably used glucose oxidase (GOD) as the redox enzyme in an attempt to produce viable glucose sensors.

The first description of the electrochemical immobilisation of an enzyme in an organic polymer appears to be by Aizawa and Yabuki⁽¹¹⁴⁾. These authors describe the characteristics of a GOD-conducting polypyrrole membrane. During the course of the work described in this thesis a number of authors have described similar experiments to those originally conducted by Aizawa and coworkers using GOD immobilised in polypyrrole.

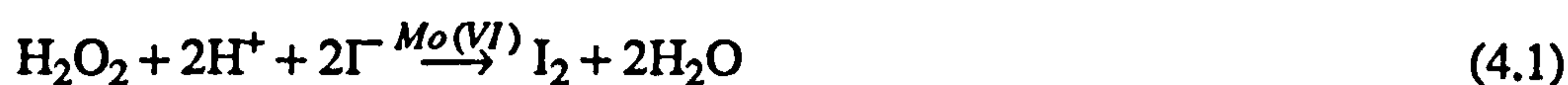
Foulds and Lowe⁽⁷⁴⁾ described a method of electrochemically immobilising GOD in polypyrrole deposited onto printed platinum substrates. Enzyme containing films were grown potentiostatically for periods of around 2½ hours (table 4.1). This presumably results in the formation of thick polymer films. The authors concentrate on the use of this system as an amperometric glucose sensor and do not describe attempts to optimise the electrode response in terms of choice of monomer, growth conditions, film thickness or enzyme loading. The effect of varying the concentration of GOD in the growth solutions was investigated. The enzyme activity included in the polymer films was found to increase linearly with the concentration of enzyme in the growth solutions over the limited range studied

(around 0 to 2.0 mg cm⁻³ enzyme). No attempt was made to determine whether the hydrogen peroxide reacts on the polypyrrole, which surrounds the enzyme, or has to diffuse to the underlying platinum substrate to be oxidised. Furthermore the effect of varying the polymer film thickness on the response was not described.

These factors are of primary importance if the response of this type of enzyme electrode is to be characterised and hence optimised.

A further report describes a very similar immobilisation procedure involving the same enzyme-polymer combination⁽¹¹⁵⁾. The results from this investigation are, however, conflicting with those obtained by Foulds and Lowe⁽⁷⁴⁾. The authors again used a potentiostatic polymer deposition method involving the lowest possible electrodeposition potential (0.65 volts vs Ag/AgCl) as shown in table 4.1. The use of this low potential was claimed to minimise possible enzyme degradation. However, there is no evidence to suggest that potentials greatly exceeding this value have any detrimental effects on this enzyme^(74,114,116). The authors conclude that hydrogen peroxide detection by electrochemical oxidation is not feasible in this system. They suggest that at the oxidative potentials (>0.8 volts vs Ag/AgCl) required for hydrogen peroxide detection the polypyrrole itself is degraded resulting in it becoming detached from the electrode. This is in contrast to the previous report⁽⁷⁴⁾ in which the authors make no mention of polymer instability or degradation in the presence of hydrogen peroxide.

Due to this proposed degradative effect hydrogen peroxide was detected using a secondary Mo(VI) catalysed iodide oxidation reaction^(187,188). The iodide produced was determined by reduction at around 0 volts (vs Ag/AgCl).



This system has the significant disadvantage of having to add iodine and catalyst to each assay solution. The rate of iodine reduction was measured as an indirect

Table 4.1

Glucose oxidase immobilised in polypyrrole

Electrodeposition method/conditions	Typical film thickness	[enzyme] in growth solution	Method of H_2O_2 determination	Useful glucose detector range	% of initial response after seven days	Ref.
Potentiostatic growth at 0.8V ^(a) in unbuffered pyrrole (<0.2 mol dm ⁻³). Printed Pt ink electrodes used. growth for up to 2.5 hours	unspecified	0 to 2.1 mg cm ⁻³ ^(b) 0 to 250 U cm ⁻³	amperometric detection of H_2O_2 at 0.70V ^(c) steady state measurement	10 ⁻³ to 10 ⁻¹ mol dm ⁻³ glucose	approx 75% ^(d)	74
potentiostatic growth at 0.65V. Polished Pt or glassy carbon electrode used. Buffered or unbuffered in KCl solution, pyrrole 0.5 mol dm ⁻³	up to 5.0 µm	8 to 19 mg cm ⁻³ 100 to 500 U cm ⁻³	indirect determination by Mo(VI) catalysed I ⁻ oxidation rate (µA min ⁻¹) measurement	10 ⁻⁴ to 10 ⁻² mol dm ⁻³ glucose	approx 3% ^(e)	115

Notes

- ^(a) All potentials vs Ag/AgCl
- ^(b) Based upon estimate of 125 000 U g⁻¹ for type VII GOD (sigma)
- ^(c) pH 7.0 phosphate buffer, 25°C
- ^(d) Stored in pH 7.0 phosphate buffer, 4°C
- ^(e) Potentiostated at 0 volts, pH 6.5 buffer

measure of the rate of hydrogen peroxide production by the enzyme. The authors claim, somewhat surprisingly, that GOD carries a net cationic charge. They attempt to increase the degree of enzyme incorporation into the polycationic polypyrrole by lowering the proposed positive charge on the enzyme.

An almost total loss of the electrode response to glucose after a seven day period was explained by proposing that strong electrostatic repulsion between GOD and the surrounding polypyrrole results in expulsion of the enzyme over this period. This must be a spurious interpretation as the isoelectric point of this enzyme is known to be in the region of 4.2 ⁽¹⁸⁹⁾. The enzyme will, therefore, carry a polyanionic charge at the pH used by these authors (pH 6.5 to 7.0).

It is apparent that there are a number of fundamental disagreements in this work. Furthermore, these reports do not describe any real attempts to characterise the electrode responses or to gain an understanding of the way in which such systems operate in terms of the kinetic and transport processes occurring. A final important consideration is that all of this work employs polypyrrole as the enzyme immobilisation matrix. It has been demonstrated previously that poly-*N*-methylpyrrole has certain advantages over the parent polymer^(180,182). The use of poly-*N*-methylpyrrole is therefore preferable in the development of a successful electrochemical immobilisation strategy.

In the next section the immobilisation of GOD in films of poly-*N*-methylpyrrole will be described. A highly successful immobilisation procedure is defined together with a kinetic model which allows the understanding and characterisation of this immobilised enzyme system.

4.5 ELECTROCHEMICAL IMMOBILISATION OF GLUCOSE OXIDASE IN POLY-*N*-METHYLPYRROLE

A new system was developed in which glucose oxidase (GOD) was immobilised in films of poly-*N*-methylpyrrole.

This procedure involves the use of buffered aqueous solutions for both enzyme immobilisation and determination of the responses to glucose. Poly-*N*-methylpyrrole is more stable than the parent polypyrrole (section 4.2) and is not degraded by hydrogen peroxide.

Hydrogen peroxide produced by the immobilised GOD, in response to additions of glucose, was detected amperometrically. The electrode responses to glucose over a range of polymer film thickness and enzyme loadings were measured. Comparison of the results with our theoretical model (section 3.1) enables a good understanding of kinetic and transport processes in the film to be achieved.

The primary objective of this work was the development of a model system rather than the production of a viable glucose sensor.

In the following section the method used to measure the enzyme reaction in the polymer film, the amperometric detection of hydrogen peroxide, will be described. Also of primary importance in gaining an understanding of the operation of this system is the determination of the site of reaction of hydrogen peroxide. This is a factor which has not been accounted for by previous authors^(74,115).

The methods used to determine the site of reaction of hydrogen peroxide at the poly-*N*-methylpyrrole/glucose oxidase (pNMP-GOD) modified electrodes are described in the section below.

4.5.1 The Detection of Hydrogen Peroxide

The oxidation of hydrogen peroxide at a pNMP-GOD modified platinum rotating disc electrodes was studied. GOD was included in the polymer films used to

ensure that they were of comparable porosity and morphology to those studied in the following sections of this chapter. All pNMP-GOD modified electrodes were produced by the potential step method described in section 4.5.2.

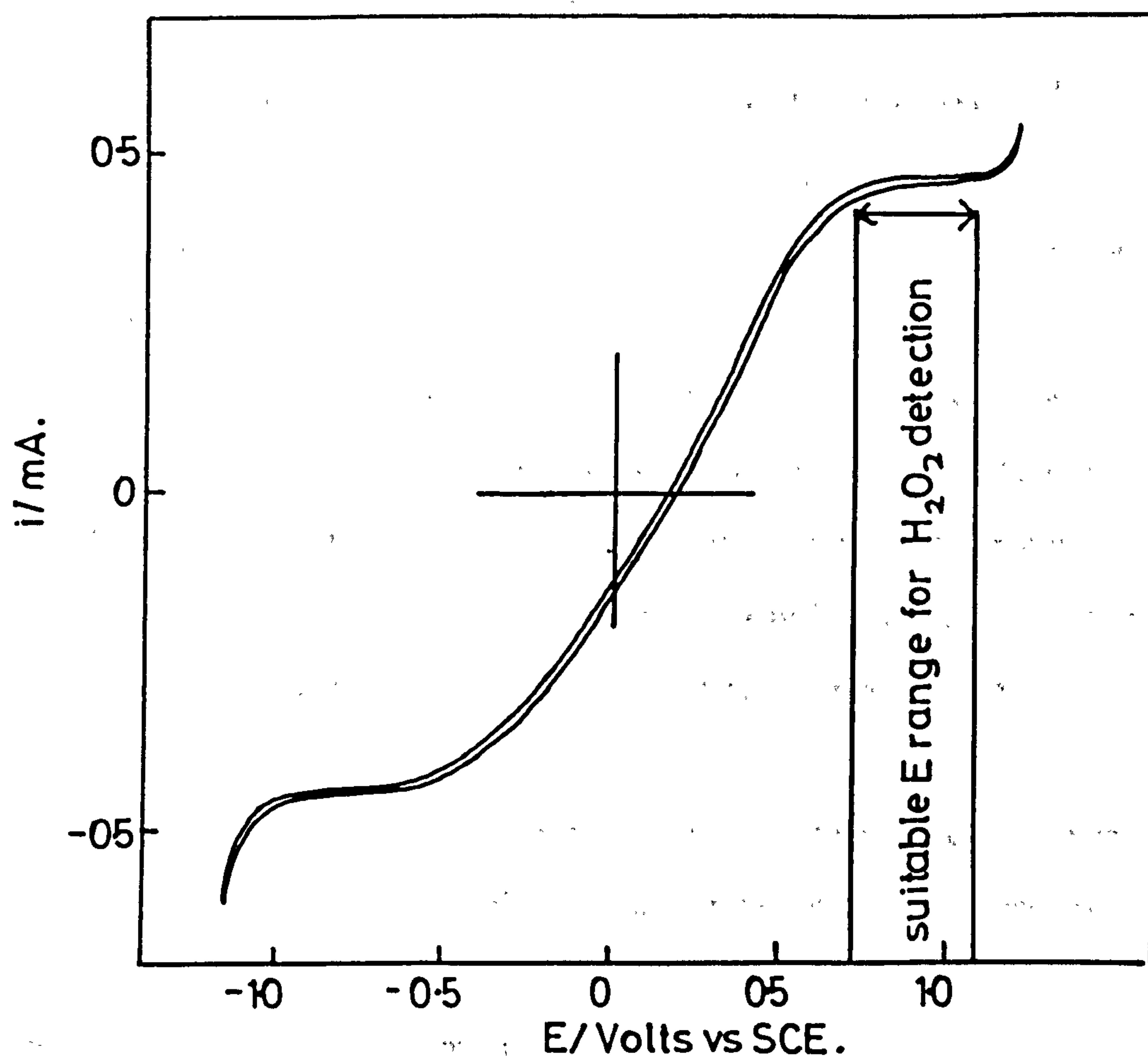
A potential of 0.80V (vs SCE) was applied to the stationary platinum electrode in a solution of *N*-methylpyrrole (0.05 mol dm^{-3}) in buffered electrolyte (0.10 mol dm^{-3} TEATFB, 0.15 mol dm^{-3} sodium phosphate at pH 7.2, 25°C) containing GOD (5 mg cm^{-3}). A total of $190 (\pm 5) \text{ mC cm}^{-2}$ was passed during each film growth. Films were washed by rotation in buffered electrolyte prior to immersion in a deoxygenated solution of hydrogen peroxide in buffered electrolyte.

Initially polarograms were recorded ($5 \times 10^{-5} \text{ mol cm}^{-3}$ hydrogen peroxide) in order to determine the limiting current for hydrogen peroxide at this type of modified electrode (figure 4.4). It is apparent that the limiting current for oxidation is reached at 0.70 volts and that for reduction at -0.60 volts.

A system of hydrogen peroxide detection based on its reduction is not feasible for the immobilised GOD system. This is because the response of the immobilised GOD to glucose is measured in air saturated solutions. The oxygen in these solutions is electroactive, being reduced at potentials below -0.30 volts, in this system. This oxygen reduction would contribute a large non-enzymic current and make the reduction of enzymically produced hydrogen peroxide difficult to quantify with any accuracy. For this reason hydrogen peroxide detection by oxidation was favoured. By poisoning the pNMP-GOD electrodes at a potential corresponding to the limiting current for the oxidation of hydrogen peroxide the enzymic reaction can be monitored. Detection potentials of between 0.80 and 0.95 volts (vs SCE) were found to be suitable, with no polymer instability or degradation apparent.

Once this suitable detection had been established, the oxidation of hydrogen peroxide at the pNMP-GOD electrodes was examined as a function of hydrogen peroxide concentration and rotation speed. For each hydrogen peroxide concentration a freshly prepared electrode was used. Concentrations in the range

Figure 4.4 Polarogram for the oxidation of hydrogen peroxide ($5 \times 10^{-5} \text{ mol cm}^{-3}$) in buffered electrolyte (0.1 mol dm^{-3} sodium phosphate, 0.15 mol dm^{-3} TEA TFB, pH 7.0, 25°C in the absence of molecular oxygen) at a poly-*N*-methylpyrrole coated platinum electrode ($A = 0.385 \text{ cm}^2$, rotation speed = 4 Hz).



5×10^{-8} to 1×10^{-6} mol cm⁻³ hydrogen peroxide were used.

The measurements were made as follows. The modified electrode was stepped to a potential of 0.9 volts in a buffered electrolyte solution (25°C, pH 7.2) and a period allowed for the resulting current to decay. A current of below 100 nAmps was reached in each case. The appropriate volume of stock hydrogen peroxide solution (30% v/v) was then injected into the cell using a glass/teflon syringe. The electrode response was measured at a series of rotation speeds for each hydrogen peroxide concentration.

The data was initially analysed in terms of the Levich equation⁽¹⁹⁰⁾.

$$i_L = 1.554nFAD^{2/3}\nu^{-1/6}W^{1/2}a_{\infty} \quad (4.3)$$

where n is the number of electrons involved, A is the electrode area (cm²), D is the diffusion coefficient of H₂O₂ in solution (cm² s⁻¹), ν is the kinematic viscosity of the aqueous medium (cm² s⁻¹), W is the rotation speed (Hz) and a_{∞} is the bulk concentration (mol cm⁻³).

This simple analysis of the limiting current is only applicable if the hydrogen peroxide can undergo a kinetically fast oxidation on the surface of the conducting pNMP-GOD matrix. Plots of i_L again $W^{1/2}$ were, however, found to be non-linear in all cases, indicating that a further degree of complexity is involved. The predicted Levich currents were reduced, the effect being particularly marked at higher rotation speeds.

This implies the existence of an additional rate limiting process of some type. The most likely explanation of this effect is that the oxidation of hydrogen peroxide on the pNMP is kinetically slow so that it must diffuse through the polymer to be oxidised at the underlying platinum surface.

This hypothesis was confirmed to be correct by using a modified Levich equation to analyse data obtained by varying hydrogen peroxide concentration and film thickness.

The Koutecky-Levich (K-L) equation⁽¹⁹¹⁾ contains a term to describe diffusion of the electroactive species through a layer of thickness l , at a modified electrode surface.

$$\frac{1}{i_L} = \frac{1}{k'_D a_\infty} + \frac{1}{nFAk'_{ME} a_\infty} \quad (4.4)$$

where k'_D is the mass transport rate constant⁽¹⁹¹⁾ given by equation 4.3, ($k'_D = 1.554nFAD^{3/2}\nu^{-1/6}W^{1/2}$) and k'_{ME} is the rate constant for the rate limiting process occurring within the modified electrode.

Where this process is diffusion the term k'_{ME} can be written as

$$k'_{ME} = KD'/l \quad (4.5)$$

where D' is the diffusion coefficient for H_2O_2 through the pNMP-GOD matrix and K is the coefficient describing partition of H_2O_2 into this matrix.

It is apparent that the slope of the K-L plots contains information about the diffusion of hydrogen peroxide in solution (D) whereas the intercept term pertains to its diffusion within the pNMP-GOD matrix (D'). Using this analysis it is not possible to separate the two transport terms contained within the K-L intercepts; diffusion and partition of hydrogen peroxide. Plots of $(i_L)^{-1}$ against $W^{-1/2}$ were found to be linear in all cases (figure 4.5a). By replotting the K-L intercepts (figure 4.5b) and K-L slopes (figure 4.5c) as a function of $(a_\infty)^{-1}$ values of D and KD' can be determined.

The gradient of the K-L slope against $(a_\infty)^{-1}$ plot is $1.02 \times 10^{-2} \text{ Amp}^{-1} \text{ s}^{1/2} \text{ mol cm}^{-3}$. Using a value for n of 2, $A = 0.38 \text{ cm}^2$ and $\nu = 1 \times 10^{-2} \text{ cm}^2 \text{ s}^{-1}$ a value for D of $7.9 \times 10^{-6} \text{ cm}^2 \text{ s}^{-1}$ was determined. This compares to 0.6 to $1 \times 10^{-6} \text{ cm}^2 \text{ s}^{-1}$ determined by anodic oxidation at a platinum surface⁽¹⁹²⁾.

The gradient of the K-L intercept against $(a_\infty)^{-1}$ plot is $3.89 \times 10^{-2} \text{ Amp}^{-1} \text{ mol cm}^{-3}$. As this slope is equal to $(k_{ME}nFA)^{-1}$ a value of k'_{ME}

Figure 4.5 a) Koutecky-Levich plots for the oxidation of hydrogen peroxide at a poly-*N*-methylpyrrole coated platinum rotating disc electrode ($A = 0.385 \text{ cm}^2$, $l = 4.18 \pm 0.11 \times 10^{-5} \text{ cm}$) at concentrations between 1×10^{-7} and $1 \times 10^{-6} \text{ mol cm}^{-3}$ hydrogen peroxide (pH 7.0, 25°C).

Figure 4.5 b) Plot of the Koutecky-Levich (K-L) intercept as a function of reciprocal hydrogen peroxide concentration.

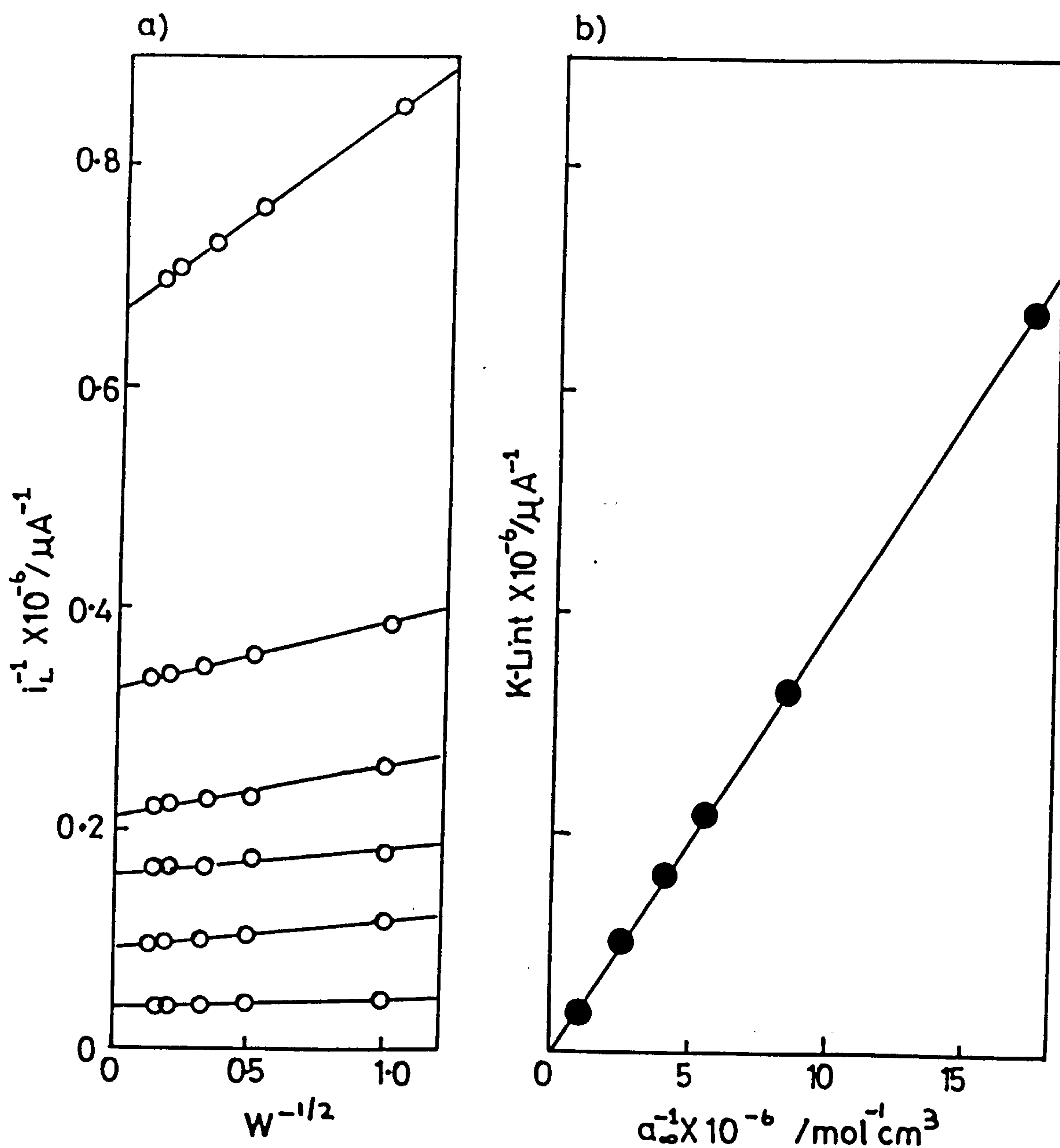
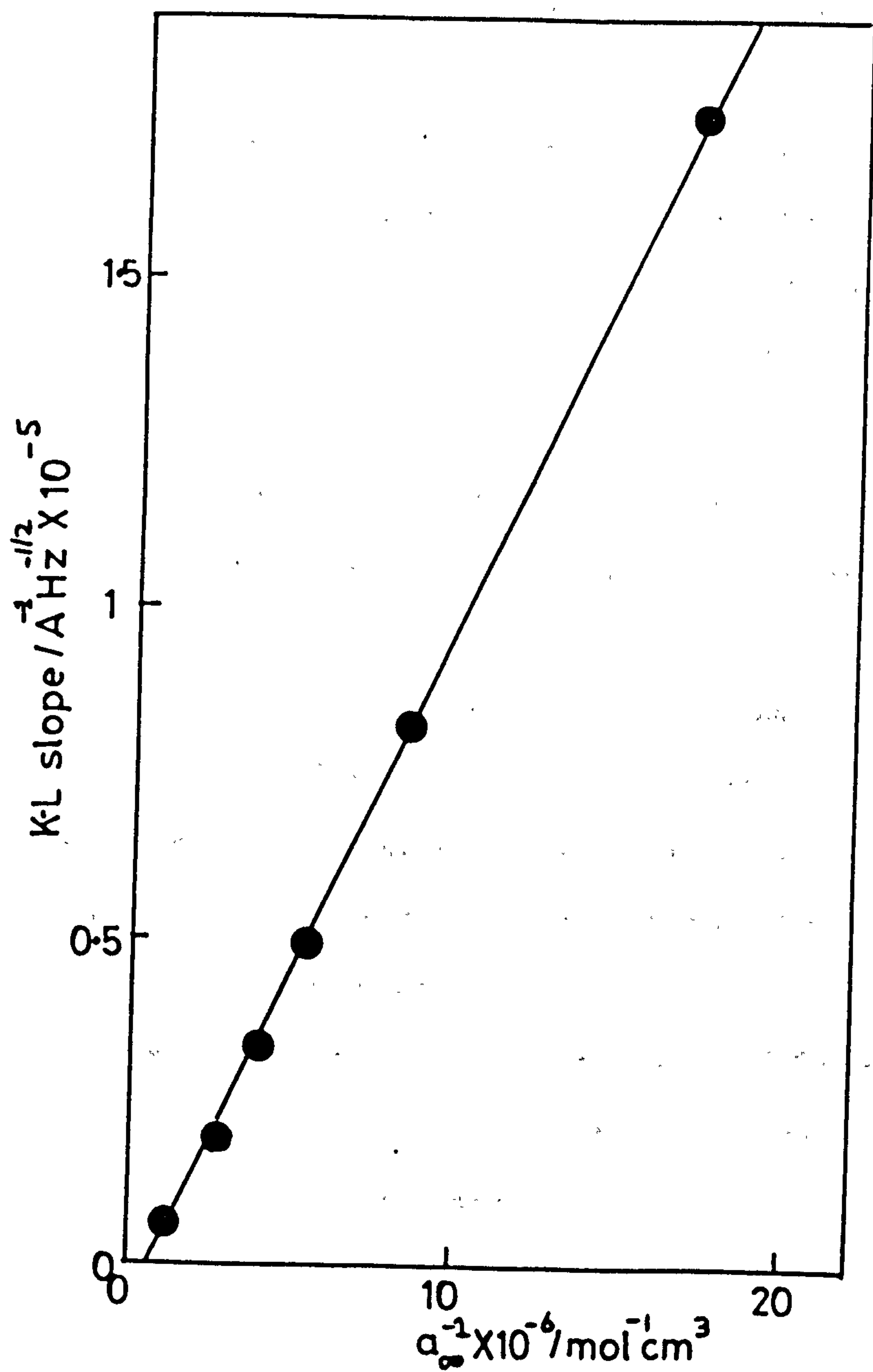


Figure 4.5 c) Plot of the K-L slope as a function of reciprocal hydrogen peroxide concentration.



can be determined. Using the constants defined above a value of k'_{ME} of $3.51 \times 10^{-4} \text{ cm s}^{-1}$. Alternatively as k'_{ME} is equal to KD'/l and as the film thickness is known ($l = 4.18 \pm 0.11 \times 10^{-5} \text{ cm}$) a value for KD' can be calculated as being in the range 1.43 to $1.51 \times 10^{-8} \text{ cm}^2 \text{ s}^{-1}$.

From equations 4.4 and 4.5 it is apparent that if this secondary diffusional process is occurring then the K-L intercept should show a linear dependence on the pNMP-GOD film thickness, l , at a fixed concentration of hydrogen peroxide.

Experiments were conducted at a range of film thicknesses. For each film thickness a K-L plot was constructed. A plot of K-L intercept against film thickness (l) is shown in figure 4.6. This plot is linear, clearly demonstrating that hydrogen peroxide diffuses through the pNMP-GOD films to react at the underlying platinum electrode. A value of KD' can be obtained from the slope of this plot since the slope is given by $(KD'nFAa_{\infty})^{-1}$ and the concentration of hydrogen peroxide is known ($1.00 \times 10^{-6} \text{ mol cm}^{-3}$). A value for KD' of $1.56 \times 10^{-8} \text{ cm}^2 \text{ s}^{-1}$ was calculated from a slope of $8.75 \times 10^8 \text{ Amp}^{-1} \text{ cm}^{-1}$.

It is interesting to note that the plot in figure 4.6 has a small intercept. This would suggest that the Levich plot obtained for oxidation of hydrogen peroxide at a clean platinum electrode (zero film thickness) would exhibit an intercept. This is known not to be the case and may suggest a systematic underestimation of film thickness or a further rate limiting process occurring.

Analysis of the data for oxidation of hydrogen peroxide at pNMP-GOD films clearly demonstrates that the process does not occur at a significant rate on the surface of the polymer. The diffusional parameters obtained are collected together in table 4.2.

Figure 4.6 Plot of the K-L intercept as a function of film thickness for hydrogen peroxide oxidation at poly-*N*-methylpyrrole coated electrodes.

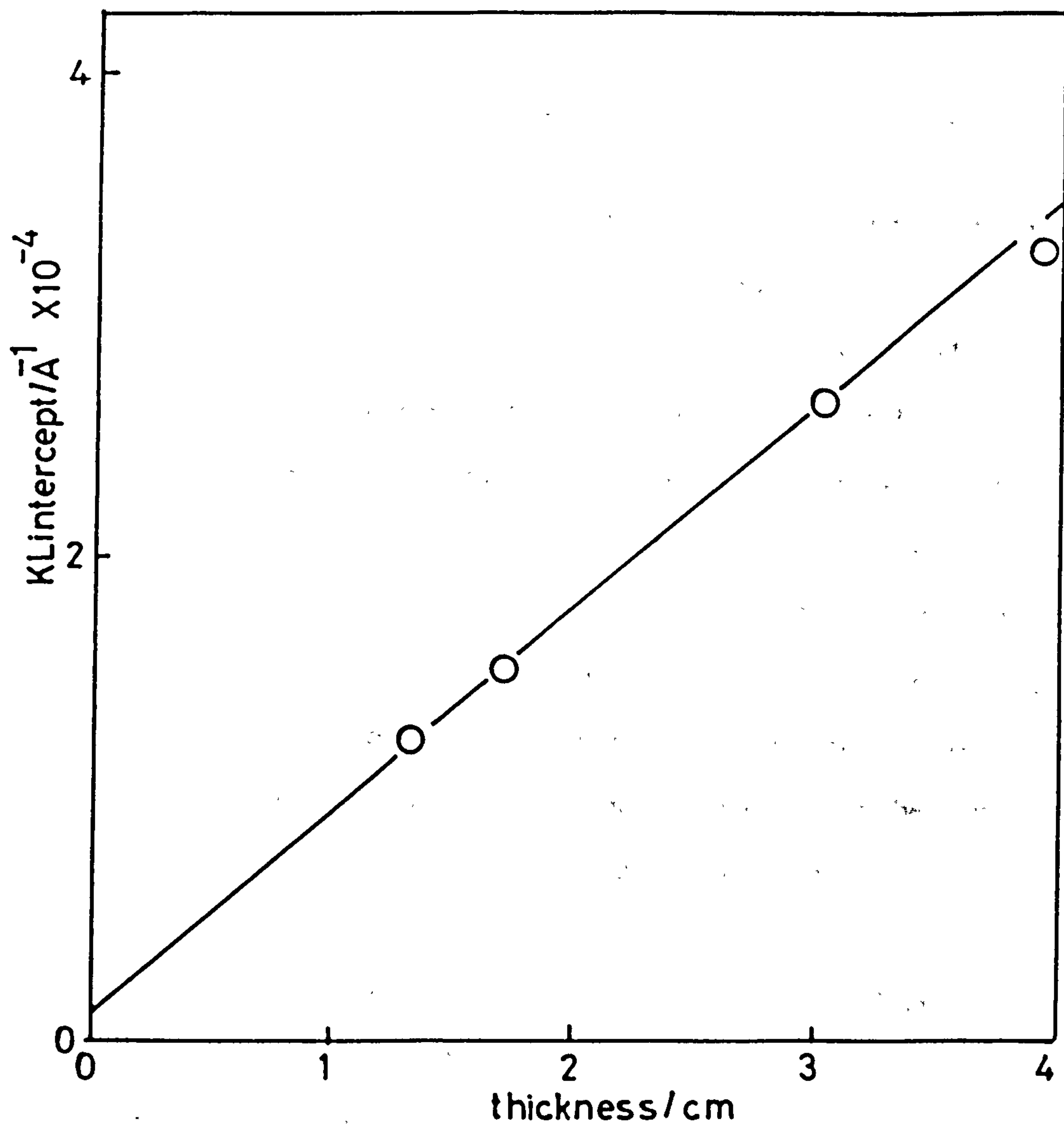


Table 4.2 Diffusional parameters for oxidation of hydrogen peroxide

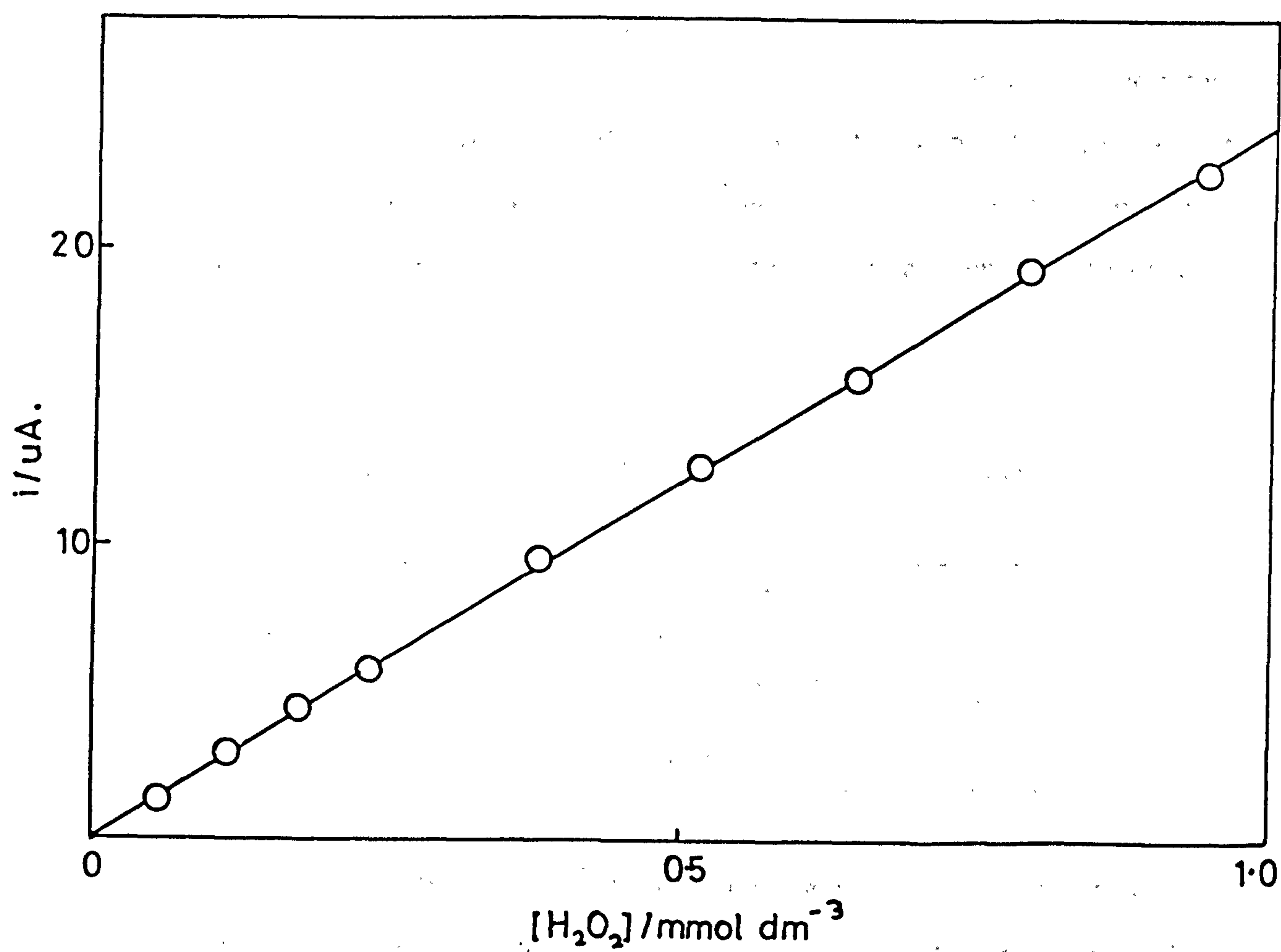
Parameter	Value (cm ² s ⁻¹)	Method of Determination
<i>D</i>	7.9×10^{-6}	Oxidation at pNMP-GOD electrode (a_{∞} varied)
	$0.6 \text{ to } 1.0 \times 10^{-6}$	Anodic oxidation at platinum ⁽¹⁹²⁾
<i>KD'</i>	$1.06 \text{ to } 1.12 \times 10^{-8}$	Oxidation at pNMP-GOD electrode at different values of a_{∞}
	1.56×10^{-8}	Oxidation at pNMP-GOD electrode at different values of l

A final investigation of hydrogen peroxide oxidation at pNMP-GOD electrodes was designed to test the stability of the polymer on prolonged exposure to hydrogen peroxide. A single modified electrode, of thickness 3.1×10^{-5} cm, was used throughout these measurements. The electrode was rotated (9 Hz) and the hydrogen peroxide concentration was increased stepwise by injecting aliquots of stock hydrogen peroxide solution. The limiting current, at 0.90V vs SCE, as a function of a_{∞} is shown in figure 4.7. A linear response was seen over the concentration range studied. The limiting current at the highest concentration studied (around 1×10^{-6} mol cm⁻³) was found to be stable for a period exceeding 2 hours. No change in the response due to polymer degradation, and no change in the visual appearance of the polymer was seen. This is in contrast to the polypyrrole/hydrogen peroxide system⁽¹¹⁵⁾.

It has been shown that the amperometric detection of hydrogen peroxide at the platinum surface of the pNMP-GOD is suited to the detection of enzymically produced hydrogen peroxide. This mode of detection was used in the work described in the following sections of this chapter.

In the next section a method for optimising the conditions of pNMP-GOD film production is described together with an analysis of the mechanism of polymer

Figure 4.7 Dependence of the limiting current on the bulk hydrogen peroxide concentration ($l=3.1\times 10^{-5}$ cm, $\omega = 9$ Hz).



growth in the presence of GOD.

4.5.2 Enzyme Immobilisation

Films of glucose oxidase containing poly-*N*-methylpyrrole (GOD-pNMP) were electro-deposited from buffered aqueous solutions (section 4.2) containing GOD (0 to 10 mg cm⁻³) and *N*-methylpyrrole (0.05 mol dm⁻³). The optimum conditions for the potentiostatic and galvanostatic growth of such films are detailed in table 4.3. No differences were observed between the films grown by these two methods. The response of a potentiostatically grown GOD-pNMP film, of defined thickness and enzyme loading, was seen to be identical to that of a comparable galvanostatically grown film. Films were normally grown in potentiostatic mode.

Table 4.3

Optimum conditions for growth of polymer films containing glucose oxidase

Method (a)	Conditions	Time/min
Potentiostatic (P)	Step from open circuit to 800 mV Typical current density (4 mA cm ⁻²)	2-8
Galvanostatic (G)	Step from $i = 0$ to 3 mA cm ⁻³ Typical voltage 750 mV	2-8

- (a) All solutions 0.05 mol dm⁻³ *N*-methylpyrrole in 0.15 mol dm⁻³ phosphate pH 7.2. 0.1 mol dm⁻³ *NEt*₄*BF*₄ containing 1 mg cm⁻³ glucose oxidase (160 U cm⁻³) degassed with nitrogen.

The film thicknesses were determined by controlling the number of coulombs passed during film growth. The enzyme loading in the films was controlled by altering the concentration of GOD in the growth solutions. Each film produced, and which subsequently had its response to glucose measured, was of a defined thickness

and enzyme loading.

The potentiostatic current transients for the electrodeposition of poly-*N*-methylpyrrole have the same form in the presence or absence of GOD. It is interesting, however, that the currents observed in the presence of GOD (1 to 10 mg cm⁻³) are typically significantly larger (50 to 100% increase). The enzyme GOD constitutes a large polyanion⁽¹⁸⁹⁾ at the pH of the growth solutions (pH 7.2). A study of the literature describing the electropolymerisation of pyrroles in the presence of other polyanions reveals that there are significant differences between the use of simple electrolyte ions and high molecular weight poly-electrolytes. Typical polyanions used as electrolytes during the electropolymerisation of pyrrole from aqueous solution are poly(vinylsulphate), PVS⁻, poly(vinyl chloride), PVC⁻, or poly(4-styrenesulphonate), PSS⁻ (193-196).

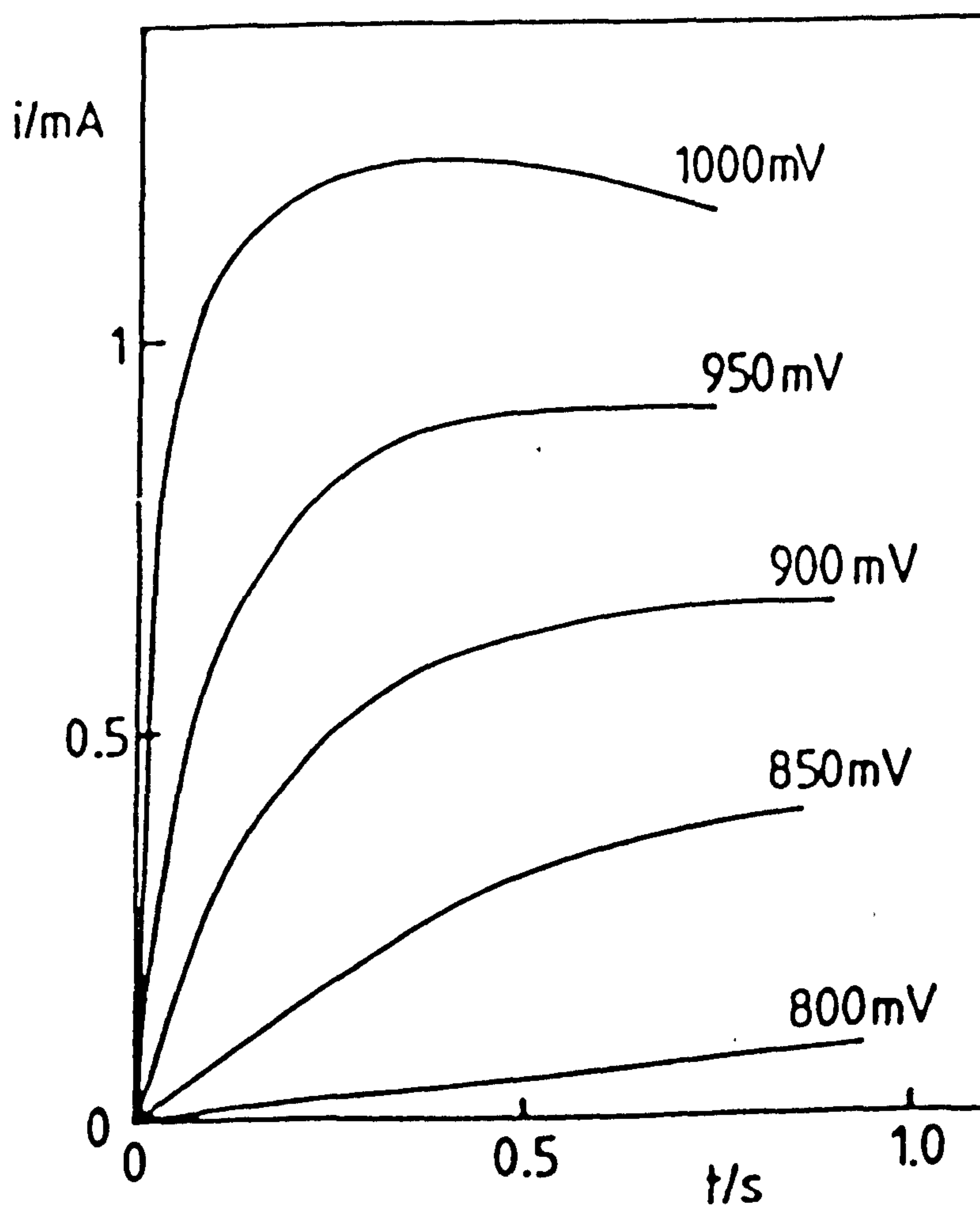
Shimidzu *et al* have studied the electrodeposition of polypyrrole-polyanion (PPy/PE) composites from aqueous solutions by potential cycling. They found that when using a simple electrolyte anion, such as Cl⁻, and a constant deposition regime a charge of 5.6 mC cm⁻² was passed for polymerisation on each potential cycle. This corresponds to a thickness increase of 14 nm for each cycle. When a high molecular weight polyelectrolyte ion, PVS⁻ or PSS⁻, was substituted for the Cl⁻ ion a two-fold increase in the charge passed, and hence thickness, produced on each potential cycle was seen. In the presence of PSS⁻, at the same concentration as that used for the Cl⁻ experiments, the charge passed per cycle increased to 13.1 mC cm⁻², corresponding to a change in thickness of 32.8 nm per cycle. It is pleasing that this increase in the charge passed during electropolymerisation when including a large polyanion in the aqueous growth solution has been described by other authors. Shimidzu *et al* rationalise this effect in terms of the concentration of the small (Cl⁻) and large (PSS⁻) electrolyte ions at the electrode surface during the electropolymerisation process. They observed that under constant potentiostatic electropolymerisation conditions, the rate of electropolymerisation of pyrrole

increases at higher concentrations of the small electrolyte ion. They suggest that the two-fold increase in the current during polymerisation of pyrrole in the presence of a polyelectrolyte is due to an increase in the concentration of this electrolyte at the electrode surface, when compared to a simple electrolyte, due to the entropic advantage of polyelectrolytes.

There are both similarities and differences between the polyelectrolytes described and GOD. Both carry a polyanionic charge, at neutral pH, and have a comparable molecular weight, $\text{PVS}^- \approx 2.5 \times 10^5$ and $\text{GOD} \approx 1.6 \times 10^5$. There are large structural differences, however, between these two species. PVS^- is essentially a linear chain molecule whereas GOD is a compact globular molecule, with exposed anionic groups on its outer surface. The PVS^- molecule obviously assumes a far higher number of negative charges than the enzyme and is thought to become entangled with the polymer chains during growth of polypyrrole. This is not the case with GOD however, which retains its globular structure in the polymer. In spite of these differences it would appear that the polyelectrolytes, PVS^- and PSS^- , act in much the same way as GOD during electrodeposition of polypyrroles. They have the effect of increasing the effective electrolyte concentration at the electrolyte/electrode interface during polymerisation. The resulting increased rate of polymerisation accounts for the increased current seen. Now that some insight into the effect of GOD on the magnitude of the current observed during polymerisation has been gained, it is interesting to determine whether or not the presence of GOD alters the mechanism of the electrodeposition process.

An investigation into the relationship between current and deposition time on the rising portion of the growth transient was undertaken. Short time growth transients were recorded for the first second of growth at a range of potentials (figure 4.8) in the presence and absence of GOD. Plots of i against t^x where $x = 1, 2$ or 3 , were constructed for the initial phase of growth. The best fits to a linear current-time relationship were found for plots of i vs t^2 over the wide potential range studied.

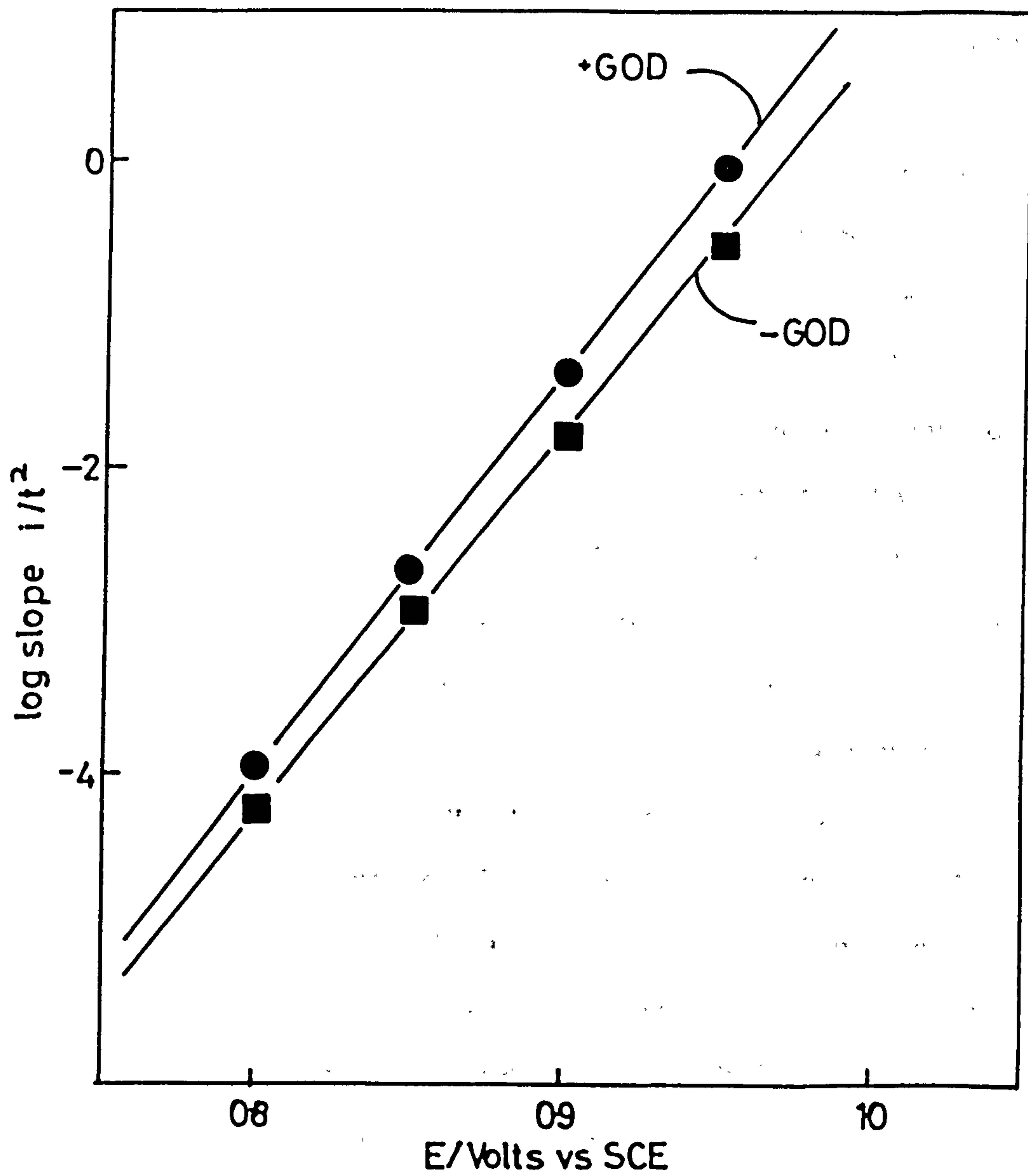
Figure 4.8 Short-time current transients for the initial phase of polymer growth from a solution containing *N*-methylpyrrole (50 mmol dm^{-3}) and glucose oxidase (5 mg cm^{-3}) at a variety of applied potentials.



This is in good agreement with the results of Pletcher *et al* for the growth of poly-*N*-methylpyrrole from neutral aqueous solutions⁽¹⁸²⁾. Plots of the logarithm of the slopes of the i vs t^2 plots against the polymerisation potential (eV) were linear for the polymerisation of *N*-methylpyrrole in the presence and absence of enzyme (figure 4.9). The slope of the plots is $(38 \text{ mV})^{-1}$. Two factors are apparent here. Firstly the data, either with or without the enzyme, are in good agreement with that of Pletcher *et al* and are consistent with a growth mechanism involving instantaneous, rather than progressive, nucleation and three dimensional growth⁽¹⁸²⁾. Secondly, although the presence of the enzyme has been shown to affect the magnitude of the current during the electrodeposition process, it does not affect the mechanism of electrodeposition. In the context of successful enzyme immobilisation it is satisfactory that the mechanism of polymerisation is not altered by the presence of GOD. No attempt was made to prove beyond any doubt that the growth does proceed via the mechanism predicted. Indeed, other growth mechanisms would account for the t^2 dependence of the transient current^(197,198).

Once the GOD containing films of poly-*N*-methylpyrrole were produced they were washed extensively by rotation in buffer solution for at least 5 minutes to remove any weakly incorporated or adsorbed enzyme. Failure to adopt this procedure resulted in release of a small amount of GOD into the bulk solution. This situation is not desirable and results in a sloping baseline on the addition of glucose when the electrode is potentiostated at a potential suitable for hydrogen peroxide detection. The sloping baseline is due to generation of hydrogen peroxide by the homogeneous GOD reaction in the bulk solution and its subsequent detection at the underlying platinum electrode. After this washing procedure the electrodes were placed in fresh buffer (pH 7.2) solution and potentiostated ready for glucose responses to be measured.

Figure 4.9 Plot of the logarithm of the slopes of the i vs t^2 plots as a function of potential applied for polymerisation.



The next section describes the way in which the response of the immobilised GOD to glucose was measured.

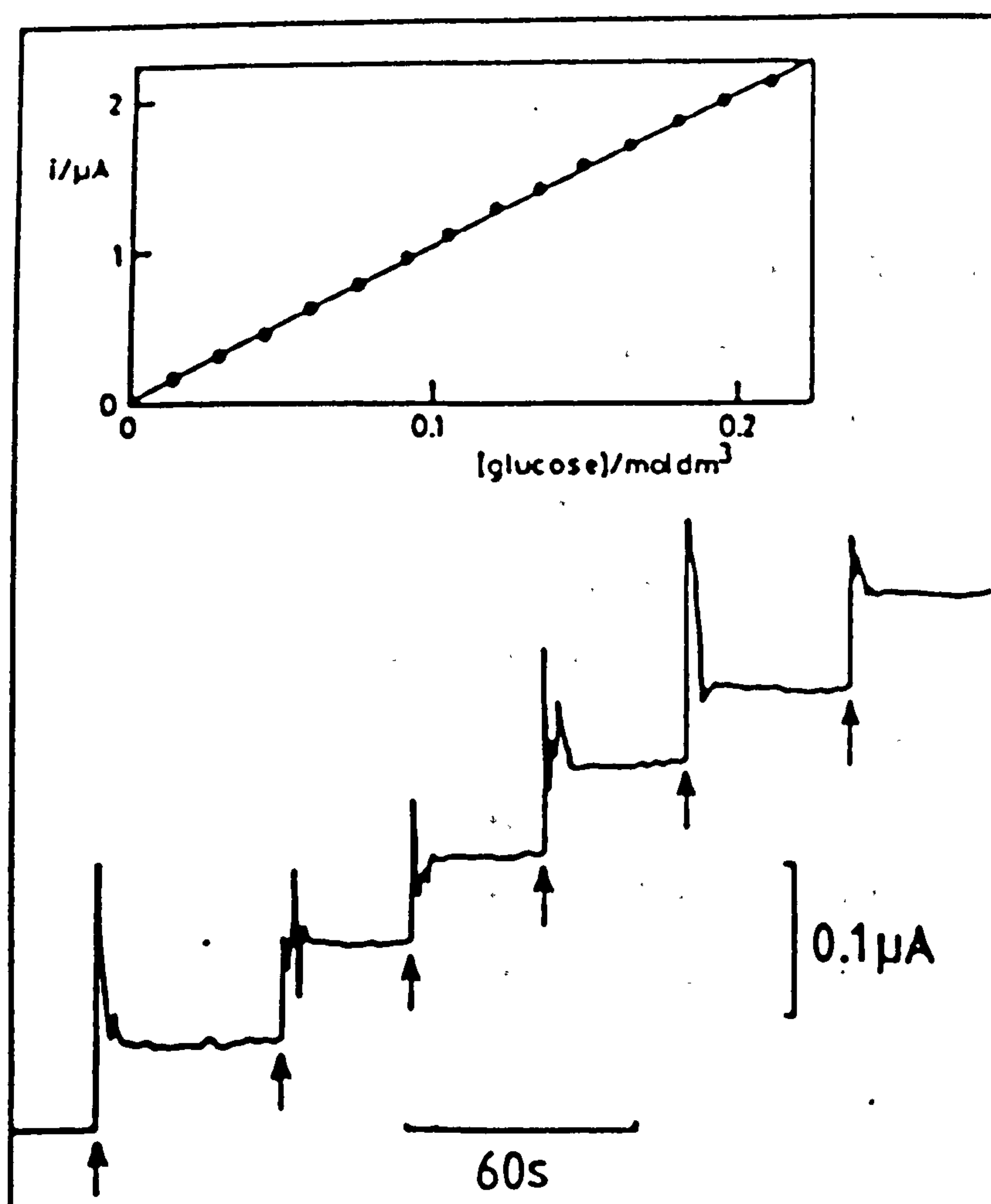
4.5.3 Response to Glucose

Glucose responses were measured at a rotating glucose oxidase - poly-*N*-methylpyrrole (GOD-pNMP) electrode (typically 9 Hz). The electrode was potentiostated at 0.90 or 0.95 volts (vs SCE) in order to detect hydrogen peroxide (H_2O_2) produced by reaction with glucose (section 4.5.1). Time was allowed for the polymer charging current to decay and a stable baseline current to be reached. Electrodes typically took 40 minutes for a stable current to be reached (< 200 nAmps) the first time they were used, and then around 5 minutes thereafter. The exact time taken was dependent on the thickness of the GOD-pNMP film, being significantly longer for very thick films, but never taking more than 40 minutes.

The glucose concentration of the buffer solution was increased step-wise by adding aliquots of a stock glucose solution (1.00 mol dm^{-3}) from a microsyringe. The solution was allowed to mix and once the resulting current increase had stabilised, taking < 20 seconds, a further injection of glucose was made. Figure 4.10 shows a typical set of current responses on consecutive additions of glucose. The inset shows the calibration curve obtained from these responses as a plot of current against bulk glucose concentration. The electrode continues to respond to glucose concentrations in excess of the Michaelis constant for the homogeneous enzyme reaction, which has a value of around $0.033 \text{ mol dm}^{-3}$ glucose, under similar conditions of pH and temperature. This effect is due to the inefficient partitioning of glucose from the bulk solution into the GOD-pNMP film resulting in a much lower glucose concentration in the film than in the surrounding solution.

The responses of GOD-pNMP films to glucose were measured in this way for a range of film thicknesses and enzyme loadings. In the next section the data are compared to the theoretical model for the electrode response (chapter 3).

Figure 4.10 The response of the glucose oxidase electrode to additions of glucose. Each arrow represents an increase in glucose concentration of 6.6 mmol dm^{-3} . The electrode was rotated at 9 Hz ($E = 0.95 \text{ V vs SCE}$). The inset shows a typical plot of current as a function of bulk glucose solution.



4.6 COMPARISON OF THE RESULTS TO THEORY

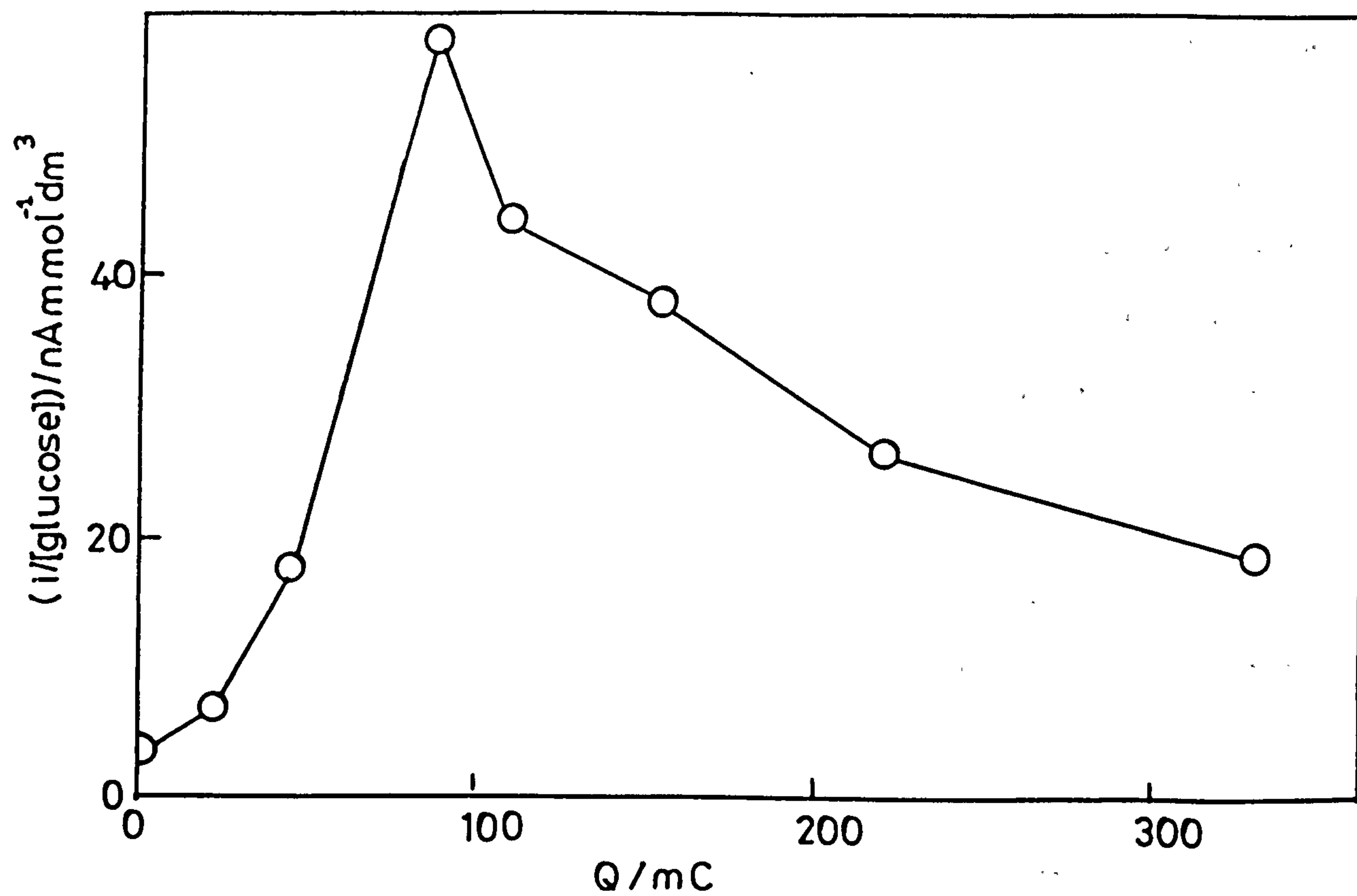
In the immobilisation system developed it is possible to vary the enzyme loading and thickness of the glucose oxidase - poly-*N*-methylpyrrole (GOD-pNMP) films with some accuracy. Glucose response data obtained from a systematic study of enzyme loading and film thickness are compared to the theoretically predicted characteristics of the electrode response in this section. Firstly the effect of varying the GOD-pNMP film thickness will be described. This will be followed by results for the variation in enzyme loading.

4.6.1 The Effect of Film Thickness

Film thickness was altered by changing the amount of charge (Q mC cm⁻²) passed during film growth. The exact correlation between Q and the film thickness, l , has been discussed previously. The charge passed was in the region 10 to 300 mC (electrode area of 0.385 cm²). A constant enzyme concentration (1.0 mg cm⁻³) was included in the growth solutions. Glucose responses were measured at a series of film thickness and a calibration plot constructed for each set of glucose data. The response curves were linear in all cases. A plot of the slope of the glucose calibration lines as a function of film thickness was constructed (figure 4.11). This shows a pronounced maximum, clearly indicating that there is an optimum film thickness (5.15×10^{-5} cm) which maximises the sensitivity of the electrode to glucose, at this enzyme loading.

This type of behaviour was predicted by the theoretical analysis presented in chapter 3 of this thesis. This corresponds to case B of this section in which the rate limiting step is the reaction of the substrate with the enzyme. The dependence of the response on the substrate concentration and the film thickness is described by equation 3.29 of section 3.3.1.

Figure 4.11 Plot of the gradient of the glucose calibration plot as a function of charge passed to grow the glucose oxidase / poly-*N*-methylpyrrole films ($A = 0.385 \text{ cm}^2$, $W = 9 \text{ Hz}$).



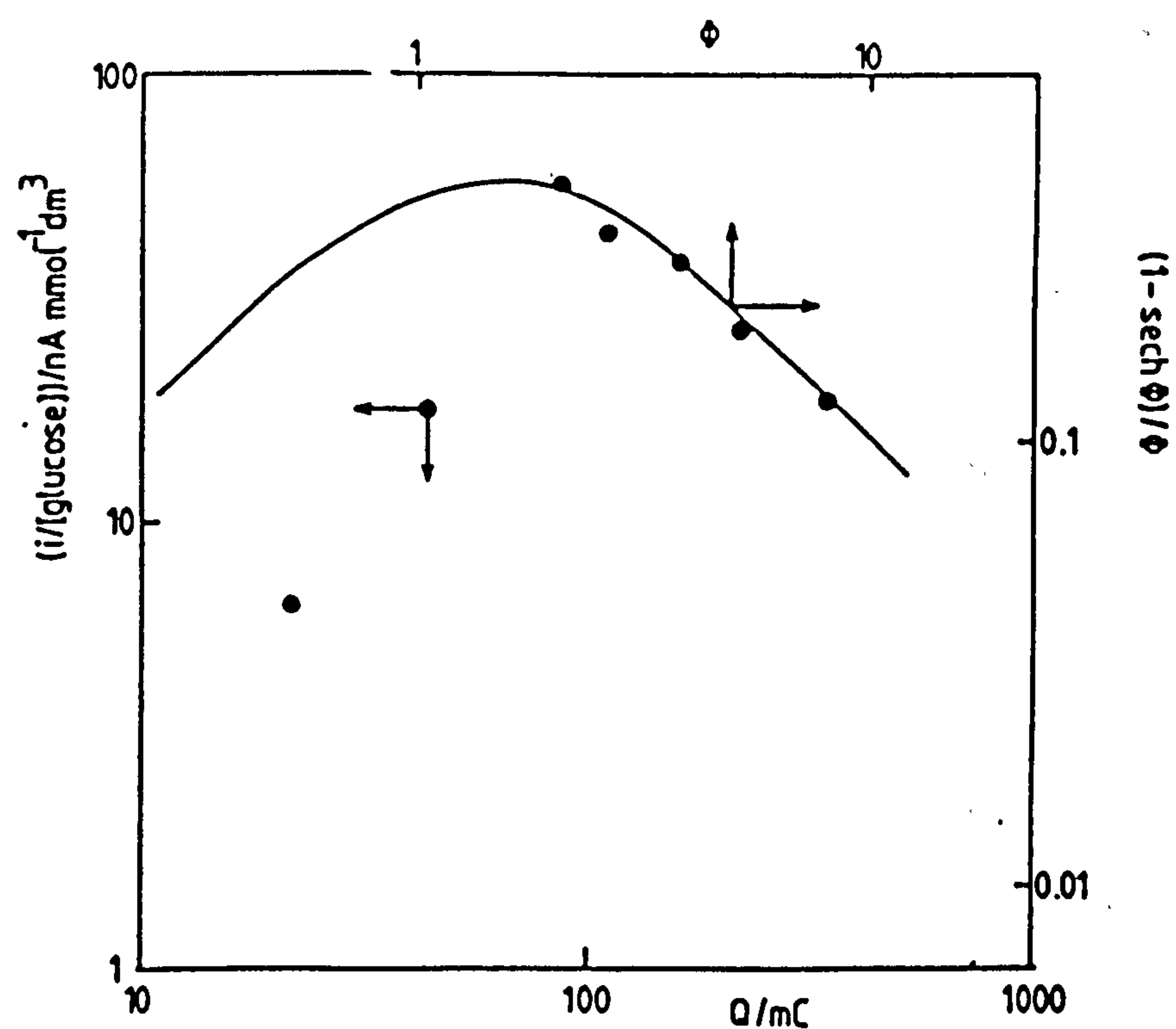
$$\frac{i}{s_{\infty}} = nFAD'_s K \left[1 - \text{sech}(l/X_K) \right] / l \quad (4.6)$$

All the terms in this equation have been defined previously. The term X_K is an expression for the kinetic length of glucose in the film, where

$$X_K = (Ds'K_M/k_{cat}e_{\Sigma})^{1/2} \quad (4.7)$$

A direct comparison of the experimental data, figure 4.10, to the theoretical response as a function of film thickness was made by constructing log-log plots. A log-log plot of the experimental data was superimposed onto a log-log plot of equation (4.6). This comparison is shown in figure 4.12. The agreement between experiment and theory is excellent for films grown by passing a charge of greater than 100 mC (260 mC cm⁻²). The current response for the thinner films is, however, significantly lower than that predicted. These deviations arise because the charge passed during polymerisation was used as a direct measure of polymer thickness. This is not a good assumption for very thin films since a large proportion of the charge passed may be non-Faradic charging current and as such is not involved in film growth. This effect will become less significant as the film thickness increases as the non-Faradic current represents a constant contribution to the total. To illustrate this effect an attempt was made to subtract off the charging current for the very thin film data. The constant non-Faradic component was estimated by measuring the charging current when the clean platinum electrode was stepped from 0 to 0.85 volts (vs SCE) in the buffer solution in the absence of poly-*N*-methylpyrrole. It was found that the largest charging currents seen resulted in the passing of 5 mC. It is apparent therefore that this non-Faradic component is not large enough to explain the deviation from theory seen in the thinnest films. An alternative explanation may lie with the washing procedure used to remove loosely bound or immobilised enzyme. It is likely that such a procedure will remove enzyme to a certain depth from each film irrespective of its thickness, assuming that the enzyme near to the film surface is

Figure 4.12 Comparison of the experimental variation of the electrode response to glucose as a function of l with the theoretical expression. The points represent the experimental data and the solid line is drawn according to equation 4.6.



less strongly immobilised than that lying deep within the film. For the thinnest films in which the response is strongly dependent on the enzyme loading, removal of this constant amount of enzyme during the washing procedure will significantly reduce the electrode response. In the thicker films, where the response becomes independent of enzyme loading, this will have little effect. There is no real evidence to support this hypothesis and it is offered only as a possible explanation of the deviation from theory seen in the thinnest films. Further work would be required to demonstrate this occurrence. Overall there is, however, good agreement between the experimental data and the theory described. The main characteristic seen, the maximum in response as a function of film thickness is fully predicted by the theory.

It has been mentioned above that the response of thin films is strongly dependent on enzyme loading whereas that in the thicker films is independent of enzyme loading. This effect will be described in the next section and the way in which this type of behaviour is predicted by the model will be presented.

4.6.2 Variation of the Enzyme Loading

Returning to equation 4.6 it can be seen that this also predicts that the response of the electrode will depend on enzyme loading in certain cases. For thick films, when $l/X_K > 1$, no dependence on enzyme loading was seen experimentally. This independence of the response is predicted by the theory. When $l/X_K > 1$

$$l/(D_S K_M / k_{cat} e_\Sigma)^{1/2} > 1 \quad (4.8)$$

In this case, corresponding to thicker films, equation 4.6 becomes

$$\frac{i}{s_\infty} \approx nFAD'_s K l \quad (4.9)$$

The theory predicts, therefore, that there will be no dependence of the electrode response on enzyme loading for thick films.

In thin films ($l/X_K \ll 1$) a strong dependence of the response on enzyme

loading is seen. This is again predicted by the theory, when $l/X_K \ll 1$ equation 4.6 becomes

$$\frac{i}{s_{\infty}} \approx nFAD'_s K_{S_{\infty}} e_{\Sigma} k_{cat} l / 2K_M \quad (4.10)$$

It is apparent that in this situation the theory predicts that increasing the enzyme loading or film thickness should increase the electrode response. The experimental data show that the response becomes dependent on enzyme loading for film of less than about 5×10^{-5} cm in thickness. Furthermore the responses for such films are seen to be rotation speed dependent. Figure 4.13 shows typical results for this rotation speed dependence in a thin film of relatively high enzyme loading. As the rotation speed increases the response decreases and approaches a plateau current. This is consistent with the concentration polarisation of hydrogen peroxide in the film. At low rotation speeds hydrogen peroxide builds up in the diffusion layer increasing the response of the electrode. At higher rotation speeds, however, the rate of loss of hydrogen peroxide to the bulk solution is increased, leading to a decrease in the response.

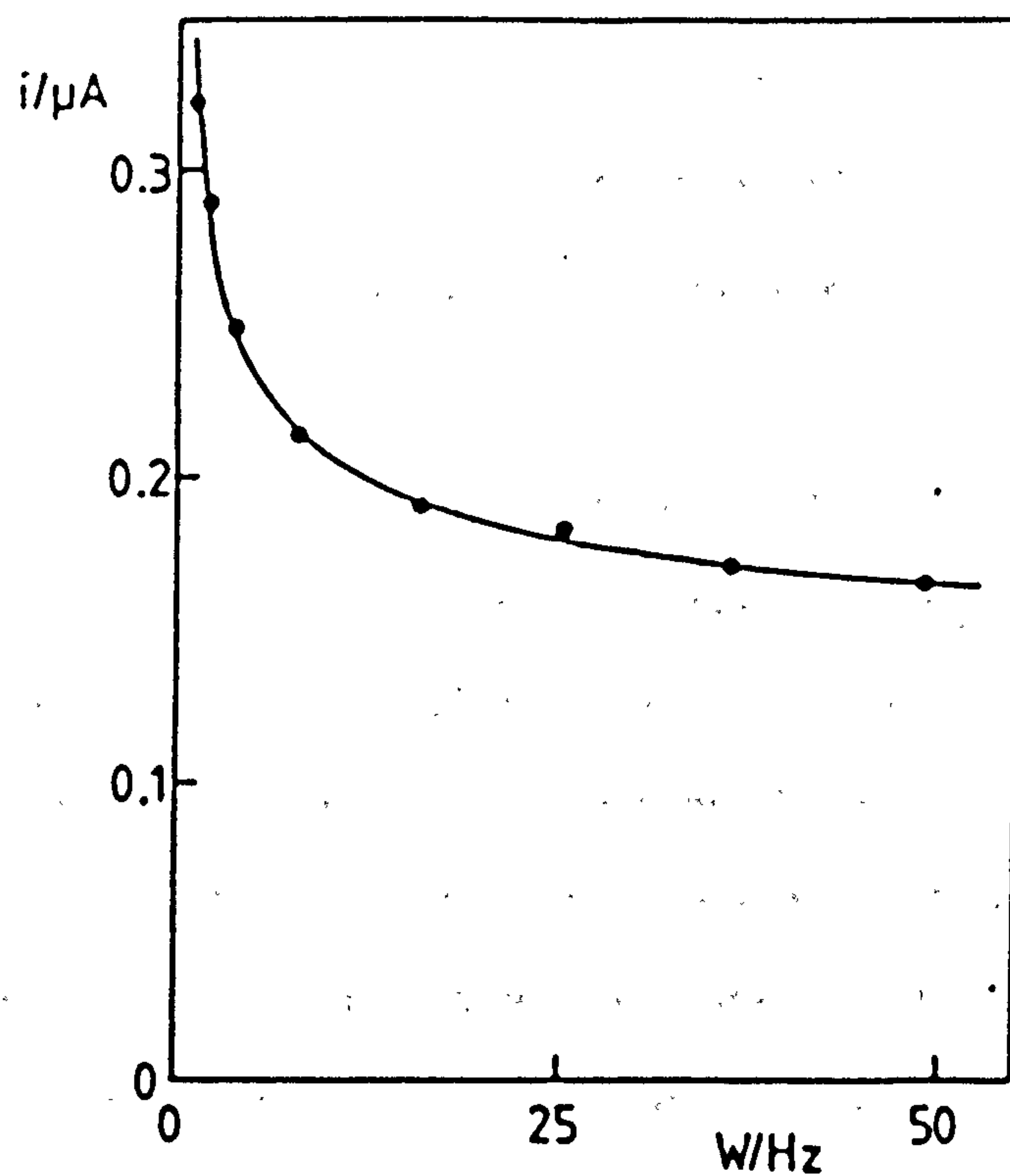
In order to model this situation we must change the boundary conditions for hydrogen peroxide at the outside of the film. Equation 3.12b was replaced by

$$x = l, \quad \frac{\partial b}{\partial x} = -k'_D b_l / K_B D_B \quad (4.11)$$

where k'_D is the mass transfer rate constant⁽¹⁹⁹⁾ for removal of hydrogen peroxide, K_B is the partition coefficient for H_2O_2 into the film, and b_l is the concentration of H_2O_2 in the film near the surface. This new boundary condition says that at the film surface the concentration gradient of hydrogen peroxide is given by the rate of removal of H_2O_2 from the film surface divided by a term describing partition and diffusion of H_2O_2 out of the film.

The mass transfer rate constant, k'_D , is given by⁽¹⁹⁹⁾

Figure 4.13 The variation of the electrode response with the rotation speed for thin films ($l \ll X_K$) with high enzyme loadings ($e_\Sigma = 2.08 \text{ mg cm}^{-3}$, $Q = 25 \text{ mC}$, $A = 0.385 \text{ cm}^2$). The glucose concentration was 6.3 mmol dm^{-3} (pH 7.0, 25°C).



$$k'_D = 1.554 D_B^{1/3} \nu^{1/6} W^{1/2} \quad (4.12)$$

At higher rotation speeds k'_D becomes greater, resulting in a decrease in the electrode response since K_B and D_B are constants.

Solution of equation 4.6 with this boundary condition gives an expression for the flux of hydrogen peroxide to the underlying platinum electrode

$$j_{obs} = \frac{j_s + j_B l k'_D / D_B}{1 + l k'_D / D_B} \quad (4.13)$$

where j_{obs} is the observed current.

This expression reduces to the previous result for j_B when k'_D is large and gives a corresponding result for j_s when k'_D is very small. A plot of j_{obs} against $W^{-1/2}$ is shown in figure 4.14. The intercept on this plot corresponds to $l k'_D / D_B \gg 1$ and gives a good estimate of j_B .

Taking the experimental values of j_B a comparison was made with the theory by constructing log-log plots of the responses as a function of enzyme concentration in the growth solutions and the equivalent dimensionless form of equation 4.6. Excellent agreement between the experimental data and theory was found for all but the very lowest enzyme loadings, corresponding to less than 0.2 mg cm^{-3} GOD in the growth solutions. These plots are shown in figure 4.15, the inset shows the experimental response as a function of enzyme concentration with the solid line drawn according to equation 4.6.

The increased response observed for very low enzyme loadings arises from the adsorption of the enzyme at the platinum electrode surface prior to the electrodeposition process. This effect is clearly demonstrated in figure 4.16. This shows that as the electrode is held in the growth solution prior to electrodeposition for periods of up to 5 minutes the electrode response increases. The enzyme adsorbs onto the metal electrode surface reaching a saturating coverage at a time exceeding 5 minutes. This process can be followed using ellipsometry. This technique clearly

Figure 4.14 Plot of j_{obs} as a function of $W^{-1/2}$. The intercept of this plot gives an estimate of j_B (data from figure 4.13).

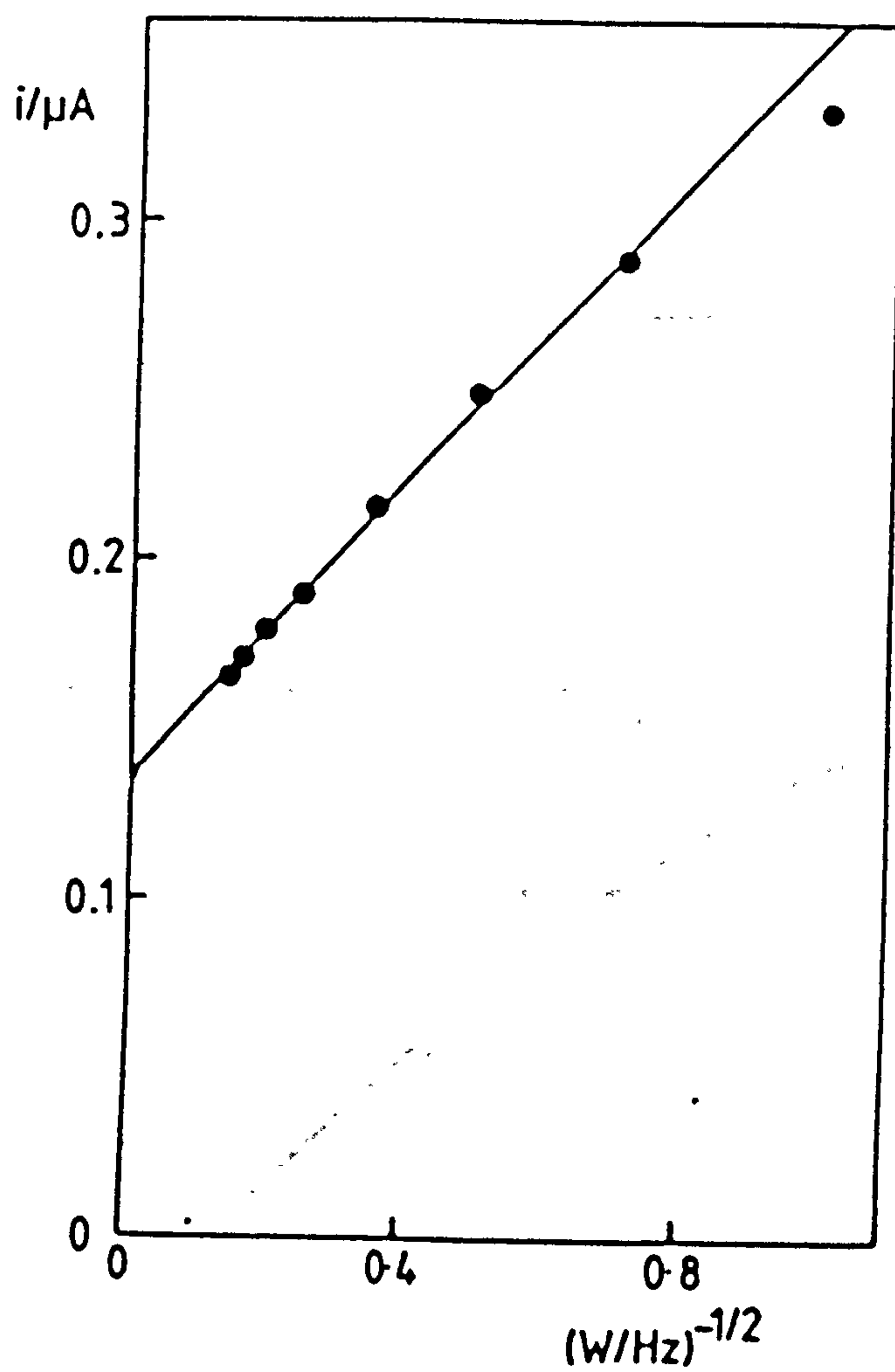


Figure 4.15 Comparison of the experimental variation of the electrode response to added glucose as a function of e_{Σ} with the theoretical expression. The points represent the experimental data and the solid line is calculated from equation 4.6. The inset shows the fit of experiment to theory ($l = 40$ mC, $A = 0.385$ cm², $W = 9$ Hz, pH 7.0, 25°C).

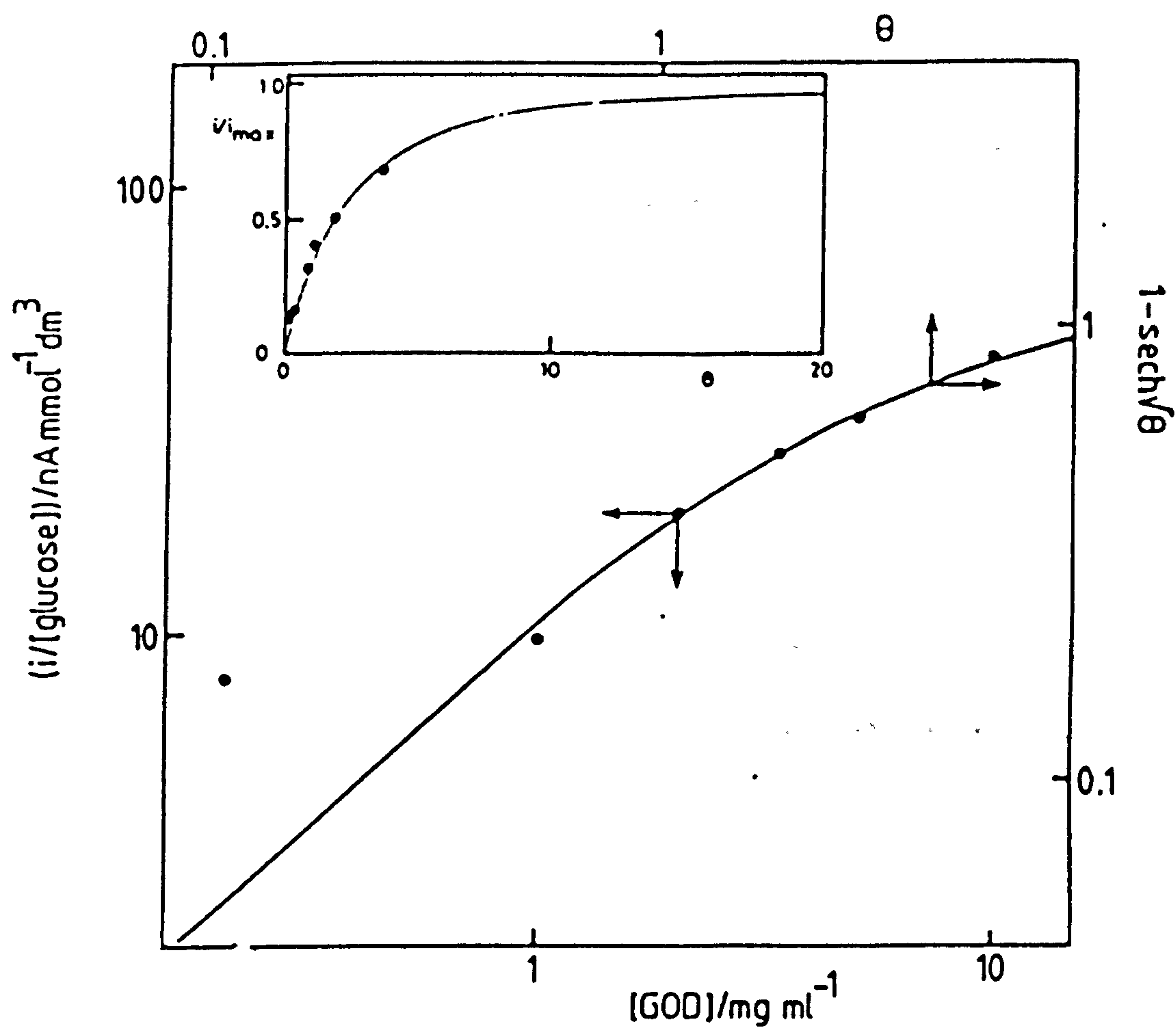
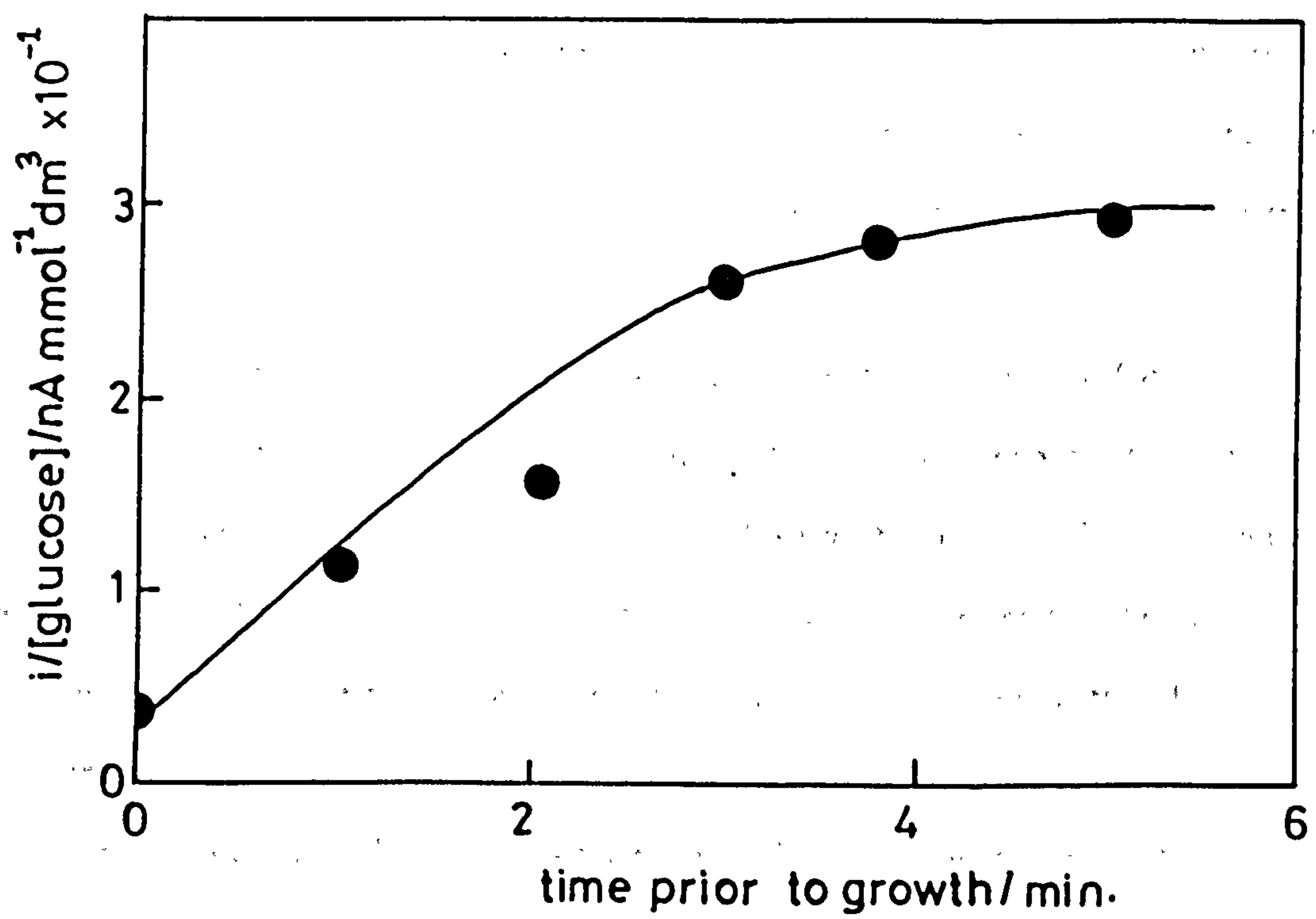


Figure 4.16 Effect of glucose oxidase concentration on the response of the resulting electrode. A plot of response as a function of the time spent in the polymerisation solution at 0 volts is shown.



demonstrates that the enzyme protein adsorbs onto a clean platinum surface over a period of minutes. Further, this technique shows that saturating coverage is not reached over the ten minute experimental period.

This pre-adsorption of glucose oxidase leads to an artificially high enzyme concentration at the electrode surface. The adsorbed enzyme is still in an active form and in thin films ($l \ll X_K$) glucose penetrates throughout the film and gives rise to an anomalously high response. This type of protein adsorption is well known⁽²⁰⁰⁾.

This unwanted effect can be removed by connecting the electrode to the potentiostat, or galvanostat, before its immersion in the growth solution. This procedure causes the electrodeposition process to begin as soon as the electrode is contacted with the growth solution. In this way unwanted enzyme preadsorption effects can be removed.

Adoption of this procedure resulted in the electrode response for the modified electrode with the lowest enzyme loading (0.18 mg cm^{-3} growth solution) being reduced by almost 60% to give a value very close to that predicted by the theory. It would appear, therefore, that this is the correct explanation for the deviation of the experimental electrode responses from the predicted responses in thin films of low enzyme loading.

Good correlation between experimental data and the theoretically predicted response has been seen for films of a wide range of thicknesses and enzyme loadings. This is satisfactory since it shows that the assumptions made in the development of the model are correct. In the following section a discussion of the results is presented, along with kinetic and transport parameters derived from the fit of experimental data to theory.

4.6.3 Discussion

There are a number of characteristics which are fundamental to the operation of the glucose oxidase / poly-*N*-methylpyrrole (GOD-pNMP) system. The results presented in section 4.5.1 clearly show that hydrogen peroxide cannot react on the conducting pNMP matrix and that it must diffuse to the underlying platinum electrode surface to be oxidised. Using this theoretical analysis the kinetic characteristics of the immobilised enzyme and the transport of the substrate, glucose, and product, hydrogen peroxide, through the polymer film were investigated. The kinetic and diffusional parameters were obtained by measuring the displacement of the experimental data from the theoretical curves using dimensionless log vs log plots (section 4.6.1 and 4.6.2). The parameters obtained in this way are presented in table 4.4.

Table 4.4

Kinetics and mass transport parameters obtained for the detection of hydrogen peroxide produced by GOD immobilised in films of poly-*N*-methylpyrrole

$X_K/D_s K$	=	$6.2 \times 10^5 \text{ cm}^{-1} \text{ s}$	a)
X_K	=	$2.2 \times 10^{-5} \text{ cm}$	b)
$1/D_s K$	=	$2.5 \times 10^{11} \text{ cm}^{-2} \text{ s}$	c)
$k_{cat} \alpha/D_s K_M$	=	$5.6 \times 10^9 \text{ cm mg}^{-1}$	d)

- a) Calculated from the shift between experiment and theory in the *y*-axis in figure 4.12.
- b) Calculated from the shift between experiment and theory in the *x*-axis in figure 4.12.
- c) Calculated from the shift between experiment and theory in the axis in figure 4.15.
- d) Calculated from the shift between experiment and theory in the *x*-axis in figure 4.15. The parameter α describes the relationship between the concentration of enzyme in the polymerisation solution, [enz], in mg cm^{-3} , and the final concentration of enzyme in the film, e_Σ , where $e_\Sigma = \alpha [\text{enz}]$.

Values of $D_s K$ of 3.4×10^{-11} and $0.4 \times 10^{-11} \text{ cm}^2 \text{ s}^{-1}$ were obtained from independent thickness and enzyme loading experiments respectively. These are in reasonably close agreement. There do not appear to be comparable parameters in the literature for partition and diffusion of glucose into polypyrrole or similar polymeric matrices. Kamin and Wilson⁽²⁰¹⁾ obtained a diffusion coefficient for glucose of $6.7 \times 10^{-6} \text{ cm}^2 \text{ s}^{-1}$. They suggest that this may be reduced by diffusional limitations resulting from cross linking in the enzyme layer but do not quantify this effect. It would seem likely that D_s in the GOD-pNMP matrix will be smaller than this value

due to the imposition of diffusional limitations on the incoming glucose.

It is apparent that K is much less than 1 for this system as even when the bulk glucose concentration exceeds 0.25 mol dm^{-3} the electrode response remains linear. This is because the concentration of substrate in the GOD-pNMP layer is still below the K_M value for the immobilised enzyme.

These observations are consistent with the low value of $D_s K$ determined.

The value of X_K determined is of the order expected for this system. It is pleasing that for "thin" films (1 to $1.7 \times 10^{-5} \text{ cm}$) l is indeed less than X_K , $2.2 \times 10^{-5} \text{ cm}$, and furthermore for "thick" films that l is greater than X_K (4 to $8 \times 10^{-5} \text{ cm}$). Using this value of X_K a value of $k_{cat} \alpha / D_s K_M$ of $2.1 \times 10^9 \text{ cm mg}^{-1}$ is obtained. This compares favourably with a value of 5.6×10^9 obtained from figure 4.15.

It can be concluded that the experimental data fits well to the theoretically predicted characteristics in the system. A procedure has been described in which the electrode response can be optimised in a systematic way. The electrode response can be optimised in two ways. Firstly the sensitivity of the electrode to glucose can be maximised by careful choice of the film thickness. Secondly for a glucose sensing device the stability of the electrode can be maximised by choosing a film thickness at which the response becomes independent of enzyme loading. In this situation loss of some enzyme activity on storage or operation should not significantly decrease the electrode response to glucose. Without a systematic study of this type it is impossible, or at best very difficult, to understand how an immobilised enzyme system is operating and therefore difficult to produce a device with the desired characteristics.

In the next section the stability of this type of device to storage and repeated operation will be described. An understanding of the mode of operation of this device allows the sensitivity of the response to loss of GOD activity to be reduced.

4.7 THE STABILITY OF THE GLUCOSE ELECTRODE

A stability study was undertaken in which the electrode was stored in buffer (pH 7.2) at room temperature between glucose assays. A film thickness was chosen which is slightly thicker than the X_K distance. In this way the “thick” film produced retained most of its sensitivity to glucose whilst having a response which was independent of the enzyme activity in the film. The film used was grown galvanostatically to a thickness of 3×10^{-5} cm from a solution containing 5 mg cm^{-3} glucose oxidase (GOD).

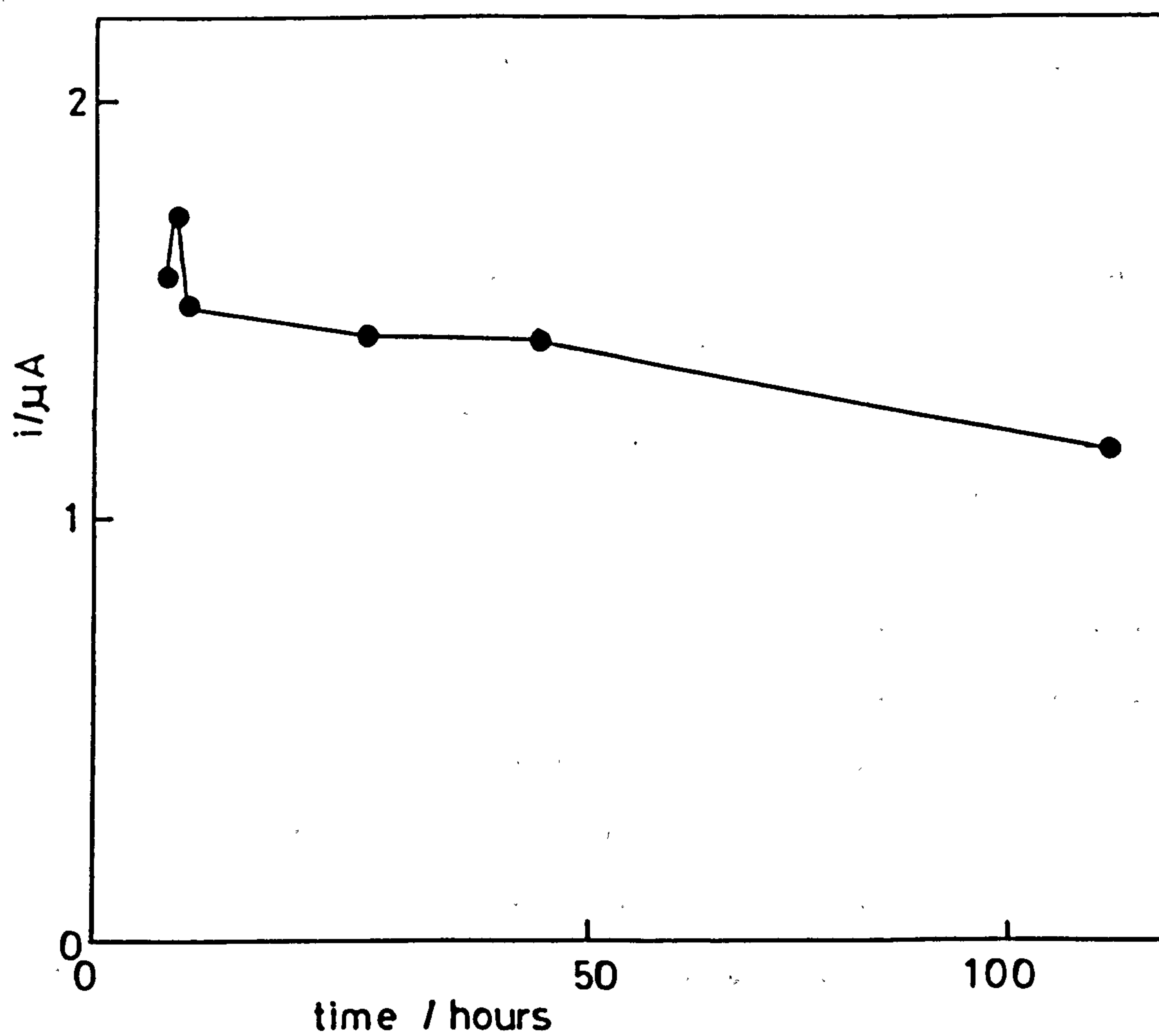
Responses to glucose (0.05 mol dm^{-3}) were measured by potentiostating the electrode at 0.95 volts (vs SCE) at set time intervals over a 5 day period. The electrode was rotated at 9 Hz to produce rapid mixing of the glucose with the bulk. The response was not rotation speed dependent in this “thick” film, high enzyme loading situation. Figure 4.17 shows the response of the electrode as a function of storage time. The electrode failed after 5 days when the polymer became detached from the platinum electrode surface.

Over the five day period in which the electrode response was measured around 25% of the initial glucose response was lost. The largest change in the response was seen between the first response measurements made immediately after production and then after 1 hour. This initial loss of response has been reported for glucose oxidase - polypyrrole system^(74,115).

The glucose oxidase - poly-*N*-methylpyrrole (GOD-pNMP) stability data can be directly compared to the literature data for the GOD-pyrrole (GOD-Py) system. In all cases the loss of response over the first day is the largest. Indeed, Umana and Waller describe a system in which around 65% of the initial response is lost over this 24 hour period. After this time the decrease in response is only small over a further 6 day period.

In a similar study Foulds and Lowe describe a loss of around 35% of the initial

Figure 4.17 The response of the glucose electrodes as a function of time stored at 25°C (pH 7.0 phosphate) after preparation. ($l = 3 \times 10^{-5}$ cm; $e_{\Sigma} = 5 \text{ mg cm}^{-3}$).



response within one day and again little change over a further 20 day period.

These results have close parallels with the GOD-pNMP system, after an initial loss of response within a 24 hour period the response becomes fairly stable.

The reason for this initial loss of response appears unclear. Foulds and Lowe do not attempt to explain this effect. Umana and Waller propose that the cause is loss of enzyme which is expelled from the polymer film by electrostatic repulsion between the polycationic polymer and the enzyme. Although the loss of activity may be due to a gradual leaching out of the enzyme in this system, their explanation as to the cause of this seems unlikely since the polymer and enzyme are known to carry opposite charges.

In the GOD-pNMP system the response of the device should be independent of enzyme activity in the film. It is difficult to explain the decrease in response in terms of loss of enzyme activity either by loss of enzyme molecules to the solution or the denaturation of the immobilised GOD. A more likely explanation is that the polymer film properties change after repeated cycles of storage and potentiostating at 0.95 volts. Any decrease in the films porosity will alter the partition and diffusion of glucose into and through the film. This would appear to be the most likely cause of the initial loss of response. After the first few response determinations the film becomes conditioned and the response remains fairly stable.

The film became detached from the electrode after 5 days. This is a simple mechanical problem and it is likely that this can be overcome by using either a rougher electrode, as used by Foulds and Lowe, or by including a polymeric plasticiser in the GOD-pNMP film during growth^(195,196).

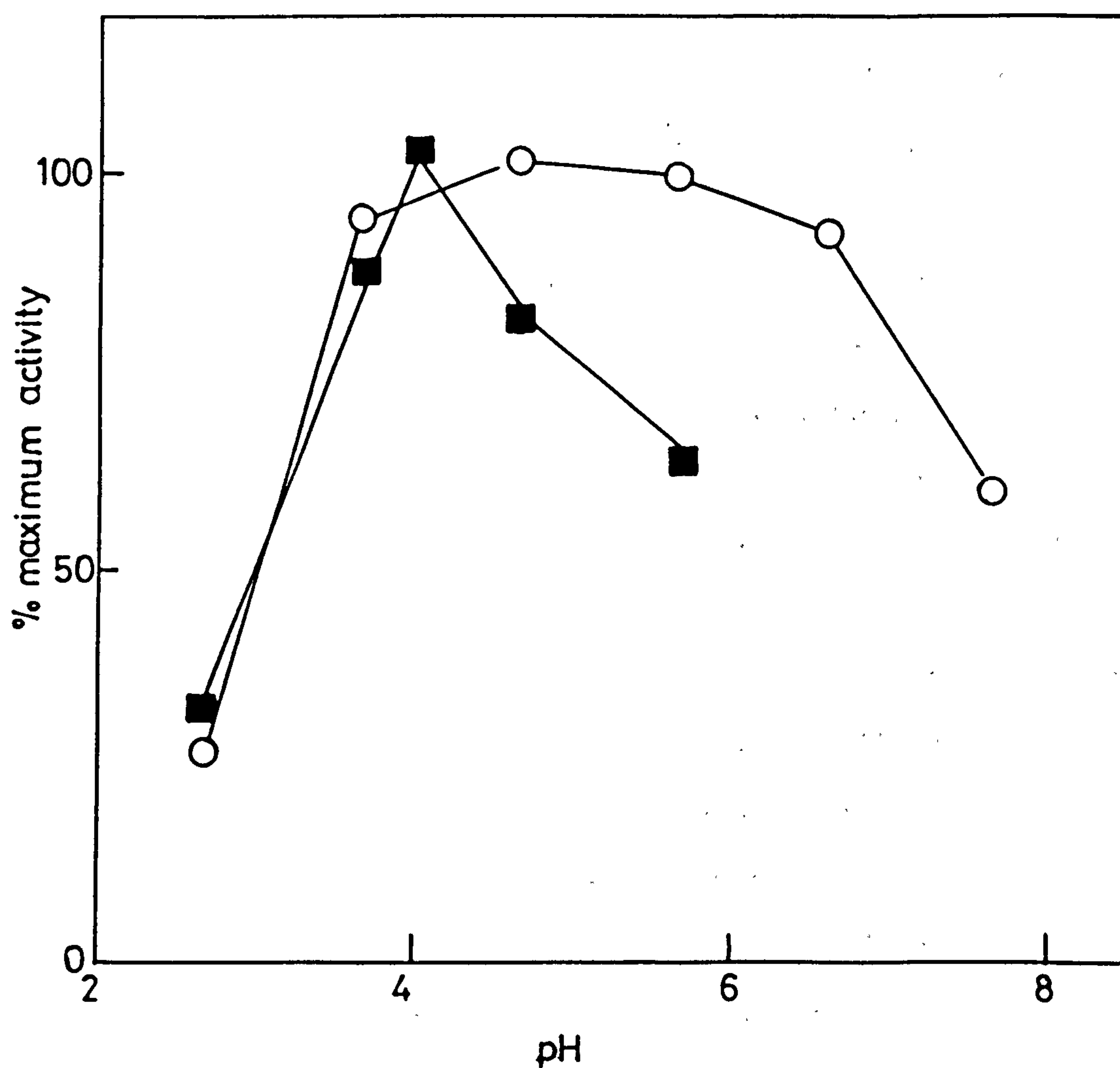
The stability of the GOD-pNMP electrodes is relatively good and compares favourably with that of the GOD-pPy electrodes described in the literature. It is likely that the small loss of response seen before a stable region is reached is due to a polymer conditioning process and not due to loss of enzyme content or activity of the thick film investigated.

In an attempt to further characterise this enzyme electrode system a pH study was undertaken. The relationship of the bulk pH to the sensor response is described in the next section. The pH profile of the GOD-pNMP system is then compared to the homogeneous pH profile and also to similar immobilised GOD systems.

4.8 DETERMINATION OF THE pH OPTIMUM OF THE IMMOBILISED ENZYME

The enzyme glucose oxidase (GOD) is typical in that it shows a pH optimum. Since all enzymes are proteins and as such composed of amino acid residues, pH changes in the bulk solution surrounding the enzyme will have marked effects on the ionic character the charged amino acid residues. A change in pH will alter the charges on amino and carboxylic acid groups at the active centres of the enzyme⁽²⁰²⁾. The enzyme will only exert its maximum catalytic effect when all the amino acid residues essential for catalysis at the active centre are in the correct ionic state. For this reason enzymes usually exert maximum catalytic activity over a narrow pH range only. Outside this range the essential residues at the active centre do not retain the required ionic character and the rate of catalysis decreases. Also in extremes of acid or base the enzyme molecule may become denatured and lose activity completely. This generally results in a bell shaped pH profile⁽²⁰³⁾. The enzyme GOD has such a pH profile for the homogeneous solution reaction. This is shown in figure 4.18. The effect of immobilising GOD in films of poly-*N*-methylpyrrole (pNMP) on the enzyme's pH optimum was investigated. Films studied were of defined enzyme loading (1 mg cm^{-3} in growth solutions) and film thickness ($1.3 \times 10^{-5} \text{ cm}$). These "thin" films ($l < X_K$) were studied because the response of the electrodes is known to be dependent on enzyme activity in this region. Therefore as the enzyme activity changes with the pH used for determination of the glucose response so the response itself will change. This would not be the case in the thick

Figure 4.18 pH profiles for free (○) and electrochemically immobilised (■) glucose oxidase. Reaction rates (0.1 mol dm^{-3} glucose) determined at 0.95 V vs SCE, 9 Hz for the immobilised enzyme.



film region ($l > X_K$) where the electrode response becomes independent of enzyme loading.

All films produced were identical and were grown potentiostatically at pH 7.2. Films were assayed for activity to glucose at a range of pH values. The pH profile of the immobilised GOD is shown in figure 4.18. There are large differences between the pH optimum for the solution and immobilised enzyme. For the homogeneous reaction the pH optimum is at pH 5.6^(70,121,204), whereas for the heterogeneous case the pH optimum has shifted to pH 4. This constitutes a large change. Also the immobilised enzyme shows a much sharper pH profile than the solution enzyme, indicating a higher sensitivity to changes in pH close to the pH optimum for the immobilised case.

It is informative to compare this data to literature reports of the pH optima of GOD immobilised in a variety of matrices. It is apparent that when GOD is immobilised in a number of ways, for example on cellophane membranes, nickel oxide, or non-porous glass beads, that the sensitivity of the enzyme to changes in pH is increased resulting in a sharper pH profile than that seen for the solution enzyme⁽²⁰⁵⁻²⁰⁷⁾.

The cause of this sharpening of the pH profile of the immobilised enzyme has not been adequately explained in the literature and it would appear that this effect is not understood. The immobilised GOD becomes much more sensitive to small changes in the pH. The reason for this may be that immobilisation imposes more constraints on the structure of this already structurally rigid protein. This effect must in some way alter the environment at the active site of the enzyme. As the pH optimum for the homogeneous enzyme is 5.6, this would indicate that a carboxylate group is present at the active site and that this group is essential for the catalytic action of the enzyme. It would therefore seem likely that the immobilisation of the enzyme in some way makes this catalytic group more susceptible to protonation/deprotonation. The catalytic action of this enzyme is, however, likely

to be caused by more than one amino acid side chain at the active site. A full explanation of the way in which immobilisation alters the microenvironment at the active site, and produces a sharpening of the pH profile of this enzyme, cannot be offered until the full three-dimensional structure of the enzyme is known.

Apart from this sharpening effect the pH optimum for the GOD-pNMP is shifted by around 1.6 pH units to a pH of 4. There are two possible explanations for this effect. Firstly immobilisation may alter the pK_a 's of the residues at the active site which are essential for maximum enzyme activity. A second and more feasible suggestion is that the pH within the polymer is different from that in solution.

Therefore, the pH optimum of 4 seen for the immobilised enzyme may simply be due to the fact that there is a barrier to entry of protons into the cationic polymer from the solution. Therefore a pH of 4 may be required in solution to maintain a pH of 5.6, the optimum value for the homogeneous reaction, in the polymer. This would seem to be the most likely explanation since the majority of literature reports for GOD immobilised at surfaces do not show a shift in the pH optimum⁽²⁰⁵⁻²⁰⁷⁾.

The pH profile of the immobilised GOD shows marked changes to that of the solution enzyme. The sharpening and shift of the pH optimum may reflect the intimate contact made between the immobilised GOD and the surrounding polymer matrix.

The GOD-pNMP system has been described in terms of film thickness, enzyme loading, pH and stability. Responses have been successfully characterised in terms of our theoretical model and the system is well understood.

As a continuation of this work, GOD was immobilised in other electrodeposited organic polymers. This work is described in the next section, and serves to demonstrate the applicability of this immobilisation method to systems other than GOD-pNMP.

4.9 THE ELECTROCHEMICAL IMMOBILISATION OF GOD IN OTHER ORGANIC POLYMERS

In this section the immobilisation of glucose oxidase (GOD) in other electrodeposited organic polymers is described. Immobilisation of GOD using polyaniline and polyphenol were successful, whereas attempts to use polyindoles as the immobilisation matrix were not. The growth of polyindole and poly(5-carboxy indole) from buffered aqueous solutions containing GOD resulted in a film which gave no response to glucose. This indicates that either GOD does not enter these types of polymer film during growth, that it is denatured or that glucose is not able to diffuse into such polymers. A very recent report indicates that GOD can be included in polyindole coats in an active state. However, in this case acetonitrile was used as the electrodeposition resulting in a different form of polyindole from that produced from aqueous solutions⁽¹¹⁶⁾.

Attention was focused on a study of the successful immobilisation systems in which GOD was included in films of polyaniline and polyphenol electrodeposited from buffered aqueous solutions by a potentiostatic technique. The glucose oxidase - polyaniline (GOD-pAn) system will be discussed first. The responses of the electrode will be compared to the theory describing the operation of this type of system (section 3.14).

4.9.1 Polyaniline

During the course of this work a report was made of the immobilisation of GOD in electrochemically synthesised polyaniline films. Shinohara *et al* describe the electrodeposition of GOD containing polyaniline film (GOD-pAn) from buffered aqueous solutions (pH 7.0) containing aniline (0.10 mol dm^{-3}) and GOD (2 mg cm^{-3} , 220 U cm^{-3}) onto platinum electrodes^(117,118). A potential of 1.2 volts (vs Ag/AgCl) was applied to the platinum electrodes for periods of up to 30 seconds

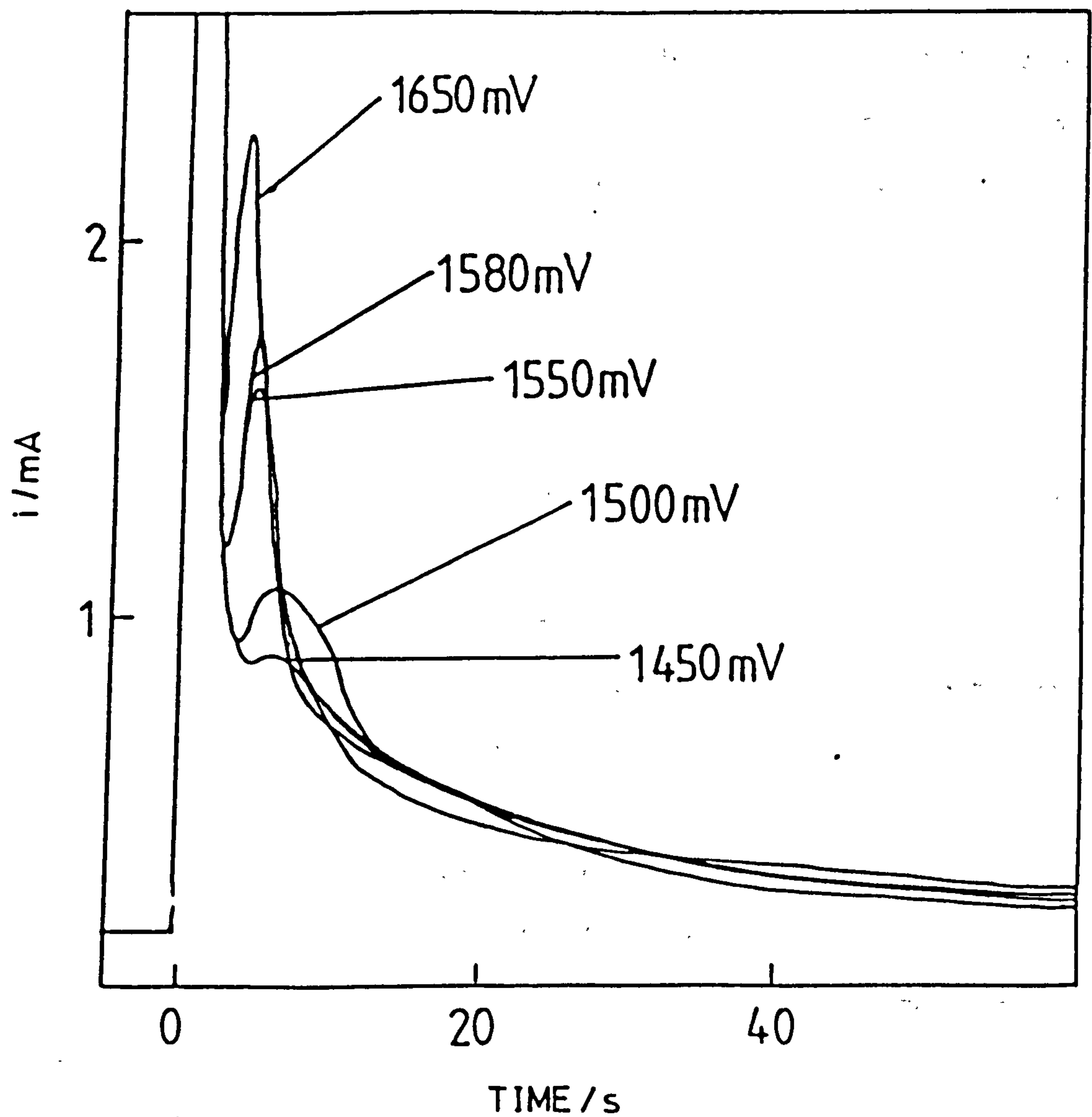
resulting in thin (2×10^{-5} cm) pAn films. These films appeared to be electro-inactive to simple redox couples and did not allow permeation of species such as ferricyanide ion to the underlying platinum electrode. This is in contrast to polypyrroles which are conducting, when oxidised, and are permeable to small molecules⁽⁸⁷⁾.

The findings of Shinohara and coworkers imply that permeation of glucose into the pAn films by diffusion is not possible, or at least is very slow, so that only enzyme exposed at the outer edge of the film can react with glucose. This idea is supported by these authors. Responses of this GOD-pAn system to glucose were determined by measuring the decrease in oxygen reduction current, at -0.5 or -0.6 volts, on the addition of glucose. This indicates that the films are at least permeable to oxygen. The response was rapid and measurable over the range 10^{-4} to 5×10^{-3} mol dm⁻³ glucose.

It should be noted that at the pH and potential used by Shinohara and coworkers for oxygen detection the pAn will be in a deprotonated and therefore insulating form⁽¹⁰⁷⁾.

As an extension to the work in which poly-*N*-methylpyrrole was used to immobilise GOD a system was developed in which polyaniline was used as an immobilisation matrix. Films were grown potentiostatically from aqueous solutions containing buffer and electrolyte (sodium phosphate 0.15 mol dm⁻³, TEATFB (0.1 mol dm⁻³), aniline (0.05 mol dm⁻³) and glucose oxidase (GOD 1 to 10 mg cm⁻³). A platinum working electrode (area 0.39 cm²) at a potential of 1.5 volts (vs SCE) was used for electrodeposition in all cases. The form of the potentiostatic transients observed at a series of potentials is shown in figure 4.19. These transients are directly comparable to those observed by Genies and Tsintavis for the potentiostatic electrodeposition of pAn from a eutectic mixture of NH₄F/HF⁽¹⁴⁷⁾. After an initial peak in the current, at times of less than 10 seconds, a common falling transient is observed at all potentials.

Figure 4.19 Potentiostatic current time transients for the polymerisation of aniline at a platinum electrode surface ($A = 0.385 \text{ cm}^2$) at a number of applied potentials.



The growth of pAn films at 1.5 volts was invariably accompanied by some solvent oxidation. However, even, adherent brown films were produced using this method.

The enzyme containing GOD-pAn films were then washed and immersed in buffered electrolyte solution. The electrodes were rotated at 9 Hz and their response to glucose measured at 0.9 volts (vs SCE). This procedure has been described previously (section 4.5.3).

There are both similarities and differences between the pAn-GOD electrode behaviour and that of the previously described pNMP-GOD electrodes. These will be discussed below along with attempts to model the operation of this system by use of an appropriate mathematical treatment (section 3.1.4).

4.9.2 Analysis of pAn-GOD Electrode Responses

Data obtained from experiments to determine the effect of film thickness and glucose concentration on the pAn-GOD modified electrode response are presented and, whenever possible, analysed in this section.

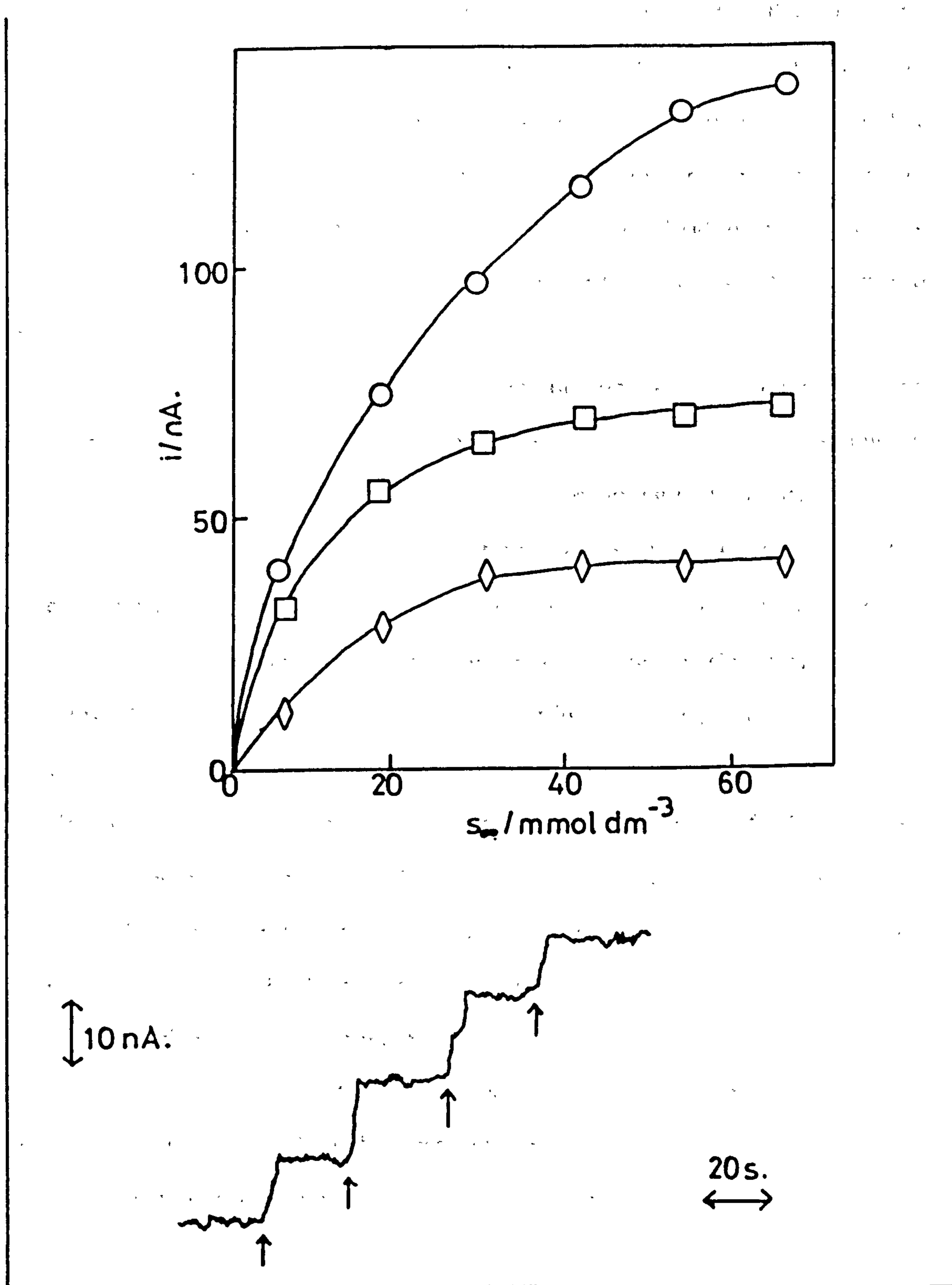
The responses of all electrodes made were seen to saturate at glucose concentrations of $5 \times 10^{-2} \text{ mol dm}^{-3}$ or less. This is in contrast to the linear responses seen in the pNMP-GOD system described previously.

An investigation into the effect of film thickness on the electrode responses at low ($< 1 \times 10^{-2} \text{ mol dm}^{-3}$) and high ($> 5 \times 10^{-2} \text{ mol dm}^{-3}$) glucose concentrations revealed definite similarities to the pNMP-GOD system.

A plot of electrode responses as a function of glucose concentration at three different film thicknesses is shown in figure 4.20. The inset shows the form of the current increases on additions of glucose.

The saturation responses could be due to one of two kinetic processes becoming rate limiting at high glucose concentrations. Either the reaction of enzyme with substrate, described by k_{cat} , or the reaction of enzyme with the mediator

Figure 4.20 Response curves for the glucose oxidase - polyaniline electrodes at three different thicknesses (circles $Q = 8$ mC, squares $Q = 24$ mC, diamonds $Q = 18$ mC). The inset shows a typical experimental $i-t$ trace with each arrow representing a 6 mmol dm^{-3} increase in the bulk glucose concentration.



oxygen, described by k_a , could be rate limiting at high substrate concentrations.

Attempts to fit the data to expressions describing a crossing of the appropriate boundary (either IV/I or V/II) with increasing substrate concentrations resulted in ill defined fits. This is largely due to the quality of the data obtained.

In the case of pNMP-GOD films data for a wide range of film thicknesses (l) and enzyme loadings (e_Σ) was acquired. However, due to the insulating nature of the polyaniline films produced only a very limited range of film thicknesses could be investigated. Furthermore, the effect of enzyme loading on the response of films of constant thickness was undefined. Changes in the enzyme loading in thin or thick films of pAn-GOD had no significant effect upon the magnitude of the response to glucose.

The effect of mediator (dioxygen) concentration on the electrode response was not determined. This information would be important when attempting to assign the turnover in the glucose response to either k_{cat} or k_a becoming rate limiting.

If k_a was rate limiting at high substrate concentrations an increase in the oxygen concentration of the bulk solution (a_∞) would lead to an increase in the current response. However if the enzyme/substrate reaction was slow then all of the enzyme would be in its oxidised (E_1) form so that increasing a_∞ would not increase the current response at saturating glucose concentrations.

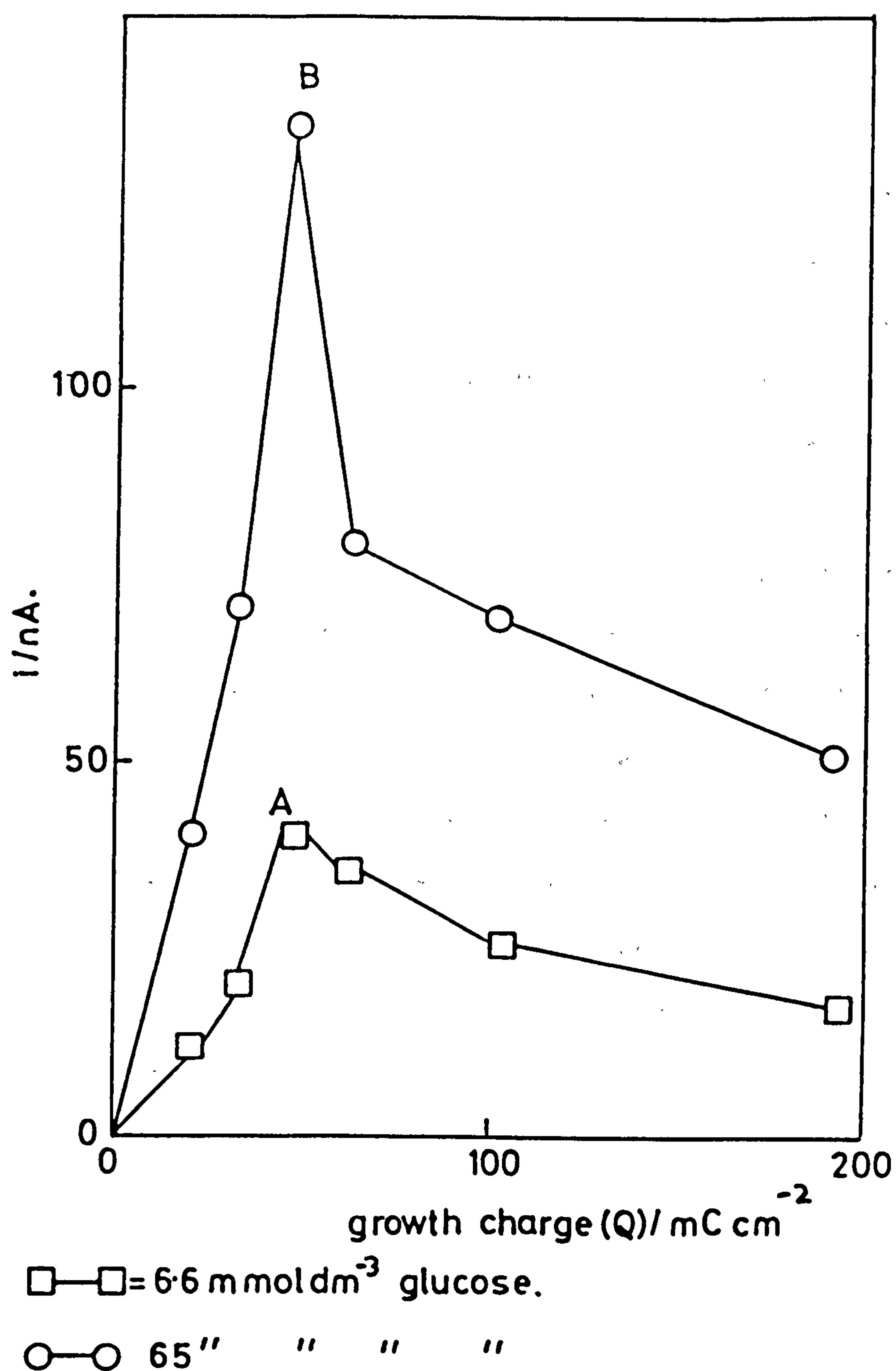
Without information regarding the effect of a_∞ on the pAn-GOD electrode responses it is not possible to distinguish between these types of kinetic turnover.

The effect of film thickness (or charge passed in film growth) to current response at low and high glucose is described by figures 4.21a and 4.21b. It is apparent that there is a maximum, in both low and high substrate plots, corresponding to an optimal film thickness. Above this thickness the current response is seen to fall sharply with increasing film thickness.

This situation is analogous to that described for the pNMP-GOD system and is

Figure 4.21 a) Electrode response, at low glucose concentration (6.6 mmol dm^{-3}) as a function of charge density for film growth.

Figure 4.21 b) Electrode response, at saturating glucose concentration (65 mmol dm^{-3}) as a function of charge density for film growth.



of the form predicted when the enzymic product, hydrogen peroxide, cannot be oxidised directly on the polymer matrix adjacent to the immobilised GOD molecules but must diffuse to the underlying platinum electrode surface for detection.

The maximum apparent in the response vs thickness plot enables an estimate of X_K , the kinetic length of glucose in the pAn-GOD film, to be made. The distance X_K corresponds to the position of the maximum for a situation of this type where the insulating pAn-GOD matrix is not able to act as a surface for rapid hydrogen peroxide oxidation.

The position of this maximum corresponds to a film thickness produced by passing around $5 \times 10^{-2} \text{ C cm}^{-2}$ of charge. It is difficult to convert this parameter into a distance (X_K) with any accuracy. Whereas in the case of pNMP-GOD films an accurate charge vs thickness ($Q-l$) relationship was established by ellipsometric studies, no such data exists for the pAn-GOD system. The literature does not provide any reasonable estimates for charge vs thickness relationships for this system.

In summary it can be seen that there are a number of practical problems associated with the study of the pAn-GOD system. This does not represent a good choice of polymer for a further detailed investigation, and serves only to demonstrate that other polymers, as well as polypyrroles, are amenable to enzyme immobilisation. Furthermore, it has been clearly shown that by changing the polymer used for immobilisation it is possible to change the substrate response characteristics of a glucose sensing device. The previous described pNMP-GOD devices gave linear current response in excess of $2 \times 10^{-1} \text{ mol dm}^{-3}$ glucose whereas the pAn-GOD device responses became saturated at glucose concentrations below $5 \times 10^{-2} \text{ mol dm}^{-3}$ glucose.

In the next section a final example of the use of an organic polymer matrix for the electrochemical immobilisation of GOD is described. Following this the

characteristics of the three devices described are summarised and compared in the form of a table.

4.9.3 Polyphenol

It has been known for some time that the electro-oxidation of phenols at simple metal electrodes results in the formation of a passivating polymeric layer on the electrode surface⁽²⁰⁸⁾. A large number of substituted phenols have been used to modify electrode surfaces using the technique of electro-oxidation^(209,212).

This work has commonly used methanol as a solvent and a potential cycling method for electropolymerising the phenol of interest. In most cases a thin, insulating polyphenylene oxide type film is deposited which results in the very rapid passivation of the electrode surface. Suggested applications for this type of polymer in the literature include their use as pH sensing materials⁽¹⁴⁹⁾ and in the field of coatings for metal protection⁽²⁰⁹⁾.

The insulating nature of these polymers means that only thin film can be electrodeposited, typically between 500 and 1000 Å⁽²⁰⁹⁾. More recent work suggests that native polyphenol deposited from acetonitrile is not electroactive in this solvent⁽¹¹³⁾. However, when such a film is placed in an aqueous solution then electroactivity of the polymer is seen, the polymer having an $E^{0'}$ close to that of the quinone/hydroquinone couple. Furthermore, the polyphenol produced in this way is highly sensitive to the pH of the bulk solution and has an $E^{0'}$ value which varies 60 mV with each unit change in pH. This implies that there is a 1:1 ratio for participation of electrons and protons in the electrode reaction.

In order to use polyphenol as an immobilisation matrix for GOD a procedure was developed which allows the reproducible electrodeposition of thin insulating films of polyphenol. When grown in the presence of GOD in the growth solution such films are found to contain enzyme in an active form.

There is little information in the literature regarding the electropolymerisation of phenol from buffered aqueous solutions. However, it is known that the electro-oxidation of phenol at 1 volt (vs SCE) at a platinum electrode results in the formation of a polyphenol film⁽¹⁴⁹⁾. The growth medium employed in this case was phenol ($2.5 \times 10^{-3} \text{ mol dm}^{-3}$) in buffer at pH 4.85. A potentiostatic growth method resulted in a rapid decay of the polymerisation current indicating rapid passivation of the platinum electrode surface.

An investigation into the use of polyphenol for the electrochemical immobilisation of GOD was undertaken. There do not appear to be any existing reports describing this type of work.

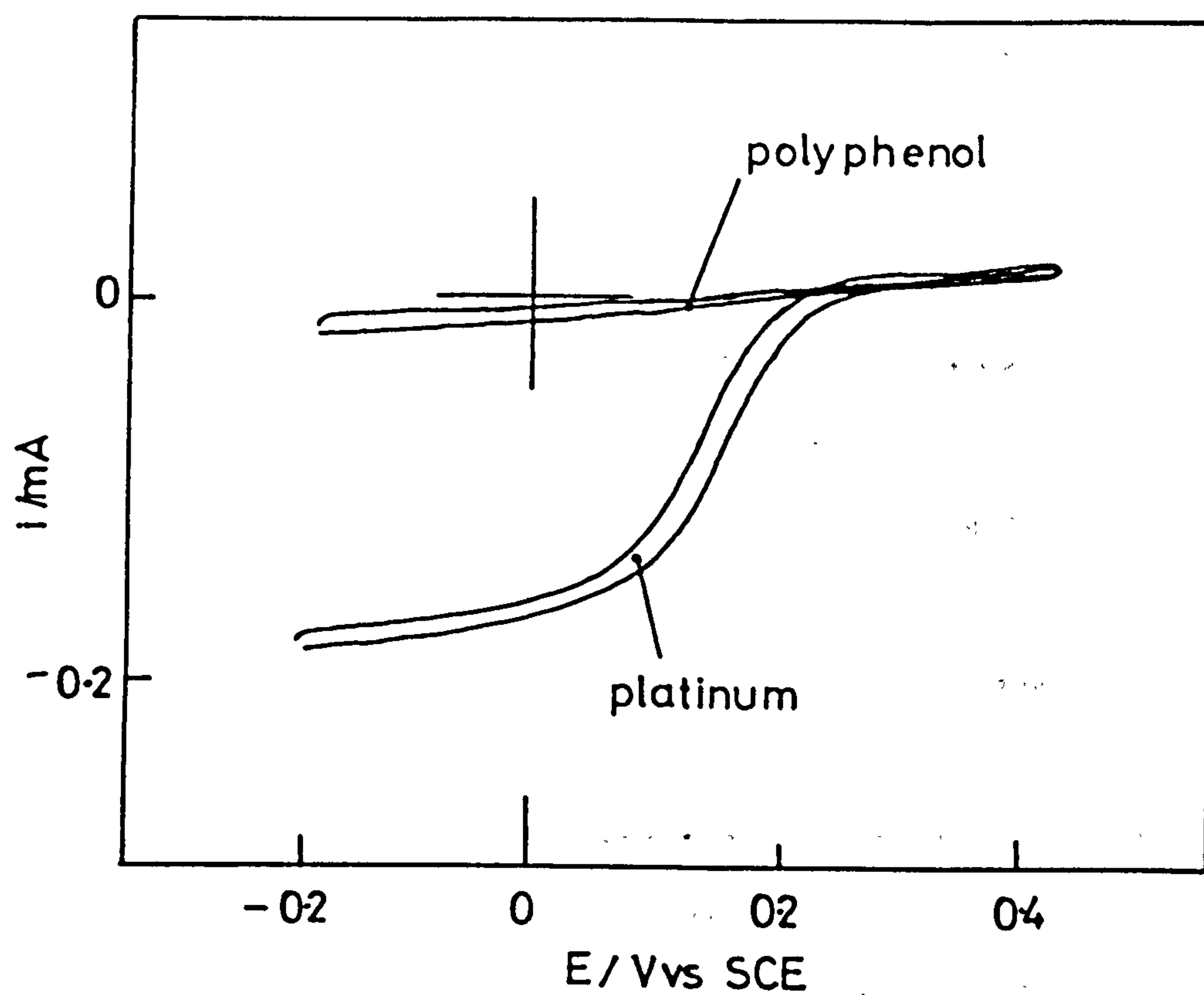
The procedure used for the preparation of polyphenol-GOD (pPh-GOD) electrodes was similar to that described for the production of pNMP-GOD and pAn-GOD electrodes.

A potentiostatic growth at 1.40 volts (vs SCE) on a clean platinum electrode was used in all cases. This potential was found to give the most even and adherent films, higher potentials being associated with solvent oxidation at the neutral pH used. Phenol (0.05 mol dm^{-3}) in buffered electrolyte (0.15 mol dm^{-3} sodium phosphate, pH 7.2, 0.1 mol dm^{-3} tetraethylammonium tetrafluoroborate) containing GOD (8.5 mg cm^{-3} , 1270 U cm^{-3}) was used as the growth solution. After passing around 5mC (electrode area = 0.385 cm^2) the current decayed to very low levels, resulting in the deposition of a thin golden film.

Films were washed and then placed in background buffered electrolyte solution for characterisation.

The permeability of this insulating film was investigated by polography in ferricyanide solution. The presence of the film completely blocked the reaction of this redox couple at the underlying platinum electrode, indicating that the film was impermeable to this molecule (figure 4.22).

Figure 4.22 Polarogram for polyphenol coated and clean platinum electrodes in ferricyanide solution (potassium ferricyanide, 5 mmol dm^{-3} , TEA TFB 0.15 mol dm^{-3} , phosphate 0.1 mol dm^{-3} , pH 7.2, 25°C) at a rotation speed of 9 Hz.



This indicates that the film may be impermeable to glucose also, resulting in only the enzyme at the outer edge of the polymer film being able to react with glucose. Due to the insulating nature of this polymer the hydrogen peroxide produced by the enzyme substrate reaction must diffuse to the platinum electrode to react.

Initial results for the response of the pPh-GOD system to additions of glucose are analysed in the next section. Data for one film thickness only is presented. A systematic variation of film thickness is not possible in this case due to the highly insulating nature of the polyphenol produced.

4.9.4 Analysis of the pPh-GOD Data

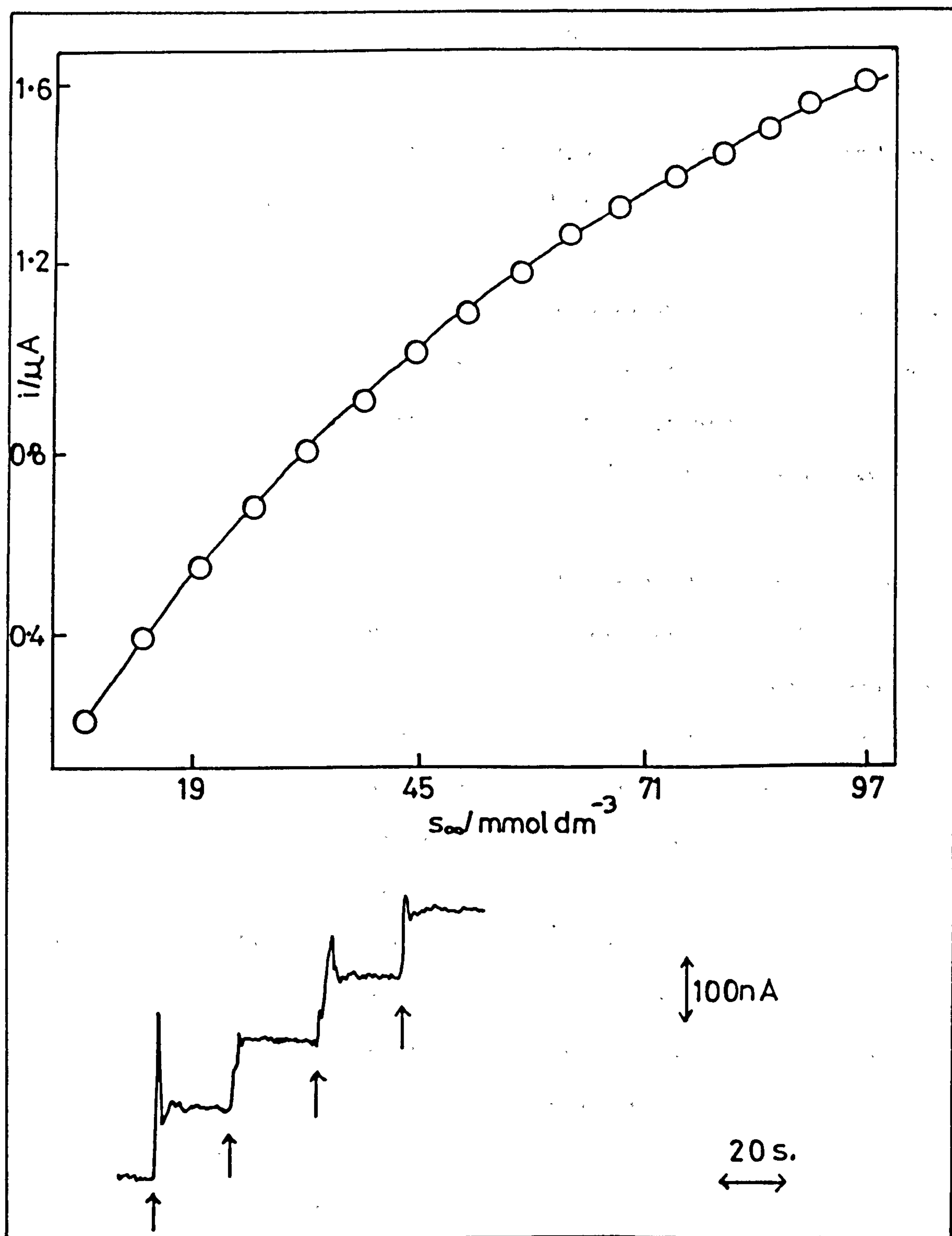
The response of pPh-GOD electrodes to glucose was determined as described previously. The responses are non-linear and continue to increase at glucose concentrations in excess of the Michaelis constant (K_M) for the homogeneous enzyme reaction⁽¹³¹⁾. Such a response is shown in figure 4.23. The inset to this figure shows the form of the current response on the addition of glucose to the bulk solution.

The shape of the substrate response curve was analysed in terms of the theoretical expression describing the current response when the reduced mediator can only become reoxidised at the underlying platinum electrode surface. This theoretical treatment is described full in section 3.1.4 of this thesis.

It is only possible to grow polyphenol to a very small thickness under the conditions used. The electrode quickly becomes passivated by the deposition of a pPh-GOD insulating layer. It is therefore apparent that since the pPh-GOD films are very thin then $l \ll X_K$.

This situation would place us on the top half of the appropriate case diagram (figure 3.5), and therefore at low concentrations of s in case IIIb. In this situation

Figure 4.23 Response curves for the glucose oxidase - polyphenol electrode to glucose. The plot shows the calibration curve obtained for additions of glucose. The inset shows the $i-t$ trace for additions of glucose. The arrows represent stepwise increases in the bulk glucose concentration of 5 mmol dm^{-3} .



increasing the substrate concentration will move us to the right hand side of the case diagram and into either case I or II.

Once again the only difference between these two cases that can be detected experimentally is the oxygen dependence of the current in this thin film / high substrate case. Referring back to table 3.3 it is apparent that the only difference between the j_B expressions for case I and II is that the former is dependent on ka_{∞} and the latter on k_{cat} .

Using the available data it is, therefore, not possible to distinguish between a kinetic turnover due to enzyme (Michaelis-Menten) kinetics, k_{cat} , or due to mediator kinetics, ka_{∞} .

The polyphenol system again serves to illustrate that an insulating polymer is a suitable choice in the development of a successful electrochemical enzyme immobilisation strategy. Further the change in polymer from poly-*N*-methylpyrrole and polyaniline to polyphenol as the immobilisation matrix has once more altered the response characteristics of the device.

A final interesting point arises from a calculation to estimate the thickness of the pPh-GOD films produced. Using an estimated molecular volume of $3.56 \times 10^{-23} \text{ cm}^3$ for each phenolic unit and assuming a close packing of the polymer, an estimate of the film thickness was made. For a charge of $4.5 \times 10^{-3} \text{ C}$ passed for electrodeposition of polyphenol the corresponding film thickness was estimated at 13 nm (or 90 monolayers of phenolic units). This dimension becomes interesting when it is known that the GOD molecule has a diameter approaching 9 nm⁽²⁹⁾. This means that the film is of a similar thickness to the enzyme molecule. This is a completely different situation to that found for pNMP-GOD films. It is highly likely therefore that glucose does not diffuse through the polyphenol matrix but may react with exposed enzyme molecules. The hydrogen peroxide produced must then diffuse over a very short distance to react on the underlying platinum electrode. This situation may account for the relatively large currents observed when additions of

glucose are made to this system.

The effect of rotating the electrode, at high glucose concentrations, was also determined. The results were directly comparable to those observed for the pNMP-GOD system, mainly that as the rotation speed increases the current decreases (figure 4.24). This effect has been explained in terms of loss of hydrogen peroxide from the polymer film being greatest at higher rotation speeds earlier in this chapter. A plot of i vs $W^{-1/2}$ reveals a straight line with an intercept corresponding to j_B (the extrapolated current response at infinite rotation speed). This has a value of $0.55 \mu A$ in the pPh-GOD system (figure 4.25).

The response of the pNMP-GOD, pAn-GOD and pPh-GOD devices to glucose are compared and contrasted in the following section. Obviously the pNMP-GOD system was the source of most of the experimental data since this system permitted wide variation in l and e_{Σ} , and produced very stable and reproducible responses. This is the most fully characterised system.

4.9.5 Comparison of Response Characteristics

The responses of the three devices, described in this chapter, to additions of glucose in the presence of oxygen are summarised in table 4.5 below. They are compared in terms of their glucose response, the site of hydrogen peroxide detection, and their stability, as well as in terms of certain enzyme loading and polymer film thickness parameters.

Figure 4.24 Plot showing the electrode response as a function of rotation speed (0.1 mol dm⁻³ glucose).

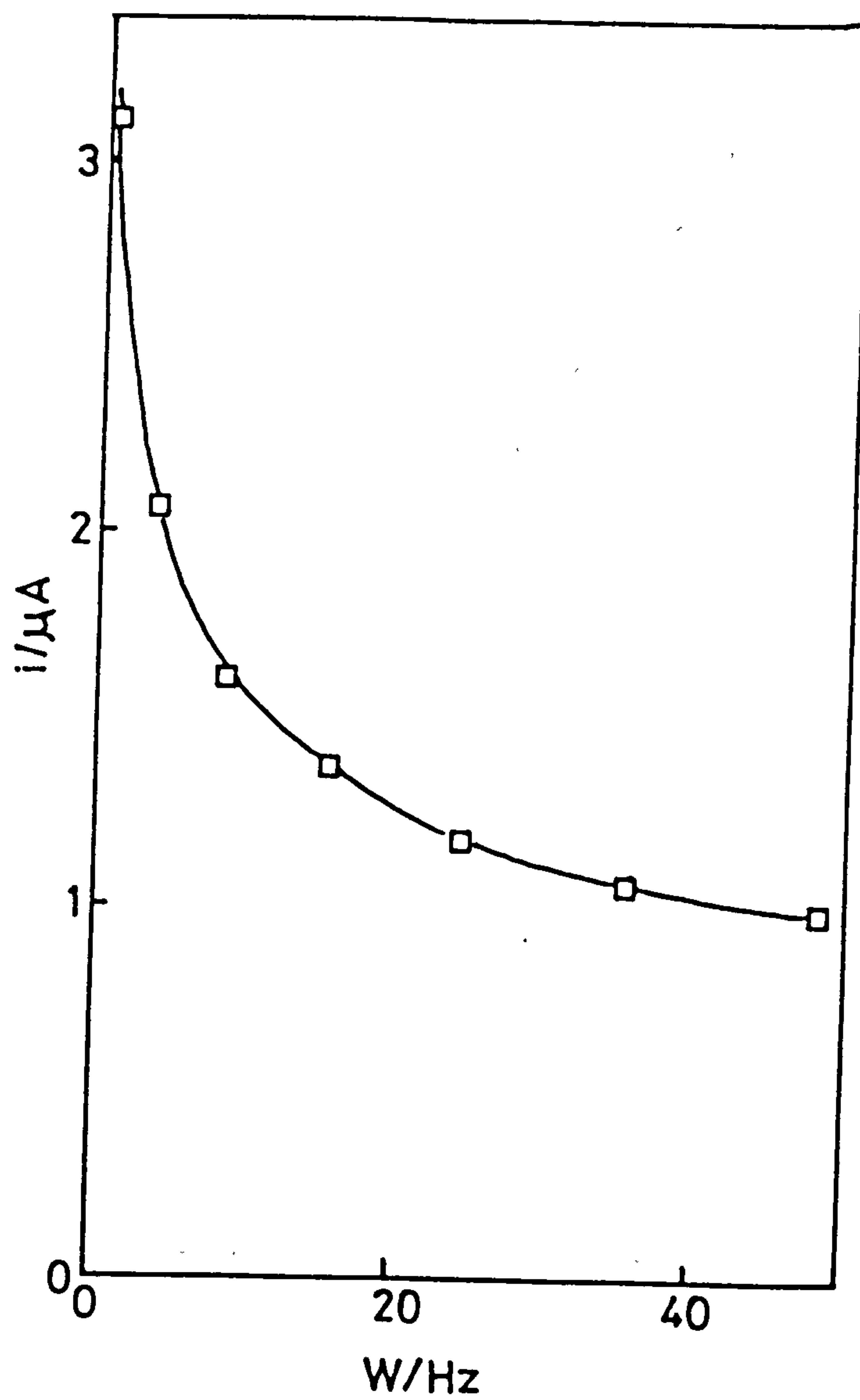


Figure 4.25 Plot of response as a function of $W^{-1/2}$ (data taken from figure 4.24).

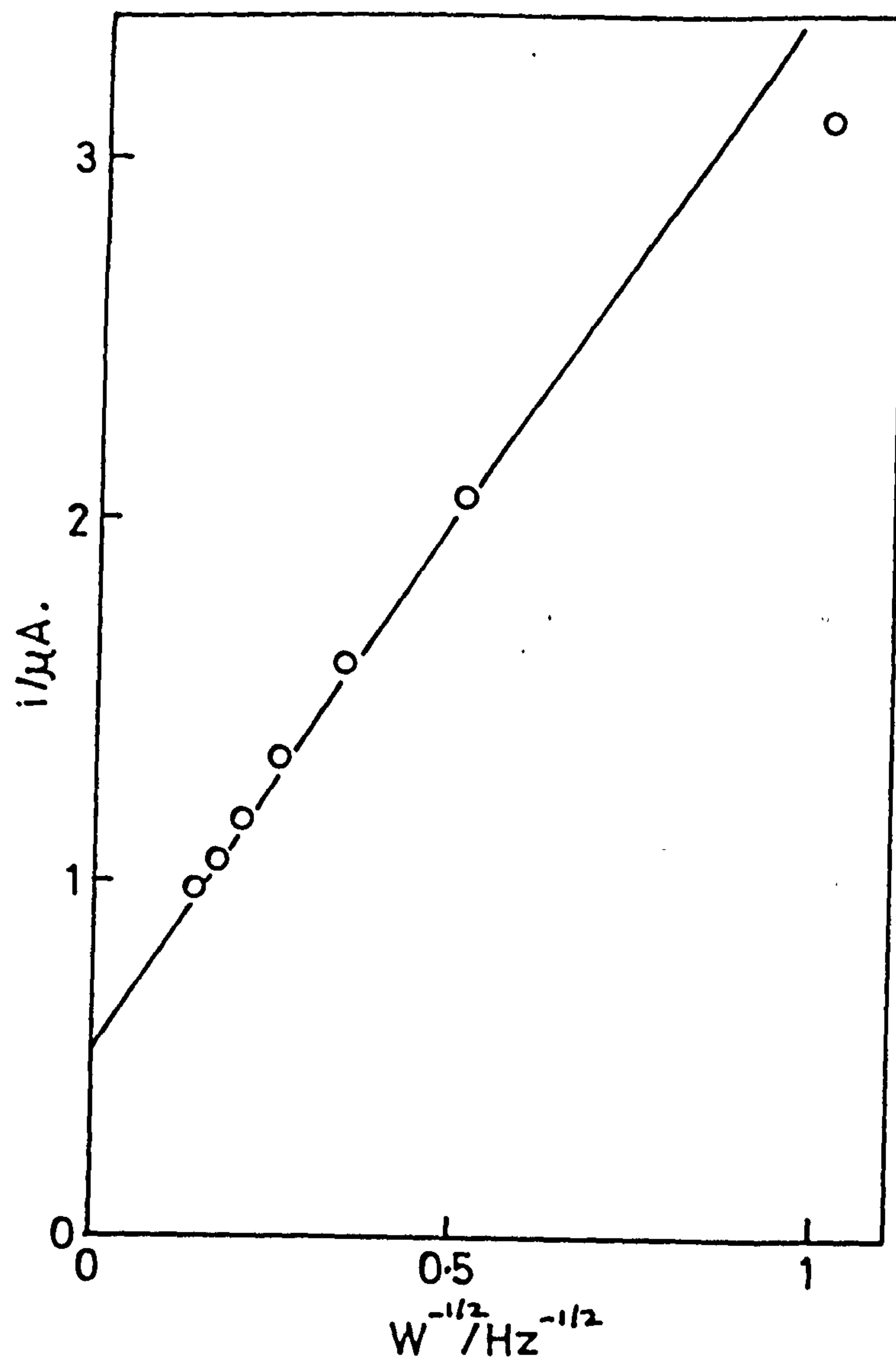


Table 4.5

Comparison of the response characteristics of the immobilised glucose oxidase systems

Parameter	pNMP-GOD	pAn-GOD	pPh-GOD
Estimated [glucose] at which saturation is reached (mol dm^{-3})	> 0.30	≈ 0.05	≈ 0.15
Site of H_2O_2 oxidation	platinum	platinum	platinum
Nature of polymeric matrix	conducting	insulating	insulating
Stability	> 5 days	≈ 2 hours	≈ 2 days
Effect of enzyme loading (e_Σ)	dependence in films of $l \ll X_K$	unclear	unknown
Effect of film thickness (l)	maximum in i vs l plot	maximum in i vs charge plot	unknown ^(a)
Effect of mediator concentration	no saturation due to a_∞	unknown	unknown ^(b)

Notes

- (a) Not possible to grow pPh-GOD films of different l due to highly insulating nature of this polymer.
- (b) No apparent O_2 limitation of reaction.

4.10 CONCLUSIONS

Examination of the data for the three immobilised enzyme / polymer systems studied reveals that the electrodeposition of organic polymers from buffered, aqueous solutions containing the monomer and redox enzyme of choice represents a successful immobilisation strategy.

Examination and interpretation of the response characteristics of these immobilised enzyme systems shows that certain characteristics are common to a number of the systems. It appears that in all cases the hydrogen peroxide produced must diffuse to the platinum electrode to react and cannot react on the polymer. This is expected for the insulators polyaniline and polyphenol but may be an unexpected result for the conducting poly-*N*-methylpyrrole matrix.

The current response is seen to be linear to very high glucose concentrations for the pNMP-GOD system. This was explained in terms of the partition of glucose into the polymer matrix being inefficient. Therefore a high glucose concentration in the bulk solution is paralleled by a low concentration in the polymer film surrounding the enzyme. In the pAn-GOD and pPh-GOD systems a saturation type response is seen. Now more glucose must enter the film, reflecting a change in its partition coefficient, K , so that k_{cat} becomes limiting at high concentrations of glucose.

Alternatively the regeneration of oxidised GOD by reaction of reduced GOD with mediator (described by k_a) could become rate limiting at high substrate concentrations.

A change in the nature of the immobilising polymer clearly produces changes in the response characteristics of the resultant device. This ability to alter the device's characteristics may be advantageous when designing a sensor for a particular application.

A detailed understanding of the mode of operation in the immobilised enzyme system has been gained. In the final part of this chapter the flexibility of the

electrochemical immobilisation method is demonstrated in terms of bi-enzyme systems developed using pNMP as the immobilisation matrix. Oxygen is again used as the mediator in these systems.

4.11 ELECTROCHEMICAL IMMOBILISATION OF TWO-ENZYME SYSTEMS

All the work previously described has involved the immobilisation of one enzyme, GOD, in a single polymer layer. In this section the feasibility of coimmobilising two enzymes in a single polymer layer is investigated. Furthermore, as it is possible to grow one layer of polypyrrole on top of another⁽¹⁶⁴⁾, it is feasible to deposit one enzyme containing layer over another. Both coimmobilisation and the production of two layer systems are described in this section. All work described involves the use of poly-*N*-methypyrrole as this has many desirable characteristics (section 4.5). The model enzyme system chosen to test this type of two enzyme system was a coupled β -fructosidase - glucose oxidase (β -Fr-GOD) system.

Initially an effective method of coupling these two enzyme reactions was determined and the pH optimum of the coupled system elucidated. This will now be described.

4.11.1 A Coupled β -fructosidase-GOD System

In this section a coupled β -fructosidase-GOD system is described. An oxygen electrode assay for this system is used to determine the pH optimum for the coupled system.

β -fructosidase (E.C. 3.2.1.26) catalyses the hydrolysis of sucrose (1-0- α D-glucopyranosyl- β D-fructofuranoside) into its constituent monomeric sugars;



The production of glucose by this enzyme was coupled to its consumption by GOD⁽¹²⁴⁾.

The α -D-glucose produced by β -fructosidase undergoes a relatively fast mutarotation to β anomer in solution. This β -D-glucose then acts as a substrate for GOD.

An oxygen electrode assay (section 2.8.1) was developed to determine the pH optimum for this coupled system.

Although assay conditions were chosen to minimise any lag due to the coupling of the two reactions, a short lag was observed on the addition of sucrose.

A trace showing depletion of oxygen on addition of substrate is shown in figure 4.26a. The pH profile determined for this coupled system is shown in figure 4.26b. A pH of 7.2 was found to give a near optimal rate and experiments to investigate the electrochemical immobilisation of this coupled system were conducted at this pH in all cases.

The coimmobilisation of this system and the production of a two layer device in which a poly-*N*-methylpyrrole- β -fructosidase layer was deposited on top of a poly-*N*-methylpyrrole-GOD layer will be described below.

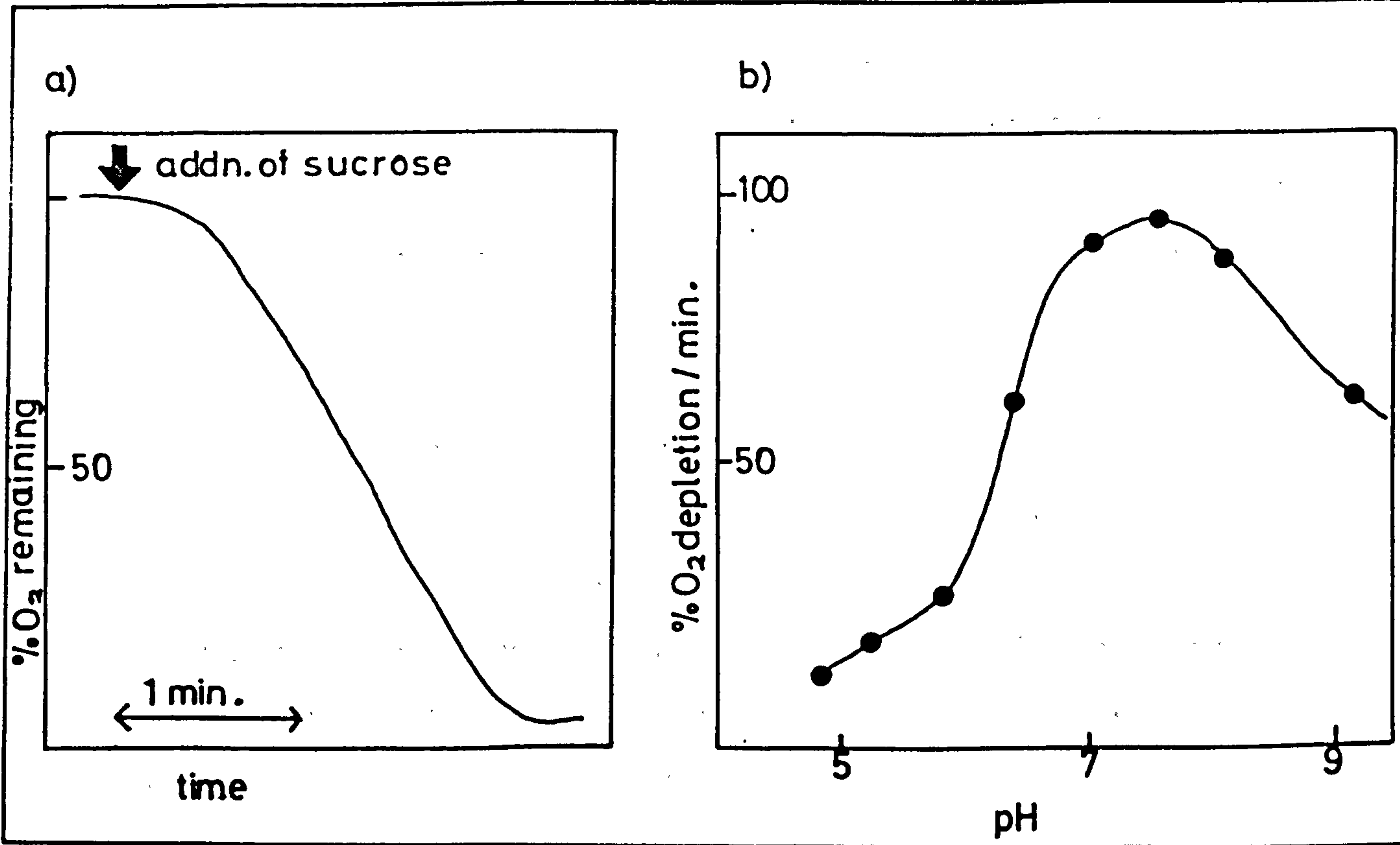
4.11.2 Coimmobilisation

Enzyme containing films were grown from solutions containing *N*-methylpyrrole (0.05 mol dm^{-3}), buffer (sodium phosphate 0.15 mol dm^{-3} pH 7.2), electrolyte (0.10 mol dm^{-3} TEATFB), GOD (1.6 mg cm^{-3} , 380 U cm^{-3}) and β -fructosidase (1.2 mg cm^{-3} , 360 U cm^{-3}). A potential of 0.8 volts (vs SCE) was applied to the platinum electrode (area of 0.385 cm^2) for potentiostatic growth. Films corresponding to a thickness of $2 \times 10^{-5} \text{ cm}$ were produced.

These coated electrodes were washed and placed in buffered electrolyte solution (pH 7.2) at 25°C and rotated at 9 Hz. A hydrogen peroxide detection potential of 0.9 volts was used. The presence of enzyme activity within the polymer

Figure 4.26 a) Oxygen electrode trace for the addition of sucrose to the coupled enzyme system in solution.

Figure 4.26 b) The pH profile for this coupled enzyme system.



was demonstrated by making additions of substrate. Additions of glucose gave current responses (figure 4.27) demonstrating that the GOD was active as expected. The electrode was then washed and placed in fresh buffered electrolyte solution. Additions of sucrose were then made and current responses were observed (figure 4.27). The responses are stable and fairly reproducible in this coimmobilised bienzyme system.

This demonstrates that coimmobilisation is possible by the electrodeposition technique. Both enzymes remain in an active state during this procedure.

In the next section the production of a bilayer device is described. This again incorporates the same coupled enzyme system but in this device the two enzymes are separated into different polymer layers.

4.11.3 Production of a Bilayer Two-Enzyme System

The bilayer system⁽¹⁶⁸⁾ was produced as follows. A GOD containing poly-*N*-methylpyrrole film was grown as previously described. The electrode was then washed and a second β -fructosidase containing layer of poly-*N*-methylpyrrole was deposited over the first layer. Films were grown potentiostatically at 0.80 and 0.90 volts (vs SCE) respectively. A slightly higher potential was required to produce the same rate of film growth for the second coating process. Both films had a thickness of around 2×10^{-5} and were found to be even and adherent.

After growth the bilayer electrode was washed and placed in buffered electrolyte solution. Addition of sucrose ($2 \times 10^{-2} \text{ mol dm}^{-3}$) to the solution produced a slow current response, taking around 20 seconds to reach a steady state current (figure 4.28). This is likely to be due to a finite time being taken for the action of the β -fructosidase enzyme to build up a concentration of glucose within the polymer film. It should be noticed that the GOD-pNMP layer above showed no response to additions of sucrose.

Figure 4.27 Responses of the coimmobilised bienzyme system. Each arrow represents a stepwise increase in the substrate concentration of 6.6 mmol dm^{-3} .

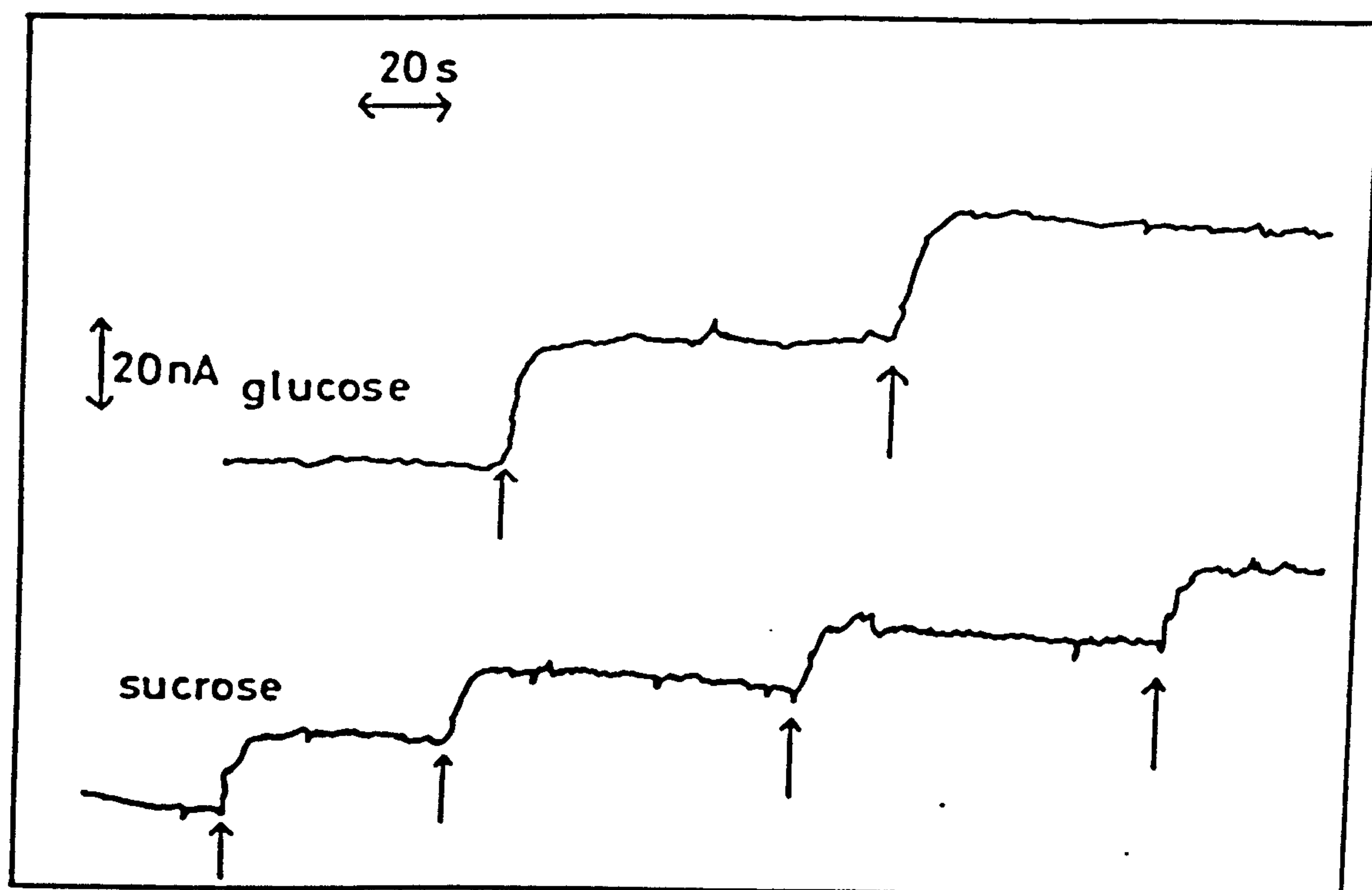
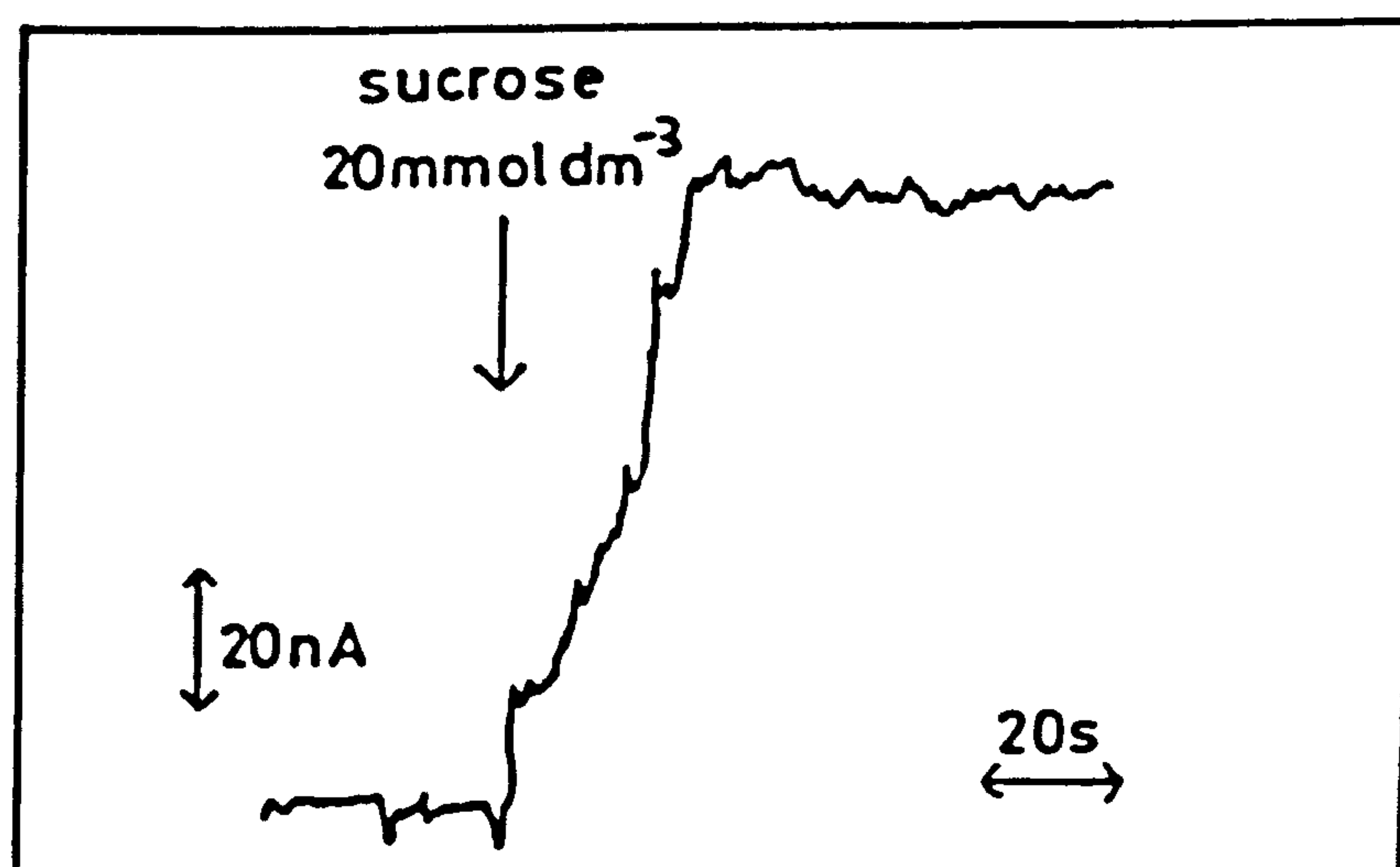


Figure 4.28 Response for the two layer bienzyme system on the addition of sucrose.



The process of electrochemical immobilisation can be used for the coimmobilisation of enzymes and furthermore for the build up of multilayer devices. This indicates that this technique may be applicable to the immobilisation of a wide range of enzyme systems.

The work presented in this chapter used oxygen as an enzyme mediator. In chapter 5 the use of an artificial electron acceptor/donor to accept electrons from substrate reduced immobilised GOD is described. A detailed theoretical analysis of the experimental data is described in full.

CHAPTER FIVE

THE IMMOBILISATION OF GLUCOSE OXIDASE IN CONDUCTING POLY-*N*-METHYLPYRROLE FILMS; MEDIATION BY A FERROCENE DERIVATIVE

In the previous chapter results were presented for the reaction of immobilised glucose oxidase (GOD) with its natural redox mediator, dioxygen, and the subsequent detection of the hydrogen peroxide produced at the underlying platinum electrode. In this chapter it was shown conclusively that hydrogen peroxide produced by GOD immobilised in films of poly-*N*-methyldpyrrole, polyaniline and polyphenol cannot be oxidised on the polymer and must therefore diffuse through the polymer to be detected at the platinum surface.

In this chapter results are presented for the GOD-pNMP system in which a water soluble ferrocene derivative is substituted for the natural mediator, dioxygen. This chapter deals exclusively with the GOD-pNMP system as this has been shown previously to have many desirable characteristics (section 4.5). A suitable ferrocene derivative was chosen as an artificial redox mediator for the GOD reaction and the electrode response was determined at a series of film thicknesses, enzyme loadings, and mediator concentrations. The responses are then described in terms of the specially developed model (section 3.2). A new situation is seen in which the ferrocene mediator is rapidly oxidised on the pNMP matrix. This redox reaction cannot, however, occur uniformly throughout the conducting polymer layer and is confined to regions at the outer surface of the polymer and close to the electrode. Evidence to support this hypothesis is presented in the theoretical section of this chapter.

In conducting this work it is essential that oxygen is excluded from the solutions. Any oxygen may interfere with the reaction mediated by the artificial redox couple under investigation. For this reason a special airtight cell was used in

all sections of this work.

In the first part of this chapter the design and characteristics of this special cell are described. Following this the requirements of a suitable mediator are described. Finally the reaction of the ferrocene mediator with GOD immobilised in films of poly-*N*-methylpyrrole is investigated and the data obtained are explained in terms of a specially developed theory.

5.1 A GAS TIGHT ELECTROCHEMICAL CELL

This section will describe the design and characteristics of an electrochemical cell in which rigorous deoxygenation of a solution and good hydrodynamics at a rotating disc electrode (RDE) are achieved. The cell is made of colourless perspex and consists of three compartments for the working (RDE), counter, and silver/silver chloride (Ag/AgCl) reference electrodes. The working electrode consists of a normal RDE (section 2.3). This electrode is attached to the rotator block and a perspex sleeve, with an inlet and outlet for nitrogen, and is fixed to the head of the rotator block by means of a rubber 'O' ring. This provides a gas tight seal. The lower end of this perspex sleeve makes a gas tight contact with the top of the cell. This arrangement allows a constant positive pressure of nitrogen to be maintained over the deoxygenated sample. No oxygen is allowed to diffuse back into the sample solution. This is essential in the present work. The system described in the previous chapter did not require this rigorous solution deoxygenation. Indeed the system required oxygen for operation, making the use of a normal water jacketed pyrex cell (figure 2.4) adequate.

A further criterion for the design of this gas tight cell is that the hydrodynamic flow of electroactive material to the RDE surface is optimised. This means that a suitable internal cell geometry must be produced, and then tested using a well characterised system such as the ferri/ferrocyanide couple in potassium chloride electrolyte. The internal cell geometry is shown as a scale drawing in figure 5.1.

The top of the sample chamber is flat, the reference electrode being retained behind a frit to prevent it protruding into the sample chamber and causing turbulence. The lower part of the sample chamber has sides which extend at a 45° angle to the glass frit at the bottom of this chamber. Below this frit is the counter electrode compartment.

It should be noted, therefore, that there are no sharp protrusions into the sample chamber, which might cause the flow of the solution to become turbulent. Also the internal geometry is such that solution leaving the electrode surface can do so with the minimum of hydrodynamic resistance.

The characteristics of this cell were determined using a number of methods, mainly by measuring Levich currents, diffusion coefficients and by performing coulometric titrations. In this way it was established that this cell geometry is well suited to use with a RDE and also the active solution volume of the cell was determined.

The results for such cell characterisation experiments are given in the following sections.

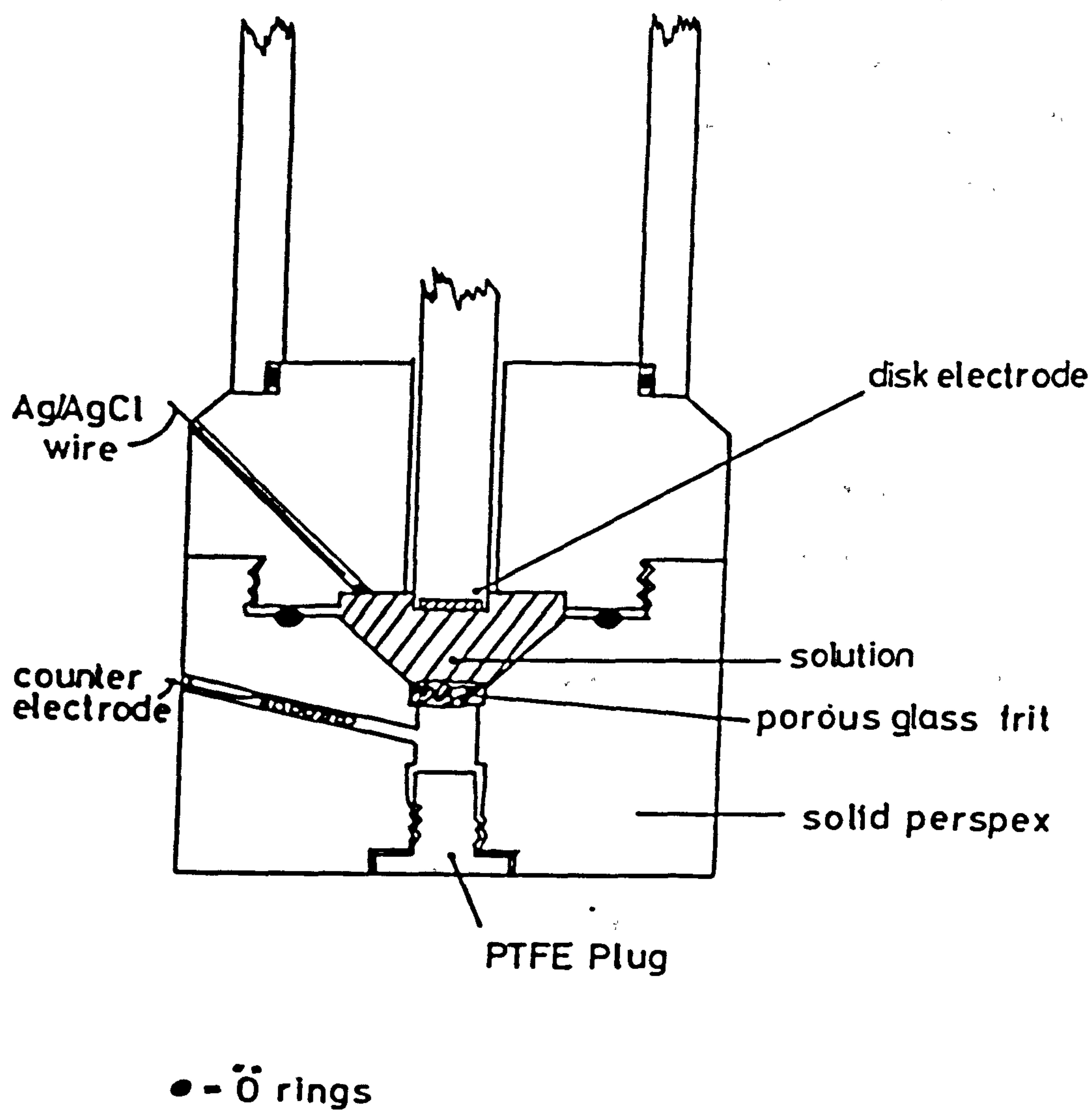
5.1.1 Levich Currents

A solution of potassium ferrocyanide ($1.00 \times 10^{-3} \text{ mol dm}^{-3}$) in potassium chloride electrolyte (0.25 mol dm^{-3}) was placed in the cell. A platinum electrode (area 0.385 cm^2) was inserted and the cell connected to the electrode rotator via the perspex sleeve. The electrode was poised at a potential corresponding to the limiting current for ferrocyanide oxidation and the rotation speed was changed step wise. As the data was collected a Levich plot was constructed. The Levich equation⁽¹⁹⁰⁾ describes the mass transport limited current at a rotating electrode.

$$i_L = 1.554nFAD^{2/3}\nu^{-1/6}\omega^{1/2}c_\infty \quad (5.1)$$

where i_L is the limiting current (amps), n the number of electrons, F is the faraday

Figure 5.1 Drawing of the perspex gas tight electrochemical cell and electrodes (to scale 1:1).



(C mol⁻¹), D is the diffusion coefficient (cm² s⁻¹), ν is the kinematic viscosity (cm² s⁻¹), W is the rotation speed (Hz), and c_{∞} is the bulk concentration of the electrode species (mol dm⁻³).

The Levich plot, i_L against $W^{1/2}$, has a slope of

$$\text{Levich slope} = 1.554nFAD^{2/3}\nu^{-1/6}c_{\infty} \quad (5.2)$$

As all parameters except D are known, a value of D can be determined. If the cell geometry of the gas tight cell is providing good hydrodynamic flow to the RDE three factors will result. Firstly the Levich plot will have a good linearity, secondly it should pass through the origin, and finally the slope of such a plot should yield a diffusion coefficient which is comparable to the accepted literature value for these experimental conditions.

All of these criteria are met in this case. The Levich plot is linear with zero intercept and a slope of $4.32(\pm 0.020) \times 10^{-5} \text{ A Hz}^{-1/2}$. This gives a diffusion coefficient for ferrocyanide in the range 6.43 to $6.53 \times 10^{-6} \text{ cm}^2 \text{ s}^{-1}$. The experimentally determined diffusion coefficient compares favourably to the accepted literature value of between 6.39 and $6.50 \times 10^{-6} \text{ cm}^2 \text{ s}^{-1}$ for a similar electrolyte medium⁽²¹⁴⁾.

This indicates that the electrode/cell combination provides a good hydrodynamic flow of the electroactive species to the RDE⁽²¹⁵⁾. Further evidence for this is presented in the following sections.

5.1.2 Alberly-Hitchman Determination of Diffusion Coefficients

As a further test of the hydrodynamics of the sample chamber of the gas tight cell, and also to determine a suitable cell solution volume, experiments were conducted to determine the diffusion coefficient of the ferrocyanide ion using the method described by Alberly and Hitchman⁽²¹⁶⁾.

In this procedure the RDE is stepped to a potential corresponding to the limiting current for ferrocyanide oxidation (0.5V vs Ag/AgCl) and the decay of the

resulting current with respect to time is measured. Conditions are chosen to give a suitably fast rate of current decay (small sample volume, high rotation speed, large electrode area). An Albery-Hitchman plot of current against time was constructed using the data from a current-time transient. A typical plot is shown in figure 5.2. The slope of this plot is given by

$$\text{Slope} = \frac{1.554 A W^{1/2} D^{2/3}}{\nu^{1/6} V} \quad (5.3)$$

where all terms have their usual meaning and V is the cell volume (cm^3).

It should be noted that in this case an accurate value for the cell volume, and not as in the case of the Levich analysis the concentration, is needed.

As A and W are known, values for D can be determined accurately by this type of experiment. Values of D for ferrocyanide were determined using a number of rotation speed / cell volume combinations, table 5.1.

Table 5.1

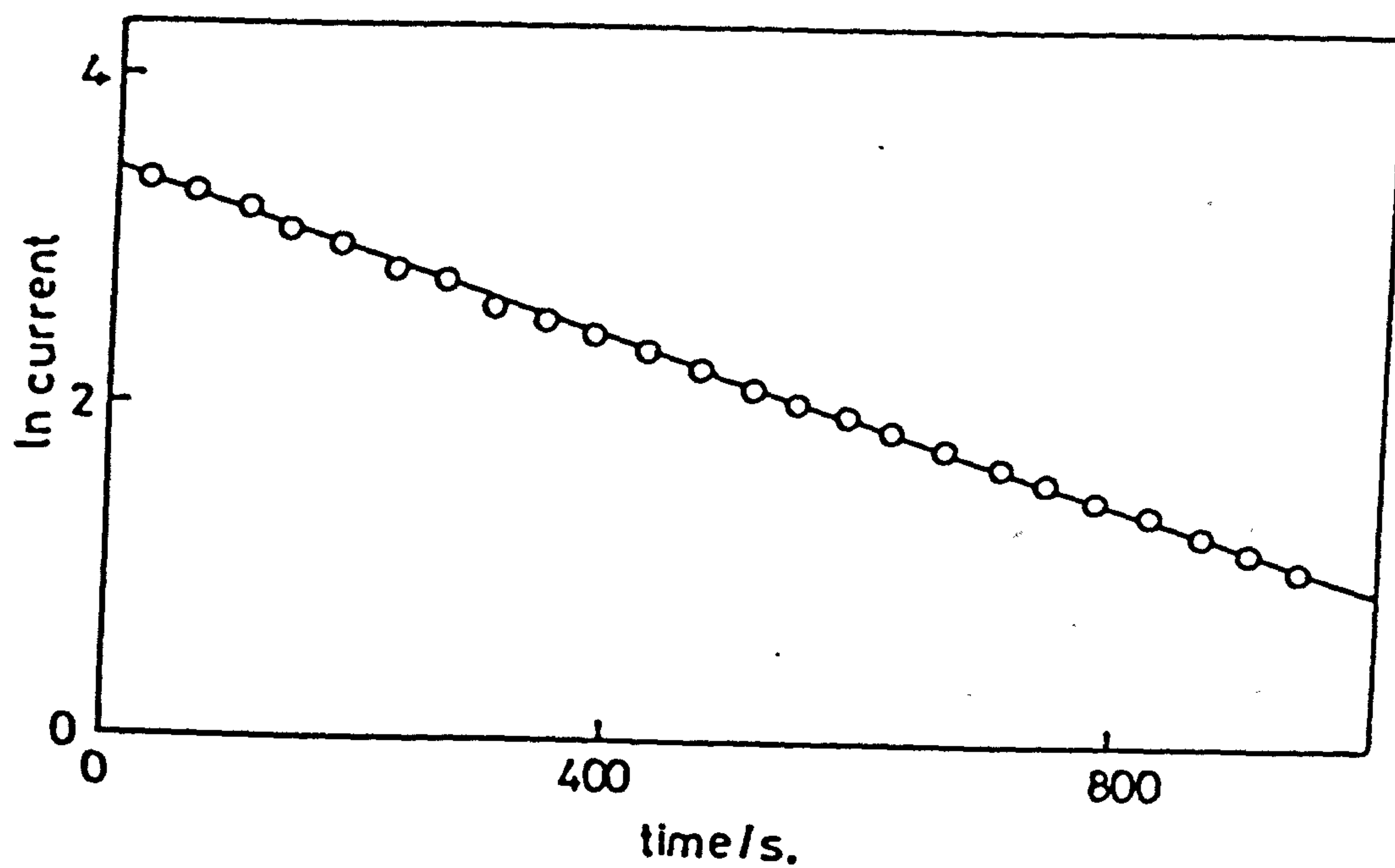
Diffusion coefficients determined by the Albery-Hitchman method

Cell volume (cm^3) ^{b)}	Rotation speed (Hz)	$D^{\text{a)}}$ obtained (cm^2s^{-1}) $\times 10^6$
4.0	16	6.60 (± 0.10)
3.5	16	6.48 (± 0.10)
3.5	25	6.42 (± 0.12)

Notes

- In a 0.25 mol dm^{-3} KCl medium, 20°C , electrode area = 0.385 cm^2
- Volume of sample chamber, working electrode compartment only. Solutions contained behind frits in reference and counter electrode compartments not included in this volume (section 5.1.1).

Figure 5.2 Albery-Hitchman plot for oxidation of ferrocyanide ion at a rotating electrode (0.5V vs Ag/AgCl).



The values of D , for ferrocyanide, determined are in excellent agreement with the value obtained from a Levich analysis (section 5.1.1) and with literature values⁽²¹⁴⁾.

This data demonstrates that the cell has the correct geometry for the hydrodynamic flow to the RDE surface to be optimal. Also it can be seen that solution volumes of between 3.5 and 4.0 cm³ are suitable for this cell. The use of smaller cell volumes was found to cause the presence of gas bubbles at the top of the cell. This situation is undesirable since it will produce turbulence in the solution flow.

In the final part of this section the cell is used for a coulometric titration. The procedure used and the titration data obtained are presented below.

5.1.3 Coulometric Titration in the Gas Tight Cell

In this work a large generator electrode was used to oxidise/reduce ferrocene acetic acid (FAA) in solution. This generator electrode consisted of platinum gauze and was found to have an active surface area of 12.5 cm² by cyclic voltammetry. During the course of the redox titration a series of polarograms were recorded at the RDE. This also served to mix the solution during the titration.

The cell was filled with 3.5 cm³ of a deoxygenated solution of FAA (7.05×10^{-4} mol dm⁻³) in buffered electrolyte (sodium phosphate 0.15 mol dm⁻³, sodium chloride 0.15 mol dm⁻³) at pH 7.0. This ferrocene derivative was used in preference to the ferri/ferrocyanide couple because it shows a marked colour change from yellow in the reduced ferrocene form to blue in the oxidised ferricinium form. This acted as an indicator to determine whether or not the solution retained behind a glass frit in the counter electrode compartment (figure 5.1) was able to mix freely with the main solution.

The large generator electrode was held at +350mV (vs Ag/AgCl) until enough charge was passed to oxidise all of the FAA to the blue FAA⁺ form. It was apparent

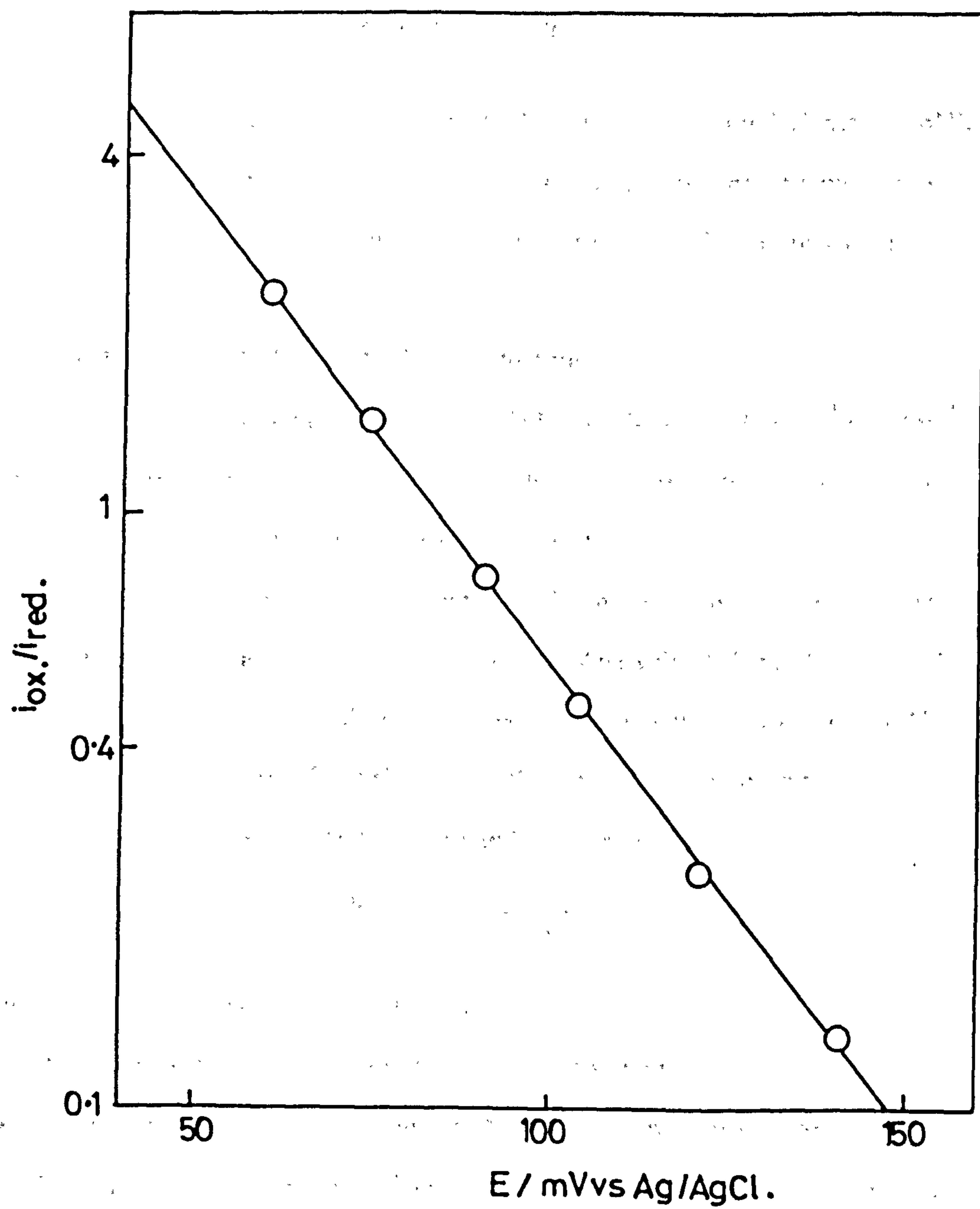
that the solution in the counter electrode compartment did not turn the blue colour produced in the sample compartment. This may be due to the fact that an opposite reaction occurs at the counter electrode to that occurring at the working electrode. It does however indicate that mixing between the FAA in the sample and counter electrode compartments is slow.

The relationship between the charge passed and the amount of material oxidised provides better evidence for the fact that only the solution in the sample compartment is in contact with the working electrode. In theory a total charge of 0.238 coulombs ($n=1$) would be required to oxidise the 3.5 cm³ of FAA solution in the sample compartment. This compares favourably with the experimentally determined value of 0.254 coulombs. This gives a value of 1.06 electrons per molecule of FAA, clearly demonstrating that the solution in the sample chamber only is accessible to the working electrode. A Nernst plot showing the progress of the oxidation of FAA is shown in figure 5.3. This has a slope of 63mV which is close to that expected for a reversible couple at this temperature; at 25°C, for a one electron reaction a slope of 59.19mV can be calculated.

The new type of gas tight perspex electrochemical cell described in this section is suited to use with a rotating electrode (RDE). It has been shown that a suitable sample volume is 3.5 to 4.0 ml and that this solution alone is in contact with the working electrode. This cell also makes the rigorous exclusion of oxygen relatively easy. This is important in the following work as there is a possibility of oxygen interfering with the glucose oxidase/mediator reaction if any is allowed to enter the solutions. For this reason the gas tight cell was used in all work described in this chapter. All potentials will therefore be expressed with respect to silver/silver chloride (Ag/AgCl).

In the following sections the reaction between substrate reduced immobilised glucose oxidase and ferrocene monocarboxylic acid (FMA) is described. Glucose

Figure 5.3 Nernst plot for the progressive oxidation of ferrocene acetic acid.



oxidase is immobilised in films of poly-*N*-methylypyrrole in all cases. The reasons for using FMA as the mediator are discussed. Initially the reaction of FMA at clean and poly-*N*-methylypyrrole coated platinum electrodes is described.

5.2 THE REACTION OF FMA AT CLEAN AND POLY-*N*-METHYL PYRROLE COATED PLATINUM ELECTRODES

In this section the site of reaction of FMA at a poly-*N*-methylypyrrole (pNMP) coated electrode is established. The diffusion coefficient and thermodynamic E° (pH 7.0) of the redox couple is determined and compared to literature values.

5.2.1. Oxidation of FMA at a Platinum Electrode

A series of polarograms were recorded for FMA ($1.035 \times 10^{-3} \text{ mol dm}^{-3}$) in buffered electrolyte solution (sodium phosphate 0.15 mol dm^{-3} , sodium chloride 0.15 mol dm^{-3}) at different electrode rotation speeds.

The electrode was polished (section 2.3) prior to each measurement. A representative polarogram is shown in figure 5.4. Analysis of this polarogram shows that the limiting current for FMA oxidation occurs at potentials anodic of 0.425V (vs SCE). The thermodynamic E° (pH 7.0) for this reaction was determined by further analysis of the polarogram using the corrected Tafel equation

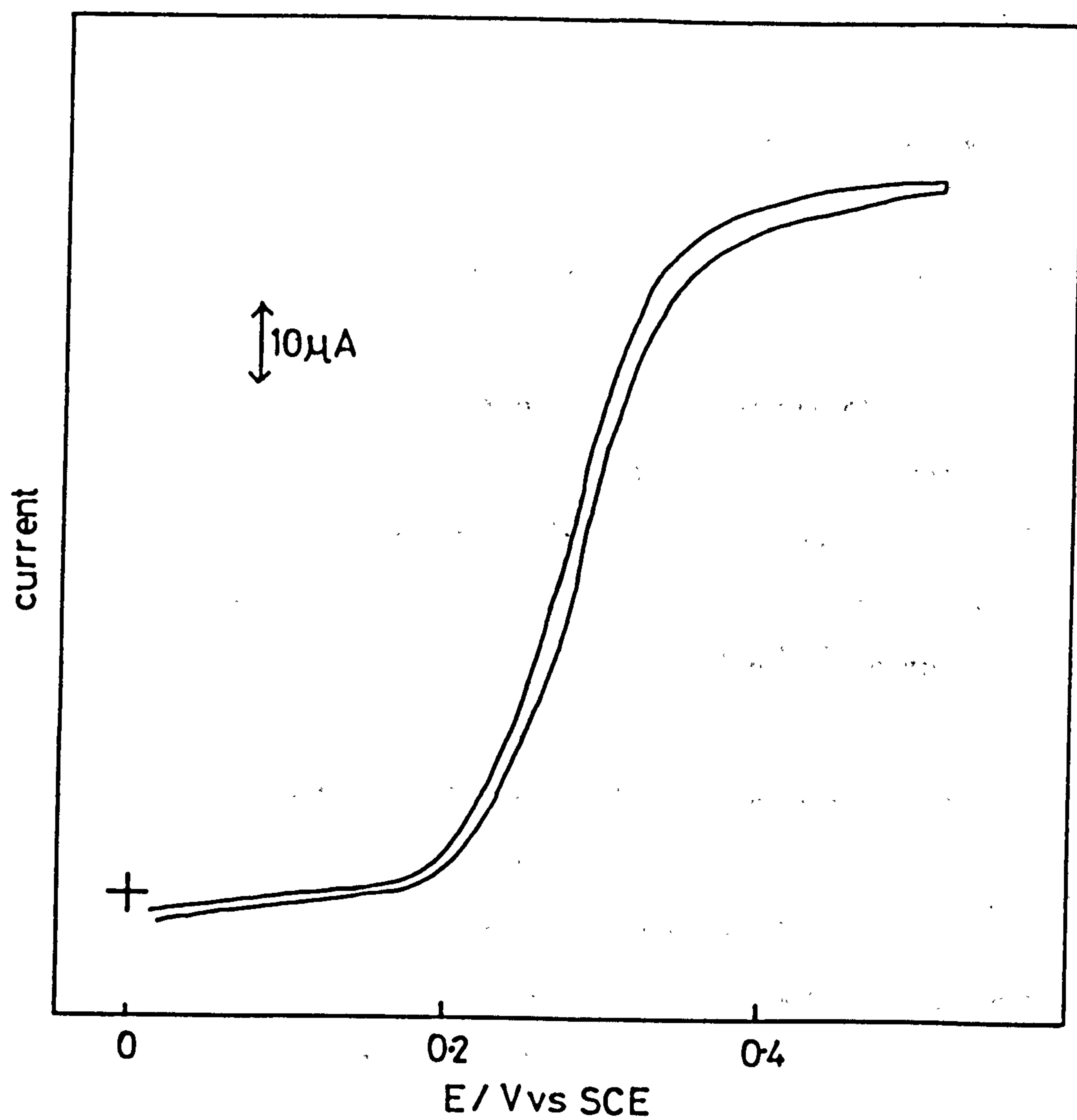
$$\ln \left[\frac{i_L}{i} - 1 \right] = \frac{RT\eta}{nF} \quad (5.4)$$

where η is the overpotential (volts vs SCE).

This form of the Tafel equation is relevant to reversible redox couples where $k' \gg k_D$ (the electrochemical rate constant \gg the mass transfer rate constant)⁽²¹⁷⁾.

The equation contains no k' term as the reaction is so fast that there is equilibrium between the oxidised and reduced species at the electrode surface. A plot of $\ln(\frac{i_L}{i} - 1)$ against η for a reversible system will yield a value for the

Figure 5.4 Polarogram for the oxidation / reduction of ferrocene monocarboxylic acid at a rotating disc electrode (9 Hz).



thermodynamic E° of this system when

$$\ln \left[\frac{i_L}{i} - 1 \right] = 0, \eta = E^\circ \quad (5.5)$$

and should have a slope equal to the Nernst slope (58.5 mV at 22°C, $n=1$).

Such a plot is shown in figure 5.5. The E° (pH 7.0, 22°C) for the FMA/FMA⁺ couple is 280mV (vs SCE). This is in good agreement with values of between 275 and 288 ±10mV (vs SCE) in the literature^(47,53,65).

The slope of this plot is 63(±3)mV indicating that the system is electrochemically reversible.

In order to determine the diffusion coefficient of the FMA molecule the platinum electrode was poised at a potential corresponding to i_L (450mV vs SCE) and the resultant limiting currents were measured as a function of rotation speed. Using this data a Levich plot (eqn 5.1) was constructed. This had a slope (eqn 5.2) of $9.545 \times 10^{-5} \text{ A cm}^{-2} \text{ Hz}^{-1/2}$ giving a value for D of $4.8 \times 10^{-6} \text{ cm}^2 \text{ s}^{-1}$ (figure 5.6). This is in good agreement with values of $6.0 \times 10^{-6} \text{ cm}^2 \text{ s}^{-1}$ determined by cyclic voltammetry under similar conditions⁽⁶⁵⁾ and $4.6 \times 10^{-6} \text{ cm}^2 \text{ s}^{-1}$ determined at a rotating disc electrode⁽²¹⁸⁾.

In this section values for E° and D of the FMA couple have been determined. This couple is stable in solution over a time scale of several hours and exhibits fast kinetics at the electrode. In the next section the reaction of this redox couple at poly-*N*-methylpyrrole coated platinum electrodes is described in an attempt to determine whether or not the FMA molecule is rapidly oxidised on this conducting polymer.

5.2.2 Reaction of FMA at Poly-*N*-methylpyrrole Coated Electrodes

The dependence of the limiting current upon the rotation speed was again determined. A Levich plot of the data was linear, indicating that the FMA was being

Figure 5.5 Corrected Tafel plot for the oxidation / reduction of ferrocene monocarboxylic acid (data from figure 5.4).

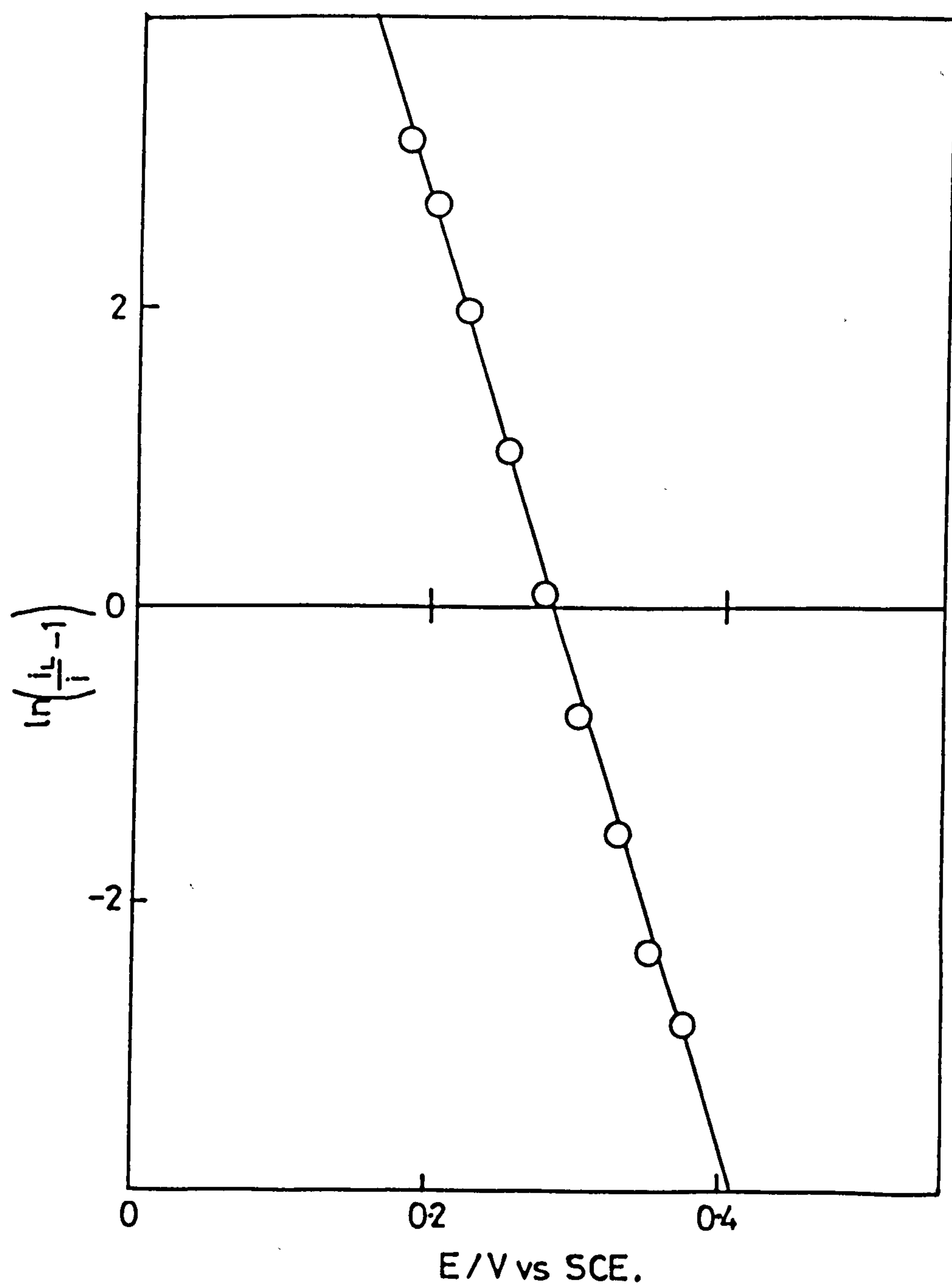
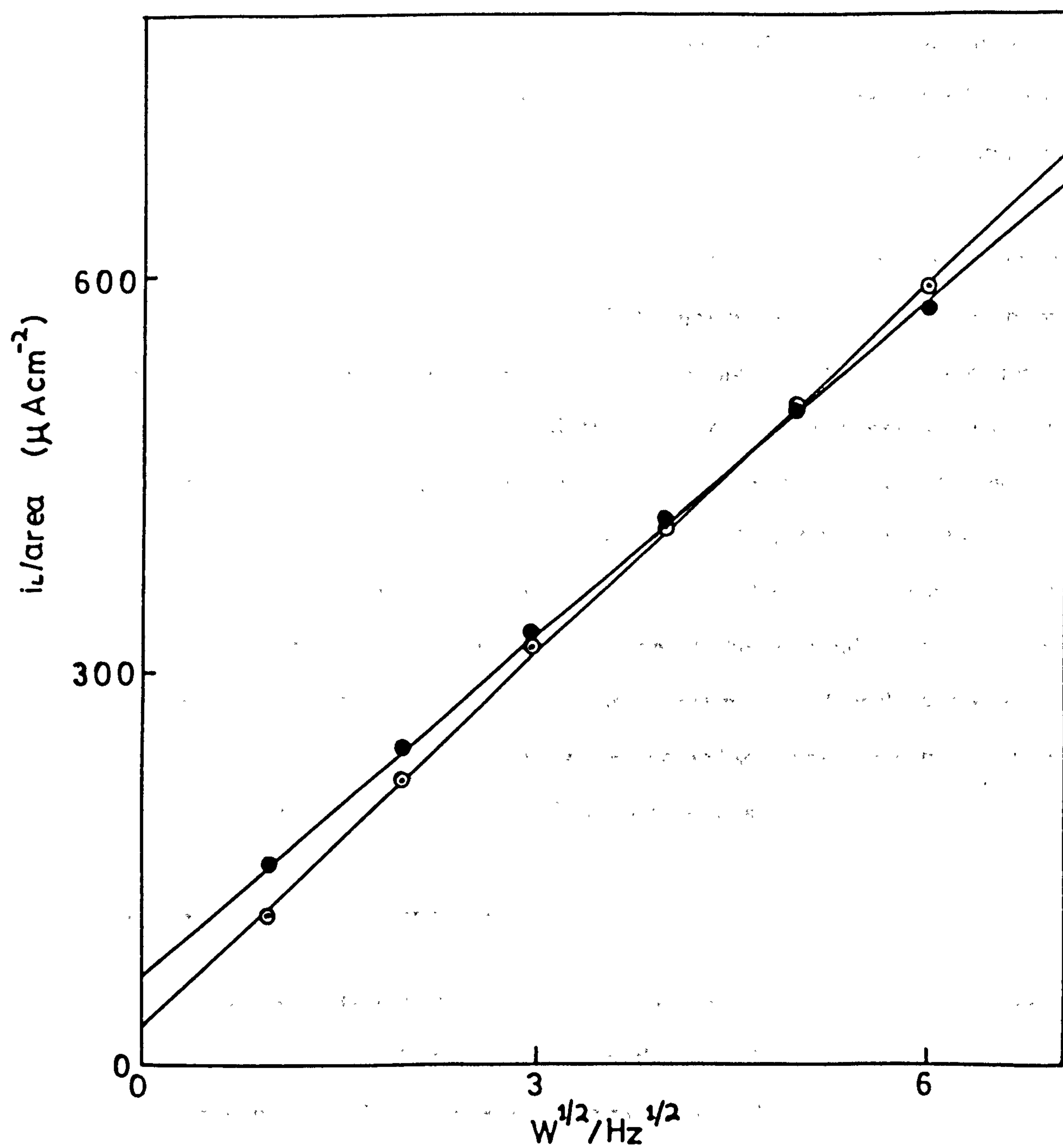


Figure 5.6 Levich plots for the oxidation of ferrocene monocarboxylic acid. Solid points for data at a pNMP-GOD coated platinum RDE, open points for data at a clean platinum RDE.



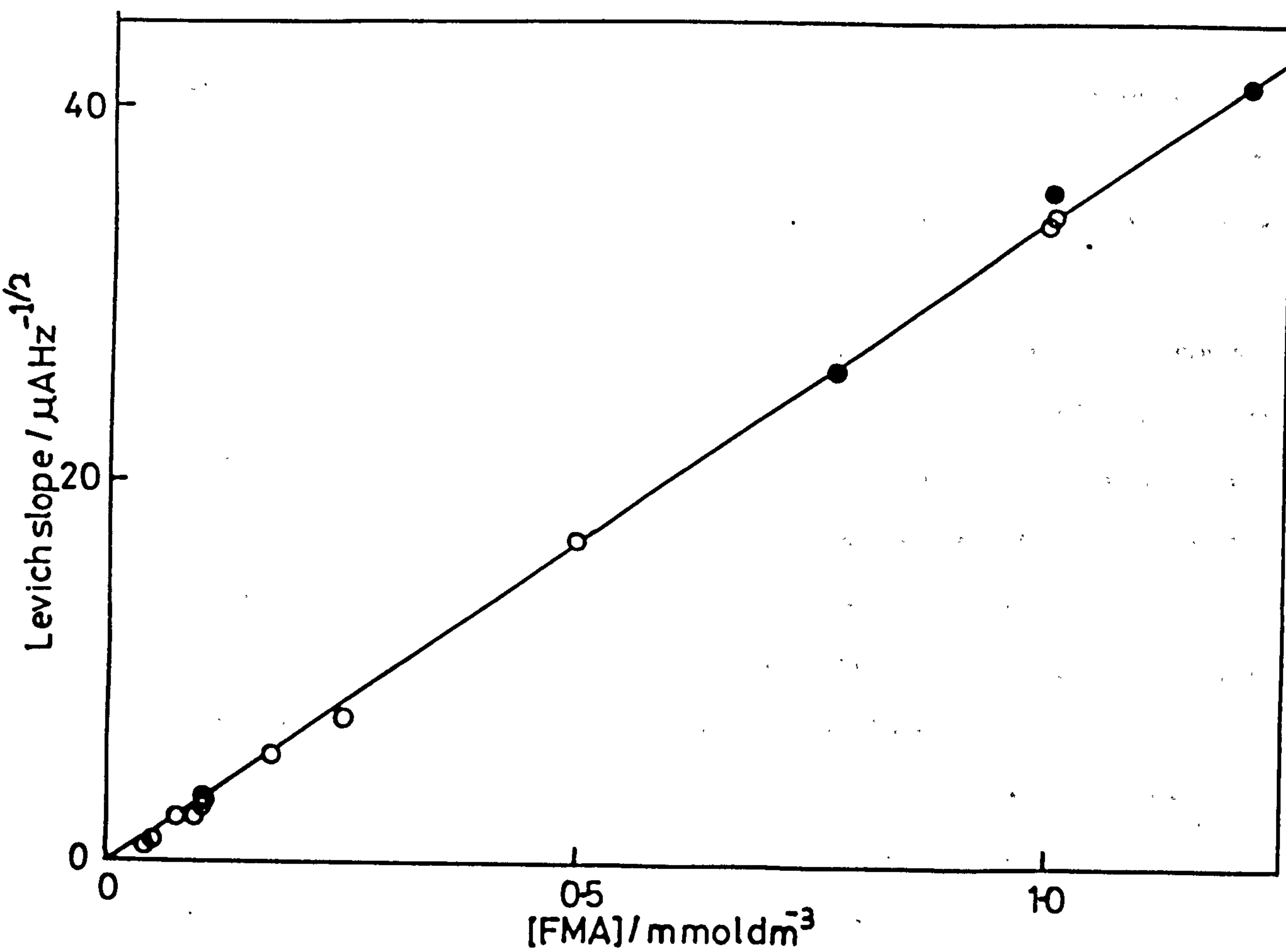
rapidly oxidised on the surface of the conducting polymer. This is opposed to the situation encountered for the oxidation of hydrogen peroxide (section 4.5.1) which must diffuse through the conducting polymer to be oxidised at the underlying platinum electrode. The Levich plot for a poly-*N*-methylpyrrole coated electrode (very thick film of around 3×10^{-4} cm) is shown in figure 5.6. This has a slope of $8.50 \times 10^{-5} \text{ A cm}^{-2} \text{ Hz}^{-1/2}$. The fact that this is very similar to the slope observed for the clean platinum case implies a facile oxidation of FMA at the conducting polymer surface. Further evidence is provided by the fact that the Levich slope is independent of film thickness and depends linearly on the bulk concentration of FMA (figure 5.7).

This observation has important implications in understanding and modeling of the reaction of this mediator with GOD immobilised in conducting poly-*N*-methylpyrrole. The reduced form of the mediator produced by the enzyme reaction can now be reoxidised on the conducting polymer. This represents a different situation to the hydrogen peroxide case presented in the preceding chapter and is one which requires the development of a new theoretical model to allow for this fact. The new situation is modelled in section 3.2 of this thesis. This model is used to interpret the data obtained for the mediation of the immobilised GOD reaction contained in this chapter. The effect of varying the polymer film thickness, enzyme loading and bulk FMA concentration on the immobilised enzyme electrode response is described and then modelled in the following sections.

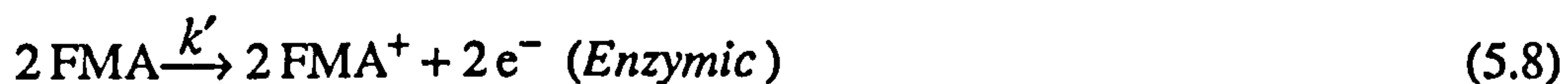
5.3 RESPONSES TO GLUCOSE

Glucose oxidase (GOD) was immobilised in films of poly-*N*-methylpyrrole (pNMP) by the method described in detail in the preceding chapter. The response of the immobilised GOD to glucose was determined when FMA was substituted for the natural enzyme mediator, dioxygen. The substrate reduced GOD is reoxidised by the

Figure 5.7 Plot of the Levich slope as a function of bulk mediator concentration. Open points for data at a pNMP-GOD coated platinum RDE, solid points for data at a clean platinum RDE.



ferricinium form of FMA (FMA^+):



The reaction in equation (5.7) probably occurs in two steps whereby the reduced enzyme donates an electron to one FMA^+ molecule to form the flavinsemiquinone state (FADH^\bullet) and then a second electron to a further FMA^+ molecule to become fully oxidised. Equation (5.9) is included to show that the oxidation of FMA produced by the enzyme at the electrode will be accompanied by the mass transport limited oxidation of FMA already present in the bulk solution.

The production of FMA by the enzymic reaction was monitored amperometrically at a potential of 0.40 volts (vs Ag/AgCl). This is approximately 0.20 volts positive of the E° of the FMA/FMA^+ couple (section 5.2) so that all of the FMA produced by the enzyme will be reoxidised to the FMA^+ form. This results in the recycling of the mediator within the polymer film (figure 5.8).

In order to measure the response of the GOD-pNMP electrode to glucose at a particular enzyme loading and film thickness the electrode was placed in a FMA solution of known concentration and potentiostated at 0.40 volts (vs Ag/AgCl). All oxygen is excluded from the cell and the Levich current at a particular rotation speed (typically 4 Hz) was measured in the absence of glucose. Then aliquots of stock glucose solution (1.00 mol dm^{-3}) were injected into the cell and the resulting current increases were measured. The Levich current, at zero glucose, was taken as the zero enzymatic current for each response measurement. A typical set of responses and the calibration curve produced by plotting the enzymatic response ($i_{\text{total}} - i_{\text{Levich}}$) is shown in figure 5.9. The current response is seen to saturate at glucose concentration of greater than $6.0 \times 10^{-2} \text{ mol dm}^{-3}$. The reasons for this current response saturation

Figure 5.8 Schematic representation of recycling of the mediator in the enzyme containing conducting polymer film.

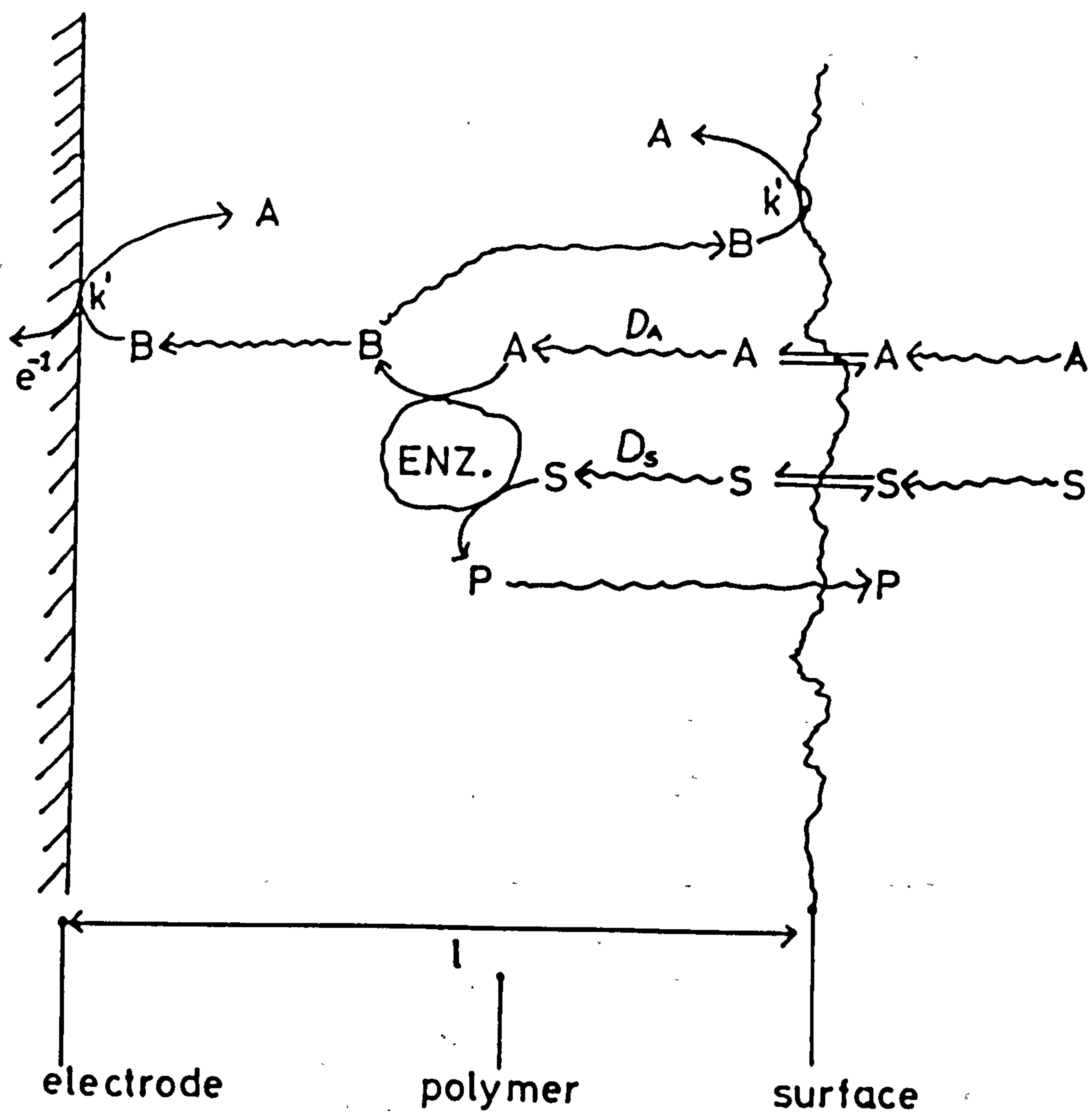
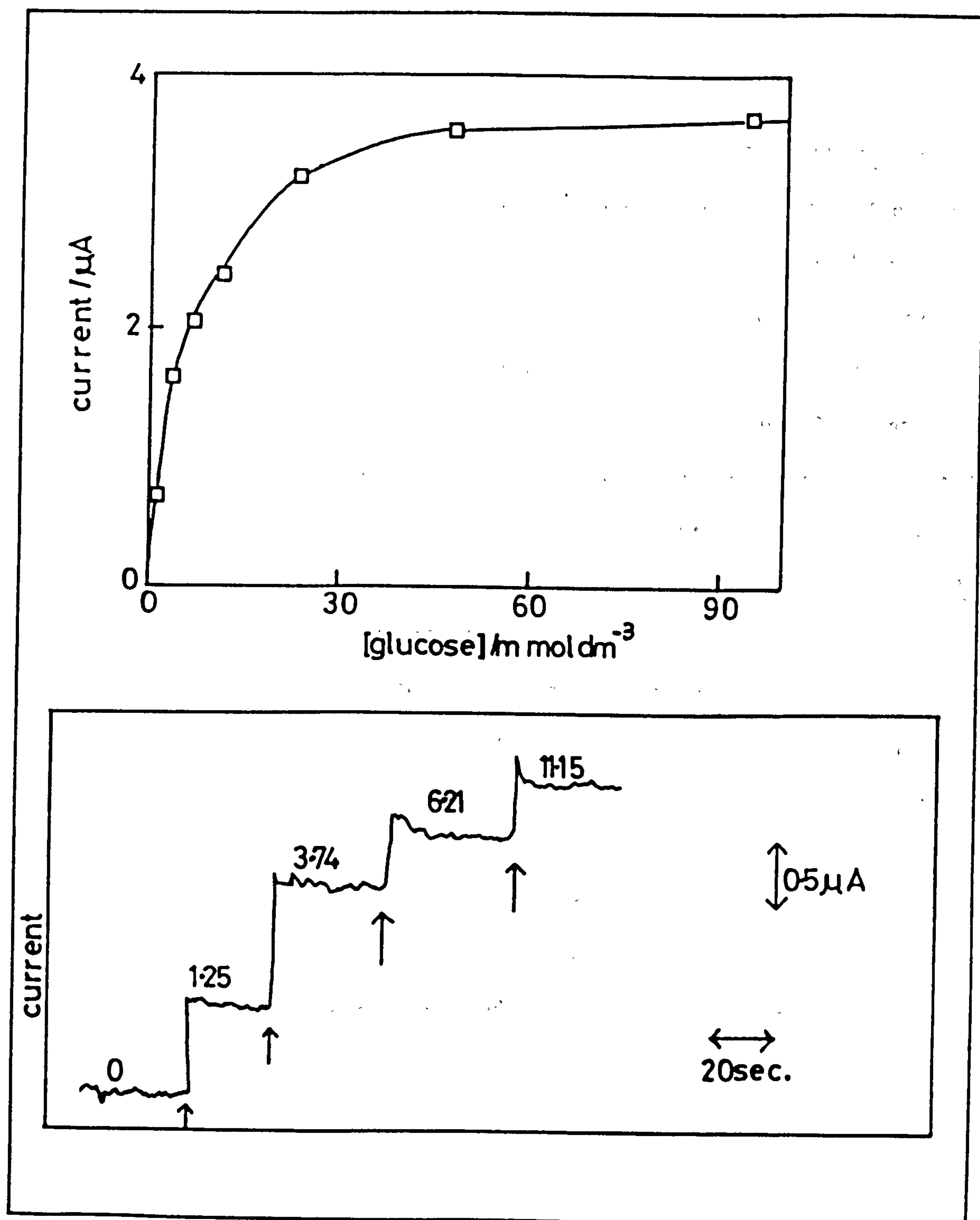


Figure 5.9 Plot of electrode response ($i_{total} - i_{Levich}$) as a function of bulk glucose concentration. The lower inset shows the experimental trace of current as a function of time. The arrows indicate the points at which glucose was injected and the numbers signify the final concentration of glucose after each addition to the bulk solution.



are explained fully in the latter sections of this chapter.

The response of this system was also investigated by cyclic voltammetry. In the next section the cyclic voltammetric responses will be presented. This is followed by the main body of this work which involves the amperometric detection of FMA produced by the immobilised GOD. These results are explained in terms of our theoretical model (chapter 3).

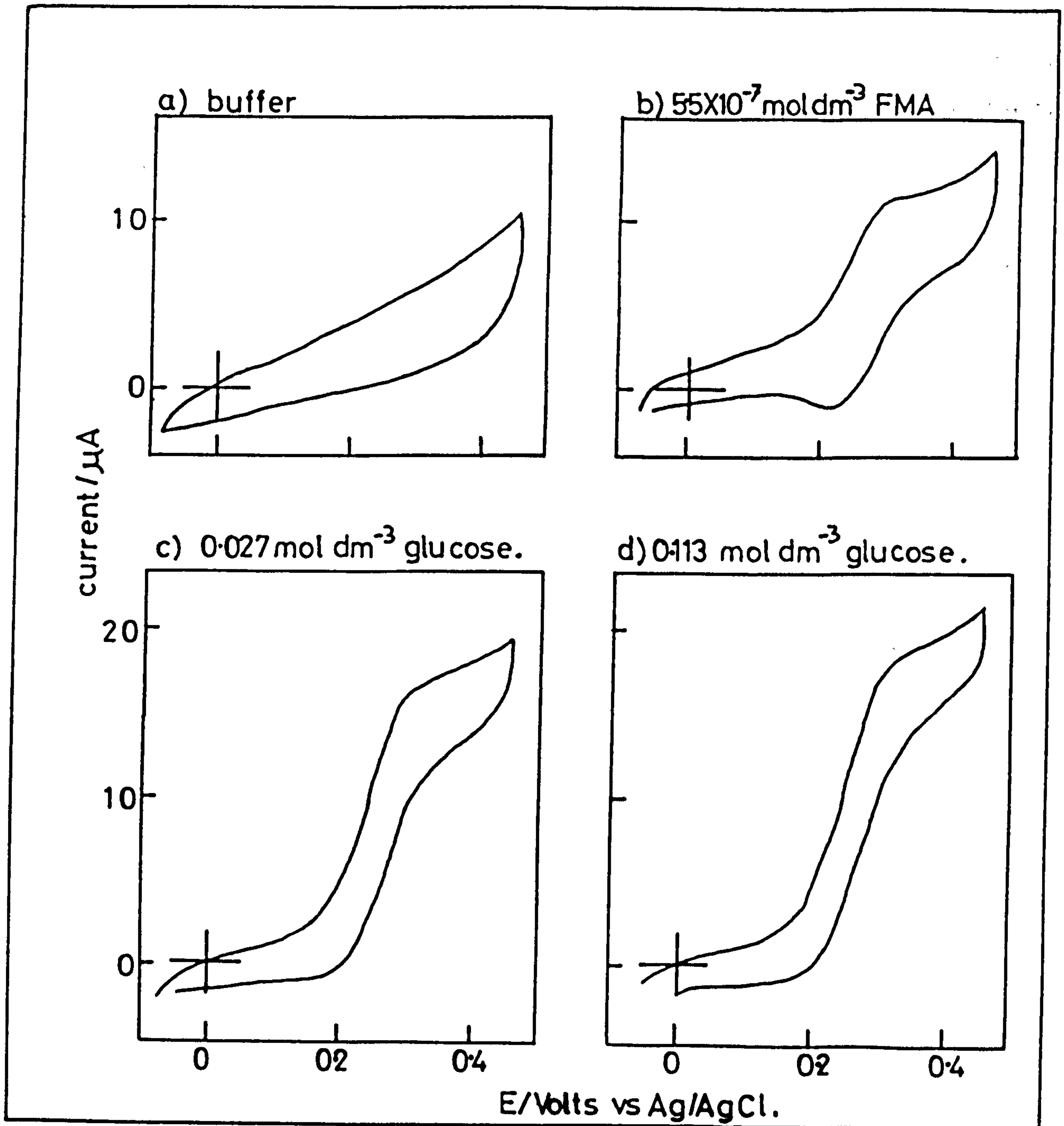
5.3.1 The Cyclic Voltammetry of the FMA Mediated GOD-pNMP System

In this short section the cyclic voltammetry of pNMP films grown potentiostatically from a buffered electrolyte solution (sodium phosphate 0.15 mol dm^{-3} , TEATFB 0.10 mol dm^{-3}) containing glucose oxidase (GOD 10 mg cm^{-3}) is described. Thin films ($1 \times 10^{-5} \text{ cm}$) were used in all cases. The films were washed and placed in a deoxygenated solution of FMA ($5.5 \times 10^{-4} \text{ mol dm}^{-3}$) at pH 7.0. Cyclic voltammetric responses were recorded in the presence of increasing amounts of glucose. Typical electrode responses, at a sweep rate of 2 mV s^{-1} are shown in figure 5.10. The development of a polarographic type wave is seen. The catalytic current is indicative of the enzyme reduction of FMA^+ .

This initial work is intended to demonstrate that mediation of the immobilised GOD reaction is feasible when using FMA added to the bulk solution. In the following sections the amperometric response of such a system to glucose additions is discussed.

Initially amperometric responses are presented and analysed in terms of the experimental variables, film thickness, enzyme loading and bulk mediator concentration. The responses presented in the next section were recorded at 4 Hz, pH 7.0, in the absence of oxygen.

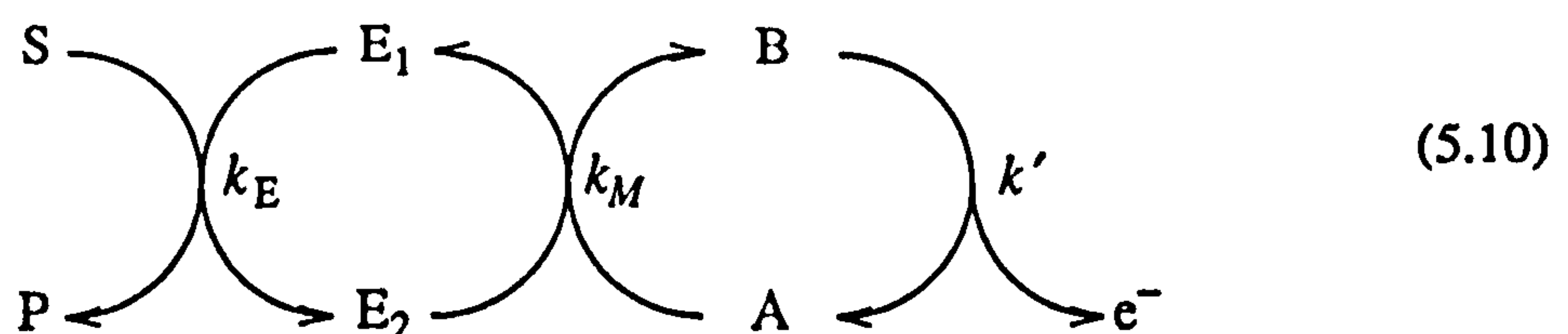
Figure 5.10 Cyclic voltammetric response for a pNMP-GOD film in the presence of FMA ($5.5 \times 10^{-4} \text{ mol dm}^{-3}$) for different concentrations of glucose.



5.4 ANALYSIS OF THE GLUCOSE RESPONSES

The characteristics of the enzyme containing film are described in terms of film thickness and enzyme loading. For each film thickness and enzyme loading the dependence of the electrode response to glucose on the bulk mediator concentration was determined.

The responses are then described in terms of our theoretical model (section 3.2). Returning to the mathematical description of this system it can be seen that the theory is based on the following reaction scheme



where S and P are the substrate and product, E_1 and E_2 are the oxidised and reduced forms of the enzyme, and A and B represent the oxidised and reduced forms of the mediator. The rate constants k_E and k_M describe the reaction of oxidised enzyme with substrate and the reaction of reduced enzyme with oxidised mediator respectively. The electrochemical rate constant k' describes the oxidation of the reduced mediator on the polymer electrode.

Returning to the theory presented in chapter 3 it can be seen that there are 5 different cases occurring in this system. The expression for the current response, j_S , has a unique combination of dependencies on l , e_Σ , s_∞ , and a_∞ for each of the five cases. The j_S expressions are given in table 5.2.

Table 5.2

The dependence of the flux j_S on the experimental variables

Case	j_S	Order with respect to			
		e_Σ	s_∞	a_∞	l
I	$-Da_\infty k' l$	0	0	1	1
II	$-Da_\infty k_M e_\Sigma l$	1	0	1	1
III	$-2a_\infty D^{1/2} k_M^{1/2} e_\Sigma^{1/2}$	$1/2$	0	1	0
IV	$-s_\infty D^{1/2} k_E^{1/2} e_\Sigma^{1/2}$	$1/2$	1	0	0
V	$-s_\infty l k_E e_\Sigma$	1	1	0	1

A case diagram showing the relationship of the different cases is shown in figure 3.8.

In the following section the effect of changing the experimental variables of l , e_Σ , s_∞ and a_∞ are described in terms of the theoretical model and accompanying case diagrams for this system.

5.4.1 Film Thickness (l)

An examination of the case diagram in figure 3.8 reveals that increasing the film thickness will move us vertically up the $\log(l/X_K)$ axis of this diagram for cases where $\gamma \ll 1$ or when $\gamma \gg 1$.

Experimental data describing the effects of increasing l at low and high substrate concentrations was obtained. In both situations the data changes from having a 1st order dependence on l for thin films to a zero order dependence on l for thick films.

5.4.1.1 The V/IV Case Boundary

Let us first consider the situation for the dependence of j_S on l for a low glucose concentration ($s_\infty = 1.25 \times 10^{-6} \text{ mol cm}^{-3}$). For thin films this places us in

case V since this is the only case where j_s is dependent on both l and s_∞ . On increasing the film thickness to a value where j_s is independent of l case IV is reached. This corresponds to travelling vertically up the case diagram for a situation when $\gamma \gg 1$ (low s_∞).

We can write an expression to describe j_s as a function of l for crossing the V/IV case boundary

$$j_{V/IV} = K_S s_\infty \sqrt{D_s \alpha [enz] k_{cat} / K_M} \tanh \left[l \left(\frac{\alpha [enz] k_{cat}}{K_M D_s} \right)^{1/2} \right] \quad (5.11)$$

Parametrisation of this expression allows us to fit the experimental data for increasing l to the theoretical expression describing the crossing of the V/IV boundary.

$$i = P [1] \tanh(l P [2])$$

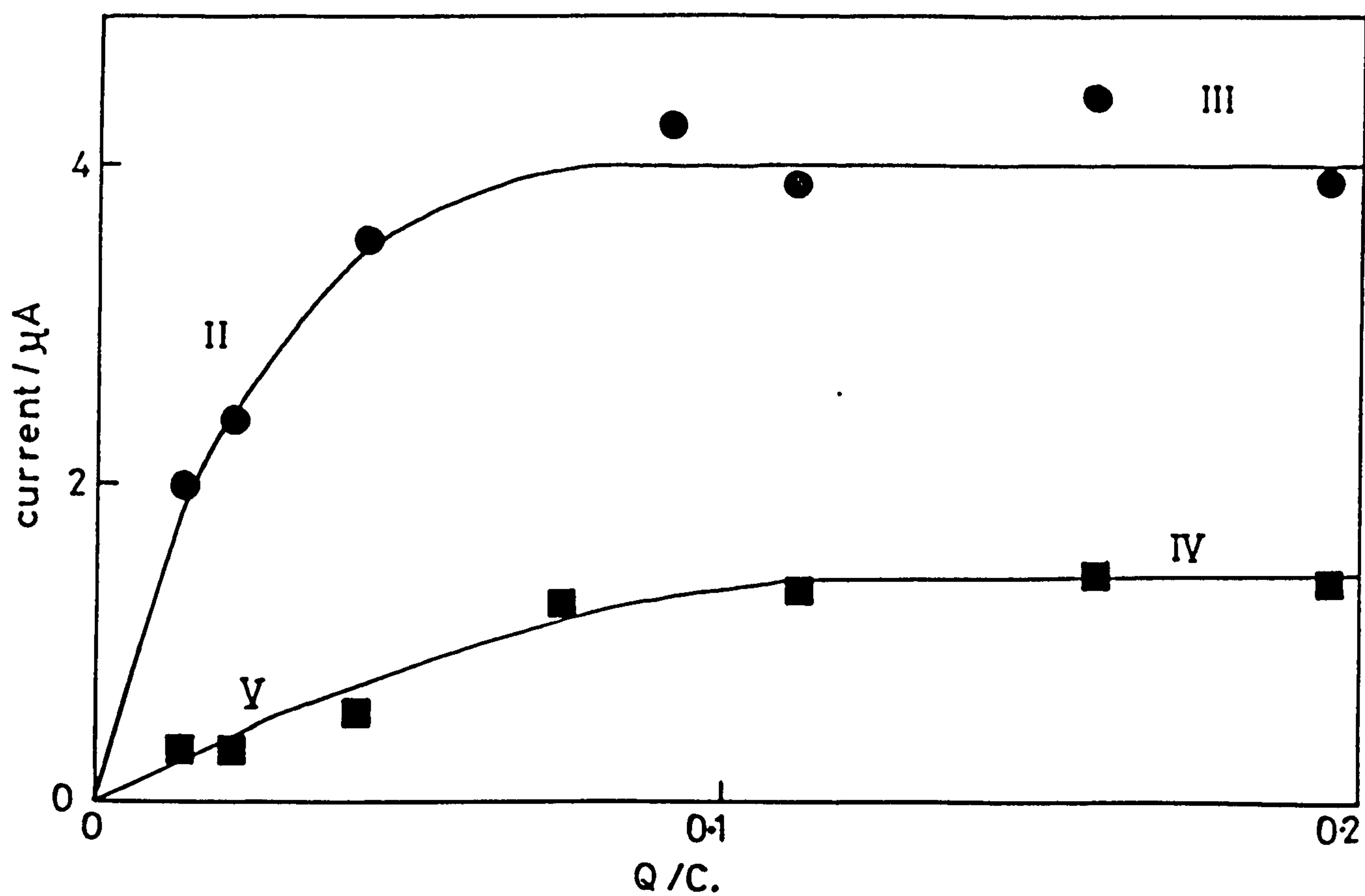
$$\text{where } P [1] = nFAK_s [s] \sqrt{D_s \alpha [enz] k_{cat} / K_M}$$

$$P [2] = \sqrt{\alpha [enz] k_{cat} / K_M D_s}$$

A knowledge of certain of the experimental variables such as $[enz]$, the concentration of GOD in the initial growth solution, s_∞ and nFA , allows us to determine the values for certain combinations of parameters. All parameters resulting from the fit of experimental data to theoretical expressions is presented and discussed in the latter part of this chapter.

A fit of experiment to theory for data which crosses the V/IV case boundary is shown in figure 5.11. The data presented in this figure correspond to $e_\Sigma = 5 \text{ mg cm}^{-3}$, $s_\infty = 1.25 \times 10^{-6} \text{ mol cm}^{-3}$ and $a_\infty = 1 \times 10^{-7} \text{ mol cm}^{-3}$. It is apparent that the fit is good. Parameters obtained from this data are compared to similar parameters obtained by variation of s_∞ , e_Σ and a_∞ later in this chapter.

Figure 5.11 Plot to show electrode response as a function of film thickness. Solid squares represent data for low glucose concentration ($1.25 \times 10^{-6} \text{ mol cm}^{-3}$) and solid circles represent data for saturating glucose ($1 \times 10^{-4} \text{ mol cm}^{-3}$).



5.4.1.2 The II/III Case Boundary

A similar experiment involving the measurement of the electrode response as a function of l for saturating substrate concentration was also undertaken.

Increasing the substrate concentration has moved us to a situation where $\gamma \ll 1$, represented by the top half of the case diagram. Now increasing l moves us vertically up this portion of the case diagram. Therefore increasing l at high substrate concentration represents a crossing of the II/III case boundary. Case II represents a situation where j_S is dependent on l and independent of s_∞ , whereas in case III j_S is independent of both l and s_∞ .

The experimental current responses as a function of l are shown in figure 5.11 together with the theoretical line calculated according to an expression describing crossing of the II/III boundary, where

$$j_{II/III} = 2K_A [a] \sqrt{D_A K_M e_\Sigma} \tanh \left[\frac{l}{2} \sqrt{k_M e_\Sigma / D_A} \right] \quad (5.12)$$

This expression is parametrised as

$$i = P[1] \tanh(X P[2])$$

$$\text{where } P[1] = 2nFAK_A [a] \sqrt{D_A K_M \alpha[enz]}$$

$$P[2] = 1/2 \sqrt{K_M \alpha[enz] / D_A}$$

Once again the fit of experiment to theory is reasonable for crossing this case boundary. The data presented in this figure correspond to $e_\Sigma = 5 \text{ mg cm}^{-3}$, $a_\infty = 1 \times 10^{-7} \text{ mol cm}^{-3}$ and $s_\infty = 1 \times 10^{-4} \text{ mol cm}^{-3}$. Parameters obtained from this fit are presented later in this chapter.

5.4.2 Substrate Concentration (s_∞)

In order to further test the validity of this model electrode responses were recorded as a function of s_∞ for a number of different film thicknesses.

5.4.2.1 The V/II Case Boundary

The effect of increasing s_{∞} on the response of a film of defined thickness was determined. A thin film corresponding to a thickness of 9.1×10^{-6} cm was used.

In order to visualise the effect of altering s_{∞} on the position of the data on the case diagram, a new case diagram was constructed. This is shown in figure 5.12 and shows a plot of $\log(\sqrt{k'/D})$ vs $\log(k_M a_{\infty}/k_E s_{\infty})$ for situations where $k_M e_{\Sigma} < k'$ and $k_M e_{\Sigma} > k'$.

Under normal experimental conditions used the data at low substrate concentration is positioned on the right hand side of the case diagram. Increasing the substrate concentration moves us to the left, corresponding to crossing the V/II case boundary.

The experimental current responses, as a function of s_{∞} , are shown in figure 5.13, together with a line drawn according to the appropriate theoretical expression describing crossing of the V/II case boundary.

$$i = \frac{nFAK_A [a] l k_M \alpha[enz]}{1 + (k_M K_A [a] / k_E K_S [s])} \quad (5.13)$$

This expression is parametrised as

$$i = P [1] X / (X + P [2])$$

$$\text{where } P [1] = nFAK_A [a] l k_M \alpha[enz]$$

$$P [2] = k_M K_A / k_E K_S$$

The experimental data represents an excellent fit to this expression. It is pleasing that not only is this a good fit but that it also gives values for the appropriate rate constant parameters which are in excellent agreement with those obtained from data crossing the V/IV and II/III boundaries.

Figure 5.12 Case diagram for situations when $k_M e_\Sigma < k'$ and $k_M e_\Sigma > k'$.

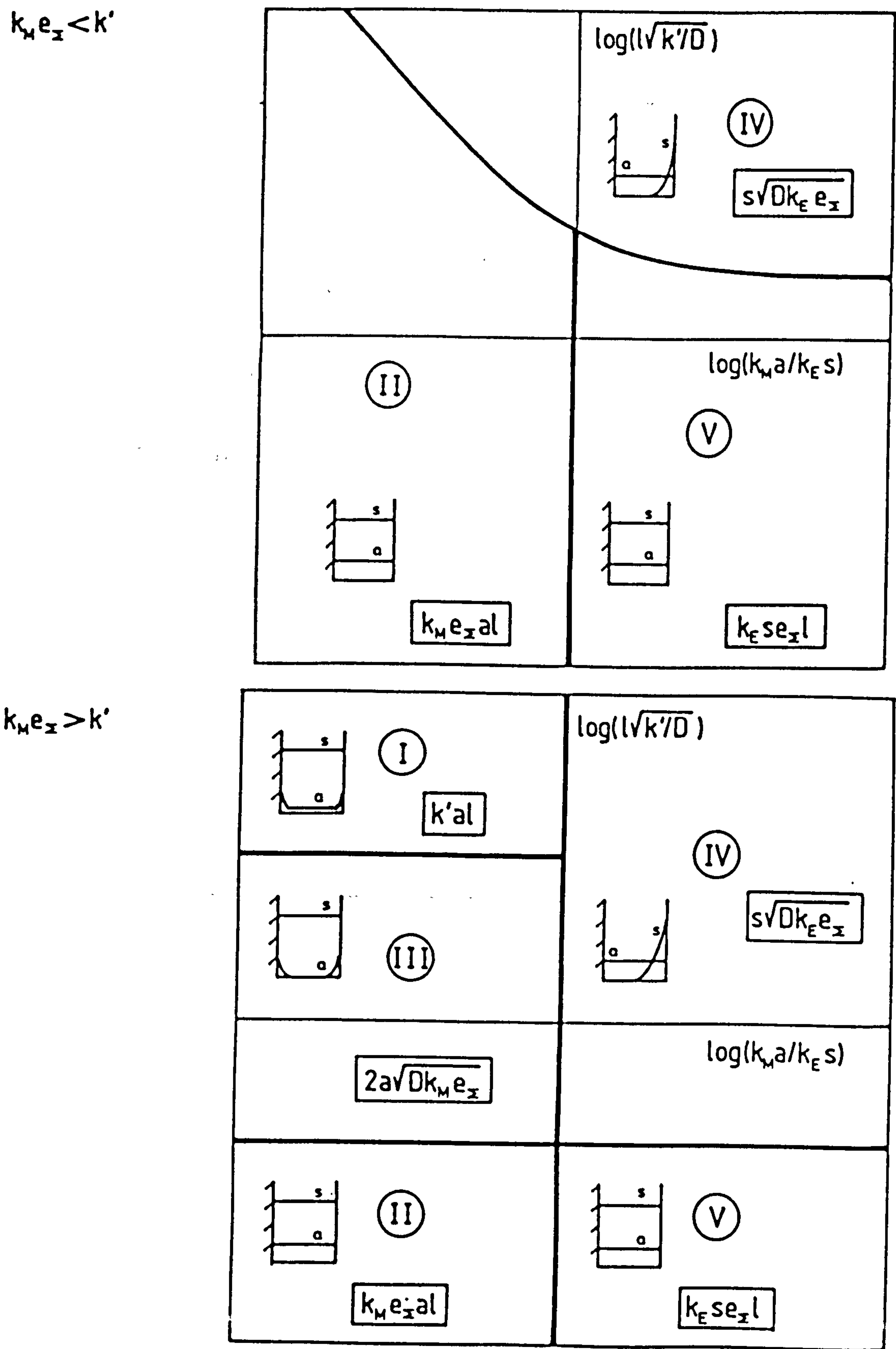
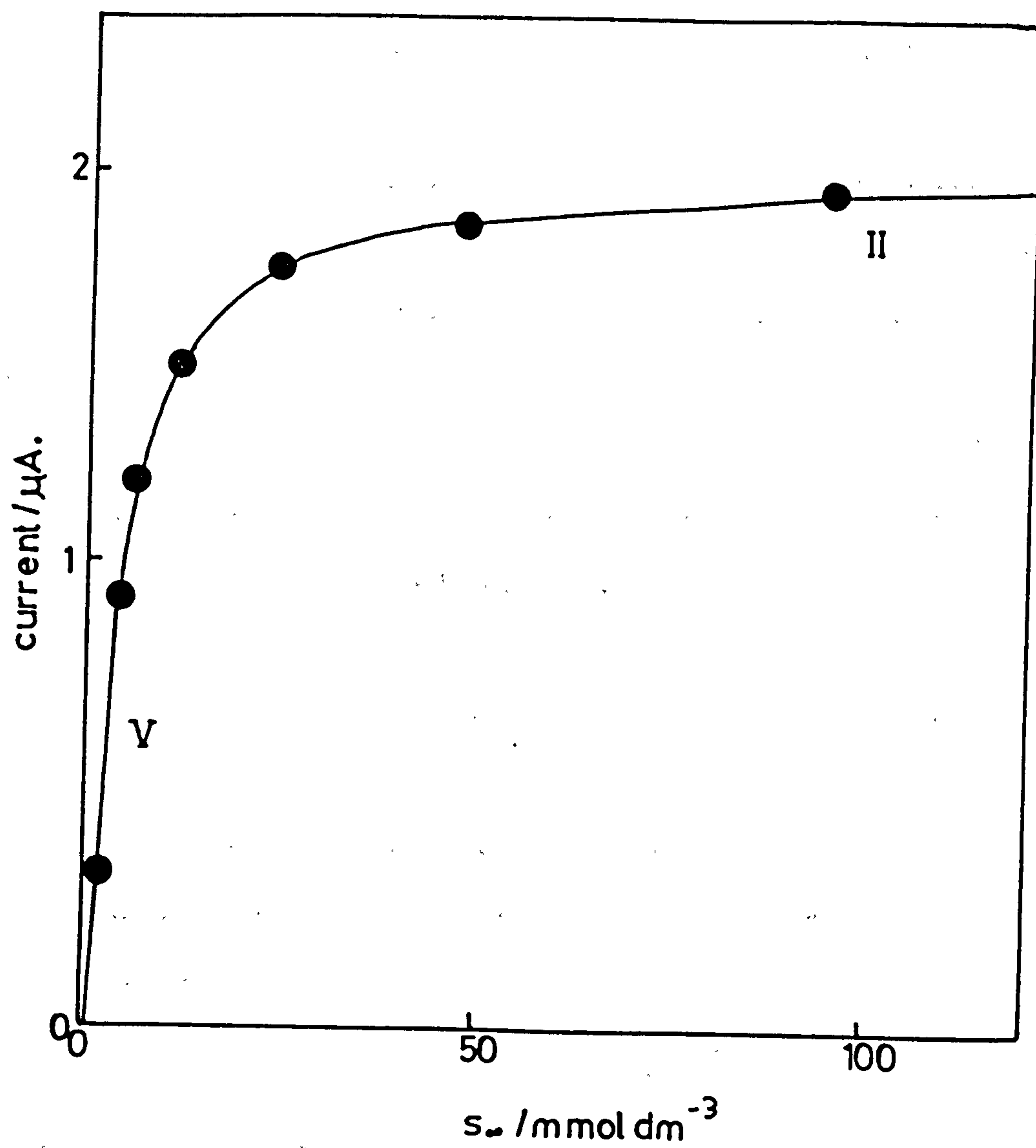


Figure 5.13 Current response as a function of substrate concentration for a “thin” film situation ($l = 9.1 \times 10^{-6}$ cm).



5.4.2.2 The IV/III Case Boundary

Similar experiments in which the response in thick films (3.2×10^{-5} cm) was measured as a function of substrate were undertaken.

Data for a thick film is positioned in the upper half of the case diagram in figure 5.12. Increasing the value of s_{∞} moves us from right to left on this diagram for a situation where $k_M e_{\Sigma} > k'$.

Case III is unusual in that it represents a situation where the FMA produced by enzymic reduction of FMA^+ is reacting at the polymer/solution and polymer/electrolyte interfaces and is not being significantly removed by reaction in the bulk of the polymer.

It has not been possible, so far, to obtain a theoretical expression for the crossing of the IV/III case boundary. It is apparent that data for increasing s_{∞} at a constant l in a thick film correspond to crossing of the IV/III boundary since a crossing from case IV to case I would move us into a situation in which j_s became once more dependent on l . This is not the case so that a IV/III boundary crossing can be identified.

Although a theoretical expression is not at present available it is still possible to obtain parameters from the limiting (linear) portions of this experimental data. Thus, at low glucose (case IV)

$$i_{IV} = nFAK_S [s] \sqrt{D_s \alpha [enz] k_{cat} / K_M} \quad (5.14)$$

The experimental data (figure 5.14) reveals a slope of $0.485 \text{ A mol}^{-1} \text{ cm}^3$ for the linear portion corresponding to case IV. Entering the known parameters, $n=2$, $A=0.385 \text{ cm}^2$, $[enz] = 5 \text{ mg cm}^{-3}$, then

$$K_S \sqrt{D_s \alpha k_{cat} / K_M} = 2.92 \times 10^{-6} \text{ mg}^{-1/2} \text{ cm}^{5/2} \text{ s}^{-1}$$

This compares very favourably with values obtained from data describing other boundary crossings.

Further, at high glucose (case III)

$$i_{III} = 2nFAK_A[a]\sqrt{D_a K_M \alpha [enz]} \quad (5.15)$$

The experimental data (figure 5.14) shows a plateau current of 4.5×10^{-6} A at saturating glucose. At $a_{\infty} = 1.035 \times 10^{-7}$ mol cm⁻³, and using the known parameters described above, then

$$K_A \sqrt{D_a k_M \alpha} = 1.3 \times 10^{-4} \text{ mg}^{-1/2} \text{ cm}^{5/2} \text{ s}^{-1}$$

This is again in excellent agreement with parameters obtained for other boundary crossings.

All the experimental parameters are compared and discussed following the presentation of all the available experimental data.

5.4.3 Mediator Concentration (a_{∞})

The effect of altering the mediator concentration under defined conditions of e_{Σ} , l and s_{∞} was investigated. The data obtained are not, however, as informative as that obtained for variations in the s_{∞} and l parameters.

Increasing the mediator concentration will move us from left to right on the case diagram in figure 5.12. However at high glucose concentrations ($s_{\infty} = 1 \times 10^{-4}$ mol cm⁻³) for a thick film (3.2×10^{-5} cm) and intermediate enzyme loading ($[enz] = 5$ mg cm⁻³) no case boundary crossing is seen, the response being linear in a_{∞} over the range 10^{-7} to 10^{-6} mol cm⁻³. This simply indicates that the increase in a_{∞} produced was not sufficient to cause a III/IV boundary crossing. The data presented in figure 5.15 is therefore all in case III. A further increase in a_{∞} is limited experimentally by the solubility of FMA in the buffer solution used. The slope of this plot will give a further estimate of the parameter $K_A \sqrt{D_A k_M \alpha}$.

Figure 5.14 Current response as a function of substrate concentration for a “thick” film situation ($l = 3.2 \times 10^{-5}$ cm).

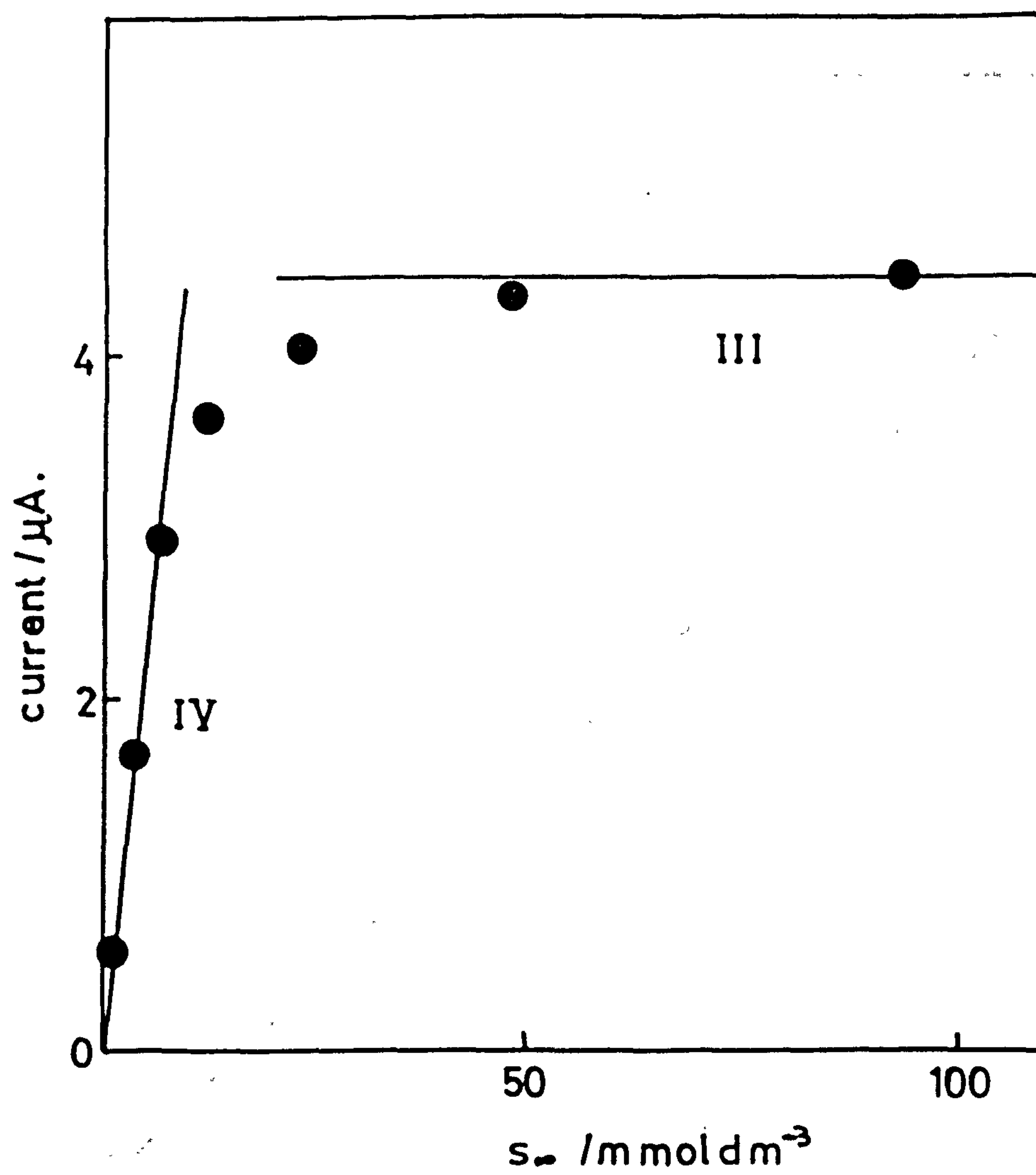
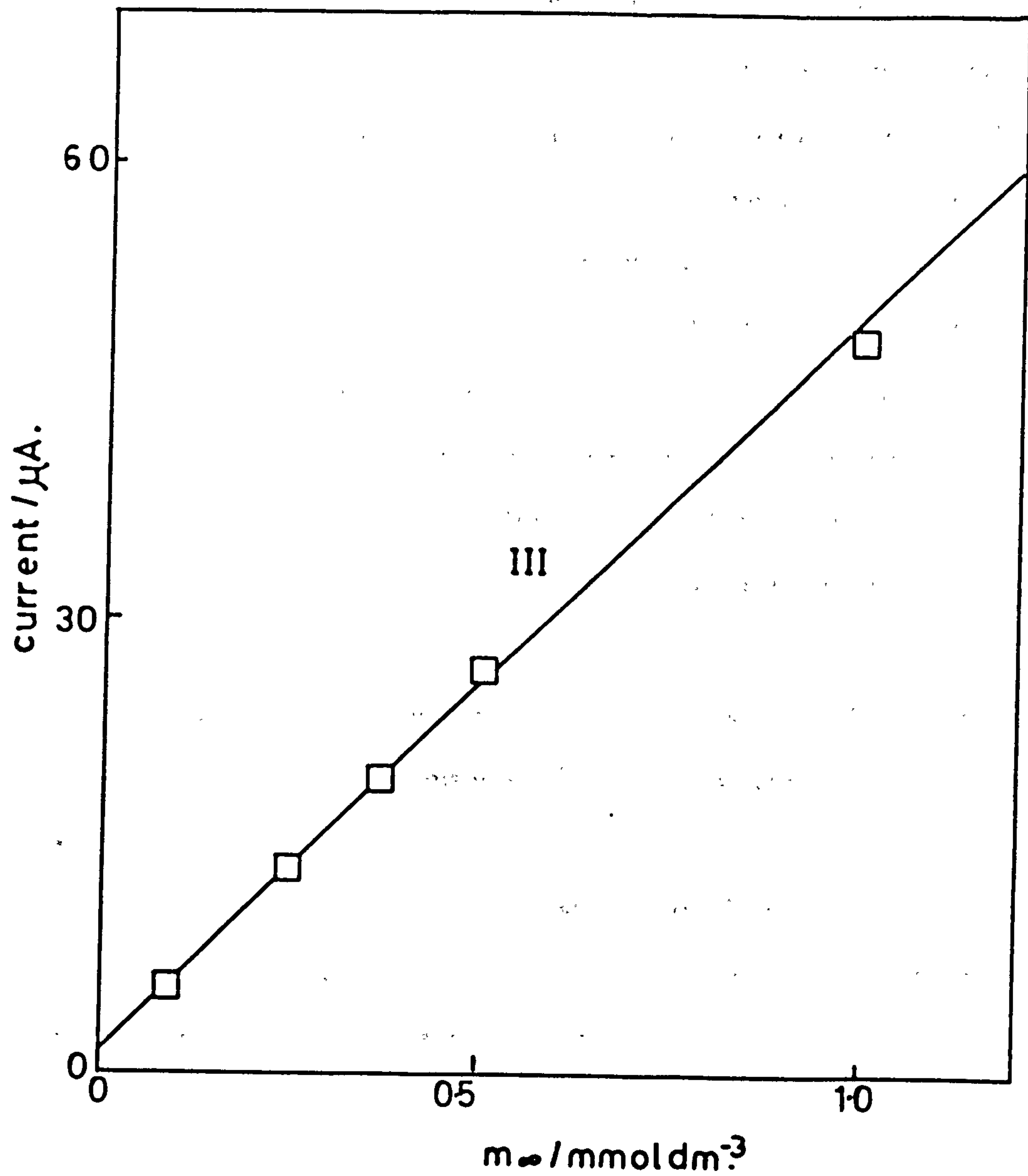


Figure 5.15 Current response as a function of mediator concentration
 ($s_{\infty} = 1 \times 10^{-4} \text{ mol cm}^{-3}$, $l = 3.2 \times 10^{-5} \text{ cm}$, $[\text{enz}] = 5 \text{ mg cm}^{-3}$).



5.4.4 Enzyme loading (e_{Σ})

The effect of altering the amount of enzyme contained within the polymer film was also investigated. This is the last of the experimental variables in the pNMP-GOD system mediated by FMA⁺.

Data was obtained using films of constant l (9.1×10^{-6} cm), a_{∞} (1.035×10^{-7} mol cm⁻³), and s_{∞} (1×10^{-4} mol dm⁻³). In this thick film, high substrate situation the data is clearly positioned in case III on the case diagram. Increasing e_{Σ} (or $\alpha[enz]$) will move us from left to right on the case diagram in figure 3.8. However, starting in case III and increasing the enzyme loading does not produce a crossing of a case boundary so that the current response is linear with $(\alpha[enz])^{1/2}$ as described by the j_s expression for case III. Data at high enzyme loadings (> 10 mg cm⁻³ in the growth solution) are excluded as there appears to be a non-linear relationship between the concentration of enzyme in the growth solution, $[enz]$, and the amount included in the polymer film at a defined film thickness, e_{Σ} or $\alpha[enz]$.

A plot of i vs $[enz]^{1/2}$ is linear, having a slope of 2×10^{-6} A mg^{-1/2} cm^{-5/2} and giving a further estimate of $K_A \sqrt{D_A k_M \alpha}$.

It is interesting that no data has been obtained which is clearly case I. Correspondingly, no direct estimate of k' , the electrochemical rate constant for the reoxidation of FMA, has been obtained.

It is however possible to put an upper limit on the value of $K_A k'$ as we know that the experimental conditions used did not produce any case I type responses. This parameter is discussed later in this chapter.

5.5 COMPARISON AND DISCUSSION OF THE EXPERIMENTALLY DETERMINED PARAMETERS

In the previous sections a number of experiments were described which enabled us to move position from one case to the next around the case diagram. This procedure provides a rigorous method of testing the validity of the model under investigation. In all cases the agreement between experimental data and theory is good, indicating that the theoretical treatment is suitable for this mediated immobilised enzyme system.

However, there are further criteria which must be met for this analysis to be acceptable. Firstly, the values for rate constants, diffusion coefficients and other combinations of parameters which result from the theoretical fit of the experimental data must be consistent from one type of experiment to the next. Also the numerical values must be of the order expected. Secondly, the parameters describing diffusion of s through the film and its reaction with the immobilised GOD must be directly comparable to those obtained when using molecular oxygen as a mediator and using the same polymer/enzyme combination. Obviously other parameters such as K_A and k_M will be different for different types of mediator.

In table 5.3 all derived experimental parameters are presented. The case boundary crossed by the experimental data giving these parameters is shown in each case. Further, the parameter for $k_{cat}K_S \alpha/K_M$ for the GOD/FMA system is compared to that for the GOD/O₂ system.

It is apparent that the parameters from all experimental data are internally consistent. Furthermore, the value for $k_{cat}K_S \alpha/K_M$ for the GOD/FMA compares very favourably to that for the GOD/O₂ system, being 6.6 to $8.5 \times 10^{-2} \text{ cm}^3 \text{ mg}^{-1} \text{ s}^{-1}$ and $2.2 \times 10^{-2} \text{ cm}^3 \text{ mg}^{-1} \text{ s}^{-1}$ respectively. This represents excellent agreement between experimental data for the two different mediators.

Table 5.3
Ferrocene monocarboxylic acid mediation – best fit data

Expt.	$k_{cat}K_S\alpha/K_M$ /cm ³ mg ⁻¹ s ⁻¹	$k_M\alpha K_A$ /cm ³ mg ⁻¹ s ⁻¹	$K_S\sqrt{D_S\alpha k_{cat}/K_M}$ ×10 ⁶ /cm ^{5/2} mg ^{-1/2} s ⁻¹	$K_A\sqrt{D_A k_M\alpha}$ ×10 ⁴ /cm ^{5/2} mg ^{-1/2} s ⁻¹	$k'K_A$ /s ⁻¹
V → II vary <i>S</i>	8.5	5.6	–	–	–
IV → III vary <i>S</i>	–	–	2.9	1.3	–
V → IV vary <i>l</i>	6.6	–	6.5	–	–
II → III vary <i>l</i>	–	4.9	–	1.2	–
III vary <i>A</i>	–	–	–	0.5	–
III vary [<i>enz</i>]	–	–	–	1.3	< 1.5
Expts with O ₂	2.2	–	–	–	–

It is clear that the current responses saturate at high substrate concentrations when using FMA as the mediator. This situation differs from the one in which molecular oxygen is used as the mediator and no saturation of the current response was seen even at glucose concentrations exceeding 0.3 mol dm⁻³.

Both of these systems use an identical polymer/enzyme combination so that we would not expect there to be any change in the substrate/enzyme reaction kinetics (denoted by K_M or k_E) from one system to another.

Analysis of the responses in the FMA mediated system reveals clearly that for both thin and thick films the responses to glucose saturate due to a changeover from the enzyme-substrate reaction (described by $k_{cat}s_\infty$) being rate limiting to the enzyme-mediator reaction (described by $k_M a_\infty$) being rate limiting at high substrate concentrations. Therefore this data is again consistent with that presented for oxygen mediation in the previous chapter of this thesis.

5.6 THE SITE OF FMA OXIDATION

An interesting and subtle difference arises between the oxygen and FMA mediated systems. In chapter 4 it was shown that when oxygen is reduced to hydrogen peroxide within a conducting poly-*N*-methylpyrrole film, or when hydrogen peroxide is added to the bulk solution, this molecule must diffuse to the underlying metal electrode to become oxidised. There is no reaction on the surface or in the bulk of the conducting poly-*N*-methylpyrrole. This behaviour is clearly indicated by Koutecky-Levich analysis.

In the case of FMA mediation the situation appears to be somewhat different. If the conducting poly-*N*-methylpyrrole film is used to oxidise FMA in solution then Levich behaviour results (section 5.2.2). FMA is able to undergo a facile oxidation on the polymer surface, as well as at the underlying platinum electrode surface (section 5.2.1). However, case III of the theoretical analysis describes a situation in which FMA can be oxidised either on the outer edge of the polymer or at the platinum electrode surface (figure 5.12). It has been shown that a large amount of the experimental data presented in this chapter is clearly in case III and as such the site of oxidation of the FMA must be one of the two sites described above. This would suggest that the bulk of the polymer is unable to act as a medium for the facile oxidation of FMA. This is an unusual situation, but one which is sensible since not only will the outer edge of the polymer be structurally different from the bulk of the polymer, but also due to the fact that the polymer is of a lower conductivity than the platinum electrode the working electrode potential, the driving force for this electrochemical reaction, will drop partly at the platinum/polymer junction and partly at the polymer/electrolyte solution interface. These are the proposed sites of FMA oxidation.

Further data would be required to fully quantify this effect. By using different mediators, and altering k_M , a better estimate of k' may be obtained.

5.7 CONCLUSIONS

By the use of two different solution mediators, oxygen and ferrocene monocarboxylic acid, it has been demonstrated that a stable system, involving electrochemically immobilised glucose oxidase, can be developed for glucose detection. More importantly, it has been possible to model the different types of electrode responses and therefore to interpret the experimental data more fully than has been previously attempted. The use of the appropriate theory allows the experimental data to be interpreted in terms of rate constants for the enzyme/substrate and enzyme/mediator reaction. This allows the rate limiting reaction to be identified in each case.

A good understanding of the way in which these systems operate has been gained. Further, it is likely that the theoretical treatments presented will be of use in understanding the way in which other immobilised enzyme systems behave.

CHAPTER SIX

THE COVALENT MODIFICATION OF REDOX ENZYMES

In the previous two chapters the characteristics of a number of mediated immobilised enzyme systems are described. In these systems a low molecular weight mediator is free to shuttle charge between the enzyme's active site and the site of mediator reoxidation.

It has been mentioned previously (chapter 1) that large flavoenzymes, such as glucose oxidase (GOD), cannot undergo direct electron transfer at simple metal electrodes. In this chapter methods for covalently attaching mediator groups to certain sites throughout GOD are described. Following this the characteristics of the resulting modified enzymes are described and interpreted in terms of a simple kinetic model. These enzymes are able to undergo direct electron transfer at simple metallic electrodes in the absence of any soluble mediating species. This represents a significant advance in the area of enzyme electrochemistry.

It was originally intended to electrochemically immobilise the modified GOD. However success in this area has not been achieved at the present time.

6.1 INTRODUCTION

This section will start by describing the effect of distance between donor and acceptor sites on the electron transfer rate in proteins. Following this, the importance of reducing this distance on the production of modified enzymes which are able to undergo fast electron exchange with simple metallic electrodes will be described. Finally the general requirements of electron relays and types of redox enzyme amenable to this type of modification will be outlined.

6.1.1 The Effect of Distance on Electron Transfer Rates

The relationship between the electron transfer rate and the distance over which this electron transfer must occur has been discussed in detail previously (chapter 1). The great significance of this effect upon achieving rapid electron exchange between redox enzymes and simple unmodified metallic electrodes will now be discussed.

It is inadequate to make general comments about the distances involved in electron transfer between redox enzymes and electrodes. For this reason, distance effects in specific examples, glucose and D-amino-acid oxidases, will be discussed.

Glucose oxidase (GOD) and D-amino-acid oxidase (D-AAO) are representative of the type of redox enzyme which have a structure suitable for modification. These proteins contain 2 flavin adenine dinucleotide (FAD) prosthetic groups closely associated, but not covalently bound, to the protein^(121,219). Given that these proteins have molecular diameters in the region of 100 Å^(29,220), it can be seen that the density of electron relaying sites within these proteins is very small. These FAD centres are located at 'active sites' towards the interior of the proteins and are not free to move at any time. This situation is ideal for the natural function of these redox enzymes (chapter 1). In the natural redox cycle the prosthetic groups are reduced by reaction with the substrate. The reduced FAD (FADH₂) centres are then reoxidised when a low molecular weight oxidant (dioxygen in the natural case) diffuses into the protein and undergoes electron, and proton, transfer with the FADH₂ centres. The reduced oxidant then diffuses out of the protein and into the bulk solution. This cycle is shown in schematic form in figure 1.4 and is discussed in detail in chapter 1.

The electron transfer distances involved in these reactions are very small. Indeed the large catalytic effect of this type of enzyme is mainly due to the arrangement at the active site which allows the substrate, prosthetic group and oxidant to come into intimate contact.

It is vital that the redox active prosthetic group is situated away from the exterior of the protein to prevent unwanted electron exchange with other redox proteins and low molecular weight solution species.

This situation may be ideal in natural systems but it represents a major problem in the study of redox enzymes by electrochemical techniques. The redox reactions of the prosthetic group can be studied by the use of low molecular weight electron shuttles to carry electrons between active site and electrode (chapter 1). The study of the direct electron transfer between the prosthetic group and a metallic electrode would, however, involve large electron transfer distances.

It is known that the electron transfer rate decreases exponentially as the distance between acceptor and donor sites increases.

$$k \propto e^{-\alpha d} \quad (6.1)$$

where k is the electron transfer, or electrochemical, rate constant, and d is distance.

This is true of electron transfers between two proteins and between proteins and an electrode (chapter 1). For example, in proteins an increase in the distance between electron donor and acceptor sites from 8 to 17 Å resulted in a decrease in the electron transfer rate constant of 10^{-4} (221).

It is informative to make an estimate of the electron transfer distance involved for direct electron transfer between the FAD centres of GOD or D-AAO and an adjacent metal electrode. Assuming that the prosthetic groups are located at the centre of the protein, there is no evidence for this, the maximum distance will be in the region of 50 Å. Although this is an overestimate of the distance it clearly shows that electron transfer between this type of redox enzyme and an electrode will occur at a very slow rate.

This explains why GOD and D-AAO exhibit no observable electrochemistry at platinum, gold or glassy carbon electrodes. When substrate is added to the enzyme in solution the FAD centres become reduced. These centres cannot however be

reoxidised at a simple electrode so that no substrate dependent current is seen. This is a major problem in the direct electrochemical study of redox enzyme in their native conformation. A new approach is required to overcome this distance effect.

For this reason the idea of modifying the enzyme by binding electron relays throughout the interior of the enzyme was developed^(136,137). In this type of system the electron transfer distances are significantly decreased by providing a series of electron relaying centres as 'stepping stones' for electrons as they are transferred between the FAD centres and the electrode, or vice versa. The significance of this type of modified redox enzyme will now be discussed.

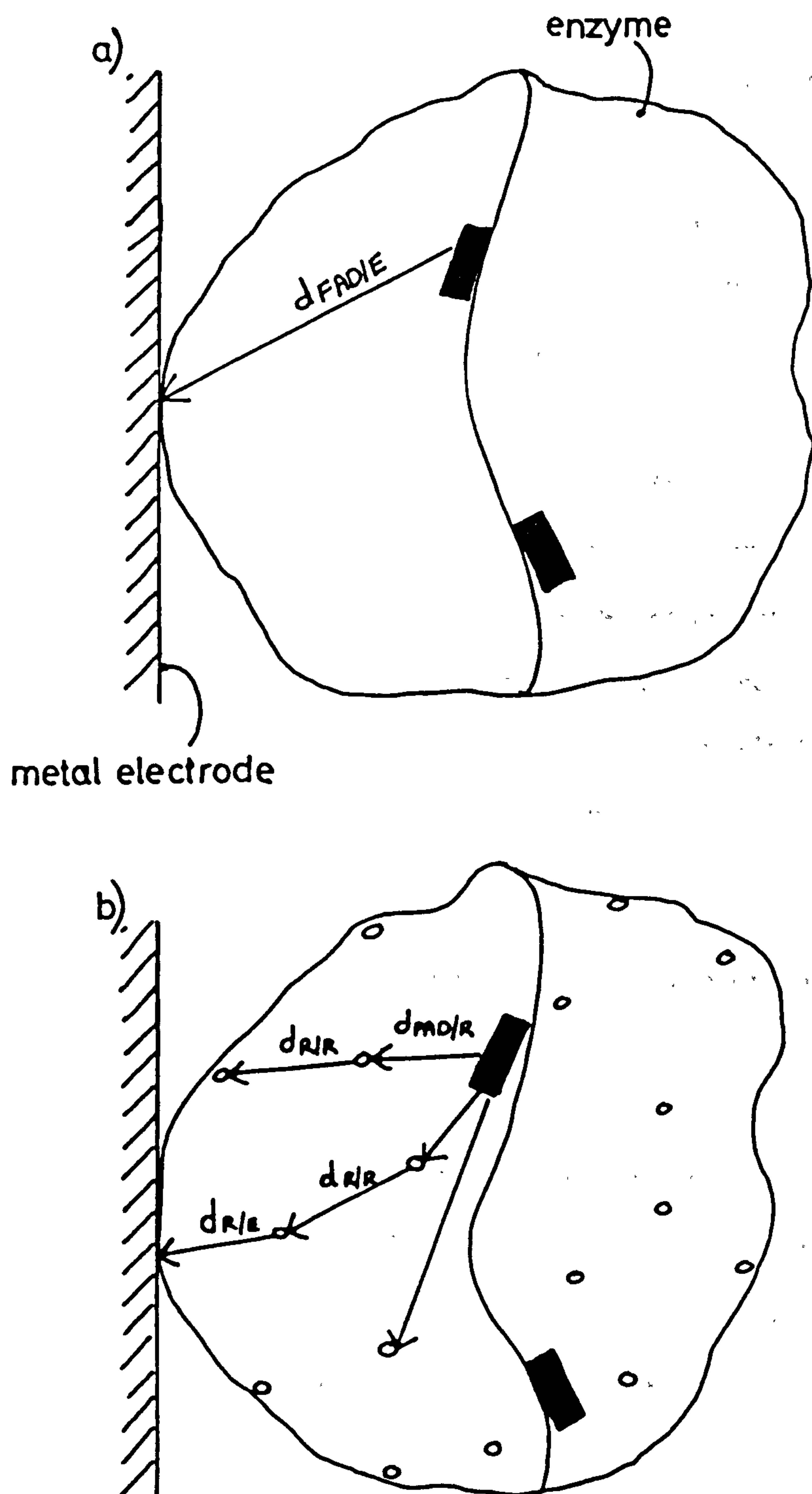
6.1.2 Electron Transfer between Modified Redox Enzymes and Simple Metallic Electrodes

The prohibitive effect of large distances upon fast electron transfer has been discussed. In order to detect a substrate dependent current from a redox enzyme at a metal electrode it is vital that the electron transfer distance is significantly decreased so that the rate of electron transfer is increased to give a measurable current.

The binding of electron relays to certain amino acid residues in the protein backbone of a redox enzyme will reduce electron transfer distances by providing a greatly increased density of electron relays within the interior, and possibly at the surface of the enzyme. If the density of relays is sufficiently high and their three dimensional arrangement is correct then electron transfer distances between the prosthetic group (FAD) and a relay (R), $d_{FAD/R}$, two adjacent relays, $d_{R/R}$, or a relay and the adjacent electrode (E), $d_{R/E}$, will all be less than the distance between the FAD centre and the electrode, $d_{FAD/E}$. These distances are shown schematically in figure 6.1.

In the modified enzyme situation, figure 6.1b, the FAD centre is reduced by substrate, gaining two electrons. These electrons can then be transferred through a series of spatially close redox centres, or possibly one centre alone, to the electrode.

Figure 6.1 Schematic representation of the electron transfer distances involved in
a) the native enzyme, and b) the redox modified enzyme.



■ : FAD
 ○ = electron relay

As the concentration of substrate increases the rate at which FAD is cycled between oxidised and reduced forms is increased and the flux of electrons between the FAD centre and the electrode, via the artificial electron relays, is increased. This means that it should be possible to measure a substrate dependent current in this system.

Previously this has only proven possible by the addition of diffusing redox couples to the enzyme solution (chapter 1), for example dioxygen.

This type of modification procedure appears feasible in theory. In the next section the type of enzymes and electron relays which may be suitable for the production of this type of system will be discussed below.

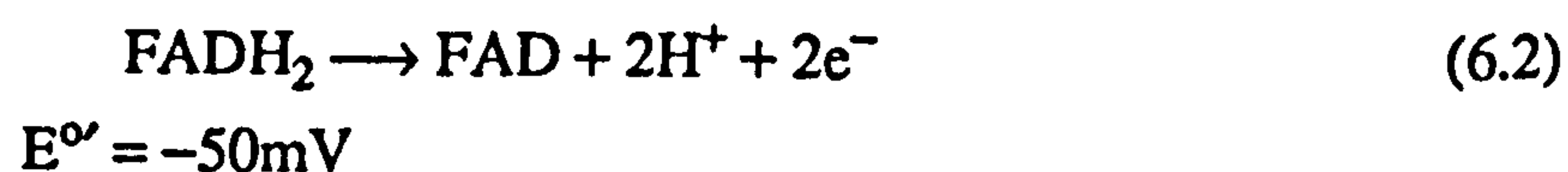
6.1.3 Techniques for the Production of Modified Flavoenzymes

There are a number of specific requirements in the electron transfer properties of relays suitable for this type of work. Also there may be certain structural features in enzymes suited to modification, although this is less clear because the three-dimensional structure of many large redox enzymes, for example GOD, is not known. These important considerations will now be discussed.

6.1.3.1 Electron Relays

In choosing the optimum type of electron relay to attach to a redox enzyme, a number of considerations, both kinetic and thermodynamic, must be taken into account.

A fundamental consideration is that the redox potential ($E^{\circ'}$) of the attached electron relay should be positive for the FAD/FADH₂ couple (equation 6.2). This will mean that the oxidation of FADH₂ by the attached relay will be thermodynamically downhill and thus favourable. This is obviously true of solution mediators as well (chapter 1).



Therefore relays with an $E^{\circ'}$ value of 0 volts or above should be chosen. It should be noted that the $E^{\circ'}$ of the electron relay will be shifted when attached to the enzyme and may also be shifted by the hydrophobic environment in the interior of the enzyme. These effects are not easily predicatable but may be important.

There are two main kinetic effects which may also be important. Firstly the redox couple should be electrochemically reversible, having an electrochemical rate constant of the order of $1 \times 10^{-2} \text{ cm s}^{-1}$ (221). This will maximise the rate of electron transfer at a relay site in the modified enzyme. Secondly it may be preferable to choose an electron relay which exhibits fast enzyme kinetics. This means that in solution the rate of reoxidation of the reduced FADH_2 centres, equation 6.3, is fast, being of the order of $10^5 \text{ dm}^3 \text{ mol}^{-1} \text{ s}^{-1}$ or greater⁽⁵³⁾.



where k_s is the second order rate constant for this reaction ($\text{dm}^3 \text{ mol}^{-1} \text{ s}^{-1}$). This consideration may however, only apply if the first electron transfer from the reduced FADH_2 centre occurs to a relay bound in very close proximity to the FADH_2 . Even if close approach is possible it is likely that the optimum molecular orientation for this electron transfer also the optimum distance will not be permitted. This will have the effect of reducing k_s if indeed the relay and FADH_2 groups are bound sufficiently closely for approach of the two centres to occur at all.

By choosing a relay with both fast electrode and enzyme kinetics it may be possible to optimise the rate of electron flux between FAD centres, electron relays and electrode. This is an area which is not understood and requires further investigation to enable a sensible choice of relays to be made.

Once a suitable relay has been proposed, and a method of binding this to the amino acid backbone of the enzyme protein devised, a choice of protein type and binding sites within the protein must be made.

These considerations will be discussed in the next section. A number of assumptions must be made as in many cases the three dimensional enzyme structure is not known and the positions of the various amino acid residues amenable to relay binding in the enzyme are undetermined.

6.1.3.2 Redox Enzymes

This section will describe the considerations which must be made in the choice of a suitable redox enzyme for protein modification.

Basic considerations to be made include enzyme stability, degree of characterisation, and amino acid composition. In order to illustrate more clearly these criteria the properties of glucose oxidase (GOD) and D-amino-acid oxidase (D-AAO) which make these enzymes good candidates for modification will be described.

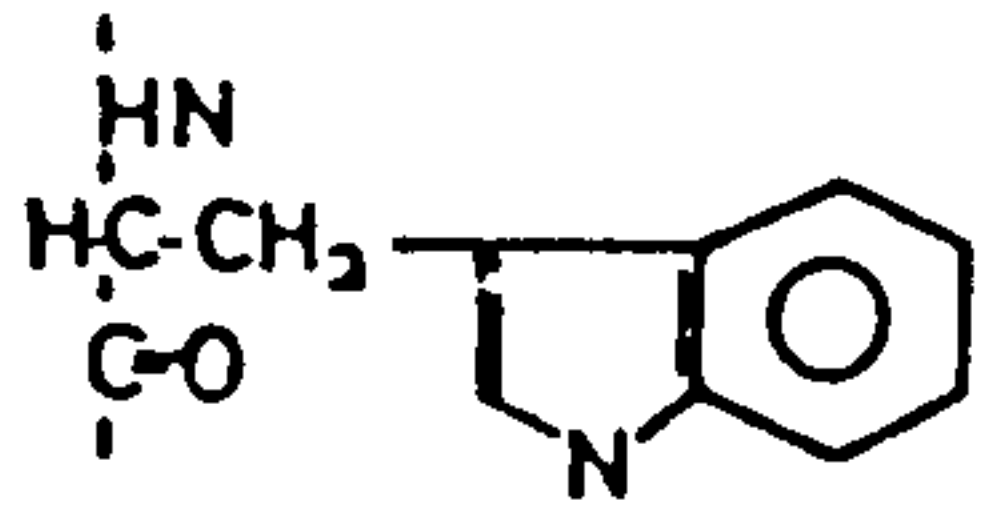
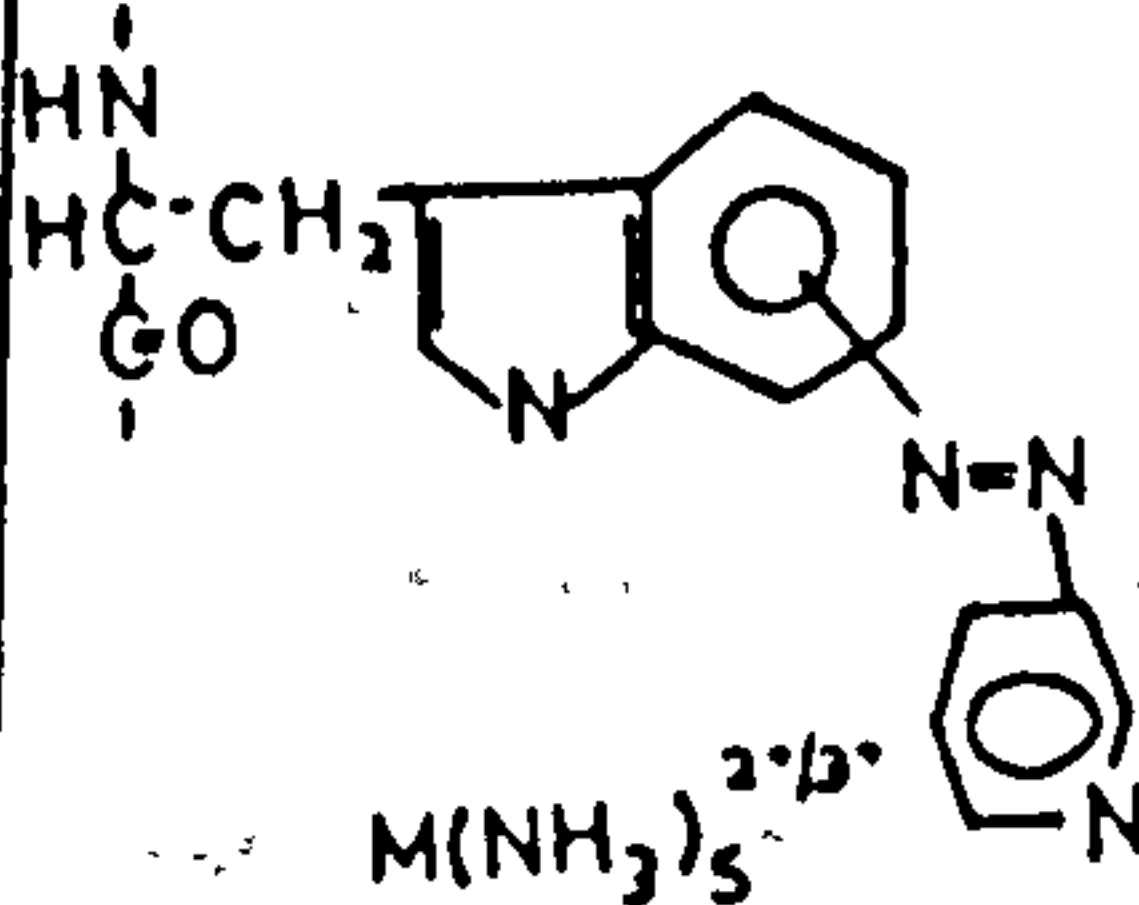
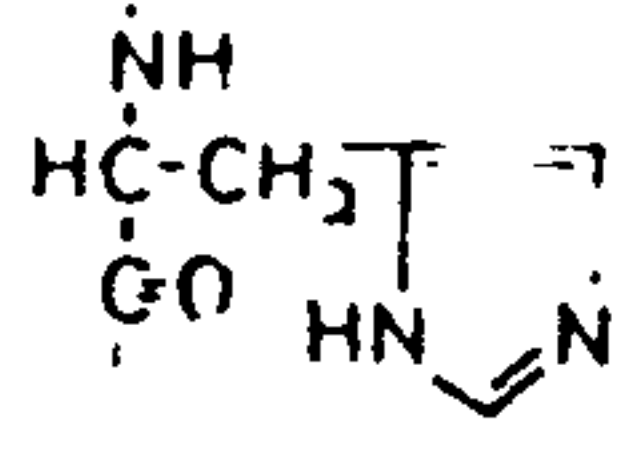
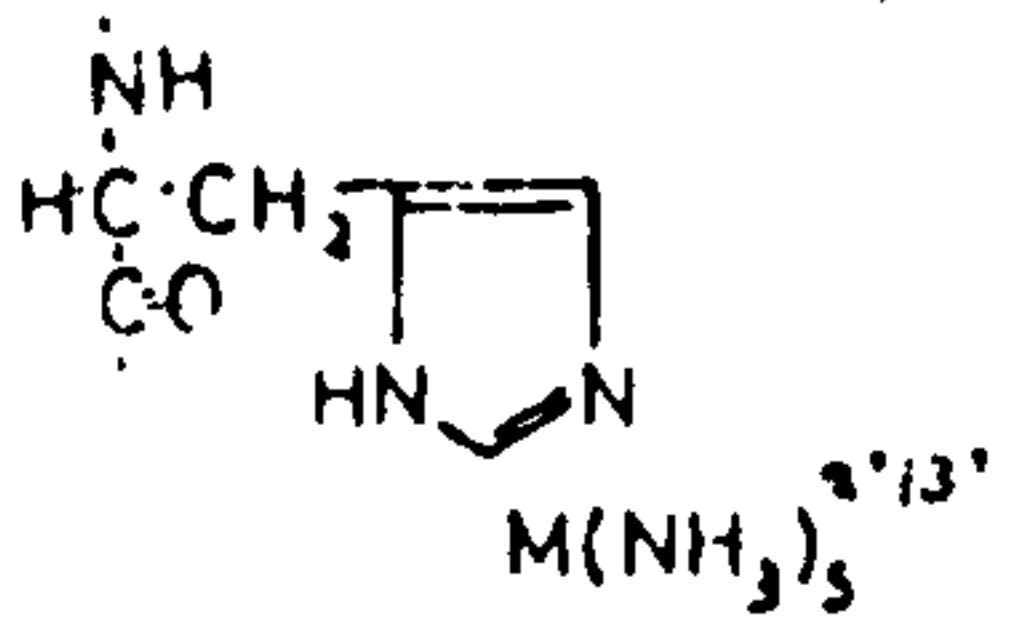
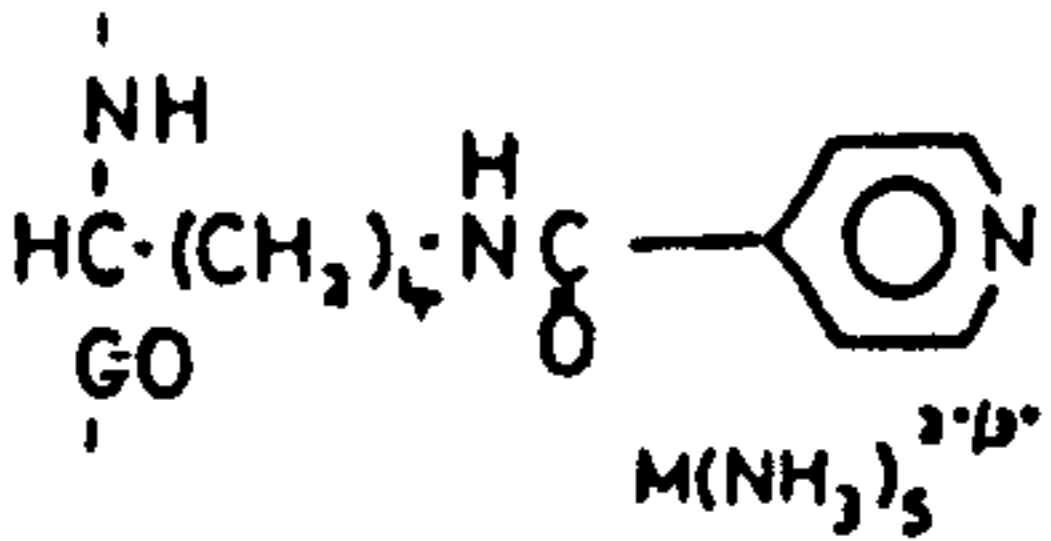
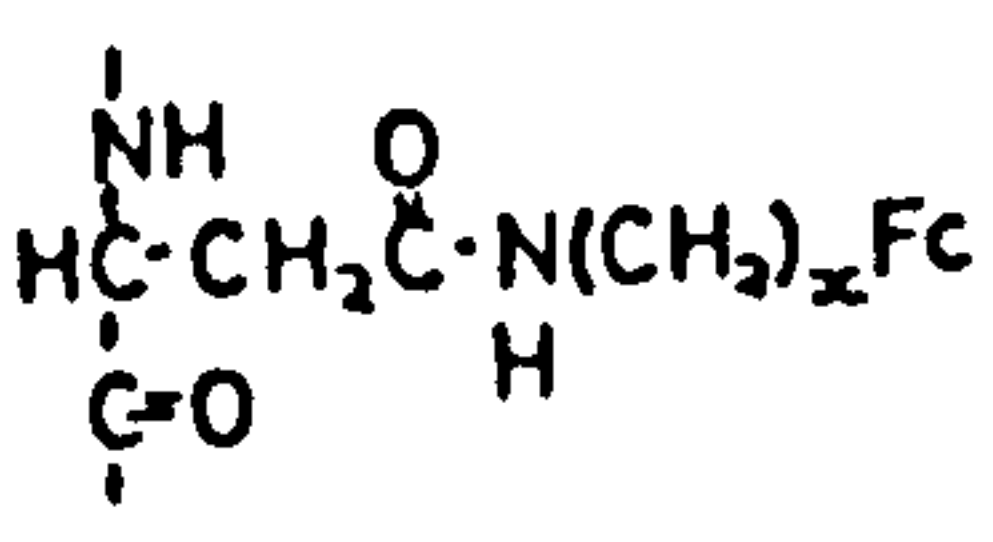
These flavoenzymes have many features in common and represent a large class of flavoprotein oxidases. The molecular weight, size, and amino acid composition of these enzymes is relatively well characterised. It appears that GOD contains two identical monomeric units each of which contains 1 FAD centre⁽²⁵⁾. D-AAO appears to be monomeric and also to contain 2 FAD centres per molecule⁽²¹⁹⁾. In considering possible modification methods, knowledge of the amino acid composition of an enzyme may be useful.

Firstly, however, possible modification sites and methods of attaching relays to these sites will be discussed. Table 6.1 details the types of amino acid residue which may be available for modification in an enzyme together with a possible coupling or coordination method for attaching an electron relay to this residue.

It is likely that if a particular amino acid residue is abundant in a protein then binding of a relay to this type of residue will produce a higher density of relays and possibly a higher rate of electron transfer through these relays. This is obviously advantageous but assumes that the protein can be reversibly unfolded to expose as

$\frac{1}{2}$ $\frac{1}{3}$ $\frac{1}{4}$ $\frac{1}{5}$ $\frac{1}{6}$ $\frac{1}{7}$ $\frac{1}{8}$ $\frac{1}{9}$ $\frac{1}{10}$ $\frac{1}{11}$ $\frac{1}{12}$ $\frac{1}{13}$ $\frac{1}{14}$ $\frac{1}{15}$ $\frac{1}{16}$ $\frac{1}{17}$ $\frac{1}{18}$ $\frac{1}{19}$ $\frac{1}{20}$ $\frac{1}{21}$ $\frac{1}{22}$ $\frac{1}{23}$ $\frac{1}{24}$ $\frac{1}{25}$ $\frac{1}{26}$ $\frac{1}{27}$ $\frac{1}{28}$ $\frac{1}{29}$ $\frac{1}{30}$ $\frac{1}{31}$ $\frac{1}{32}$ $\frac{1}{33}$ $\frac{1}{34}$ $\frac{1}{35}$ $\frac{1}{36}$ $\frac{1}{37}$ $\frac{1}{38}$ $\frac{1}{39}$ $\frac{1}{40}$ $\frac{1}{41}$ $\frac{1}{42}$ $\frac{1}{43}$ $\frac{1}{44}$ $\frac{1}{45}$ $\frac{1}{46}$ $\frac{1}{47}$ $\frac{1}{48}$ $\frac{1}{49}$ $\frac{1}{50}$ $\frac{1}{51}$ $\frac{1}{52}$ $\frac{1}{53}$ $\frac{1}{54}$ $\frac{1}{55}$ $\frac{1}{56}$ $\frac{1}{57}$ $\frac{1}{58}$ $\frac{1}{59}$ $\frac{1}{60}$ $\frac{1}{61}$ $\frac{1}{62}$ $\frac{1}{63}$ $\frac{1}{64}$ $\frac{1}{65}$ $\frac{1}{66}$ $\frac{1}{67}$ $\frac{1}{68}$ $\frac{1}{69}$ $\frac{1}{70}$ $\frac{1}{71}$ $\frac{1}{72}$ $\frac{1}{73}$ $\frac{1}{74}$ $\frac{1}{75}$ $\frac{1}{76}$ $\frac{1}{77}$ $\frac{1}{78}$ $\frac{1}{79}$ $\frac{1}{80}$ $\frac{1}{81}$ $\frac{1}{82}$ $\frac{1}{83}$ $\frac{1}{84}$ $\frac{1}{85}$ $\frac{1}{86}$ $\frac{1}{87}$ $\frac{1}{88}$ $\frac{1}{89}$ $\frac{1}{90}$ $\frac{1}{91}$ $\frac{1}{92}$ $\frac{1}{93}$ $\frac{1}{94}$ $\frac{1}{95}$ $\frac{1}{96}$ $\frac{1}{97}$ $\frac{1}{98}$ $\frac{1}{99}$ $\frac{1}{100}$

[illegible]

Amino acid residue	Electron relay	Coupling method	Structure of bound relay
tryptophan 	$M^{2+/3+}(NH_3)_5$	complexed to azo bonded 4 pyridine function	
histidine 	$M^{2+/3+}(NH_3)_5$	coordination to heterocyclic rings (imidazoles)	
lysine 	$M^{2+/3+}(NH_3)_5$	complex with pyridyl amides of lysine	
aspartic acid 	$Fc (CH_2)_x NH_2$	amide bonding	

many of these potential binding sites as possible. This problem will be discussed later.

Therefore with a knowledge of the amino acid composition of an enzyme a potential binding strategy can be developed. Table 6.2 lists the amounts of the eight possible amino acid residues for modification in the proteins GOD and D-AAO. It can be seen that both of these enzymes are relatively rich in all of these residues, so that a modification procedure based on any one or a number of these residues might prove successful. This may not, however, be true of other enzymes, so it is important that a survey is made.

Table 6.2

The amino acid composition of two flavoenzymes

Residue	Glucose oxidase		D-amino-acid oxidase
	No. of residues per monomer		No. of residues per monomer
	a)	b)	c)
lysine	15	17.4	11.2
glutamic acid / glutamine	48	54.2	40.2
aspartic acid / asparagine	62	79.8	32.3
tyrosine	18	27.6	13.8
tryptophan	11	10.3	9.6
histidine	17	15.4	8.2

Notes

- a) Based on a molecular weight of 80 000 per subunit. Not accounting for carbohydrate content⁽²⁵⁾.
- b) Based on a molecular weight of 67 000 per subunit (due to calculation of carbohydrate content)⁽²⁹⁾.
- c) Based on a molecular weight of 46 000 per monomer⁽²²³⁾.

Another important consideration is the accessibility of the amino acid residues to the coupling reagent during the modification procedure. A method which reversibly opens or unfolds the protein structure must be used to maximise the probability of coupling to the interior of the enzyme and not simply binding relays to its outer surface. A successful strategy must allow binding close to the active site and throughout the interior of the protein as well as possibly requiring relays bound at the periphery. The opening process must be reversible if the modified enzyme is to retain activity and in particular its substrate specificity.

A suitable procedure for achieving this reversible structure unfolding will now be described.

Urea at a concentration of 2 to 3 mol dm⁻³ is known to reversibly open GOD and DAAO^(136,137). A higher concentration of urea (6 mol dm⁻³) is known to irreversibly open enzymes, resulting in damage to their structure⁽²²⁴⁾. Therefore the addition of urea in a suitable concentration to the reaction mixture upon enzyme modification will result in opening of the structure and increase the accessibility of the residues to the coupling or complexing reagents. Removal of the urea will then allow renaturation of the modified enzyme protein.

The modification of a number of amino acid residues appears feasible in this type of enzyme. By assessing the properties of both the electron relay and the enzyme and proposing a possible coupling procedure (which includes urea or a similar 'unfolding agent') it should be possible to produce a range of modified enzymes.

In the next section work involving these modification techniques will be reviewed and the properties of the resulting modified enzymes will be discussed.

6.2 TYPES OF MODIFIED REDOX ENZYME PRODUCED

This section will review the work of Degani and Heller^(136,137) on the modification of glucose oxidase (GOD) and D-amino-acid oxidase (D-AAO) with series of electron relays. The modification procedures will be described together with the electrochemical response of the resulting modified enzymes to their substrate.

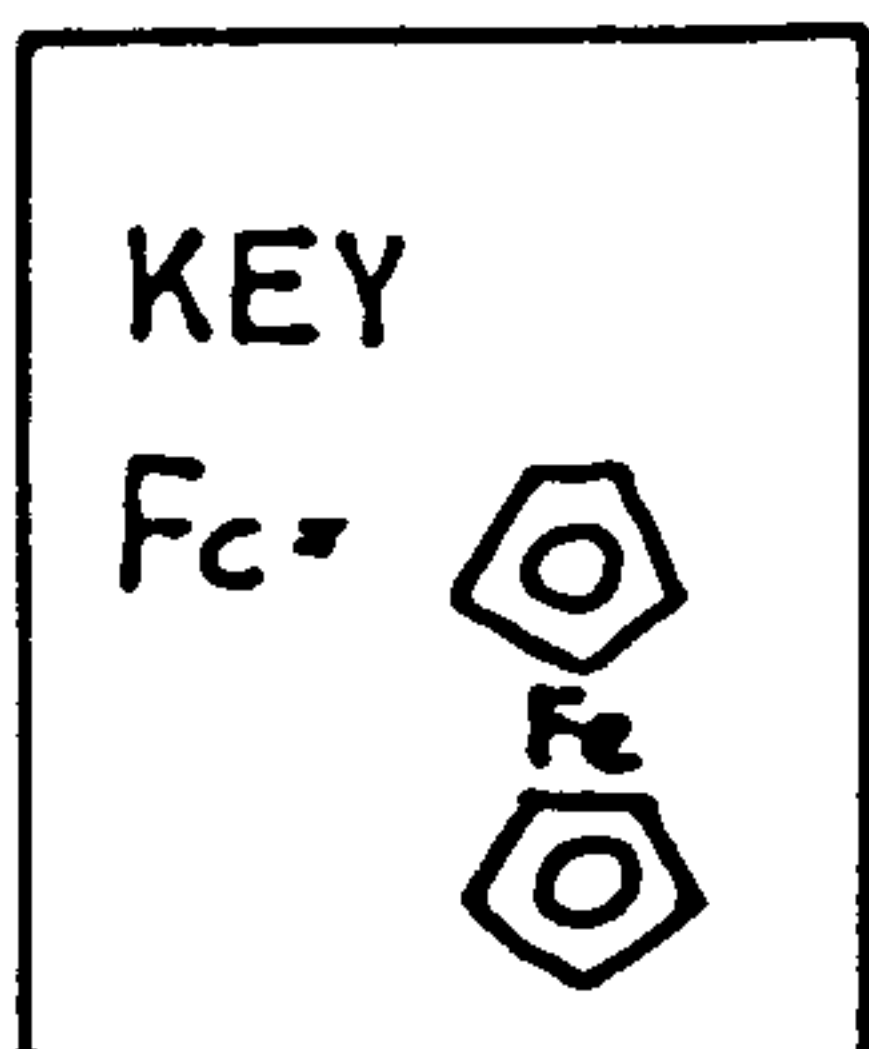
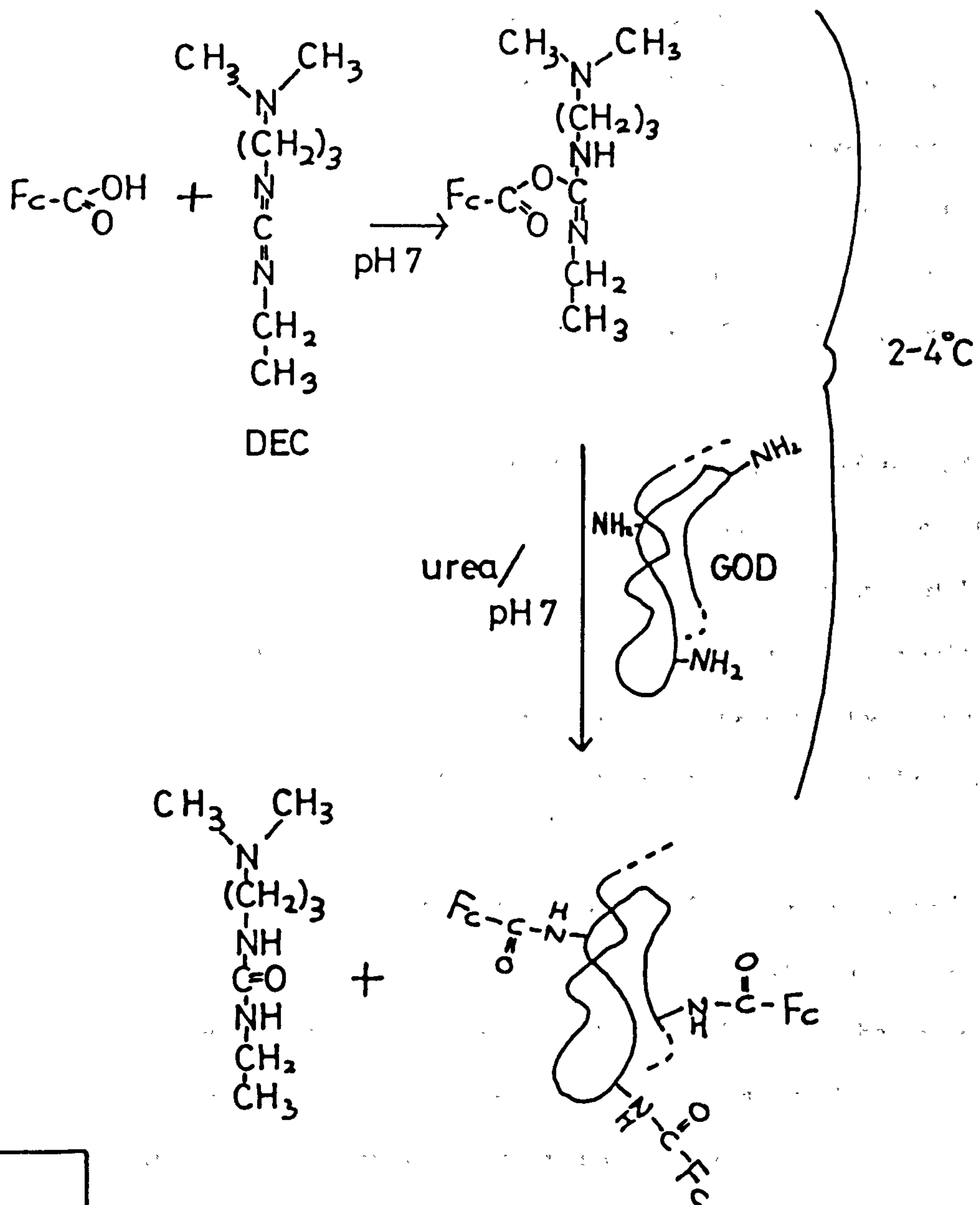
6.2.1 Ferrocene Modified Flavoenzymes

The first report⁽¹³⁶⁾ detailing the production of a modified redox enzyme by simple carbodiimide coupling of ferrocene electron relays to lysine residues of GOD described an enzyme which was able to exchange electrons with a simple carbon or platinum electrode. The authors demonstrated that the modified GOD gave a substrate concentration dependent current indicating that the modification procedure was successful. They also clearly demonstrated that the resulting current was not due to the presence of diffusible electron relays either in the form of low molecular weight ferrocene derivatives or ferrocene modified, but enzymically inactive, GOD. Therefore the current measured on addition of glucose was attributed to the presence of the covalently bound ferrocene electron relay groups.

The electron relay, ferrocene carboxylic acid, was chosen because of its fast electrode and enzyme kinetics⁽⁵³⁾ and because the carboxylic function provided a simple coupling site. The coupling procedure employed a water soluble carbodiimide reagent to produce amide bonds^(225,226) between the amine functions of the lysine residues on GOD and the carboxylate functions of the ferrocene carboxylic acid. The reaction sequence is shown in figure 6.2.

The coupling reaction was carried out at ice temperature. Ferrocene carboxylic acid (80 mg) was added to 4 cm³ of a 0.15 mol dm⁻³ sodium-HEPES (4-(2-hydroxyethyl)-1-piperazine ethane sulphonate) buffer solution to give a turbid

Figure 6.2 Reaction sequence for coupling of electron relays to a redox enzyme via amide bonds.



solution of pH 7.3 ± 0.1 . The pH was adjusted to this value by adding drops of hydrochloric acid solution (0.10 mol dm^{-3}) and stirring, where necessary. DEC (1-(3-dimethyl-aminopropyl)-3ethylcarbodiimide hydrochloride, 100 mg) was added and dissolved. This was followed by addition of 810 mg of urea to give a final concentration of approx. 3 mol dm^{-3} . The pH was adjusted to within the range 7.2 to 7.3 and 60 mg (7080 Units) of GOD was added. The pH was again checked and adjusted to the range 7.2 to 7.3 if necessary. The solution was placed in a sealed glass vial and left in an ice water bath for around 15 hours. The resulting mixture was then centrifuged and the supernatant filtered through a 0.2μ pore filter. The modified enzyme was then separated by gel filtration on a column of Sephadex G-15 in a Na_2HPO_4 ($0.085 \text{ mol dm}^{-3}$, pH 7.0) running buffer. The authors observed that the enzyme was eluted in the first, orange fraction, of 4 cm^3 or less.

The enzymic activity and iron content of the enzyme before and after modification were determined. It was found that the modified enzyme retained between 50 and 60 % of the activity of the native enzyme and contained 14 iron atoms per molecule whereas the native enzyme contained only 2. Therefore the authors demonstrated that 12 ferrocene centres had been attached to the enzyme and that a dramatic loss of enzyme activity during the modification procedure, and in particular the use of urea, had been avoided.

The electrochemical response of the modified GOD in the presence and absence of glucose was studied by d.c. cyclic voltammetry at gold, platinum or carbon electrodes in the absence of oxygen. They found that in the absence of glucose the presence of the ferrocene relays on the GOD was barely visible in the d.c. cyclic voltammogram. However, as the glucose concentration was increased a catalytic current was seen to flow when the potential was greater than 0.4 volts (vs NHE).

This clearly demonstrated that the modified GOD could be reduced by glucose and that the electrons from the reduced FADH_2 centres of the enzyme could be

transferred, via the ferrocene electron relays, to the electrode at a sufficient rate for the current to be measurable.

The authors also prepared a modified but enzymically inactive GOD by removing the FAD centres from the molecule. When this enzyme was mixed with native GOD no electrochemical response to glucose was seen. This demonstrates that the ferrocene relays on the enzymically inactive modified GOD could not act as diffusible electron relays for the unmodified but enzymically active native GOD.

This work clearly demonstrates that modification of GOD with ferrocene electron relays is feasible and further that the spatial distribution of the relays within the modified enzyme has sufficiently reduced the electron transfer distances involved so that a substrate dependent current can be observed in the absence of any diffusible mediating species.

During the course of this work the modification of GOD with ferrocene acetic acid and the modification of D-AAO with ferrocene carboxylic acid was reported⁽¹³⁷⁾. These modified enzymes were produced by the same procedure as that described above⁽¹³⁶⁾. The modification of GOD with ferrocene acetic acid produced an enzyme containing $13(\pm 1)$ ferrocene centres per enzyme molecule and having 60% of the activity of the native enzyme. This is directly comparable to the ferrocene carboxylic acid modified GOD. The potentials at which a catalytic current flows in the presence of glucose are however reduced to positive of 0.25 volts (vs SCE). This is expected since the $E^{\circ'}$ of the acetic acid derivative of ferrocene is 0.165 volts negative of the $E^{\circ'}$ of the carboxylic acid derivative⁽⁴⁷⁾. The ferrocene acetic acid modified GOD does however appear to give a larger current response, at a fixed glucose concentration, than the ferrocene carboxylic acid modified enzyme. This effect will be discussed in detail later.

The modification of D-AAO with ferrocene carboxylic acid does not appear to be as successful as the GOD modifications. The authors only manage to attach $3(\pm 1)$ ferrocene electron relays to this enzyme and the resulting low electron relay density

only produces a small change in the d.c. cyclic voltammogram in the presence of the D-alanine substrate. This effect may be connected to the fact that the D-AAO molecule contains only 11 lysine residues whereas the GOD molecule contains between 30 and 35 lysine residues^(25,29) (table 6.2). Also, it is likely that urea will open the structure of the two enzymes to different degrees making the accessibility of lysine residues to the coupling reagent non-equivalent in the two proteins. It may be surprising that 3 (± 1) electron relays on D-AAO provide a sufficient density of relays for a substrate dependent current to be measured at all.

The authors have determined the stability of these enzymes by measuring the period taken for a 10% loss in current to be observed at a fixed glucose concentration. The three types of ferrocene modified enzyme appeared to be of equal stability 2(± 0.5 h) elapsing before the catalytic current was decreased by 10%. This indicates that the loss of activity is due to a process which is independent of the number of electron relays attached to the protein.

The modifications reviewed so far have successfully utilised ferrocene relays. In the next section work describing the use of ruthenium pentaamine relays to modify GOD and DAAO will be reviewed.

6.2.2 Ruthenium Pentaamine Modified Flavoenzymes

A ruthenium(II) pentaamine pyridyl complex has been shown to act as a soluble mediator of glucose oxidase (GOD). The second order rate constant for the reaction between reduced GOD and the ruthenium(III) form of the complex is comparable to that for the GOD-ferrocene carboxylic acid reaction⁽⁵³⁾. Also, the ruthenium II/III couple exhibits fast electrode kinetics at a glassy carbon electrode with a heterogeneous rate constant (k) of $1 \times 10^{-2} \text{ cm s}^{-1}$ ⁽⁵⁹⁾. Therefore, this electron relay meets with the criteria described previously for choosing a candidate for the modification of GOD.

This section reviews methods which have been used to complex or coordinate this electron relay to GOD. Also, the electrochemical properties of the resulting modified GODs are discussed.

A single report exists of the modification of redox enzymes with ruthenium based relays⁽¹³⁷⁾. Again the authors employ GOD and they present three different strategies for incorporating the $\text{Ru}(\text{NH}_3)_5^{2+/3+}$ relay into the enzyme. In all modification procedures urea (2 mol dm^{-3}) was used as a reversible protein 'opening' reagent. Iron and ruthenium contents of all modified enzymes were determined by atomic absorption spectroscopy.

Amides between the ruthenium pentaamine complex of isonicotinic acid and GOD amines were formed by reacting isonicotinoyl chloride hydrochloride with the available lysine residues of GOD. The isonicotinoyl-modified GOD was then purified by gel filtration chromatography on Sephadex G-15. Ruthenium(II) pentaamine chloride was then added to the enzyme to form the ruthenium modified enzyme (figure 6.3). This modified enzyme was then purified by ion exchange on Sephadex G-25 cation exchange resin.

This modification procedure incorporated $6(\pm 1)$ relays per enzyme molecule and produced an enzyme of good stability ($10 \pm 2 \text{ h}$ to a 10% loss in current).

A second modification procedure employed the pyridyl azo binding of ruthenium pentaamine to GOD. L-aminopyridine was covalently coupled to the activated aromatic rings of available tyrosine or tryptophan residues in GOD via an azo bond (figure 6.4). The enzyme was then purified by gel filtration on Sephadex G-15. The bound pyridine functions were then coordinated to the $\text{Ru}(\text{NH}_3)_5^{2+}$ and the resulting modified enzyme purified by ion exchange on Sephadex G-25 cation exchange resin. The resulting modified enzyme contained only $2(\pm 0.3)$ electron relays per molecule, but again had a stability identical to that of the ruthenium pentaamine isonicotinamide modified GOD.

Figure 6.3 Ruthenium pentaamine isonicotinamide modified glucose oxidase coupling site.

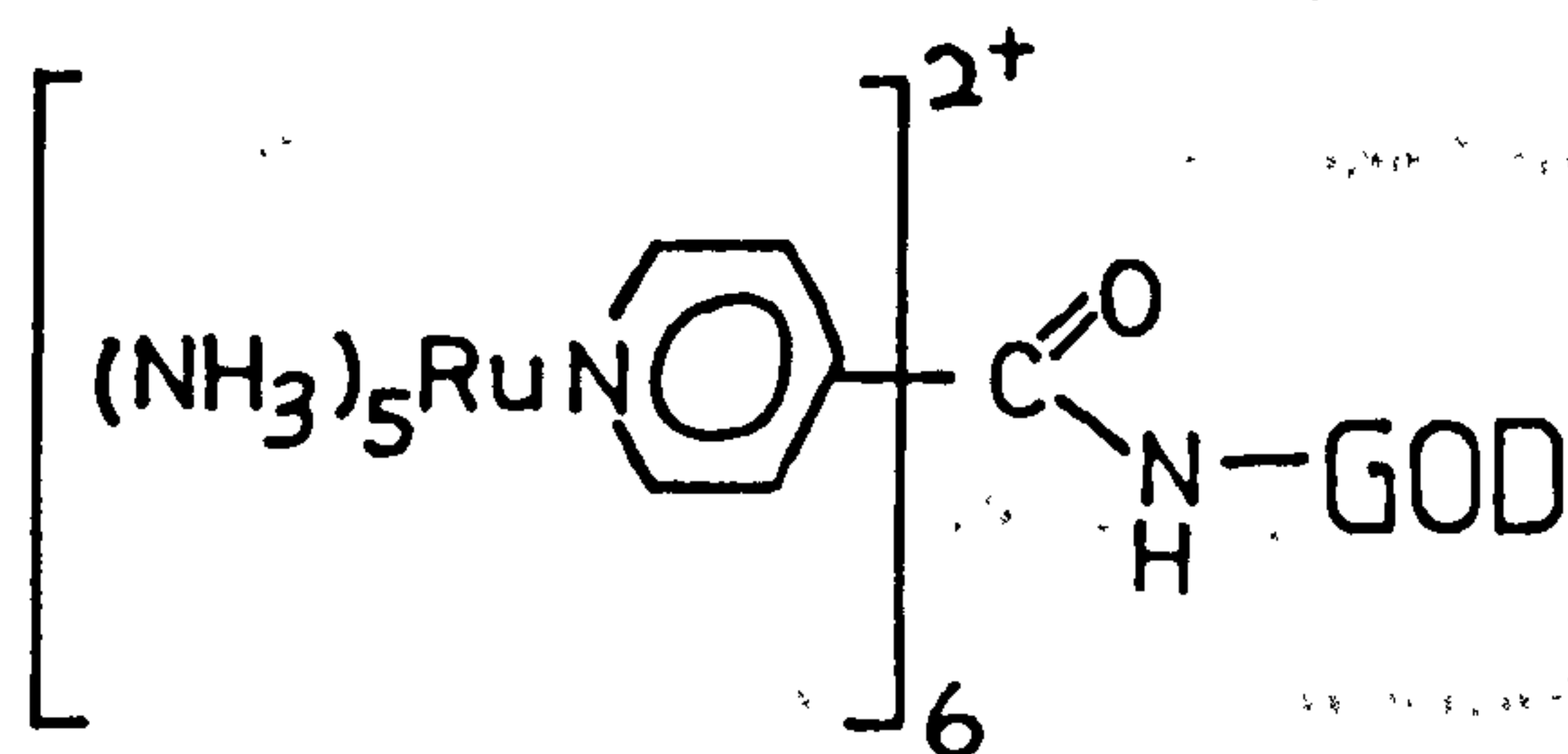
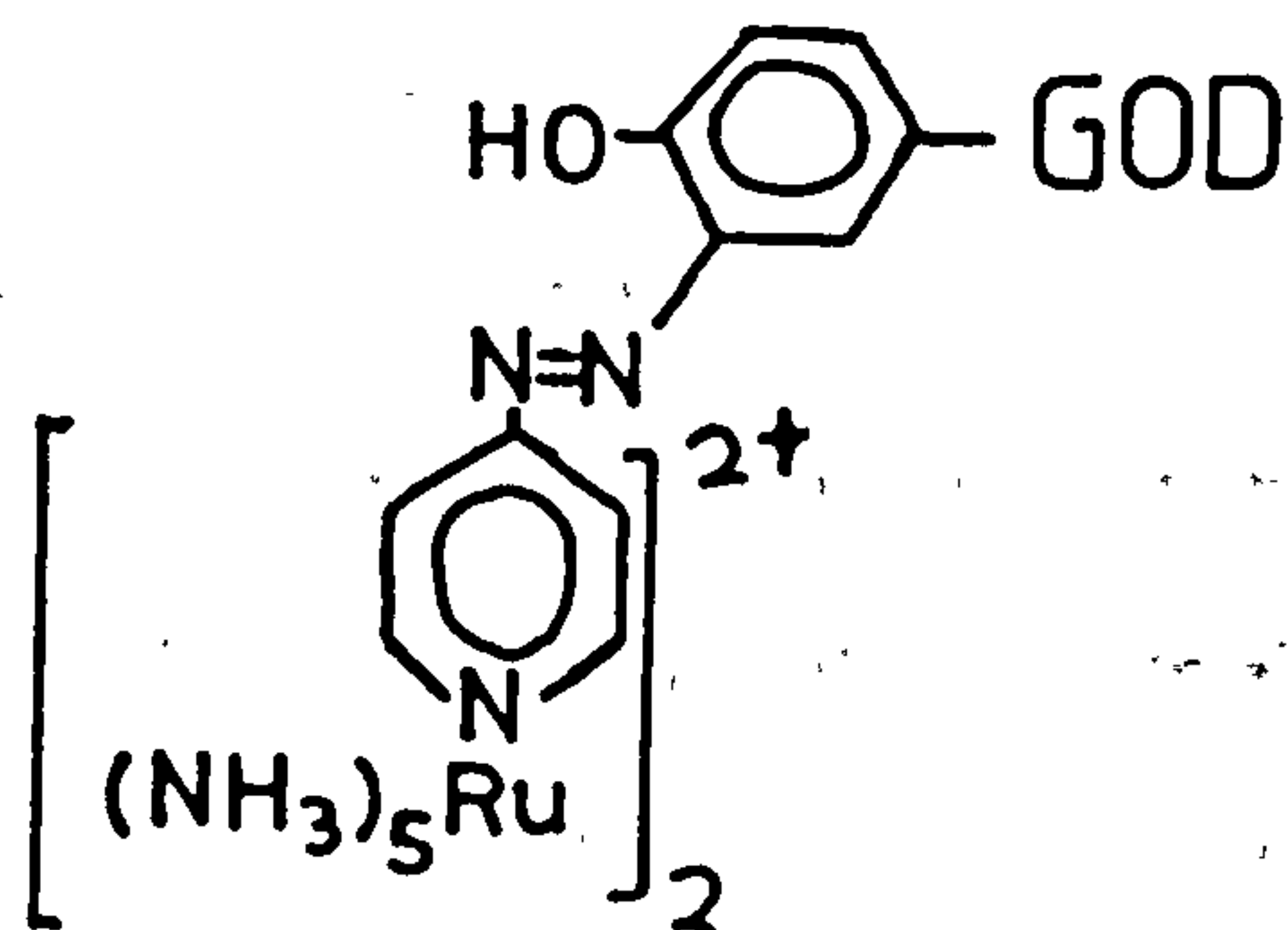


Figure 6.4 Ruthenium pentaamine azo coupling site.



The third and final type of modification involved coordination of the ruthenium pentaamine to the nitrogens of imidazole rings⁽²²⁷⁾ on available histidine residues of GOD (figure 6.5). Following coordination to the ruthenium pentaamine modified enzyme was purified by ion exchange on Sephadex G-25 ion exchange resin. The resulting modified enzyme contained $14(\pm 1)$ electron relays per molecule and had a stability of greater than 7 days (prior to loss of 10% of current) when stored in the ruthenium(III) form. This stability was reduced to less than 5 mins, however, when stored as the ruthenium(II) form.

A number of important conclusions can be drawn from this work. Firstly, it is clear that the enzyme modification of GOD with ruthenium based electron relays is relatively unsuccessful when compared to the production of ferrocene modified GODs. The addition of glucose to any of the three ruthenium modified GODs results in only a small increase in current at potentials positive of the E^o' of the bound relay. Addition of glucose ($0.020 \text{ mol dm}^{-3}$) to the GOD modified with ruthenium pentaamine pyridyl azo functions results in a broad and very small increase in the catalytic current, and no indication of a plateau current is seen. This is probably not surprising since this modified enzyme contains only 2 bound electron relays per molecule. The situation is not however, much improved in the case of the enzyme containing 14 histidine coordinated electron relays.

Secondly, it appears that it is not the number but the type of electron relay attached to the enzyme that determines its stability. Hence all the ferrocene modified enzymes have an identical stability (2 hours to loss of 10% of current) as do the ruthenium modified enzymes (10 hours to loss of 10% of current). This may simply reflect the stability of the electron relays and not the stability of enzymic activity. This will be discussed in detail later in this chapter.

Finally, there appears to be no correlation between the abundance of a particular type of amino acid residue in GOD and the number of relays that can be coupled to this residue (table 6.3).

Figure 6.5 Ruthenium pentaamine relays coordinated to available imidazole rings of glucose oxidase.

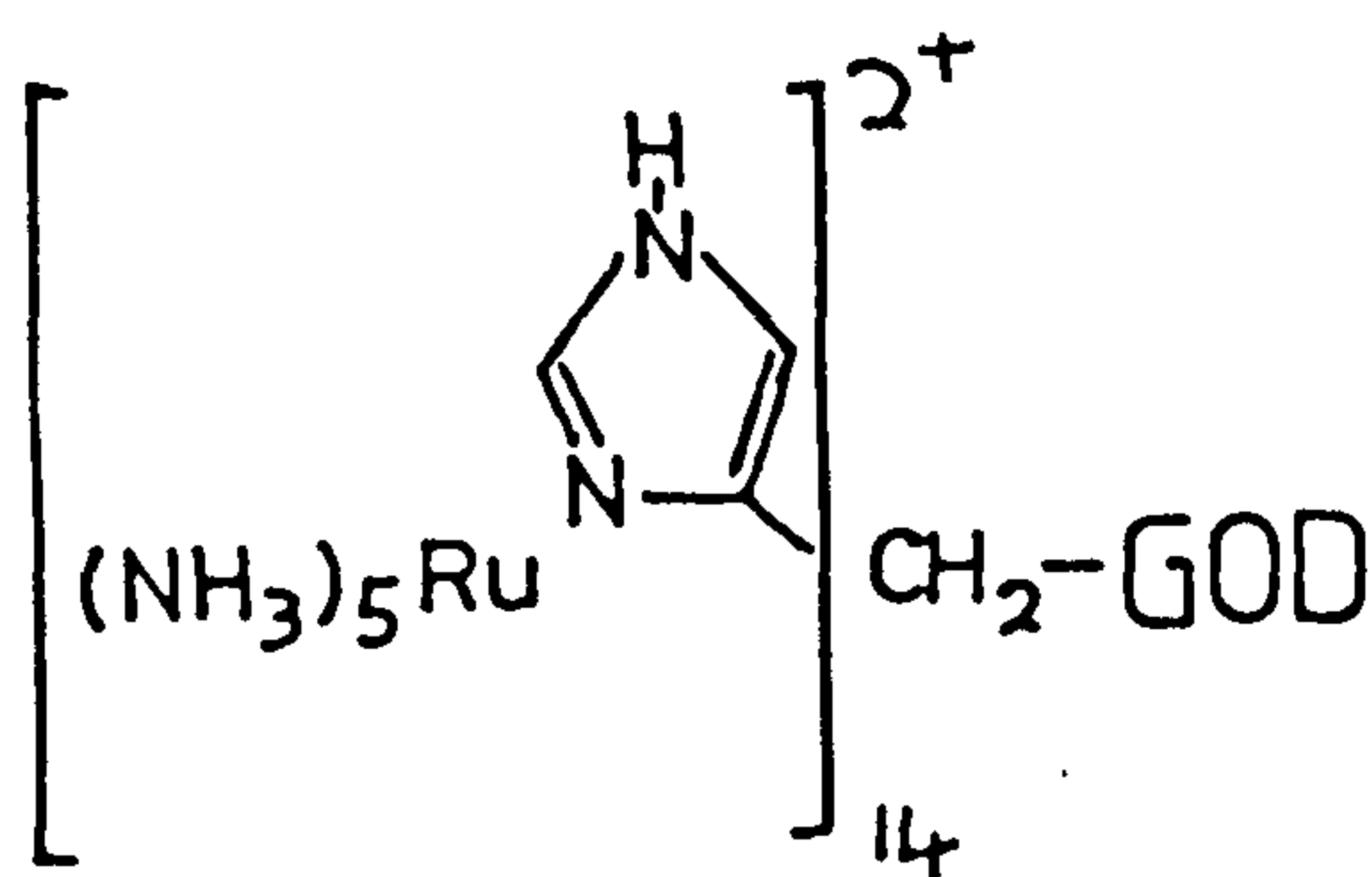


Table 6.3

Comparison of no. of relays incorporated to no. of possible coupling sites in GOD

Residue	No. of residues per enzyme molecule ⁽²⁹⁾	Coupling method	No. of relays per molecule ⁽¹³⁷⁾
lysine	35	Amide bound to $\text{Fc}-(\text{CH}_2)_{\text{ox}}-\text{COOH}$	13 ± 1
		Coordination of $\text{Ru}(\text{NH}_3)_5^{2+/3+}$ to amide lined pyridine	6 ± 1
tyrosine / tryptophan	total of 75	Coordination of $\text{Ru}(\text{NH}_3)_5^{2+/3+}$ to azo bound pyridine	2 ± 0.3
histidine	31	Coordination to imidazole ring	14 ± 1

This may be expected since the abundance of a type of residue is no measure of its accessibility to the coupling reaction employed.

In conclusion, the work of Degani and Heller demonstrates that modification procedures which employ the coupling of ferrocene electron relays to the enzymes GOD and D-AAO are more successful than modifications using ruthenium relays. The electrochemical studies of a range of modified enzymes show that ferrocene modified GOD gives the most pronounced and measurable, if not the most stable, response to glucose, making enzymes containing ferrocene relays most suited to an electrochemical investigation.

In an attempt to study the kinetics of the modified enzymes and to improve their stability a series of ferrocene modified GODs were produced.

In the next section the behaviour of three ferrocene modified GODs in the presence and absence of substrate, will be described and attempts to determine the cause of activity loss after preparation will be discussed.

6.3 A SERIES OF FERROCENE CARBOXYLIC ACID MODIFIED ENZYMES

In this section the electrochemical behaviour of a series of three ferrocene modified glucose oxidase (GOD) molecules is described.

6.3.1 Preparation and Determination of Iron Content

The method of Degani and Heller⁽¹⁰⁾ was used in each case for modified enzyme preparation and purification with some minor modifications (section 2.9). GOD was modified with a series of three ferrocene carboxylic acid derivatives⁽²²⁸⁾.

The degree of modification was estimated by atomic absorption spectroscopy (section 2.9) of the resulting modified enzymes. The iron content of the enzymes is detailed in table 6.4.

Table 6.4

The iron content of the various modified enzymes

Modifying electron relay	Number of iron atoms per enzyme molecule
none	2 ^(a)
$\text{Fc}-\overset{\text{O}}{\underset{\sim}{\text{C}}}$	13 ^(b)
$\text{Fc}-\text{CH}_2-\overset{\text{O}}{\underset{\sim}{\text{C}}}$	22 ^(b)
$\text{Fc}-(\text{CH}_2)_3-\overset{\text{O}}{\underset{\sim}{\text{C}}}$	29

(a) Heller obtained a value of 2 for the native enzyme⁽¹³⁶⁾.

(b) Heller obtained a value of 14⁽¹³⁷⁾.

The iron content was determined for duplicate preparations of each enzyme at two or more concentrations. Buffers used were found to be essentially iron free. As each ferrocene contains one iron centre, this represents a direct determination of the number of covalently linked ferrocenes on each type of modified GOD.

6.3.2 Electrochemistry

Electrochemical measurements were performed in a 2 cm³ volume glass cell (section 2.5) using platinum working electrodes, area 0.127 cm² or 0.393 cm² (table 2.1), Pt wire or gauze counter electrodes and a SCE. All experiments were performed in the buffer used to elute modified enzyme samples from the column (0.085 mol dm⁻³ phosphate, pH 7.0). All solutions were deoxygenated and experiments performed under a positive pressure of oxygen free nitrogen.

The enzyme content and activity of all modified enzyme solutions was determined by the procedures previously described (section 2.8).

In the next section the effect of varying the glucose and enzyme concentrations on the electrochemical response is described for each of the three modified enzymes.

6.4 RESPONSES TO GLUCOSE

In this section the response of the different types of ferrocene modified GOD to glucose are presented. The great majority of the work presented deals with the ferrocene acetic acid modified enzyme as this has a number of desirable characteristics.

6.4.1 Stationary Electrode Studies

In this work a stationary glassy carbon or platinum electrode was used as a working electrode. The glucose concentration of the solution was increased stepwise by injection of aliquots of stock glucose solution (1.00 mol dm^{-3}). A d.c. cyclic voltammogram was recorded at each glucose concentration. Figure 6.6 shows d.c. cyclic voltammograms for each of the modified enzymes at zero glucose concentration. It is apparent that there is a small 'ferrocene' signal in each case. This is, however, broad and indistinct. On addition of glucose a catalytic wave emerges (figure 6.7). The magnitude of the current is seen to be glucose dependent in each case. Figure 6.8 shows a plot of limiting current as a function of glucose concentration for the ferrocene acetic acid modified enzyme.

It is apparent that the ferrocene acetic acid modified enzyme gives far higher catalytic currents (at fixed glucose and enzyme concentration) than the ferrocene monocarboxylic and ferrocene butanoic acid modified enzymes (figure 6.7).

For this reason and because of the improved stability of the ferrocene acetic acid modified enzyme to storage this preparation was the one used in most of this work.

Figure 6.6 D.c. cyclic voltammograms for: a) the unmodified GOD enzyme in buffered electrolyte (0.085mol dm^{-3} phosphate pH 7.0) at zero glucose (platinum or glassy carbon electrode, 5 mV s^{-1}); b) the ferrocene carboxylic acid modified GOD (4.6 mg cm^{-3}); c) the ferrocene acetic acid modified GOD (2.0 mg cm^{-3}); d) the ferrocene butanoic acid modified GOD (0.65 mg cm^{-3}).

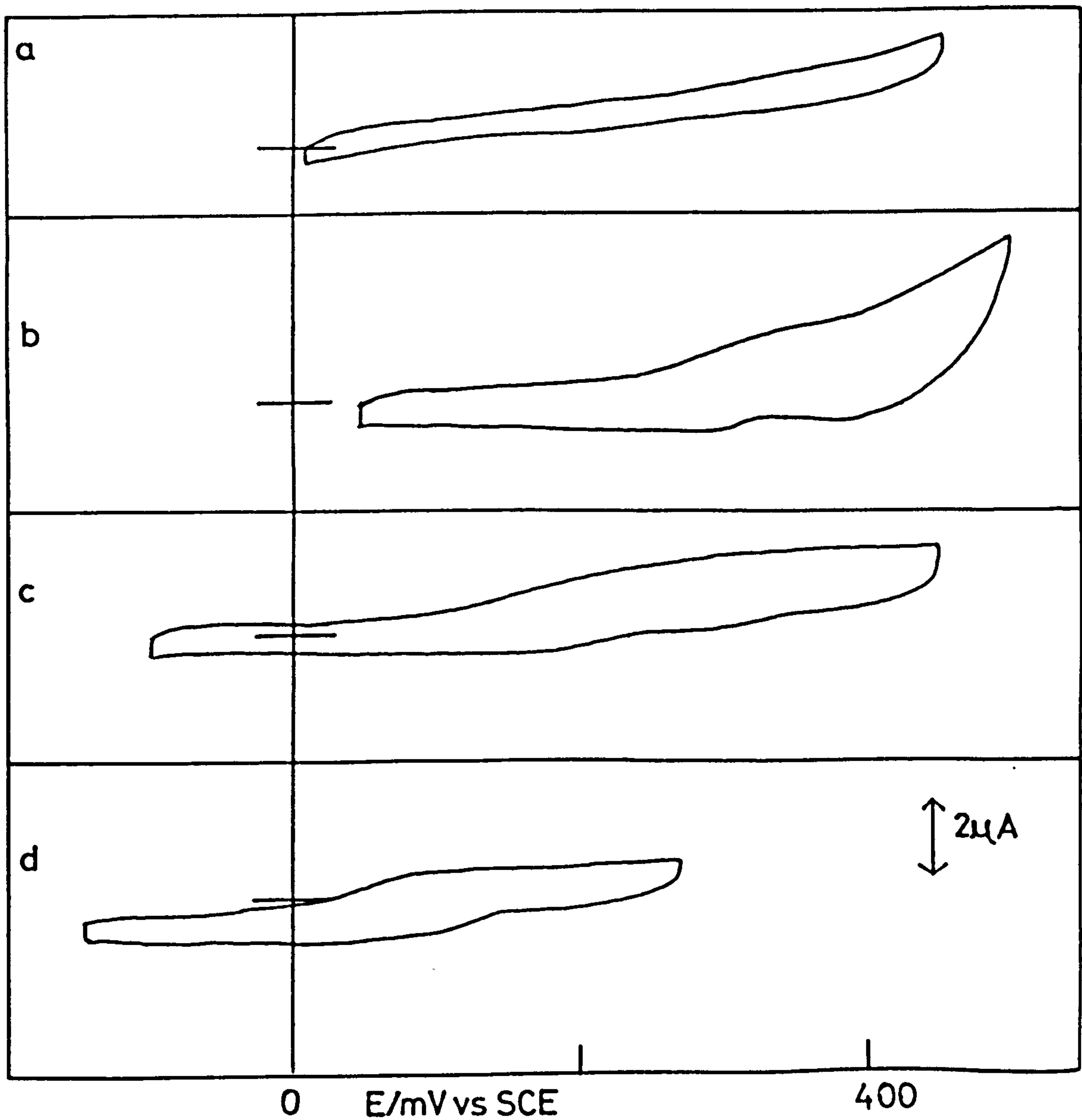


Figure 6.7 D.c. voltammogram for: (a) ferrocene acetic acid, (b) ferrocene butanoic acid, and (c) ferrocene carboxylic acid modified glucose oxidase at a glassy carbon electrode (3mm diameter), sweep rate 5 mV s^{-1} . In all cases the glucose concentration is 100 mmol dm^{-3} and the enzyme concentration is 1 mg cm^{-3} . All at pH 7.0, 25°C .

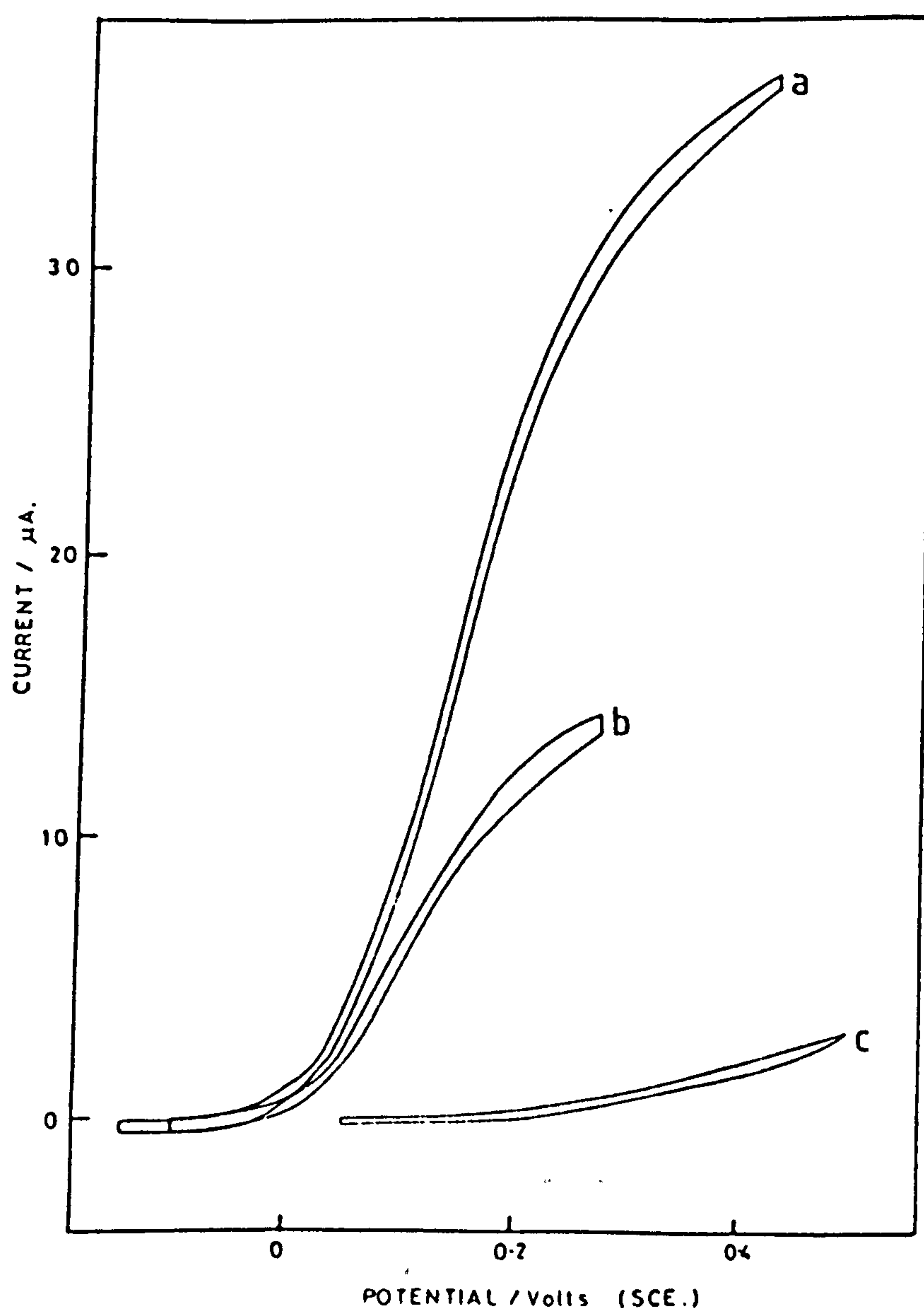
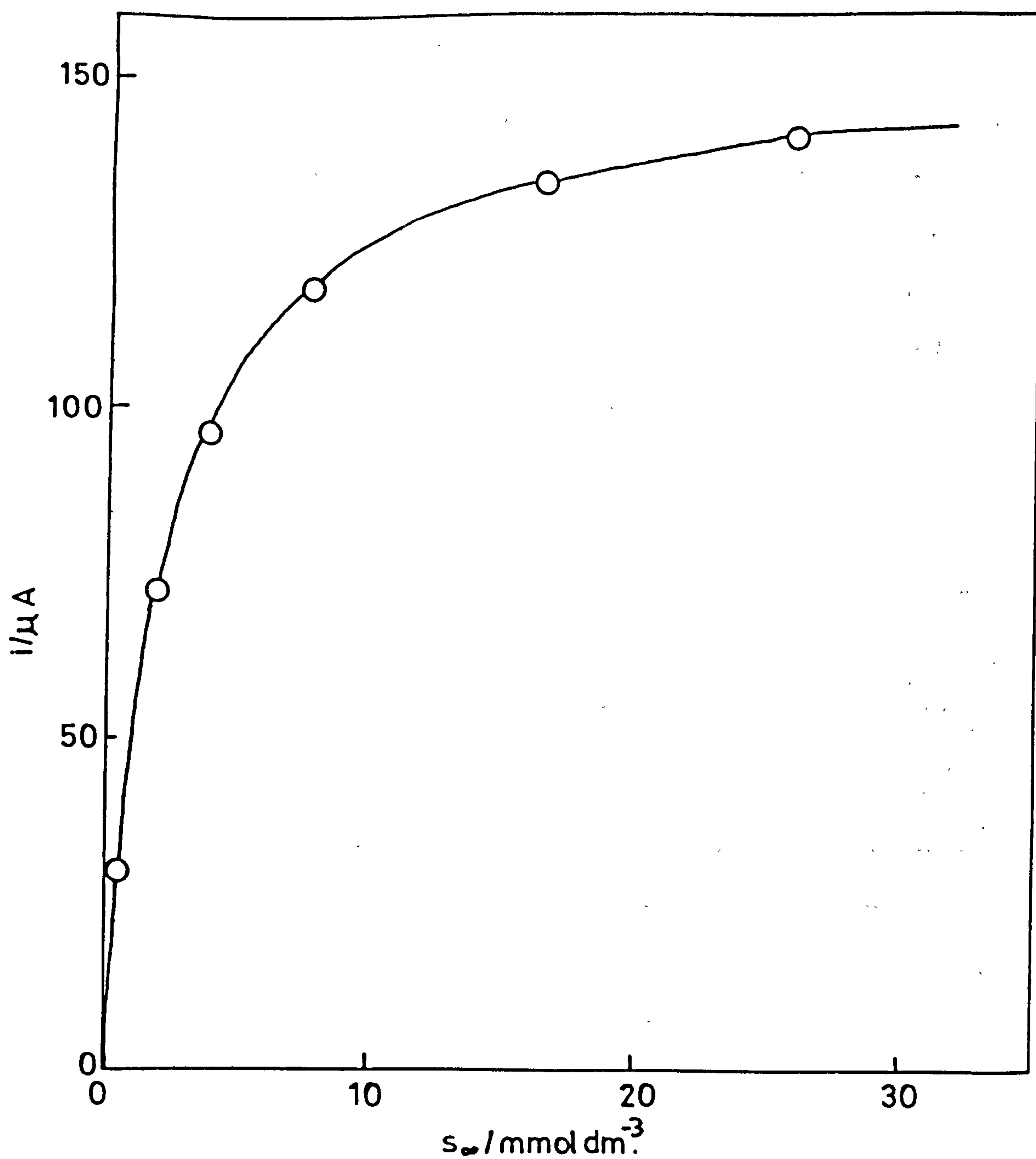


Figure 6.8 Glucose response curve for the ferrocene acetic acid modified GOD (4.5 mg cm⁻³) at a glassy carbon electrode (3mm diameter) at pH 7.0, 25°C in the absence of atmospheric oxygen.



6.4.2 Analyses of the Glucose Responses

If we assume Michaelis-Menten kinetics for the reaction between the modified enzyme with its substrate glucose we can derive the following expression (see chapter 3)

$$\frac{i_L}{nFA} = [\text{enzyme}] \left[\frac{D_E k_{cat} s_{\infty}}{K_M + s_{\infty}} \right]^{1/2} \quad (6.4)$$

The terms in this equation are defined fully in the theoretical section of this thesis. It is apparent that plots of $([\text{enzyme}]/i_L)^2$ vs $(s_{\infty})^{-1}$ should be linear. Figure 6.9 shows an example of such a plot. From the slopes and intercepts of this type of plot it is possible to obtain estimates of K_M and k_{cat} , if we know the value of the electrode area and D_E , the diffusion coefficient of the enzyme. The values for k_{cat} and K_M determined in this way are presented in table 6.5.

Table 6.5

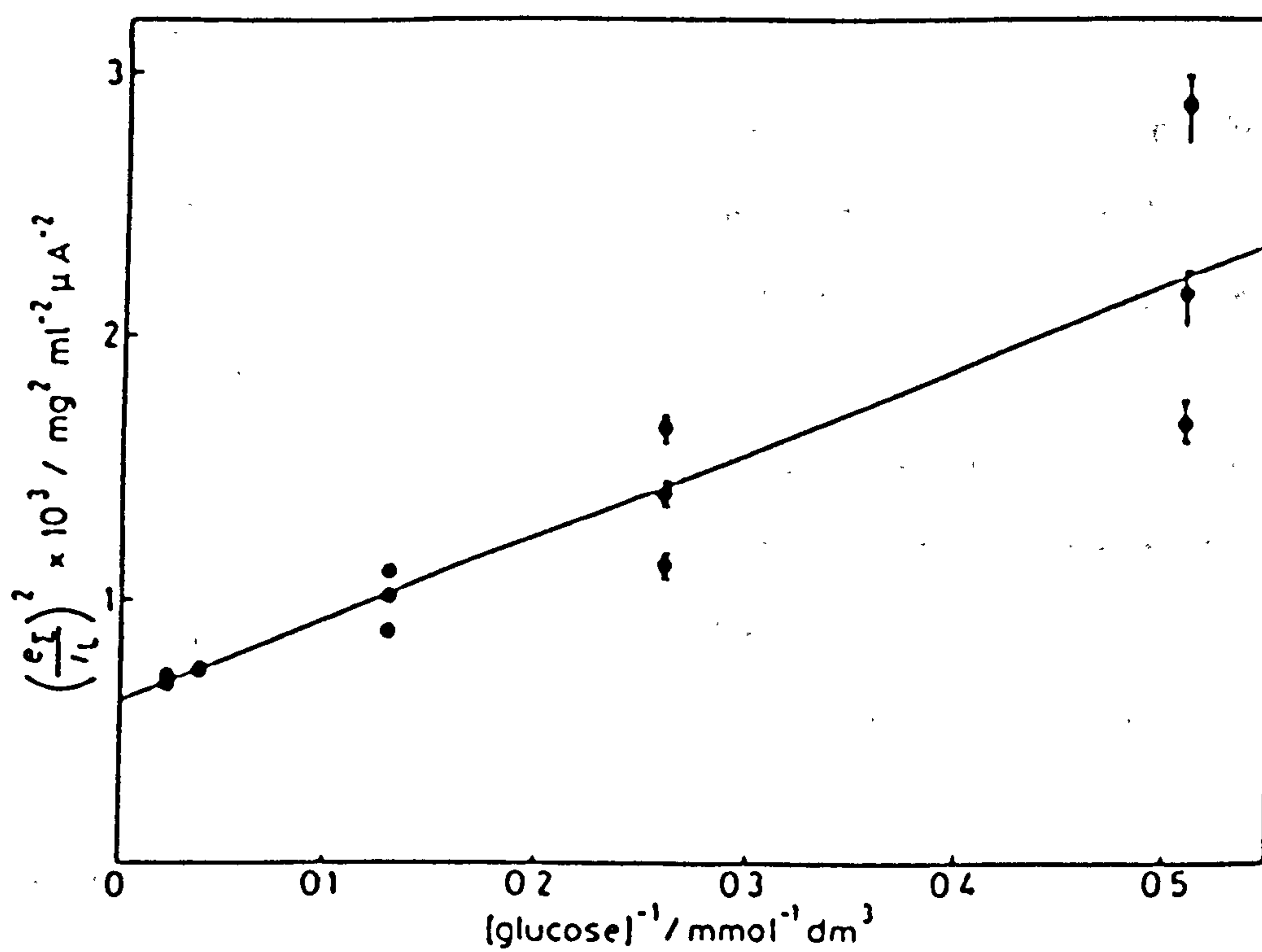
Kinetic constants determined for the modified GOD-glucose reactions

	Glucose oxidase	Enzyme modifier		
		Ferrocene carboxylic acid	Ferrocene acetic acid	Ferrocene butanoic acid
k_{cat}/s^{-1}	800 ⁽¹²³⁾	5 ^{a)}	1100	50
$K_M/\text{mol dm}^{-3}$	0.020 ⁽⁷⁰⁾	0.001	0.005	0.002

- a) Kinetic constants were calculated using a value for D_E , the diffusion coefficient of the enzyme, of $5 \times 10^{-7} \text{cm}^2 \text{s}^{-1}$, and an n value of 2 electrons per substrate molecule.

It is apparent that the value of k_{cat} for the ferrocene acetic acid modified GOD is comparable to that of native GOD and is far in excess of that for the other two enzymes. This is clearly the cause of the large catalytic currents seen for the

Figure 6.9 Plot of equation 6.4 for ferrocene acetic acid modified GOD using data for three different enzyme concentrations (0.45, 1.13 and 4.5 mg cm⁻³).



reaction of this enzyme with glucose.

The precise reason for this large catalytic effect is unknown at the present time. A number of possible explanations will now be presented. The rate constant k_{cat} describes the rate of reaction between glucose and the electron accepting FAD centres at the enzyme's active site when saturating glucose is present. At this glucose concentration ($> 0.080 \text{ mol dm}^{-3}$) the enzyme kinetics become independent of glucose concentration and k_{cat} is reached.

It is possible that the widely different values of k_{cat} obtained for the different types of modified enzyme are due mainly to changes in structure at or close to the active FAD containing centres. A disruption of the optimal steric arrangement, as found in the native enzyme, could easily explain why the k_{cat} values for the ferrocene carboxylic and butanoic acid modified enzymes are so low. However, this type of structural effect could not explain the increase in k_{cat} obtained for the ferrocene carboxylic acid modified enzyme. Furthermore, there is no apparent correlation between the number of ferrocene centres per enzyme molecule (table 6.4) and k_{cat} .

The modified enzymes have similar values of K_M for glucose, 1 to 5 mmol dm^{-3} . These values are all much lower than that for the native enzyme⁽⁷⁰⁾. This simply reflects the fact that the response becomes saturated more quickly for the modified enzymes. Again it is not possible to explain the reduction in K_M which occurs on modification on the basis of the data currently available.

The value of K_M is a measure of the point at which the response turns over from being 1st order in glucose at very low concentrations, to zero order in glucose, at high concentrations. It is apparent that all three modified enzymes are more sensitive to glucose than the native enzyme. This may again reflect subtle changes at the active centres of the enzyme. The extent of any structural changes incurred on modification cannot be assessed until the three dimensional structure of the enzyme

is known.

It is clear however that the ferrocene carboxylic acid modified GOD produces by far and away the largest catalytic currents in the presence of glucose. This effect is due to the large k_{cat} value associated with this enzyme.

In the following section the redox potentials of the modified enzymes are estimated, and the effect of varying the redox potential on the characteristics of the resulting enzyme discussed.

6.4.3 Estimation of the Redox Potentials of the Modified Enzymes

The redox potentials of each modified enzyme species was determined by analysis of the waveshape in the presence of glucose. The waveshapes, at sufficiently high glucose concentration to saturate the enzyme kinetics, have been shown previously in figure 6.7.

Analysis of these waves using a corrected Tafel plot (section 5.2.1) gives an estimate of the thermodynamic E° of the modified enzymes. Tafel plots for each of the three types of enzyme are shown in figure 6.10. It is clear that as the E° value of the free ferrocene derivatives used for modification decreases, so the E° value of the resulting enzyme decreases (table 6.6)

Figure 6.10 Corrected Tafel plots for the modified enzymes: A) ferrocene butanoic acid modified, B) ferrocene acetic acid modified, and C) ferrocene carboxylic acid modified. All for saturating glucose concentration (0.1 mol dm^{-3} , pH 7.0).

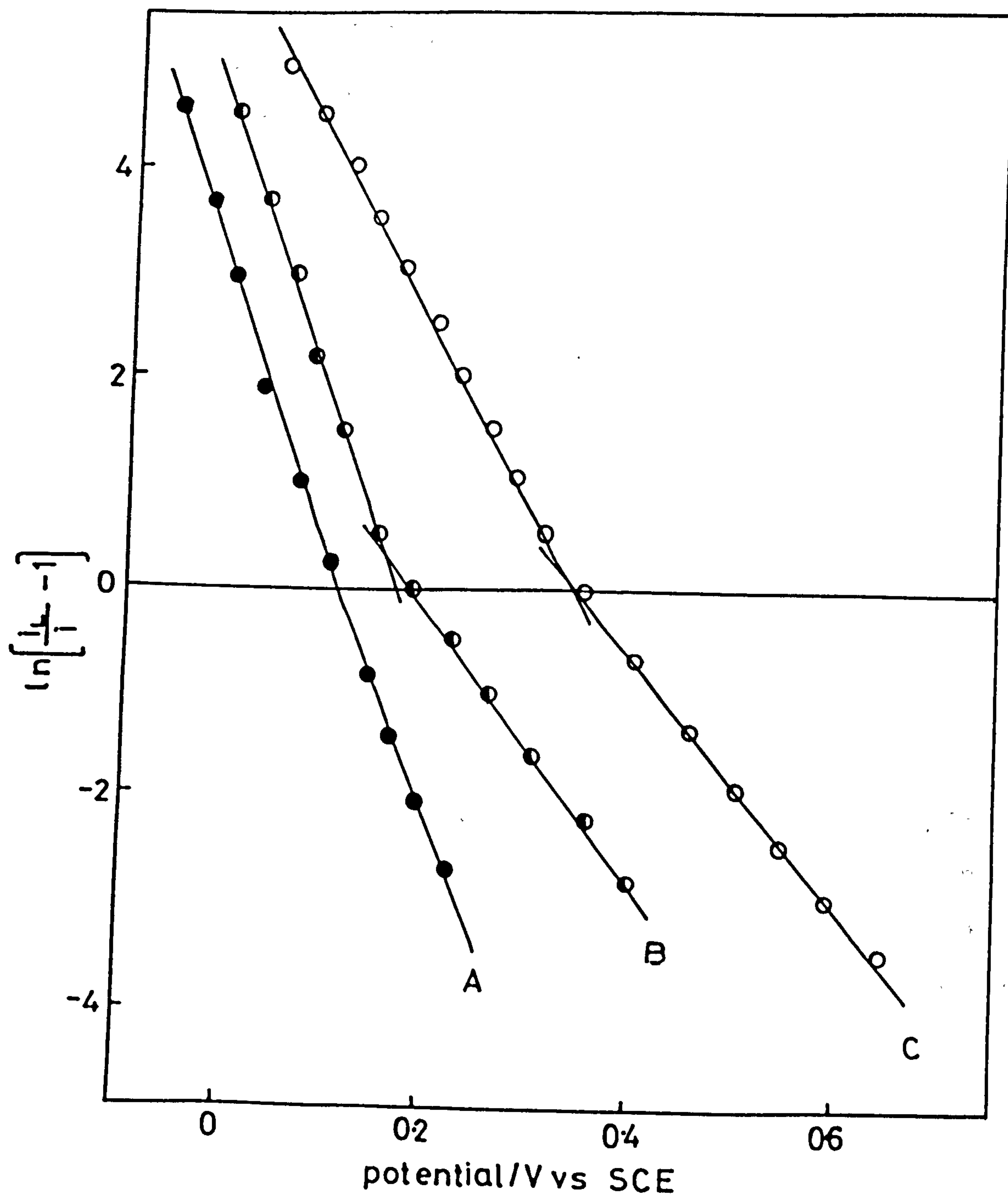


Table 6.6

Redox potentials for the modified enzymes

Enzyme modifier	E° (mV vs SCE)	Enzyme E° ^{a)} (mV vs SCE) pH 7.0, 25°C
Ferrocene carboxylic acid	290	300 to 330
Ferrocene acetic acid	113	130 to 180
Ferrocene butanoic acid	95	90 to 110

- a) A range of E° values are given in each case to demonstrate that there is some dependence on the glucose concentration.

The dependence of the E° value on the concentration of glucose may imply a more complex situation than that described previously (section 6.4.2). The corrected Tafel plots presented in figure 6.10 are composed of two linear portions. This is due to the fact that it is difficult to make a realistic estimate of i_L for such systems as the current retains a weak potential dependence on the portion of the current voltage curve approximating to a limiting current. Further work is required to study the waveshape and potential dependence of the current as a function of glucose concentration.

It is clear that the E° of the modified enzymes reflects the E° of the ferrocene modifier employed. While it was thought preferable to make an attempt to decrease the E° of the modified enzyme, by use of different modifying mediating groups, it was found that if the E° of the resulting enzyme was too low then this was oxidised in the air. Therefore it was found that in contact with atmospheric oxygen the ferrocene butanoic acid modified GOD became a brilliant green colour, indicating its oxidation to the ferricinium ion form. This oxidised form is unstable and quickly decomposes. It is likely that the ferricinium ion form disproportionates to give ferric hydroxide. Due to loss of the ferrocene functions this enzyme quickly loses any

electrochemical activity and hence is of little practical use.

The ferrocene carboxylic acid and acetic acid modified enzymes are far more air stable, having significantly higher E^0 values, and retain their activity for prolonged periods.

In the next section the stability of the different enzyme species is discussed. Little attention is given to the ferrocene butanoic acid derivative due to its acute air sensitivity.

6.5 STABILITY STUDIES

In this section the stability of the modified enzymes will be described in terms of loss of activity, with time, under a variety of operation and storage conditions. The 'operational' stability describes the stability of the enzymes to continuous potential cycling in the presence of glucose. This section will also discuss the reasons for this loss of activity with time. A number of factors can contribute to this effect.

6.5.1 Stability on Storage

It is obviously advantageous to use a modification procedure which results in a product that is stable to simple cold storage (2 to 4 °C) in solution. In order to assess the storage stability properties of the modified enzymes, cold stored samples were assayed for remaining enzymic activity over a six day period. Activity was assayed using the dye linked (4-aminoantipyrene) spectrophotometric assay described in detail in section 2.8. The assay determines the activity of the enzymes only and does not give any indication of their electrochemical response to glucose. Attempts to determine whether loss of ferrocene occurs as a function of time are described in the next section.

Initially the stability of ferrocene carboxylic acid modified GOD to storage was studied under three different storage conditions. Storage of enzyme samples, in buffer solution ($0.085 \text{ mol dm}^{-3}$ phosphate, pH 7.0) contained in sealed polythene vials was either at 4°C with the presence or absence of catalase (approximately $2000 \text{ Units cm}^{-3}$), to decompose any hydrogen peroxide formed in the presence of traces of oxygen and glucose, or at room temperature (not thermostated) to provide an indication of 'bench-top' stability. Figure 6.11 shows how the activity of an enzyme sample was affected by the different storage methods. It could be seen that there was an initial loss of activity of 30 to 40% over the first two hours. After this time it was apparent that simple cold storage (4°C), in the absence of catalase, represented the most effective storage method. The loss of activity over a six day period was linear with time and constituted a loss of 3% per day. Storage at 4°C in the presence of catalase or at room temperature resulted in a larger activity loss over a six day period.

The storage stability (4°C) of the ferrocene acetic acid modified GOD was also assessed. This enzyme was found to be significantly more stable than the original modification (figure 6.12), retaining 88% of its original activity after a six day period, as opposed to a 50% retention for the original, ferrocene carboxylic acid modification.

Modification of GOD with ferrocene butanoic acid produces an enzyme which is very unstable to storage. Samples become an intense green colour within 2 hours of column purification. This is indicative of the ferricinium form of the electron relay which is far less stable than the reduced Fe(II) form. This effect is discussed in detail in the following section. This enzyme retained less than 10% of its activity after a six day cold storage period (4°C) and was therefore of little use in any investigation of the kinetics of ferrocene modified glucose oxidase systems. The stability data is summarised in table 6.7.

Figure 6.11 The effect of different storage conditions on the activity of the ferrocene carboxylic acid modified GOD to glucose.

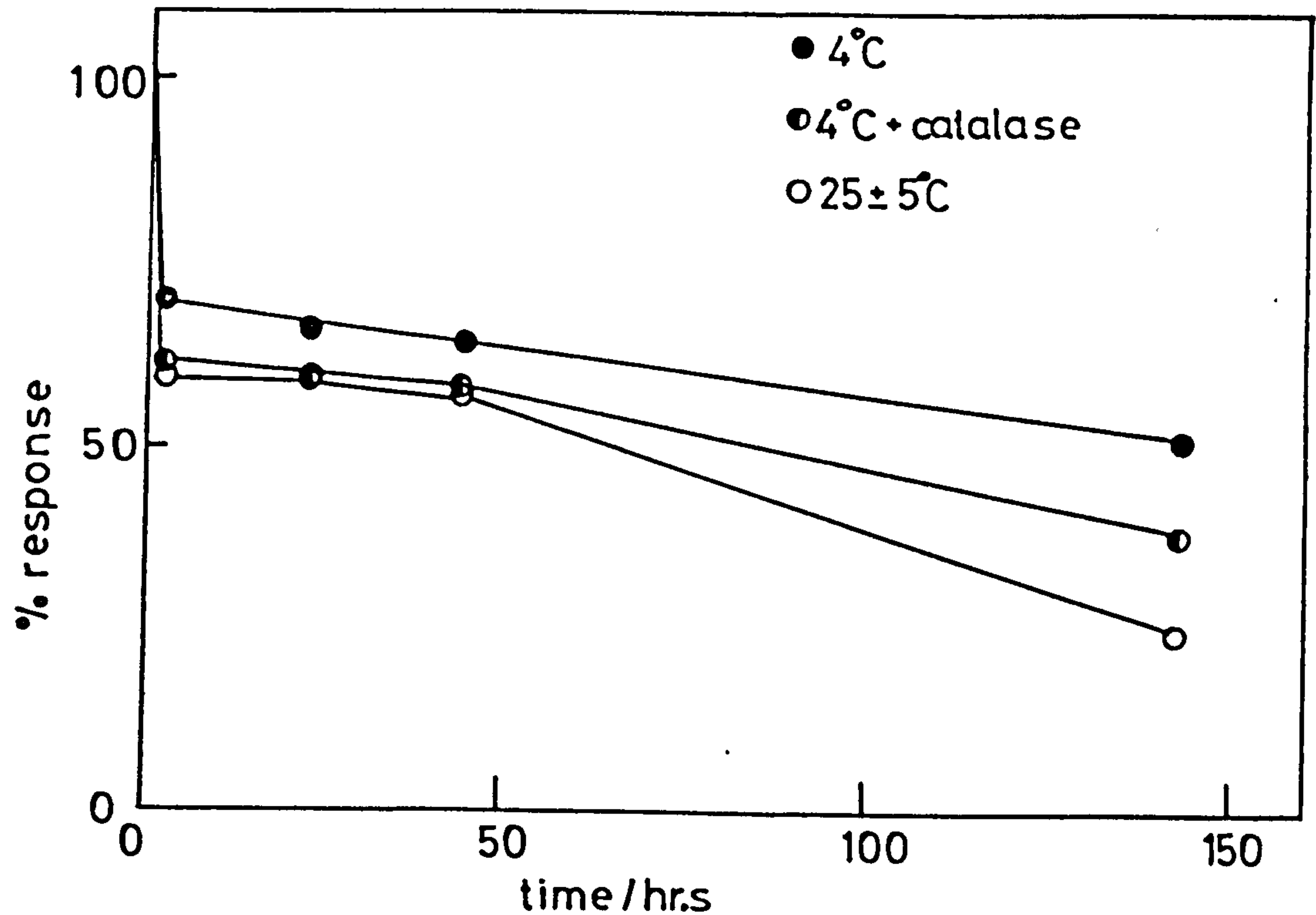


Figure 6.12 Comparison of the storage stability of: a) ferrocene acetic acid modified GOD to b) ferrocene carboxylic acid modified GOD, at 4°C, pH 7.0, in the absence of atmospheric oxygen.

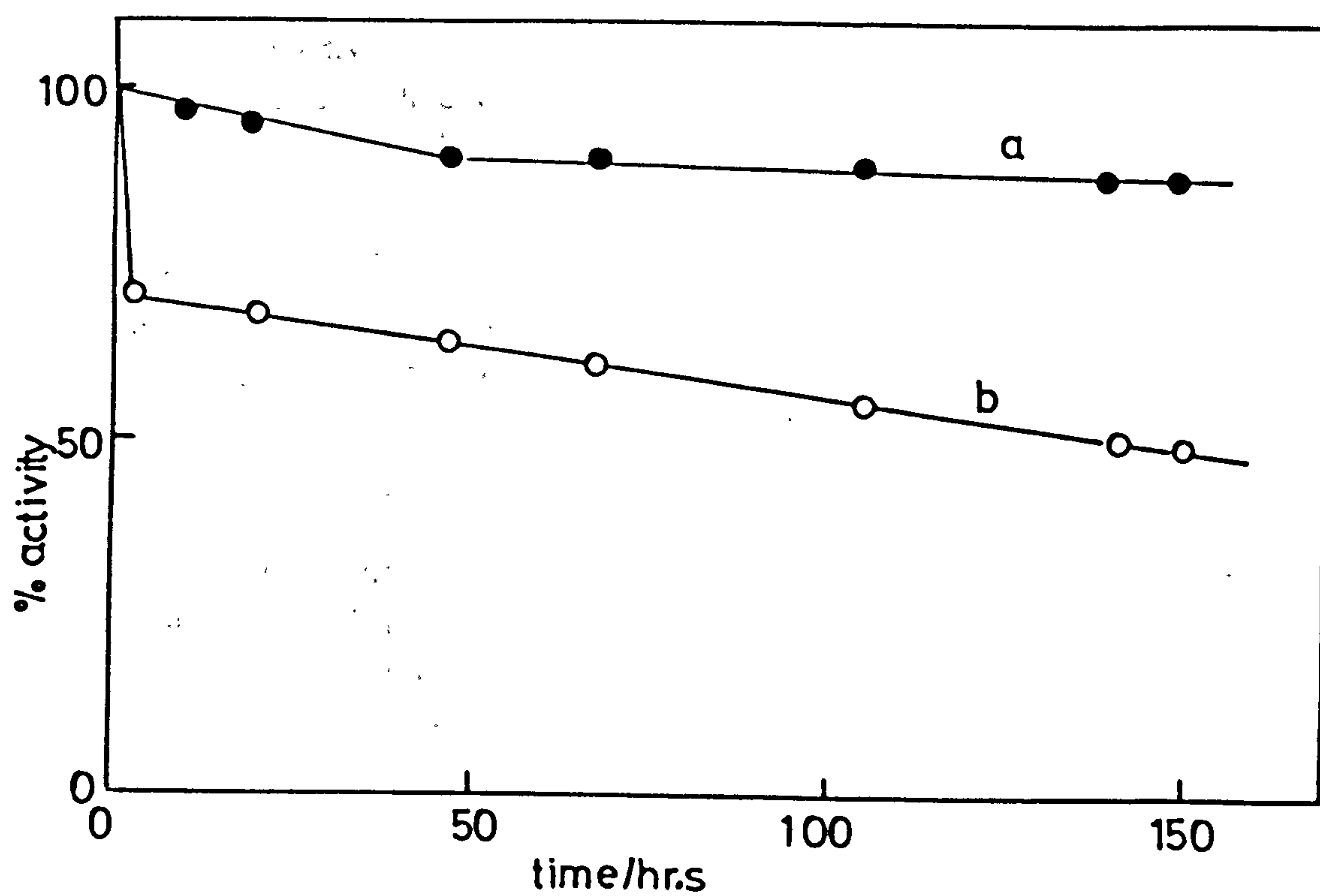


Table 6.7

Stability data for the ferrocene modified glucose oxidases

Procedure	Enzyme modifier		
	Ferrocene carboxylic acid	Ferrocene acetic acid	Ferrocene butanoic acid
A. Cold Storage			
% of initial activity remaining after 10 hours storage at 4°C (pH 7.0 under N ₂)	69	97	≈ 20
% of initial activity remaining after 150 hours storage at 4°C (pH 7.0 under N ₂)	49	88	< 10
B. Potential Cycling			
% of initial current remaining after 2 hours potential cycling at 5 mV s ⁻¹ (20°C, pH 7.0 under N ₂)	98	92	—
% of initial current remaining after 28 hours potential cycling at 5 mV s ⁻¹ (20°C, pH 7.0 under N ₂)	28	29	—

Hence it can be seen that the ferrocene acetic acid modified GOD exhibits the best stability on simple cold storage at 4°C. In the following section the electrochemical response of the ferrocene carboxylic and acetic acid modified GODs as a function of time will be described.

6.5.2 Operational Stability

This describes the stability of the modified enzymes to continuous potential

cycling under defined conditions. Electrochemical responses were measured by d.c. cyclic voltammetry at a glassy carbon electrode ($A = 0.126 \text{ cm}^2$). This was done by cycling the potential continuously and measuring the current response after predetermined periods of time. The electrode was polished prior to each measurement of the current response on the plateau region at saturating substrate concentration ($>0.08 \text{ mol dm}^{-3}$ glucose).

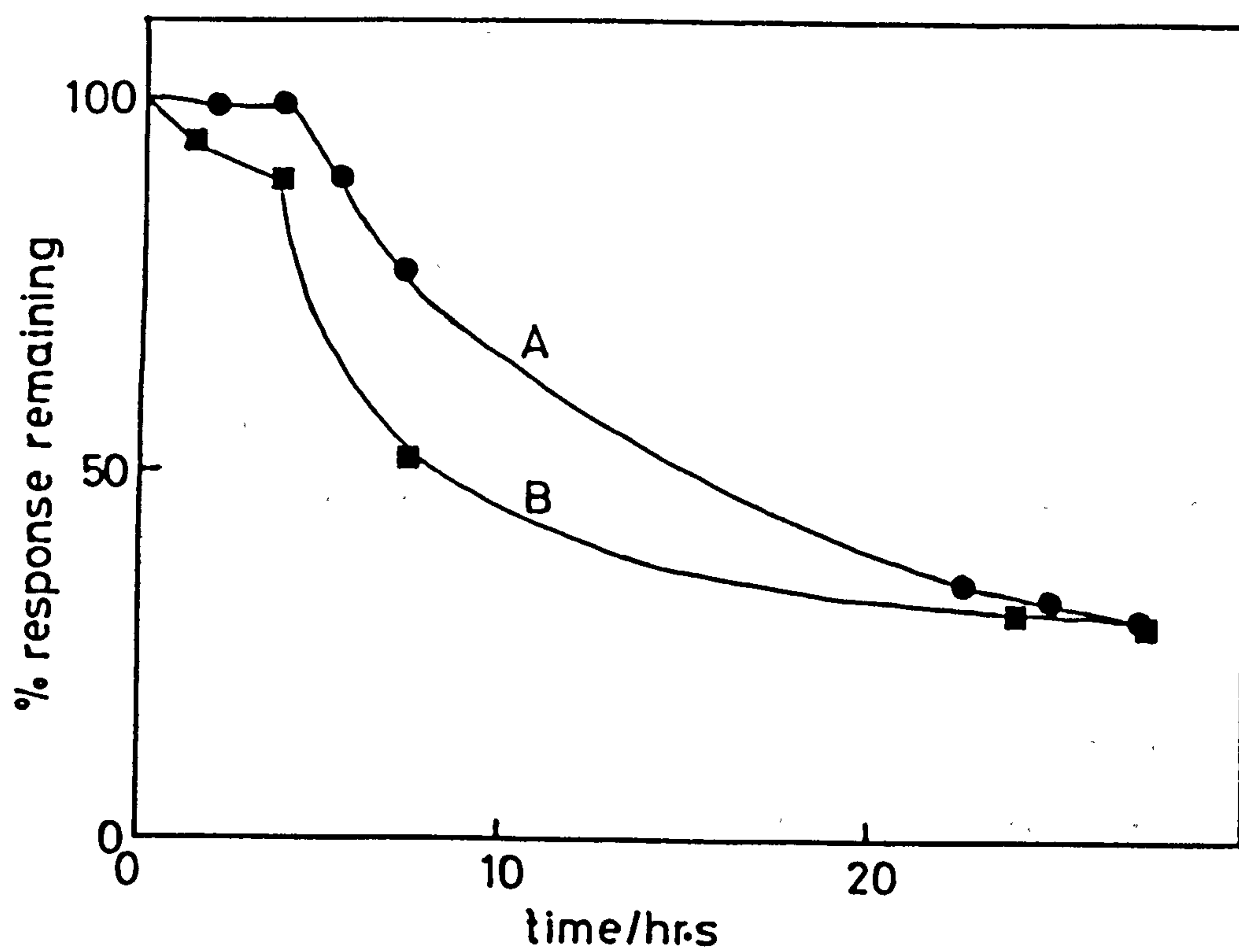
The properties of the initial response remaining as a function of the time after enzyme preparation for the ferrocene carboxylic and acetic acid modified enzymes are shown in figure 6.13.

It is apparent that there is little difference between the stability of the two preparations when continuously in operation. Table 6.7 summarises the storage and operational stability data obtained for the various enzyme preparations.

It is apparent that the ferrocene acetic acid modified GOD is significantly more stable to cold storage than the ferrocene carboxylic acid preparation. However, there appears to be little difference between the operational stabilities of these two preparations. The shape of the activity vs time plot in figure 6.13 is interesting. Little activity is lost by either preparation over the first 4 hours after collection from the column. After this plateau region there is a rapid loss of activity over the next 25 hrs until a further plateau is approached, corresponding to around a 70% loss of response. It therefore appears that two factors are in operation here. Initially it seems likely that ferrocene centres are lost from the enzyme (see next section) but sufficient remain for the response to be independent of the number of remaining centres. After this plateau region further loss of ferrocene centres occurs and the resulting current decreases rapidly as it becomes strongly dependent on the number of electron relays remaining.

The source of this loss of activity is investigated and discussed in the next section.

Figure 6.13 The stability of A) ferrocene acetic acid modified and B) ferrocene carboxylic acid modified GOD to continuous potential cycling (5 mV s^{-1} , 20°C).



6.5.3 Loss of Electrochemical Response

An investigation into the cause of the loss of current response described in the last section was undertaken. There are a number of possible reasons for this loss of electrochemical response.

Firstly the enzyme may become denatured or inactivated in some way producing a decrease in its activity to glucose. This can simply be investigated by measuring the enzyme activity in freshly prepared and aged samples using the dye-linked spectrophotometric assay described in chapter 2 of this thesis (section 2.8).

Secondly the loss of enzyme activity, if indeed this has occurred, may be due to dissociation of FAD required for the catalytic enzymic oxidation of glucose. Attempts were made to separate any dissociated FAD from enzyme in an aged preparation and then to reconstitute the enzyme with fresh FAD.

Finally, loss of the electrochemical response may be due to loss of ferrocene electron relays or loss of electroactive iron ions from these centres. In order to quantify this effect a number of experiments were undertaken. The iron content of fresh and aged modified enzyme was determined by atomic absorption spectroscopy. Furthermore, an attempt was made to separate any free ferrocene from an aged preparation by chromatography. All work described in the following section involves use of the ferrocene acetic acid modified GOD as this was the most stable.

6.5.3.1 Loss of Enzyme Activity

The activity of fresh and aged ferrocene acetic acid modified GOD samples was determined at saturating glucose concentration (section 2.8). The $\Delta A_{450} \text{ min}^{-1}$ for a fresh ($t=0$) and aged ($t=312$ hrs storage at 4°C , pH 7.0, $0.085 \text{ mol dm}^{-3}$ phosphate buffer) enzyme samples were measured. The activities of the two samples were as follows:

$$t = 0 \quad \Delta A_{450} \text{ min}^{-1} = 29$$

$$t = 312 \text{ hrs} \quad \Delta A_{450} \text{ min}^{-1} = 16$$

These activities were measured for a 1 mg cm^{-3} solution in each case. This demonstrates that 55% of the initial catalytic activity of the glucose oxidase remained after this time period.

6.5.3.2 Loss of FAD

The possible loss of FAD was first determined by a second column purification (G-25 Sephadex, section 2.9) of an aged sample. This procedure will separate the enzyme from any low molecular weight species present. Any free FAD was measured by recording the A_{450} of the resulting column fractions. This 'separation' yielded no observable 2nd fraction. The A_{450} readings were zero for all but the enzyme containing fraction. Furthermore, the absorption spectra for the freshly prepared enzyme was identical to that of the aged sample, indicating no significant or detectable loss of FAD.

Attempts were made to regain activity in the second aged ($t = 312 \text{ hr}$) sample by 'reconstitution' with pure FAD (final concentration $1 \times 10^{-6} \text{ mol dm}^{-3}$). This procedure did not increase the activity of the aged sample.

6.5.3.3 Loss of Ferrocene Centres

The effect on ferrocene centres of aging of the enzyme sample was assayed in two ways. Firstly the aged sample was subjected to a second column purification (G-25 Sephadex, section 2.9) after 312 hours cold storage. Electrochemical monitoring of each fraction by cyclic voltammetry (5 mV s^{-1} , 0 to +0.5V vs SCE) revealed no traces of ferrocene derivatives in the eluate. However, atomic absorption spectroscopy of the fresh and aged samples revealed that the number of ferrocene centres had decreased from 22 (± 2) at $t=0$ to 6.5 (± 1) at $t=312 \text{ hrs}$. Presumably this ferrocene is lost by disproportionation of the ferrocene centres to produce ferric hydroxides, and therefore is not recovered as a ferrocene derivative upon column separation.

Table 6.8 summarises the data collected for the stability studies in an attempt to determine the cause of the loss of electrochemical response.

Table 6.8

Stability data for the ferrocene acetic acid modified glucose oxidase

	Time		% Remaining
	$t=0$	$t=312$ hrs	
Enzyme activity ^{a)} ($\Delta A_{450} \text{ min}^{-1}$) of 1 mg cm^{-3} solution	29	16	55
FAD content (% of initial FAD content remaining)	100	≈ 100	≈ 100 ^{b)}
Ferrocene centre content per enzyme molecule ^{c)}	22	6.5	30

Notes

- a) Saturating glucose ($>0.08 \text{ mol dm}^{-3}$, pH 7.0)
- b) Indicates no detectable loss of FAD
- c) Measured by atomic absorption spectroscopy of duplicate samples

6.5.3.4 Conclusions

It appears that the loss of electrochemical response observed with aging of the sample is likely to be due to a combination of a loss of enzyme activity and a loss of ferrocene electron relay groups. This accounts for the biphasic loss of activity seen in figure 6.13. In order to relate a specific cause of activity loss to the second phase seen in this figure more detailed measurements of activity and ferrocene content as a function of time are required. No loss of electrochemical response can be apportioned to loss of FAD.

6.6 REAGENTLESS MEMBRANE ELECTRODES

In this section the responses of membrane electrodes constructed using ferrocene carboxylic acid modified glucose oxidase (GOD) is described. The responses are interpreted in terms of an established model describing kinetic and mass transport processes in membrane electrodes.

The resulting enzyme electrodes are termed 'reagentless' as there is no requirement for the presence of molecular oxygen or any other low molecular weight diffusible mediator in such a system.

6.6.1 Electrode Construction

Freshly prepared modified GOD was incorporated into a carbon ink by mixing 0.45g of carbon powder with 1 cm³ of a 9 mg cm⁻³ enzyme solution in phosphate buffer (0.085 mol dm⁻³, pH 7.0).

This ink (100 µl) was then applied to the surface of a glassy carbon disc electrode (3mm diameter) and allowed to dry. A dialysis membrane (Visking, Medicell) was then applied to the electrode and secured by means of a tight fitting silicone rubber 'O' ring. The membrane was pretreated, prior to application to the electrode, by boiling in a sodium carbonate solution as specified by the manufacturers.

The electrode was then washed copiously with water and placed in a deoxygenated buffer solution (0.085 mol dm⁻³ phosphate, pH 7.0). The electrode was then cycled 10 times between 50 and 450 mV (vs SCE) to obtain a constant background response. The response of this electrode to additions of glucose was then determined.

6.6.2 Response to Glucose

The buffer solution (2.5 cm³) was stirred by means of a small magnetic flea.

The glucose concentration was increased stepwise by the injection of quantities of glucose stock solution (1.00 mol dm^{-3}). After each addition the solution was allowed to mix before a d.c. cyclic voltammogram was recorded (5 mV s^{-1}). Figure 6.14 shows the electrode response as a function of glucose concentration. A catalytic current develops at potentials exceeding 200 mV (vs SCE) on the addition of glucose. The relatively large currents seen are due to the very large surface area of the porous carbon ink in intimate contact with the modified enzyme behind the dialysis membrane.

Glucose diffuses through the membrane and reduces the modified enzyme which is then directly reoxidised at the electrode surface. This type of device removes the need for diffusible mediators employed in similar devices^(53,54).

6.6.3 Analysis of the Glucose Response

The electrode response (figure 6.14) can be analysed using the model for enzyme membrane electrodes⁽²²⁹⁾. This type of analysis demonstrates whether the response is controlled by diffusion of glucose through the dialysis membrane, enzyme kinetics, or a combination of these two processes.

Initially a value of k_{ME}' must be determined. This constant, the electrochemical rate constant for the electrode process at low substrate concentrations is defined as:

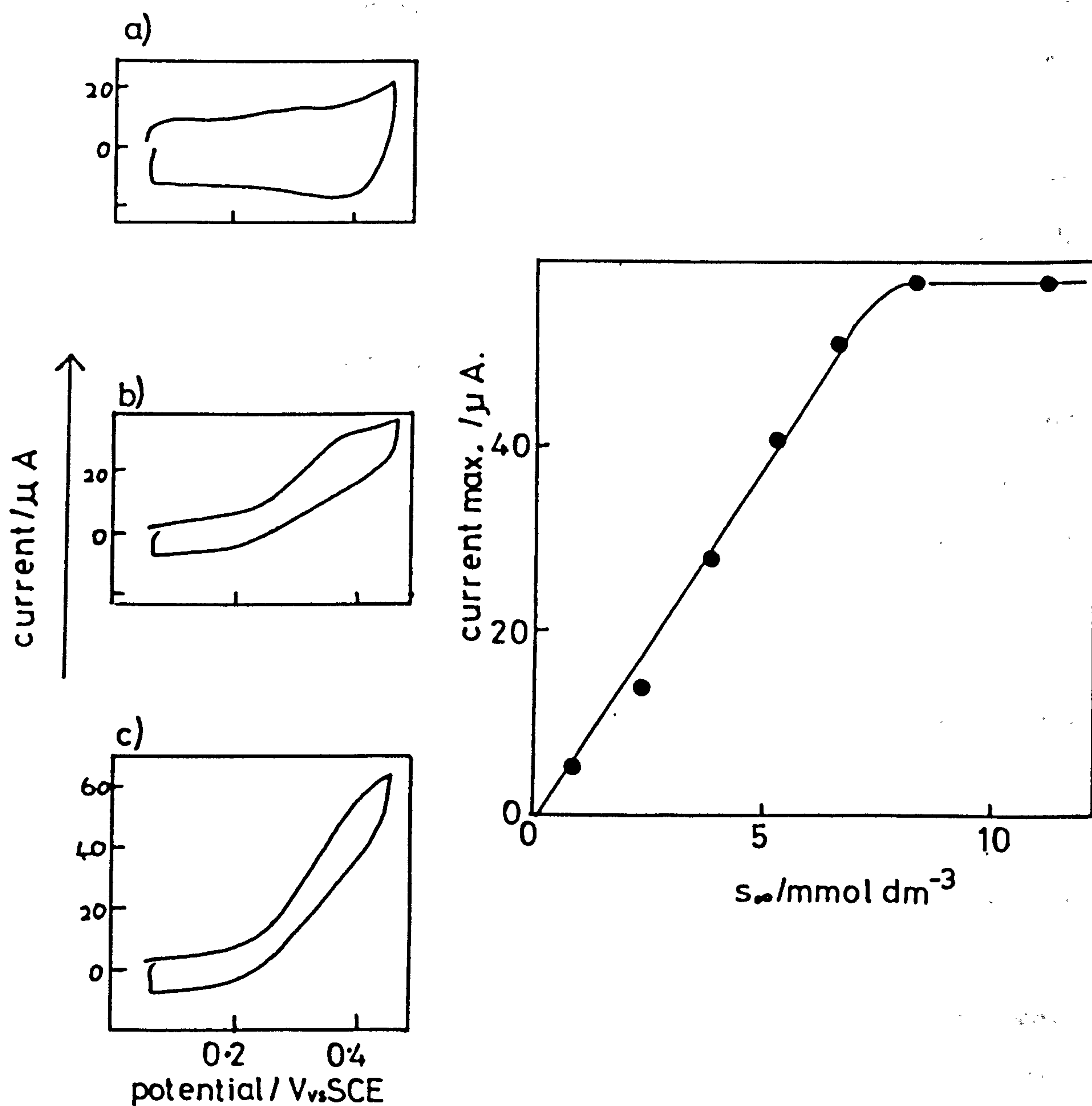
$$1/k_{ME}' = K_M/(e_{\Sigma} L k_{cat}) + 1/k_S' \quad (6.5)$$

where L is the thickness of the reaction layer behind the membrane and k_S' describes the rate of transport of glucose through the dialysis membrane.

The constant k_{ME}' is determined by constructing a plot of s_{∞}/i vs s_{∞} , where s_{∞} is the bulk glucose concentration and i is the resulting current.

$$s_{\infty}/i = \frac{1 + (s_{\infty}/K_{ME})(1 - i/[nFAk_S' s_{\infty}])}{n F A k_{ME}'} \quad (6.6)$$

Figure 6.14 Membrane electrode responses to a) zero glucose, b) 2.4×10^{-3} mol dm⁻³, and c) 6.54×10^{-3} mol dm⁻³ glucose, with inset calibration curve showing plateau current as a function of bulk glucose concentration (20°C, pH 7.0).



where

$$K_{ME} = \frac{K_M / (Lk_{cat}) + e_{\Sigma} / k_S'}{1 / (Lk_{cat}) + 1 / k'} \quad (6.7)$$

and k' is the heterogeneous rate constant describing direct reoxidation of the modified electrode at the electrode surface. Such a plot is shown in figure 6.15a. The limiting value of s_{∞}/i as $s_{\infty} \rightarrow 0$ gives $[s_{\infty}/i]_0 = (nFAK_{ME}')^{-1}$. This gives a value for k_{ME}' of $6.6 \times 10^{-4} \text{ cm s}^{-1}$.

The second stage in this analysis is to plot Y against ρ (where $\rho = (1/nFAK_{ME}')/(s_{\infty}/i)$ and $Y = (\rho - 1)/s_{\infty}$). Such a plot is shown in figure 6.15b. From the intercepts at $l=0$ and $Y=0$ we obtain estimates of $1/K_{ME}$ and k_S'/k_{ME}' respectively. We find that $K_{ME} = 7.2 \text{ mmol dm}^{-3}$ and $k_S'/k_{ME}' = 1.0$.

The constant K_{ME} is analogous to the Michaelis constant used in standard enzyme kinetics. For glucose concentrations below K_{ME} the electrode response is substrate dependent and for glucose concentrations well in excess of K_{ME} the electrode response saturates.

In this case we find that K_{ME} is greater than the apparent value for K_M (table 6.5). Using the values of K_{ME} , K_M and k_S'/k_{ME}' determined we find that $k_{cat}L/k' \gg 1$.

This indicates that the response in the plateau region is determined by the rate of electrochemical oxidation of the modified enzyme, denoted by the electrochemical rate constant k' .

In the region where the electrode response is dependent on the glucose concentration the ratio of k_S'/k_{ME} has a value of 1.0 demonstrating that the rate limiting process in this region of the response curve is transport of glucose through the membrane by diffusion.

The various parameters are collected together in table 6.9.

Figure 6.15 Analysis of the modified enzyme membrane electrode response.

a) Plot of s_{∞}/i against s_{∞} , giving an estimate of k_{ME}' .

b) Plot of Y against ρ , giving an estimate of K_{ME} and k_s'/k_{ME}' .

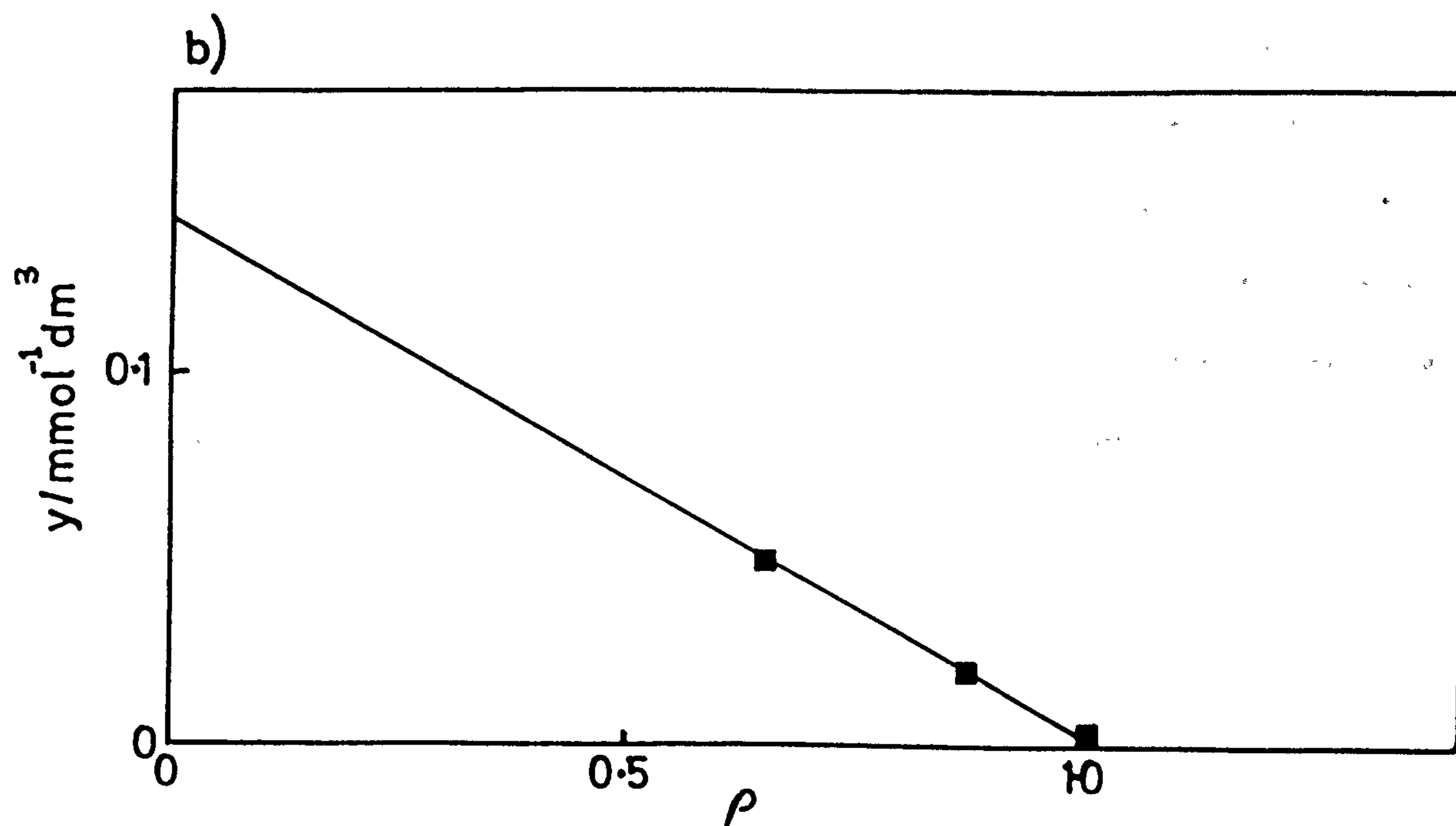
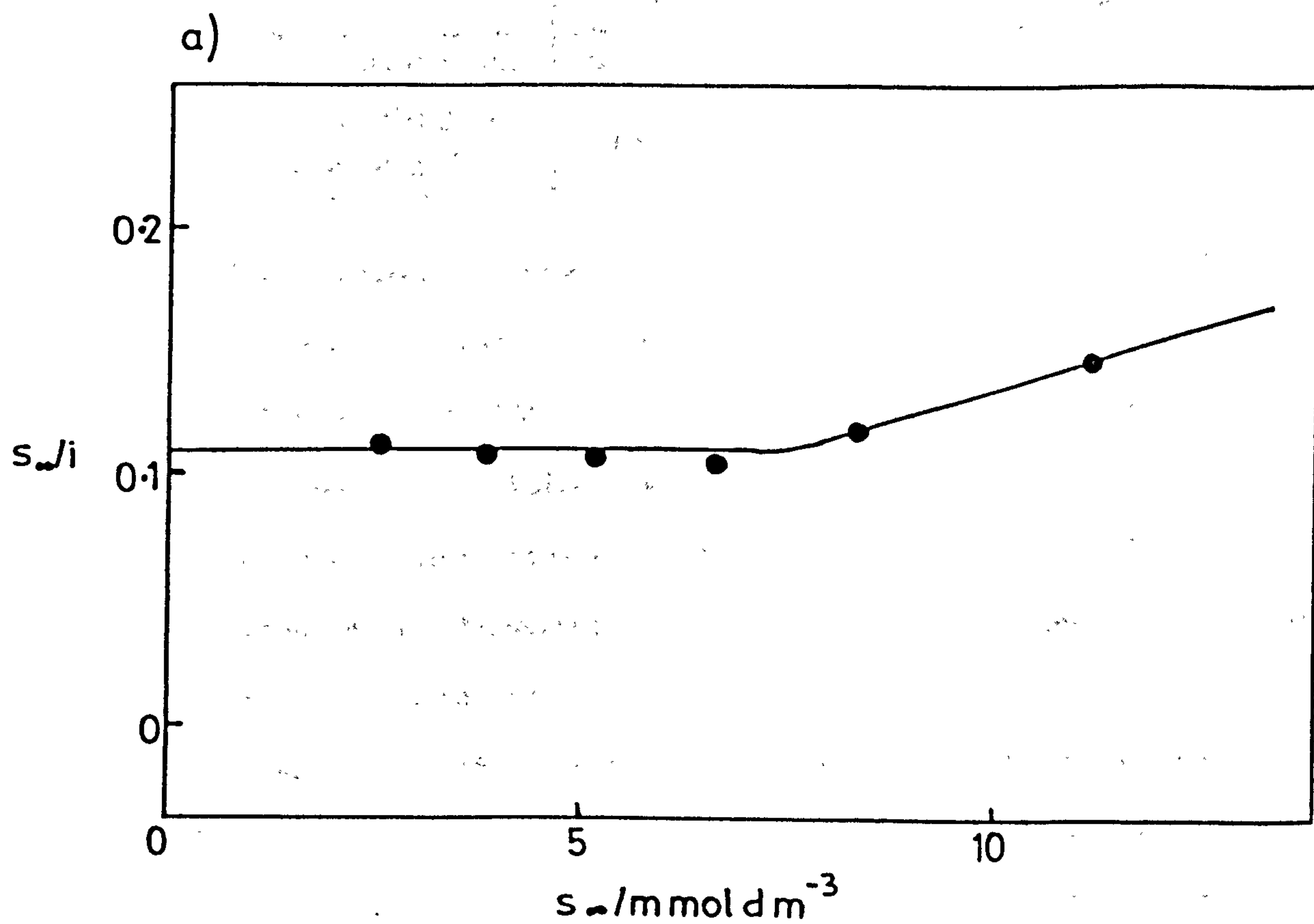


Table 6.9

The kinetic parameters obtained for the modified GOD-membrane electrode

	$k_s'/\text{cm s}^{-1}$	$K_{ME}/\text{mmol dm}^{-3}$	$k_{cat}L/k'$
Freshly prepared	6.6×10^{-4}	7.2	$\gg 1$
After 390 days storage at 4°C	5.6×10^{-5}	5.0	16

The experiment was repeated after storage of the carbon ink for 390 days (4°C, pH 7.0, under N_2). Analysis of the data obtained produced the kinetic parameters presented in table 6.9. The smaller value of k_s' obtained using the aged sample reflects differences in the dialysis membranes used for the two experiments; a thicker membrane being used in the latter experiment. Also, although the value of $k_{cat}L/k'$ is smaller in the second experiment, the response in the plateau region is still limited by electrode kinetics and not by enzyme kinetics.

It can be concluded therefore that the modified GOD ink can be stored for extended periods of time. Although a large proportion of the enzyme activity is undoubtedly lost during this period it still allows the construction of a reagentless glucose sensor in which the plateau response is independent of the enzyme activity and is controlled by the rate of electrochemical oxidation of the substrate reduced enzyme. Furthermore, use of such an electrode will not pollute the sample glucose solution with diffusible ferrocene derivatives. This may have advantages for *in vivo* glucose sensing. This electrode also operates at a low overpotential, reducing the problem of electrochemical interference in biological samples.

6.8 CONCLUSIONS

In this section conclusions about the modification of redox enzymes with electron relaying groups will be drawn.

In this chapter the modification of glucose oxidase with 3 ferrocene carboxylic acid derivatives has been described. Modification using ferrocene acetic acid has proven particularly successful, mainly due to the large k_{cat} for this enzyme, and the correspondingly large catalytic currents obtained, but also because of the improved storage stability of this preparation. It is clear that this type of covalent redox enzyme modification has great potential in the area of fundamental research into enzyme electrochemistry as well as possible applications in the field of biosensors.

The unique ability of this type of modified enzyme to undergo direct electron transfer at simple metal electrodes opens up an area of direct enzyme electrochemistry which has not previously been possible. A large range of potential candidates for modification are available, and it is to be expected that this will be a growing area for research in future years.

The original aim of producing such modified GOD molecules was as an extension to the work on the electrochemical immobilisation of GOD in organic polymers described in chapters 4 and 5 of this thesis. However, the electrochemical immobilisation of ferrocene acetic acid modified GOD has not been possible so far. This may be a result of the enzyme gaining many positive charges upon modification. If the enzyme becomes polycationic on modification then it will no longer be electrostatically included as a counter ion in oxidatively grown, polycationic, polypyrroles.

It is likely that a negatively charged polymer, such as a sulphonated pyrrole⁽²³⁰⁾, is required for the successful electrochemical immobilisation of this modified enzyme. It is encouraging however that the modified enzyme is able to undergo direct reoxidation at poly-*N*-methylpyrrole electrodes. Direct electron

transfer between the immobilised enzyme molecule and the surrounding polymer matrix is essential for such a device to succeed due to the absence of any freely diffusible mediator.

The electrochemical immobilisation of a redox modified enzyme appears to be feasible given the correct enzyme / polymer combination. This would allow the easy preparation of reagentless and specific glucose sensitive electrodes.

CHAPTER SEVEN

CONCLUDING REMARKS

7.1 Overall Conclusions

The work presented in this thesis deals with two main areas. Firstly the electrochemical immobilisation of redox enzymes in conducting or insulating organic polymer films is described. Data obtained for a variety of systems is analysed according to specially developed kinetic models describing diffusion and reaction of substrate and mediator in the polymer films. Useful information is extracted from this data.

Secondly the methods used to covalently modify redox enzymes are described and examples of successful modifications are given. The electrochemical responses of the resulting modified enzymes are analysed in order to determine the values of the kinetic constants for the reactions. A significant improvement over previous literature procedures is described.

7.2 Future Work

A number of interesting openings have appeared during the course of this work. Furthermore, certain of the research projects undertaken over the period allowed for the research leading to a PhD remain unfinished at the present time. Although such work is not included in this thesis it is informative to mention briefly the kind of work which appears to be worth pursuing. There are two main areas here.

Firstly, the production of a self contained system in which an enzyme and its mediator are immobilised together in a single step electrochemical procedure may have applications in the development of small and stable sensing devices. This type

of system has been investigated in the form of a poly-*N*-methyldopamine / glucose oxidase / ferricyanide ion electrode and is relatively easy to produce. Furthermore, the stability of such a system is greatly enhanced by the electrostatic attraction between the mediating ion and the polycationic polymer. This overcomes many of the problems associated with previous systems.

Secondly, attempts to immobilise a modified enzyme, such as ferrocene acetic acid modified glucose oxidase, have so far proven unsuccessful by an electrochemical method. This may be due to unfavourable charge interactions between enzyme and immobilisation matrix when using poly-*N*-methyldopamine. There is still much to be learned about the way in which redox enzymes can be usefully modified to undergo direct electron transfer at simple metallic electrodes. Also, the way in which such enzymes behave is not well understood and suitable electrochemical immobilisation procedures have yet to be developed. It is likely that this area of research will receive a great deal of attention in future years, due both to an academic interest in the fundamentals of biological electron transfer reactions and a commercial interest in successful biosensing.

REFERENCES

1. A.L. Lehninger, *Biochemistry*, 2nd ed., (1981), Worth, New York, 477-508.
2. M. Dixon and E.C. Webb, *Enzymes*, 3rd ed., (1979), Longman, London, 277-290.
3. L.D. Bowers and P.W. Carr, *Advances in Biochemical Engineering*, **15**, (1980), 89.
4. L.D. Bowers, *Anal. Chem.*, **58**, (1986), 513A.
5. G. Dryhurst, K.L. Kadish, F. Scheller and R. Renneberg, *Biological Electrochemistry* Vol.1, (1982), Academic Press, New York and London, 399-421.
6. A. Fersht, *Enzyme Structure and Mechanism*, (1977), Freeman, Reading and San Francisco, 274-287.
7. D.G. Nicholls, *Bioenergetics*, (1982), Academic Press, London.
8. H.R. Mahler and E.H. Cordes, *Basic Biological Chemistry*, (1968), Harper Int. Ed., Japan, 362-371.
9. E.A. Dawes, *Quantitative Problems in Biochemistry*, 6th edn., (1980), Longman, New York, 215-217.
10. D.E. Metzler, *Biochemistry*, Int. Ed., (1977), Academic Press, New York, 582-609.
11. S.S. Isied, *Prog. Inorg. Chem.*, **32**, (1984) 443.
12. G. McLendon, T. Guarr, M. McGuire, K. Simolo, S. Strauch and K. Taylor, *Coord. Chem. Rev.*, **64**, (1985) 113.
13. R.A. Marcus and N. Sutin, *Biochem. Biophys. Acta*, **811**, (1985), 265.
14. G. McLendon, *Acc. Chem. Res.*, **21**, (1988), 160.

15. W.J. Albery, *Electrode Kinetics*, O.U.P., Oxford, (1975), 115.
16. J.T. Hupp and J. Weaver, *J. Electroanal. Chem.*, 152 (1983), 1.
17. R.A. Marcus, *J. Chem. Phys.*, 43, (1965), 679.
18. M. Dixon and E.C. Webb, *Enzymes*, 3rd edn., (1979), Longman, London, 479.
19. C. Walsh, *Acc. Chem. Res.*, 13, (1980) 148.
20. A.L. Lehninger, *Biochemistry*, 2nd edn., (1981), Worth, New York, 487.
21. P. Hemmerich, C. Veeger and H.C.S. Wood, *Angew. Chem. Internat. Ed.*, 4, (1965), 671.
22. B. Janik and P.J. Elving, *Chem. Rev.*, 68, (1968), 295.
23. G. Dryhust, K.L. Kadish, F. Scheller and R. Renneberg, *Biological Electrochemistry Vol.1*, (1982), Academic Press, New York and London, 459.
24. M. Dixon and E.C. Webb, *Enzymes*, 3rd edn., (1979), Longman, London, 483.
25. H. Tsuge, O. Natsuaki and K. Ohashi, *J. Biochem*, 78 (1975), 835.
26. M. Dixon and E.C. Webb, "Enzymes", 3rd edn., (1979), Longman, London, 712.
27. P. Hemmerich, V. Massey, H. Michel and S. Schug, *Advances in Biochemical Engineering*, 17 (1982) 119.
28. V. Massey, G. Palmer and R. Bennet, *Biochim. Biophys. Acta*, 48 (1961) 1.
29. S. Nakamura, S. Hayashi and K. Koga, *Biochim. Biophys. Acta*, 445 (1976) 294.
30. L.M. Schopfer, V. Massey and A. Caiborn, in "Flavins and Flavoproteins", Eds. V. Massey and C.H. Williams, Elsevier, New York, (1982) 102.
31. G.E. Schultz, R.H. Schirmer and E.F. Pai, *J. Mol. Bio.*, 160 (1982) 287.
32. A.E.G. Cass, G. Davis, M.J. Green and H.A.O. Hill, *J. Electroanal. Chem.*, 190 (1985) 117.

33. C. Tanford, *J. Amer. Chem. Soc.*, **74** (1952) 6036.
34. F. Scheller, M. Jänchen, J. Lampe, H-J. Prümke, J. Blanck and E. Palacek, *Biochim. Biophys. Acta*, **412** (1975) 157.
35. T. Kakutani, K. Toriyama, I. Ideka and M. Senda, *Bull. Chem. Soc. Jpn.*, **53** (1980) 947.
36. K.S.V. Santhranam, N. Jespersen and A.J. Bard, *J. Amer. Chem. Soc.*, **99** (1977) 274.
37. F. Scheller, G. Strand, B. Neuman, M. Kuhn and W. Ostrowski, *Bioelectrochem. Bioenerg.*, **6** (1979) 117.
38. B. Kuznetsov, N. Mestechkina and G. Shumakovich, *Bioelectrochem. Bioenerg.*, **4** (1977) 1.
39. G. Dryhust, K.L. Kadish, F. Scheller and R. Renneberg, "Biological Electrochemistry", vol.1, (1982), Academic Press, New York and London, 436.
40. P.R. Duke, R.N. Kusti and L.A. King, *J. Electrochem. Soc.*, **116** (1969) 32.
41. E. Knobloch, in "Methods in Enzymology", Academic Press, New York, **18B** (1971) 375.
42. H. Durliat and M. Comtat, *Anal. Chem.*, **56** (1984) 148.
43. R.M. Ianniello, T.J. Lindsay and A.M. Yacynych, *Anal. Chim. Acta*, **141** (1982) 23.
44. R.M. Ianniello, T.J. Lindsay and A.M. Yacynych, *Anal. Chim. Acta*, **54** (1982) 1980.
45. C. Bourdillion, J.P. Bourgeois and D. Thomas, *J. Amer. Chem. Soc.*, **102** (1980) 4231.
46. F.R. Shu and G.S. Wilson, *Anal. Chem.*, **48** (1976) 1679.
47. R. Szentrimay, P. Yeh and T. Kuwana, in "Electrochemical Studies of Biological Systems", Ed. D. Sawyer, ACS, Washington DC, (1977) 143.

48. A.P.F. Turner, S.P. Hendry and M.F. Cardosi, in "Biosensors, Instrumentation of Processing", The World Biotech. Report, vol.1, Online Publications, Pinner, (1987) 125.
49. J.E. Frew and H.A.O. Hill, *Phil. Trans. R. Soc. Lond.*, **316** (1987) 95.
50. G. Davis, *Biosensors*, **1** (1985) 161.
51. G. Davis, in "Biosensors, Fundamentals and Applications", (1987), Eds. A.P.F. Turner, I. Karube and G.S. Wilson, OUP, Oxford, 247.
52. R.S. Nicholson and I. Shain, *Anal. Chem.*, **37** (1965) 178.
53. A.E.G. Cass, G. Davis, G.D. Francis, H.A.O. Hill, W.J. Aston, I.J. Higgins, E.V. Plotkin, L.D.L. Scott and A.P.F. Turner, *Anal. Chem.*, **56** (1984) 667.
54. A.E.G. Cass, G. Davis, H.A.O. Hill, I.J. Higgins, E.V. Plotkin, A.P.F. Turner and W.J. Aston, in "Charge and Field Effects in Biosystems", (1984), Eds. M.J. Allen and P.N.R. Usherwood, Abacus, p.475.
55. H.A.O. Hill, *Analytical Proceeding*, **22** (1985) 201.
56. J.E. Frew, M.J. Green, H.A.O. Hill, *J. Chem. Tech. Biotechnol.*, **36** (1986) 357.
57. G.A. Robinson, H.A.O. Hill, R.D. Philo, J.M. Gear, S.J. Rattle and G. Forrest, *Clin. Chem.*, **31** (1985) 1449.
58. K. DiGleria, M.J. Green and H.A.O. Hill, *Anal. Chem.*, **58** (1986) 1203.
59. A.L. Crumbliss, H.A.O. Hill and D.J. Page, *J. Electroanal. Chem.*, **206** (1986) 327.
60. A.P.F. Turner, W.J. Aston, I.J. Higgins, J.M. Bell, J. Colby, G. Davis, and H.A.O. Hill, *Anal. Chim. Acta.*, **163** (1984) 161.
61. A.P.F. Turner, W.J. Aston, G. Davis, I.J. Higgins, H.A.O. Hill and J. Colby, in "Microbiol. Gas Metabolism, Mechanistic, Metabolic and Biotech. Aspects", *Soc. Gen. Microbiol.*, (1985) 161.

62. A.E.G. Cass, G. Davis, H.A.O. Hill and D.J. Nancarrow, *Biochim. Biophys. Acta.*, 828 (1985) 51.
63. M. Ball, J.E. Frew, M.J. Green and H.A.O. Hill, in "Electrochemical Sensors for Biomedical Applications", ed. C.K.N. Li, The Electrochem. Soc., (Proceedings Volume) 86-14 (1986) 16.
64. J.M. Dicks, W.J. Aston, G. Davis and A.P.F. Turner, *Anal. Chim. Acta.*, 182 (1986) 103.
65. I. Taniguchi, S. Miyamoto, S. Tomimura and F.M. Hawkridge, *J. Electroanal. Chem.*, 240 (1988) 333.
66. J. Mahenc and H. Aussaresses, *C. R. Acad. Sci. Paris*, 289 (1979) 357.
67. J.R. Mor and R. Guamaccia, *Anal. Biochem.*, 79 (1977) 319.
68. M.K. Weibel and C. Dodge, *Arch. Biochem. Biophys.*, 169 (1975) 146.
69. R. Racine and W. Mindt, *Experientia Suppl.*, 18 (1971) 525.
70. Y.A. Aleksandrovski, L.V. Bezhikina and Y.V. Rodinov, *Biokhimiya* (trans.), 46 (1981) 708.
71. V. Massey, G. Palmer, C.H. Williams, B.E.P. Swoboda and R.H. Sands, in "Flavins and Flavoproteins", ed. E.C. Slater, Elsevier, Amsterdam (1966) 133.
72. D.L. Williams, A.P. Doig Jr. and A. Korosi, *Anal. Chem.*, 42 (1970) 118.
73. M.A. Lange and J.Q. Chambers, *Anal. Chim. Acta.*, 175 (1985) 89.
74. N.C. Foulds and C.R. Lowe, *J. Chem. Soc. Faraday Trans.*, 82 (1986) 1259.
75. R.M. Ianniello, T.J. Lindsay and A.M. Yacynych, *Anal. Chem.*, 54, (1982) 1980.
76. G. Davis, H.A.O. Hill, I.J. Higgins and A.P.F. Turner, in "Implantable Sensors for Closed Loop Prosthetic Systems", ed. W.H. Ko, Futura, New York, (1985), p.189.

77. G. Davis, M.J. Green and H.A.O. Hill, *Enzyme Microb. Technol.*, **8** (1986) 1203.
78. S.L. Brooks, R.E. Ashby, A.P.F. Turner, M.R. Calder and D.J. Clarke, *Biosensors*, **3** (1987/88) 45.
79. C. Iwakura, Y. Kajiya and H. Yoneyama, *J. Chem. Soc. Chem. Commun.*, (1988) 1019.
80. L.B. Wingard Jr., *Bioelectrochem. Bioenerg.*, **9** (1982) 307.
81. N.K. Cenas, A.P. Pocius and J.J. Kulys, *Bioelectrochem. Bioenerg.*, **11** (1983) 61.
82. N.K. Cenas and J.J. Kulys, *Bioelectrochem. Bioenerg.*, **8** (1981) 103.
83. G. Johnsson and L. Gorton, *Biosensors*, **1** (1985) 355.
84. A.P.F. Turner, S.P. Hendry, M.F. Cardoso and E.W. Neuse, *BDA Autumn Meeting*, Liverpool (1987), Diabetic Medicine (in press).
85. J.J. Kulys and N.K. Cenas, *Biochim. Biophys. Acta.*, **744** (1983) 57.
86. G.B. Street and T.C. Clarke, *IBM Res. Develop.*, **25** (1981) 51.
87. A.F. Diaz, J.M. Vasquez Vallejo and A. Martinez Duran, *IBM Res. Develop.*, **25** (1981) 42.
88. A.F. Diaz and K.K. Kanazawa, in "Extended Linear Chain Compounds", ed. J.S. Miller, vol.3 (1983) Plenum Press, NY and London, pp.417-441.
89. A.G. MacDiarmid and M. Maxfield, in "Electrochemical Science and Technology of Polymers - 1", ed. R.G. Linford, (1987), Elsevier, NY and London, pp.67-98.
90. A.F. Diaz, K.K. Kanazawa and G.P. Gardini, *J. Chem. Soc. Commun.*, (1979) 635.
91. A.F. Diaz and J.I. Castillo, *J. Chem. Soc. Commun.*, (1980) 397.

92. R.C.M. Jakobs, L.J.J. Janssen and E. Barendrecht, *Recl. Trav. Chim. Pays-Bas.*, 103 (1984) 275.
93. R. Qian, J. Qiu and D. Shen, *Synth. Metals*, 18 (1987) 13.
94. M. Takakuno, *Synth. Metals*, 18 (1987) 53.
95. P.G. Pickup, *J. Electroanal. Chem.*, 225 (1987) 273.
96. K. Kaneto, Y. Kohno, K. Yoshimo and Y. Inishi, *J. Chem. Soc. Chem. Commun.*, (1983) 382.
97. R.J. Waltman, J. Bargon and A.F. Diaz, *J. Phys. Chem.*, (1983) 1459.
98. C. Tournillon and F. Garnier, *J. Electroanal. Chem.*, 161 (1984) 51.
99. M. Sato, S. Tanaka and K. Kaerlyama, *J. Chem. Soc. Chem. Commun.*, (1985) 713.
100. M. Sato, S. Tanaka and K. Kaerlyama, *Synth. Metals.*, 14 (1986) 279.
101. J. Roncali, F. Garnier, R. Garreau and M. Lemaine, *J. Chem. Soc. Chem. Commun.*, (1987) 1500.
102. P. Marque, J. Roncali and F. Garnier, *J. Electroanal. Chem.*, 218 (1987) 107.
103. G. Tourillon and F. Garnier, *J. Electroanal. Chem.*, 135 (1982) 173.
104. R.J. Waltman, A.F. Diaz and J. Bargon, *J. Phys. Chem.*, 88 (1984) 4343.
105. A.F. Diaz and J.A. Logan, *J. Electroanal. Chem.*, 111 (1980) 111.
106. A. Kitani, J. Yano and K. Sasaki, *Chem. Letts.*, (1984) 1565.
107. W. Huang, B.D. Humphrey and A.G. MacDiarmid, *J. Chem. Soc. Faraday Trans.*, 1 82 (1986) 2385.
108. R.J. Waltman and J. Bargon, *J. Electroanal. Chem.*, 194 (1985) 49.
109. G. Schiavon, G. Zotti and G. Bontempelli, *J. Electroanal. Chem.*, 194 (1985) 327.

110. G. Brilmyer and R. Jasinski, *J. Electrochem. Soc.*, 129 (1982) 1950.
111. G. Schiavon, S. Zecchin, G. Zotti and S. Cattarin, *J. Electrochem. Soc.*, 213 (1986) 53.
112. G. Mengoli, *Adv. Polym. Sci.*, 33 (1979) 26.
113. N. Oyama, T. Ohsaka, T. Hirokawa and T. Suzuki, *J. Chem. Soc. Chem. Commun.*, (1987) 1133.
114. M. Aizawa and S. Yabuki, *Proc. 51st Ann. Meet. Jpn. Chem. Soc.*, (1985) 6.
115. M. Umana and J. Waller, *Anal. Chem.*, 58 (1986) 2979.
116. P.C. Pandey, *J. Chem. Soc. Faraday Trans.*, 1 84 (1988) 2259.
117. H. Shinohara, T. Chiba and M. Aizawa, *Proc. 6th Sensor Symp.*, Tsukuba, Japan, May (1986) 134-2.
118. H. Shinohara, T. Chiba and M. Aizawa, *Sensors and Actuators*, 1 (1988) 79.
119. P.C. Reeves, *Organic Syntheses*, 56 p.28.
120. J. Okuda and I. Miwa, *Methods of Biochemical Analysis*, 21 (1978) 159.
121. D. Keilin and E.F. Hartree, *Biochem. J.*, 42 (1948) 221.
122. H.J. Bright and M. Appleby, *J. Biol. Chem.*, 244 (1969) 3625.
123. M.K. Weibel and H.J. Bright, *J. Biol. Chem.*, 246 (1971) 2734.
124. I. Satoh, I. Karube and S. Suzuki, *Biotechnol. Bioeng.*, 18 (1976) 269.
125. J. Okuda and I. Miwa, *Methods of Biochemical Analysis*, 21 (1978) 158.
126. J. Okuda and I. Miwa, *Methods of Biochemical Analysis*, 21 (1978) 169.
127. P. Trincer, *Ann. Clin. Biochem.*, 6 (1969) 24.
128. D. Barham and P. Trunder, *Analyst*, 97 (1972) 142.
129. *Personal Communication*, Medisense (UK) Inc.

130. J.H. Pazur and K. Kleppe, *Biochemistry*, 3 (1964) 578.
131. B.E. Swoboda and V. Massey, *J. Biol. Chem.*, 240 (1965) 2209.
132. S. Hayashi and S. Nakamura, *Biochim. Biophys. Acta*, 657 (1981) 40.
133. L.G. Whitby, *Biochem. J.*, 54 (1953) 437.
134. K. Kusai, I. Sekuzu, B. Hagihara, K. Okuniki, S. Yamauchi and M. Nakai, *Biochim. Biophys. Acta*, 40 (1960) 555.
135. E.A. Dawes, "Quantitative Problems in Biochemistry", 6th edn., (1980), Longman, New York, p.178.
136. Y. Degani and A. Heller, *J. Phys. Chem.*, 91 (1987) 1285.
137. Y. Degani and A. Heller, *J. Amer. Chem. Soc.*, 110 (1988) 2615.
138. R.M.C. Dawson, D.C. Elliot, W.H. Elliot and K.M. Jones, in "Data for Biochemical Research", 3rd. edn., Oxford Scientific Publications, (1986), pp.514-519.
139. R.M.A. Azzam and N.M. Bashara, "Ellipsometry and Polarised Light", (1979), North Holland Publishing Company, Amsterdam.
140. A.J. Bard and L.R. Faulkner, "Electrochemical Methods, Fundamentals and Applications", (1980), Wiley, New York, pp.588-592.
141. A. Hammett, *Personal Communication*, ICL, Oxford.
142. A. Fersht, "Enzyme Structure and Mechanism", Freeman, Reading (1977), p.89.
143. J.G. Dauber and A.T. Moore, "Chemistry for the Life Sciences", 2nd edn., MacMillan, Surrey (1980), p.320.
144. N. Bartlett and R.G. Whitaker, *J. Electroanal. Chem.*, 224 (1987) 27.
145. L.D. Mell and J.T. Maloy, *Anal. Chem.*, 47 (1975) 299.

146. S.W. Feldberg, *J. Amer. Chem. Soc.*, 106 (1984) 4671.
147. E.M. Genies and C. Tsintavis, *J. Electroanal. Chem.*, 195 (1985) 109.
148. R.V. Subramanion, *Adv. Polym. Sci.*, 33 (1979) 43.
149. G. Cheek, C.P. Wales and R.J. Nowak, *Anal. Chem.*, 55 (1983) 380.
150. L. Coche, A. Deronzier and J-C. Moutet, *J. Electroanal. Chem.*, 198 (1986) 187.
151. A. Haimerl and A. Merz, *Angew. Chem. Int. Ed. Engl.*, 25 (1986) 180.
152. T. Inagaki, M. Hunter, X.Q. Yang, T.A. Skotheim and Y. Okamoto, *J. Chem. Soc. Chem. Comm.*, (1986) 126.
153. N.C. Foulds and C.R. Lowe, *Anal. Chem.*, 60 (1988) 2473.
154. G. Bidan, A. Deronzier and J-C. Moutet, *Nouv. J. Chim.*, 8 (1984) 501.
155. S. Cosnier, A. Deronzier and J-C. Moutet, *J. Electroanal. Chem.*, 198 (1986) 187.
156. J.G. Eaves, H.S. Munro and D. Parker, *Inorg. Chem.*, 26 (1987) 644.
157. F. Daire, F. Bedioui, J. Devynck and C. Bied-Charreton, *J. Electroanal. Chem.*, 205 (1986) 309.
158. P. Audebert, G. Bidan and M. Lapkowski, *J. Chem. Soc. Chem. Commun.*, (1986) 887.
159. J.P. Collin and J-P. Sauvage, *J. Chem. Soc. Chem. Commun.*, (1987) 1075.
160. A. Deronzier and J.M. Latour, *J. Electroanal. Chem.*, 224 (1987) 295.
161. A. Bettelheim, B.A. White, S.A. Raybuck and R.W. Murray, *Inorg. Chem.*, 26 (1987) 1009.
162. F. Bedioui, A. Merino, J. Devynck, C. Mestres and C. Bied-Charreton, *J. Electroanal. Chem.*, 239 (1988) 433.

163. B. Zinger and L.L. Miller, *J. Amer. Chem. Soc.*, 106 (1984) 6861.
164. J. Tietje-Girault, J.M. Anderson, I. MacInnes, M. Schroder, G. Tennant and H.H. Girault, *J. Chem. Soc. Chem. Commun.*, (1987) 1096.
165. O. Ideka, K. Okabayashi and H. Tamura, *Chem. Lett.*, (1983) 1821.
166. F. Bedioui, C. Bongars, J. Devynck, C. Bied-Charreton and C. Hinnen, *J. Electroanal. Chem.*, 207 (1986) 87.
167. T. Skotheim, M. Velasquez-Rosenthal and C.A. Linkous, *J. Chem. Soc. Chem. Commun.*, (1985) 612.
168. P.N. Bartlett and R.G. Whitaker, *Biosensors*, 3 (1987/88) 359.
169. A.F. Diaz and K.K. Kanazawa, *J. Chem. Soc. Chem. Commun.*, (1979) 381.
170. K.K. Kanazawa, A.F. Diaz, R.H. Geiss, W.D. Gill, J.F. Kwak, J.A. Logan, J.F. Rabolt and G.B. Street, *J. Chem. Soc. Chem. Commun.*, (1979) 854.
171. A.F. Diaz, J. Crowley, J. Bargon, G.P. Gardini and J.B. Torrance, *J. Electroanal. Chem.*, 121 (1981) 255.
172. G.B. Street, T.C. Clark, M. Krouribi, K.K. Kanazawa, V. Lee, P. Pfluger, J.C. Scott and G. Weiser, *Mol. Cryst. Liq. Cryst.*, 83 (1982) 253.
173. G. Kirchner, M.P. Scollar and A.M. Klibanov, *J. Amer. Chem. Soc.*, 107 (1985) 7072.
174. J. Grunwald, B. Wirz, M.P. Scollar and A.M. Klibanov, *J. Amer. Chem. Soc.*, 108 (1986) 6732.
175. G.P. Gardini, in "Advances in Heterocyclic Chemistry", (1983), eds. A.R. Katritzky and A.J. Boulton, Academic Press, New York, p.67.
176. R.B. Bjorklund, *J. Chem. Soc., Faraday Trans.*, 1 83 (1987) 1507.
177. A. Dall'Olio, G. Dascola, V. Varacca and V. Bocche, *Compt. Rend. (Paris)* 267C (1968) 433.

178. T. Iyoda, A. Ohtani, T. Shimidzu and K. Honda, *Synth. Met.*, 18 (1987) 725.
179. W. Wernet, M. Monkenbusch and G. Wegner, *Makromol. Chem., Rapid Commun.*, 5 (1984) 1574.
180. E.M. Genies and A.A. Syed, *Synth. Met.*, 10 (1984/85) 21.
181. S. Asavapiriyant, G.K. Chandler, G.A. Gunawardena and D. Pletcher, *J. Electroanal. Chem.*, 177 (1984) 229.
182. S. Asavapiriyant, G.K. Chandler, G.A. Gunawardena and D. Pletcher, *J. Electroanal. Chem.*, 177 (1984) 245.
183. T. Shimidzu, A. Ohtani, T. Iyoda and K. Honda, *J. Electroanal. Chem.*, 224 (1987) 123.
184. B.L. Funt and S.V. Lowen, *Synth. Met.*, 11 (1985) 129.
185. O. Inganäs, R. Erlandsson, C. Nylander and I. Lundström, *J. Phys. Chem. Solids*, 45 (1984) 427.
186. A.F. Diaz, J. Castillo, K.K. Kanazawa and J.A. Logan, *J. Electroanal. Chem.*, 133 (1982) 233.
187. H.V. Malmstadt and H.L. Pardue, *Anal. Chem.*, 33 (1961) 1040.
188. R.W. Murray, in "Electroanalytical Chemistry", vol.13, ed. A.J. Bard, (1983), Marcel Dekker, New York, p.165.
189. R. Bentley, in "The Enzymes", vol. 7, eds. P.D. Boyer, H.A. Lardy and H. Myrback, (1973), Academic Press, New York, p.567.
190. V.G. Levich, "Physicochemical Hydrodynamics", (1962) Prentice Hall, Eaglewood Cliffs, New Jersey, pp.60-72.
191. W. J. Albery and A.R. Hillman, "Modified Electrodes", *Ann. Rep. C., R. Soc. Chem.*, (1981) 377.
192. K. Sasaki, M. Ioi and K. Ohashi, *Electrochim. Acta.*, 12 (1967) 363.

193. T.T. Wang, S. Tasaka, R.S. Hutton and P.Y. Lu, *J. Chem. Soc. Chem. Commun.*, (1985) 1343.
194. T. Shimidzu, A. Ohtani, T. Iyoda and K. Honda, *J. Chem. Soc. Chem. Commun.*, (1986) 1415.
195. T. Iyoda, A. Ohtani, T. Shimidzu and K. Honda, *Chem. Lett.*, (1986) 687.
196. T. Shimidzu, A. Ohtani, T. Iyoda and K. Honda, *J. Electroanal. Chem.*, 224 (1987) 123.
197. The Southampton Electrochemistry Group, "Instrumental Methods in Electrochemistry", (1985), Ellis Horwood, Chichester, pp.303-311.
198. A.R. Hillman and E.F. Mallen, *J. Electroanal. Chem.*, 220 (1987) 351.
199. W.J. Albery, in "Electrode Kinetics", (1975), Oxford University Press, Oxford, pp.58-60.
200. C. Bourdillon, J. Bourgeois and D. Thomas, *Biotechnol. Bioeng.*, 21 (1979) 1877.
201. R.A. Kamin and G.S. Wilson, *Anal. Chem.*, 52 (1980) 1198.
202. B.L. Williams and K. Wilson (eds.), "Principles and Techniques of Practical Biochemistry", (1979), Arnold, London, pp.6-9.
203. M. Yudkin and R. Offord, in "Comprehensive Biochemistry", (1975), Longmans, Worldwide Publishers, pp.131-132.
204. R. Bentley, in "The Enzymes", vol.17, (1963), Academic Press, New York, p.572.
205. G. Brown, E. Selegny, S. Avrameas and D. Thomas, *Biochim. Biophys. Acta*, 185 (1969) 260.
206. H.H. Weetall and L.S. Hersh, *Biochim. Biophys. Acta*, 206 (1970) 54.
207. K.B. Ramachandran and D.D. Perlmutter, *Biotechnol. Bioeng.*, 18 (1976) 669.

208. F. Bruno, M.C. Pham and J.E. Dubois, *J. Electrochim. Acta.*, **22** (1977) 451.
209. M.C. Pham, P.C. Lacaze and J.E. Dubois, *J. Electroanal. Chem.*, **86** (1978) 147.
210. M.C. Pham, J.E. Dubois and P.C. Lacaze, *J. Electroanal. Chem.*, **99** (1979) 331.
211. M.C. Pham, G. Tourillon, P.C. Lacaze and J.E. Dubois, *J. Electroanal. Chem.*, **111** (1980) 385.
212. J.E. Dubois, P.C. Lacaze and M.C. Pham, *J. Electroanal. Chem.*, **117** (1981) 233.
213. M.C. Pham, A. Hachemi and J.E. Dubois, *J. Electroanal. Chem.*, **161** (1984) 199.
214. R.N. Adams, "Electrochemistry at Solid Electrodes", (1969), Marcel Dekke, New York, p.219.
215. A.J. Bard and L.R. Faulkner, "Electrochemical Methods, Fundamentals and Applications", (1980), Wiley, New York, pp.283-298.
216. M.L. Hitchman and W.J. Albery, *Electrochim. Acta*, **17** (1972) 787.
217. J. Albery, "Electrode Kinetics", (1975), Clarendon Press, Oxford, pp.66-67.
218. P.J. Heywood, *Personal Communication*, University of Warwick (1988).
219. K. Yagi and T. Ozawa, *Biochim. Biophys. Acta*, **81** (1964) 599.
220. K. Yagi, T. Ozawa and T. Ooi, *Biochim. Biophys. Acta*, **54** (1961) 199.
221. S.L. Mayo, W.R. Ellis, R.J. Crutchley and H.B. Gray, *Science*, **233** (1986) 948.
222. The Southampton Electrochemistry Group, "Instrumental Methods in Electrochemistry", 1st. edn., (1985), Ellis Horwood, pp.184-185.
223. S.C. Tu and D.B. McCormick, *J. Biol. Chem.*, **248** (1973) 6339.
224. N. Sugiura, H. Ohama, A. Kotaki and K. Yagi, *J. Biochem.*, **73** (1973) 901.
225. D. Hoare and D.E. Koshland, *J. Amer. Chem. Soc.*, **88** (1966) 2057.

226. D. Hoare and D.E. Koshland, *J. Biol. Chem.*, **242** (1967) 2447.
227. K.M. Yocom, J.B. Shelton, J.R. Shelton, W.A. Schröder, G. Worosila, S.S. Isied, E. Bordignon and H.B. Gray, *Proc. Natl. Acad. Sci. USA*, **79** (1982) 7052.
228. P.N. Bartlett, R.G. Whitaker, M.J. Green and J. Frew, *J. Chem. Soc. Chem. Commun.*, (1987) 1603.
229. W.J. Albery and P.N. Bartlett, *J. Electroanal. Chem.*, **194** (1985) 211.
230. N.S. Sundaresan, S. Basak, M. Pomerantz and J.R. Reynolds, *J. Chem. Soc. Chem. Commun.*, (1987) 621.